

Yudi Rusman

**ISOLATION OF NEW SECONDARY METABOLITES
FROM SPONGE-ASSOCIATED
AND PLANT-DERIVED ENDOPHYTIC FUNGI**

 Cuvillier Verlag Göttingen

**ISOLATION OF NEW SECONDARY METABOLITES
FROM SPONGE-ASSOCIATED AND PLANT-DERIVED
ENDOPHYTIC FUNGI**

*ISOLIERUNG VON NEUEN NATURSTOFFEN AUS
SCHWAMMASOZIIERTEN UND AUS PFLANZEN GEWONNENEN
ENDOPHYTISCHEN PILZEN*

**Inaugural-Dissertation
zur
Erlangung des Doktorgrades
der Mathematisch-Naturwissenschaftlichen Fakultät
der Heinrich-Heine-Universität Düsseldorf**

**vorgelegt von
Yudi Rusman
aus Bogor, Indonesien**

Düsseldorf, 2006

Bibliografische Information Der Deutschen Bibliothek

Die Deutsche Bibliothek verzeichnet diese Publikation in der Deutschen Nationalbibliografie; detaillierte bibliografische Daten sind im Internet über <http://dnb.ddb.de> abrufbar.

1. Aufl. - Göttingen : Cuvillier, 2007

Zugl.: Düsseldorf, Univ., Diss., 2006

978-3-86727-128-8

Gedruckt mit Genehmigung der Mathematisch-Naturwissenschaftlichen Fakultät der Heinrich-Heine-Universität Düsseldorf

Gedruckt mit Unterstützung des Deutschen Akademischen Austauschdienstes (DAAD)

Eingereicht am: 6.7.2006

Referent: Dr. Rainer Ebel, Juniorprofessor

Koreferent: Prof. Dr. Peter Proksch

Tag der mündlichen Prüfung: 23.10.2006

© CUVILLIER VERLAG, Göttingen 2007

Nonnenstieg 8, 37075 Göttingen

Telefon: 0551-54724-0

Telefax: 0551-54724-21

www.cuvillier.de

Alle Rechte vorbehalten. Ohne ausdrückliche Genehmigung des Verlages ist es nicht gestattet, das Buch oder Teile daraus auf fotomechanischem Weg (Fotokopie, Mikrokopie) zu vervielfältigen.

1. Auflage, 2007

Gedruckt auf säurefreiem Papier

978-3-86727-128-8

Erklärung

Hiermit erkläre ich ehrenwörtlich, dass ich die vorliegende Dissertation mit dem Titel „Isolierung von neuen Naturstoffen aus schwammassoziierten und aus Pflanzen gewonnenen endophytischen Pilzen“ selbst angefertigt habe. Außer den angegebenen Quellen und Hilfsmitteln wurden keine weiteren verwendet. Diese Dissertation wurde weder in gleicher noch in abgewandelter Form in einem anderen Prüfungsverfahren vorgelegt. Weiterhin erkläre ich, dass ich früher weder akademische Grade erworben habe, noch dies versucht habe.

Düsseldorf, den 7.7.2006

Yudi Rusman

ACKNOWLEDGEMENTS

I acknowledge my appreciation and grateful to Prof. Peter Proksch and Dr. Rainer Ebel, Juniorprofessor who gave the opportunity to pursue the doctoral research as well as their supervision and guidance.

I am indebted to Dr. R.A. Edrada Ebel for her scientific advices and guidance in the interpreting NMR spectra during the study as well as conducting antimicrobial and antifungal assays.

Special thanks are given to Dr. Victor Wray (GBF, Braunschweig) for his 600 MHz ^1H NMR and 150 MHz ^{13}C NMR measurements, Prof. W.E.G. Müller (Univ. Mainz) for conducting the cytotoxicity assays, Dr. Michael Kubbutat and his coworkers at ProQinase GmbH (Freiburg) for the protein kinase inhibition assays, and Prof. W. Frank (HHU-Düsseldorf) for the X-ray crystallography experiment as well as Prof. J. Ernst and Dr. C. Lengsfeld (HHU-Düsseldorf) for the *Candida albicans* death cell supply. I would like also to deeply thank Dr. Peter and his colleagues (HHU-Düsseldorf) for 500 MHz ^1H NMR and 125 MHz ^{13}C NMR measurement as well as Dr. Keck and Dr. Tommes (HHU-Düsseldorf) for conducting EI and FAB-mass spectrometry experiment.

I am also indebt to Arnulf Diesel for his helps und co-operation as a lab-mate that I finished the lab work on time. I wish to thank the (former) ESI-MS, antimicrobial assay, and molecular biology team at the institute for their helps in conducting ESI-MS measurement, antimicrobial and antifungal assays, and fungal identification, respectively.

I am grateful to Frau Schlag, Frau Kohnert and Frau Thiel for technical and administrative support, respectively. I'd like to thank the (former) members of fungal group, Dr. F. Teuscher, Dr. H. Effendi, I. D. Indriani, A. Diesel, C. Freitas, J. Jacob, A. Hassan, and A. Debbab. The special thanks also are also given to all Indonesian students as well as all other doctoral students at the Institute for their cooperation by sharing the places and works as well as the nice time during the study.

Finally, I express my appreciation to DAAD which gave me the financial support during my stay in Germany.

ZUSAMMENFASSUNG

Schwammassoziierte und aus Pflanzen gewonnene endophytische Pilze produzieren Naturstoffe mit einer Vielfalt an chemischen Strukturen, die in vielen Fällen kommerziell einsetzbaren synthetischen Ansätzen nicht zugänglich sind. Darüber hinaus weisen viele dieser Sekundärstoffe biologische Aktivitäten in pharmakologisch relevanten Assaysystemen auf die sie zu potentiellen Leitstrukturen für die Entwicklung neuer Arzneistoffe machen.

Ziel dieser Arbeit war die Isolierung von Sekundärstoffen aus Pilzen – assoziiert mit tropischen marinen Schwämmen sowie Endophyten terrestrischer Pflanzen – gefolgt von Strukturaufklärung und Untersuchung ihres pharmakologischen Potentials. Drei schwammassoziierte Pilze (*Aspergillus niger*, *Penicillium citreonigrum* sowie ein unidentifizierter Pilz) und zwei endophytische Pilze aus Pflanzen (*Pestalotiopsis longisetula* und *Chaetomium globosum*) wurden als Naturstoffquellen ausgewählt und über einen Zeitraum von drei bis vier Wochen in 300 mL Standkulturen in Flüssigmedien angezogen. Die aus der folgenden Extraktion erhaltenen Ethylacetatfraktionen wurden zur Isolierung der Naturstoffe weiteren Trennmethoden unterzogen.

Die Isolierung wurde mit Hilfe verschiedener chromatographischer Methoden durchgeführt. Dazu wurden Verfahren der Massenspektrometrie (MS) und Kernresonanzspektroskopie (NMR) angewendet, um das Molekulargewicht zu bestimmen beziehungsweise die Strukturen der Verbindungen aufzuklären. Zusätzlich wurde die Röntgenkristallographie bei einigen Verbindungen angewendet, um die absolute bzw relative Konfiguration der Stereozentren im Molekül zu bestimmen. Schließlich wurden die bioaktiven Eigenschaften in verschiedenen Biotests untersucht, darunter antimikrobielle, antifungale und cytotoxische Eigenschaften sowie die Wirkung gegen Malaria und als Inhibitoren verschiedener Proteinkinasen.

Citreonigrine A – I stellen strukturell außerordentlich komplexe meroterpene dar die zum teil für Naturstoffe neuartige Kohlenstoffe grüngerüste aufweisen. Sie werden isoliert aus *P. citreonigrum*, einem mit dem 1996 im Bali Bali Barat Nationalpark, Indonesien, gesammelten Schwamm *Pseudoceratina purpurea* assoziierten Pilz. Des weiteren wurden

aus dieser Art sechs neue Drimene sesquiterpenlactone, zwei neue Citreoviridinole, ein neues Diketopiperazin und ein neues Vermistatinderivat isoliert. Citreonigrin B und citreodrimene D weisen inhibitorische Aktivität gegenüber Proteinkinasen auf. Außerdem zeigten citreodrimenes A, B und C ausgeprägte cytotoxische Eigenschaften in Tests mit der Zelllinie L-5178Y (murines T-Zell Lymphom) und HeLa (humanes Cervixcarcinom).

Asperhillus niger ist ein Isolat aus dem 1999 auf Elba gesammelten Schwamm *Axinella damicornis*. Aus diesem Pilz wurden neue Derivate des Asperazins und Aflavinins sowie zwei neue γ – Pyrone isoliert. In den Biotests zeigte das neue Aflavininderivat nicht nur antimikrobielle Aktivität gegen *Bacillus subtilis*, *Staphylococcus epidermis* und *S. aureus*, sondern ebenfalls cytotoxische Aktivität in Tests mit der Zelllinien L-5178Y, HeLa und PC-12 (adrenales Phäochromocytom der Ratte).

Aus der im Gewächshaus der Heinrich-Heine-Universität Düsseldorf angezogenen Pflanze *Aglaia odorata* wurde 2002 der Pilz *P. longisetula* isoliert. Daraus konnten ein neues Gamahorinderivat, ein neues Herbarinderivat und ein neues Variecoxanthonderivat isoliert werden. Aufgrund der zu geringen vorliegenden Menge wurden diese beiden Verbindungen keinen Biotests unterzogen.

Insgesamt wurden in dieser Arbeit mehr als fünfzig Verbindungen isoliert und mindestens dreißig davon – nach bestem Wissen – als neue Verbindungen identifiziert. Die Diskussion beschränkt sich auf die neuen Verbindungen sowie in Rahmen diese Arbeit erzielte neue Befunde zur Aktivität einiger bekannter Verbindungen wie Chaetomin (aus *C. globosum*), Meleagrinen (aus einem unidentifizierten Pilz), das Antibiotikum RF 3192-C (aus *A. niger*) und Atromentin (aus *A. niger*).

TABLE OF CONTENTS

1	INTRODUCTION	1
1.1	Natural Products Drug Discovery and Its Current Status	1
1.1.1	Traditional Medicines and Natural Products in the Past	1
1.1.2	Natural Products Today	2
1.2	Fungi as Natural Products Sources	5
1.2.1	Sponge-Associated Fungi	6
1.2.2	Terrestrial Endophytic Fungi	9
1.3	Aims and Scopes of the Study	12
2	MATERIAL AND METHODS	13
2.1	Materials	13
2.1.1	Fungal Origin	13
2.1.2	Media	14
2.1.2.1	Medium for Isolation of Plant Endophytic Fungi	14
2.1.2.2	GPYNS Medium for Isolation of Sponge Associated Fungi	14
2.1.2.3	Wickerham Medium for Liquid Culture	14
2.1.2.4	Malt Agar (MA) Medium	15
2.1.2.5	Rice Media	15
2.1.2.6	Modified Abe Medium	15
2.1.2.7	Modified Potatoes Dextrose Agar (PDA) Medium	16
2.1.2.8	White Bean (<i>Phaseolus vulgaris L</i>) Medium	16
2.1.2.9	Modified Czypek Yeast Agar (CYA) Medium	16
2.1.2.10	Luria Bertoni (LB) Medium	17
2.1.2.11	Yeast Medium	17
2.1.2.12	Fungal Medium for Bioassays	18
2.1.2.13	Potatoes Dextrose Agar (PDA) Medium for Bioassays	18
2.1.3	Chemicals	18
2.1.3.1	Technical Grades Solvent for Separation	18
2.1.3.2	Solvents for HPLC and LC/MS	19
2.1.3.3	Solvents for NMR	19
2.1.3.4	Chemicals for Media	19

2.2	Methods	20
2.2.1	Collection and Isolation of Fungi	20
2.2.2	Isolation of Terrestrial Endophytic Fungi	20
2.2.2.1	Isolation of Sponge Associated Fungi	20
2.2.3	Fungal Identification and Taxonomy	20
2.2.3.1	Morphological Characteristic Identification	20
2.2.3.2	Fungal Identification using Molecular Biology Approach	21
2.2.3.3	Taxonomy	23
2.2.4	Fungal Cultivation	23
2.2.4.1	Fungal Culture for short Term Storage	23
2.2.4.2	Fungal Culture for isolation of Secondary Metabolites	24
2.2.5	Fungal Extraction	24
2.2.5.1	Solvent-Solvent Extraction	27
2.2.6	Isolation, Purification and Identification of Secondary Metabolites	27
2.2.6.1	Chromatography	32
2.2.6.1.1	Thin Layer Chromatography	32
2.2.6.1.2	Column Chromatography	33
2.2.6.1.2.1	Silica Column	33
2.2.6.1.2.2	Reverse Phase (RP) Column	34
2.2.6.1.2.3	Sephadex Column	34
2.2.6.1.2.4	Flash Chromatography	35
2.2.6.1.2.5	Vacuum Liquid Chromatography (VLC)	35
2.2.6.1.2.6	Semi Preparative HPLC	36
2.2.6.1.2.7	Analytical HPLC	37
2.2.6.1.3	Gas Chromatography	38
2.2.6.2	Determination of Maximum UV Absorption	39
2.2.6.3	Determination of Molecular Weight	40
2.2.6.3.1	Mass Spectrometry	40
2.2.6.3.1.1	Electron Impact (EI) Mass Spectrometry	41
2.2.6.3.1.2	Fast Atom Bombardment (FAB) Spectrometry	41
2.2.6.3.1.3	ElectroSpray Impact (ESI) Mass Spectrometry	42
2.2.6.3.2	LC/MS	42
2.2.7	Structure Elucidation of Pure Secondary Metabolites	44

2.2.7.1	NMR Measurements	44
2.2.7.1.1	One Dimensional NMR	44
2.2.7.1.2	Proton (¹ H) NMR	44
2.2.7.1.2.1	Carbon (¹³ C) NMR	45
2.2.7.1.2.2	DEPT	45
2.2.7.1.3	Two Dimensional NMR	46
2.2.7.1.3.1	COSY NMR	47
2.2.7.1.3.2	HMQC NMR	47
2.2.7.1.3.3	HMBC NMR	48
2.2.7.1.3.4	ROESY NMR	48
2.2.7.2	X-Ray Crystallography	49
2.2.8	Derivatization of Isolated Compounds	50
2.2.8.1	p-Bromobenzoate Esters (Hu, et al.,2001)	50
2.2.8.2	Marfey Analysis (Marvey, 1984)	50
2.2.9	Optical Rotation	51
2.2.10	Bioactivity	52
2.2.10.1	General Cytotoxicity Assay using <i>Artemia salina</i>	52
2.2.10.2	Anti-bacterial and Anti-fungal Assays	53
2.2.10.2.1	Anti-bacterial Assays	53
2.2.10.2.2	Anti-fungal Assays	53
2.2.10.3	Cytotoxicity Assays	54
2.2.10.4	Protein Kinase Assays	54
3	RESULTS	59
3.1	Secondary Metabolites from Sponge Associated Fungi	59
3.1.1	Secondary Metabolites from <i>Penicillium citreonigrum</i>	59
3.1.1.1	New Neoaustin-type Meroterpenes	59
3.1.1.1.1	Citreonigrin A	59
3.1.1.1.2	Citreonigrin B	65
3.1.1.2	New Austinoneol-type Meroterpenes	69
3.1.1.2.1	Citreonigrin C	69
3.1.1.2.2	Citreonigrin D	75
3.1.1.3	New Preaustinoid A-type Meroterpenes	79
3.1.1.3.1	Citreonigrin E	79

3.1.1.3.2	PC 3.3.6.8.4.F	85
3.1.1.3.3	PC 3.3.6.8.4.A	89
3.1.1.4	New Paraherquonin-type Meroterpenes	92
3.1.1.4.1	Citreonigrin G	92
3.1.1.4.2	Citreonigrin I	99
3.1.1.4.3	PC 3.3.6.6.3.A	103
3.1.1.4.4	Citreonigrin F	107
3.1.1.4.5	Citreonigrin H	113
3.1.1.5	Others New Meroterpenes	117
3.1.1.5.1	PC 3.3.6.6.3.B	117
3.1.1.5.2	PC 3.3.22.D	122
3.1.1.6	Biological Activities of New Meroterpenes	126
3.1.1.7	New Sesquiterpene Lactones	129
3.1.1.7.1	Citreodrimene A	129
3.1.1.7.2	Citreodrimene B	134
3.1.1.7.3	Citreodrimene C	137
3.1.1.7.4	Citreodrimene D	141
3.1.1.7.5	Citreodrimene E	147
3.1.1.7.6	Citreodrimene F	150
3.1.1.8	Biological Activity of New Sesquiterpene Lactones	155
3.1.1.9	New Vermistatin Derivate	158
3.1.1.10	Known Isolated Metabolites from <i>P. citreonigrum</i>	162
3.1.2	Secondary Metabolites from <i>Aspergillus niger</i>	164
3.1.2.1	2-(Hydroxy(phenyl)methyl)-4-pyrone	164
3.1.2.2	6-Benzyl-4-oxo-4H-pyran-3-carboxamide	166
3.1.2.3	New Aflavinine Derivate	170
3.1.2.4	Known Isolated Metabolites from <i>A. niger</i>	185
3.1.3	Meleagrins, a Known Secondary Metabolites from Unidentified Fungus	186
3.2	Secondary Metabolites from Plant Endophytic Fungi	188
3.2.1	Secondary Metabolites from <i>Pestalotiopsis longisetula</i>	188
3.2.1.1	PL 3.8 D	188
3.2.1.2	PL 5.12.A	192
3.2.1.3	New Herbarin Derivate	195

3.2.1.4	Known Metabolites from <i>P. longisetula</i>	198
3.2.2	Chaetomin, a Known Secondary Metabolites from <i>Chaetomium globosum</i>	199
3.3	The Biological Activity of Some Known Metabolites	200
4	DISCUSSION	202
4.1	Secondary Metabolites from Sponge-Associated Fungi	202
4.1.1	Secondary Metabolites from <i>P. citreonigrum</i>	202
4.1.1.1	The Isolated Meroterpenes	202
4.1.1.1.1	Farnesylpyrophosphate and 3,5-Dimethylorselinic Acid as Precursors in the Meroterpenes Biosynthetic Pathways	202
4.1.1.1.2	Proposed Biosynthetic Pathways of New Preaustinoid A Type Meroterpenes (Citrinigrin E, PC 3.3.6.8.4.A and PC 3.3.6.8.4.F)	209
4.1.1.1.3	Proposed Biosynthetic Pathways of New Neoaustin Type Meroterpenes (Citrinigrin A and B)	212
4.1.1.1.4	Proposed Biosynthetic Pathways of New Austinoneol A Type Meroterpenes (Citrinigrin C and D)	214
4.1.1.1.5	Proposed Biosynthetic Pathways of Paraherquonin Type Meroterpenes (Citrinigrin F, G, H, I, and PC 3.3.6.6.3.A)	219
4.1.1.1.6	Proposed Biosynthetic Pathways of PC 3.3.6.6.3.B and PC 3.3.22.D	222
4.1.1.1.7	Biological Activities of the Isolated Meroterpenes	224
4.1.1.2	Sesquiterpene Lactones	227
4.1.1.2.1	Biogenesis of the Isolated Sesquiterpene Lactones	227
4.1.1.2.2	Biological Activity – Structure Relationships of the Isolated Sesquiterpene Lactones	229
4.1.1.3	14,15-Dihydroversmitatin and Vermistatin	233
4.1.2	Secondary Metabolites from <i>A. niger</i>	235
4.1.2.1	New γ -Pyrone ((2-(hydroxy(phenyl)methyl)-4-pyrone and 6-benzyl-4-oxo-4H-pyran-3-carboxamide)	235
4.1.2.2	New Aflavinine Derivate	236
4.1.2.3	New Asperazine Derivate	237
4.2	Secondary Metabolites from Terrestrial Endophytic Fungi	238
4.2.1	Secondary Metabolites from <i>P. longisetula</i>	238
4.2.1.1	PL 3.8.D	238
4.2.1.2	PL 5.12.A	239

4.2.1.3 PL 4.2.7.5	239
5 CONCLUSION	241
6 REFERENCES	243
7 ATTACHMENTS	261

1 INTRODUCTION

1.1 Natural Products Drug Discovery and Its Current Status

Natural products are chemical compounds derived from living organisms, such as plants, animals, insects, and microorganisms. Since they are highly diverse and often provide highly specific biological activity, natural products have been the basis of human diseases treatment and a major source of new drugs. Many successful drugs in the market today were originally synthesized to mimic the action of molecules found in nature (Feher and Schmidt, 2003).

Natural product derived drugs are usually secondary metabolites and their derivatives. And today they must be pure and highly characterized compounds. Secondary metabolites are those products (chemical compounds) of metabolism that are not essential for normal growth, development or reproduction of organism. They may serve as (Demain, 2000):

- competitive weapons used against other bacteria, fungi, amoebae, plants, insects, and large animals
- metal transporting agents
- agents of symbiosis between microbes and plants, nematodes, insects, and higher animals
- sexual hormones
- differentiation effectors

1.1.3 Traditional Medicines and Natural Products in the Past

The use of natural products, mainly as plant preparations, as medicinal agents has begun since the ancient time. The usefulness of plants to treating diseases was recorded in the Emperor Shennung's classic herbals (the earliest recorded Chinese herbal medicine, 2700 BC) and Eber's papyrus in Egypt (1550 BC). Ayurveda, the term used for the traditional medicinal system in India, is being used for more than three thousand years, and the earliest Vedic texts, dating from 1500 – 1200 BC were especially concerned with aging, various afflictions and the prescription of cures involving prayers and herbal medicines.

Later, the Greek physician Galen (AD 129 – 200) devised the first pharmacopoeia describing the appearance, properties and use of many plants of his time (Patwardhan et al., 2004).

Today, most knowledge of traditional medicines and therapies has been lost in the daily life, since it was only sporadically recorded in epics and folklore. This fact is not only found in mostly developed countries, but also some developing countries where the indigenous population has been marginalized. Although some traditional medicines and therapies have still survived and are being applied, their percentage is very small compared to modern medications (Patwardhan et al., 2004).

Nevertheless, the wisdoms of ancient medicines have often been the basis of modern drug discovery. Thus, some ideas of the currently accepted modern medicine is based on the traditional medicines and therapies. In addition, due to the high cost of modern medications research and production, most developing countries, especially subtropical and tropical countries with a higher biodiversity of plants, still rely on traditional medicine. Today the largest users of traditional medicines are the Chinese, with over 5000 plants and plant products in their Pharmacopoeia (Strobel et al., 2000).

1.1.4 Natural Products Today

Natural products are the most successful source of drug leads and continue to provide greater structural diversity than standard combinatorial chemistry, and so they offer major opportunities for finding novel molecules. In the modern area of drug discovery, they will continue to be important as targets for production by biotechnological approaches, a source of lead compounds of novel chemical structures, and as the active ingredients of useful treatments derived from traditional systems of medicine (Harvey, 1993).

The discovery of pure natural compounds as active principles was first described at the beginning of the 19th century. Morphine, produced and commercialised by E. Merck for the first time in 1826, was one among the first isolated active compounds (Newman et al., 2000). Today, a vast range of drugs, which represent the cornerstones of modern pharmaceutical care, are either natural products themselves or have been derived from

them. Currently, there are more than 183.000 known natural products, and new structure are being published at a rate about 10.000 per annum (Dictionary of Natural Products, 2004).

Some analytical and separation techniques have been developed in order to reduce the time required for isolation and characterization of natural compounds. High performance liquid chromatography (HPLC) has been the most reliable tool for the separation of complex mixtures of small molecules. More recently, the advent of electrospray (ESI) and atmospheric pressure chemical ionization (APCI) have provided mass spectrometry (MS) interfaces which are applicable to the analysis of a wide range of molecules and are compatible with liquid chromatography (LC) (Elsewijk and Irth, 2003). The high field NMR (originally 200 MHz and then up through 600 – 800 MHz) allows the complete structure elucidation in amount of compounds less than 1 mg.

The rapid identification of already known natural products is an important strategy to screen novel bioactive compounds from natural resources. LC-MS, LC-UV or combination of the two have become a widely used tool for the dereplication of natural products. Data from UV and MS alone will rarely provide sufficient information to distinguish between the known isomers. Even when this is achieved, possible novel isomers have also to be considered. Recently, the use of LC-NMR at this stage has been advocated (Bradshaw et al., 2001).

It is estimated that about one third of currently marketed drugs are related to natural products (Elsewijk and Irth, 2003). The percentage of natural product and natural product derived drugs in the top 35 worldwide ethical drug sales for 2000, 2001 and 2002 are shown in figure 1.1. Their relative percentage of all marketed drugs was 40 % in 2000 and remained approximately constant at 24 % in 2001 and 26 % in 2002 (Butler, 2004).

Most natural product and natural product derived compounds introduced between 1981 – 2002 were compounds with antibacterial and cytotoxic potential, while only one was used as an antiviral agent (see figure 1.2). It thus can be concluded that natural products still serve a major role as anticancer and antibacterial agents.

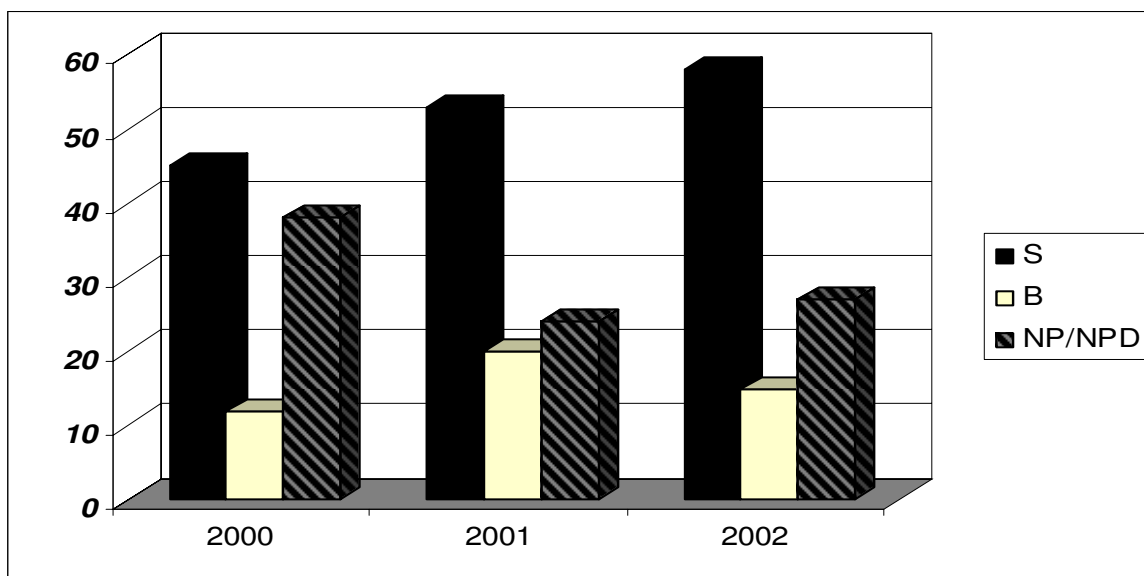


Figure 1.1 Percentage of synthetic (S), biologic (B) and natural product (NP)/natural product-derived (NPD) drugs in the top 35 worldwide ethical drug sales for 2000, 2001, and 2002 (Butler, 2004).

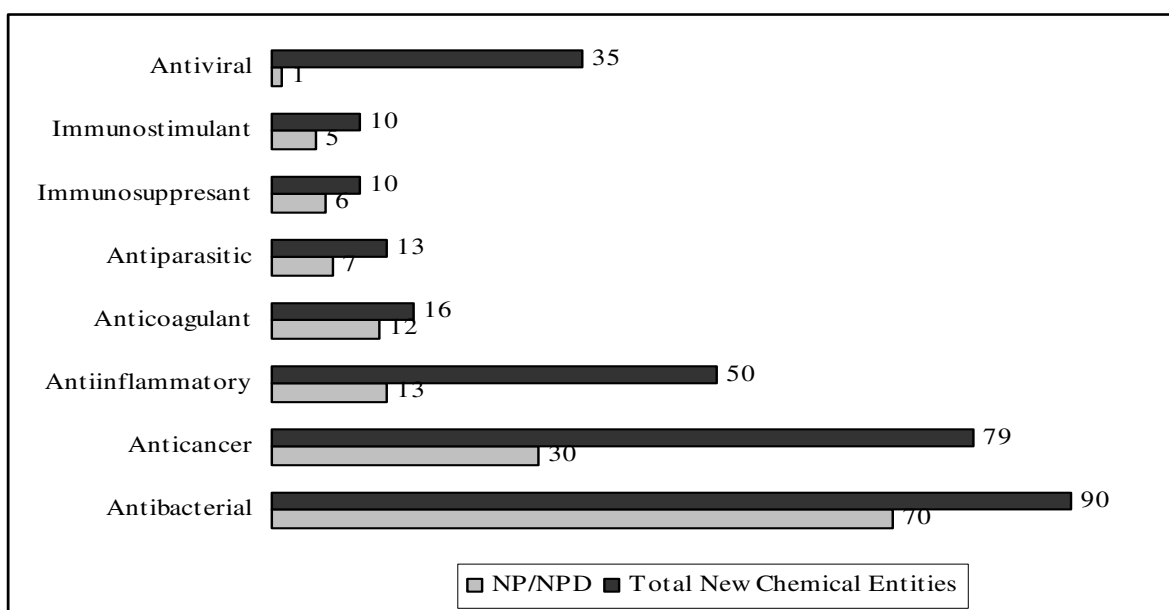


Figure 1.1 Comparison of new natural product (NP) and natural product derived (NPD) compounds to total new chemical entities per selected medical indication in the frame time 1981 – 2002 (Newman et al., 2003).

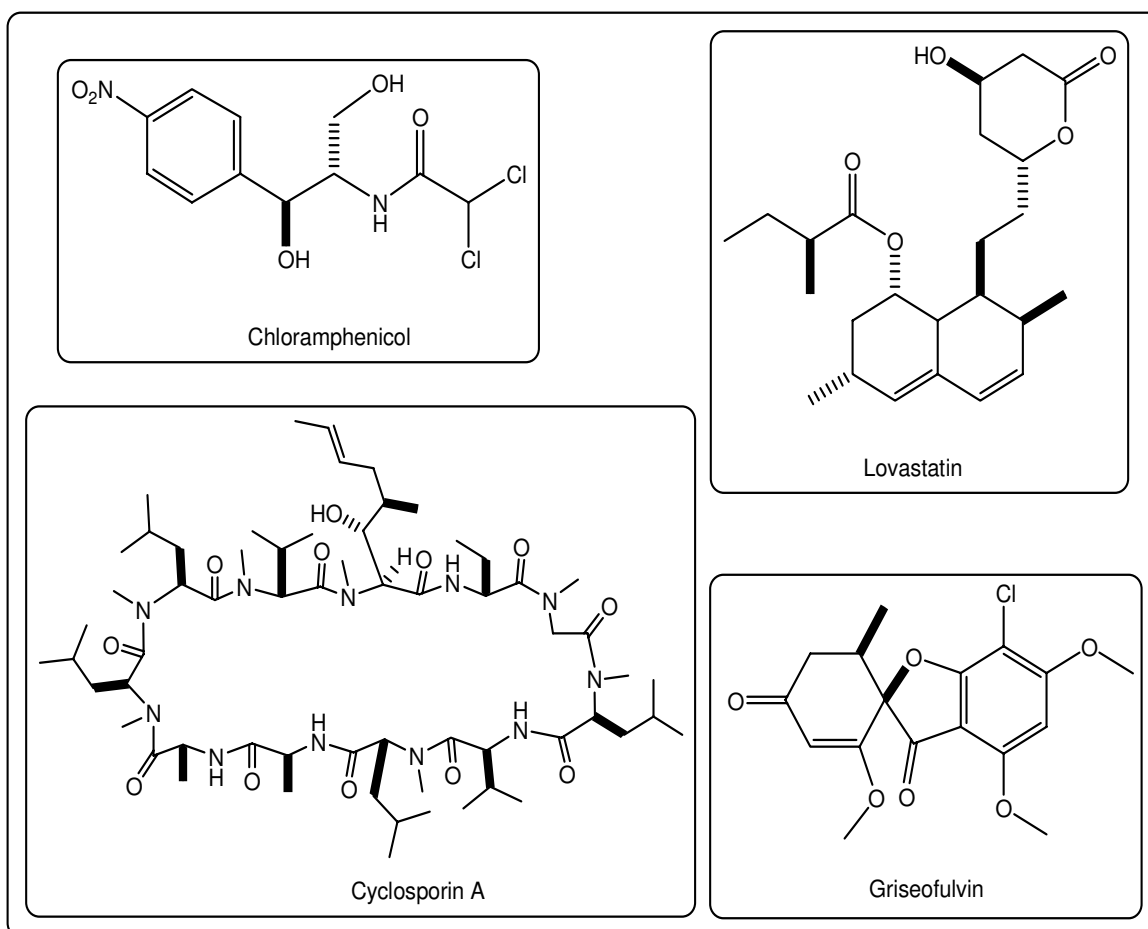
In the frame time 1998 – 2004 at least 21 natural product and natural product derived drugs have been launched onto the market in USA, Europe, and Japan. The 21 drugs can be classified as 3 natural products, 10 semi synthetic natural products, and 8 natural product-derived drugs. Although the number was low, there are still many natural product-derived

compounds in Phase III or registration that may be launched in 2005 and 2006 (Butler, 2005)

1.2 Fungi as Natural Products Sources

Fungi are heterotrophic eukaryotes that lack chlorophyll. Thus they must absorb all required nutrients from external sources, but since they are independent of light, they can also inhabit damp and dark places. As true eukaryotes, they have membrane bound organelles such as nuclei, mitochondria, endoplasmic reticulum, etc. Fungi are characterized by a distinctive, filamentous, multinucleate vegetative structure known as the mycelium. It is composed of hyphae, a branching system of tubular structures which contain protoplasm and continually extend by apical growth and lateral branching (Ainsworth and Sussman, 1965).

Fungi are remarkable organisms that produce a wide range of secondary metabolites. In many cases, the benefit these compounds confer on the organism is unknown. However, interest in these compounds is considerable, as many natural products are of medical, industrial, or agricultural importance (Calvo et al., 2002). The exploration of fungal bioactive secondary metabolites was initiated by the discovery of penicillin in 1928 by Alexander Fleming, further re-isolation and clinical studies by Chain, Florey and co-workers in early 1940s, and its subsequent commercialization in a synthetic form (Butler, 2004). About twenty years after the discovery of penicillin, several other antimicrobial agents such as chloramphenicol (Long and Troutman, 1949) and griseofulvin (Grove et al., 1952) had been discovered from fungi. Furthermore, cyclosporine A (Traber et al., 1982 and Traber et al., 1987), and lovastatin (Endo, 1979) are fungal metabolites used as immunosuppressants during organ transplantation and antihyperlipidaemic agents, respectively.



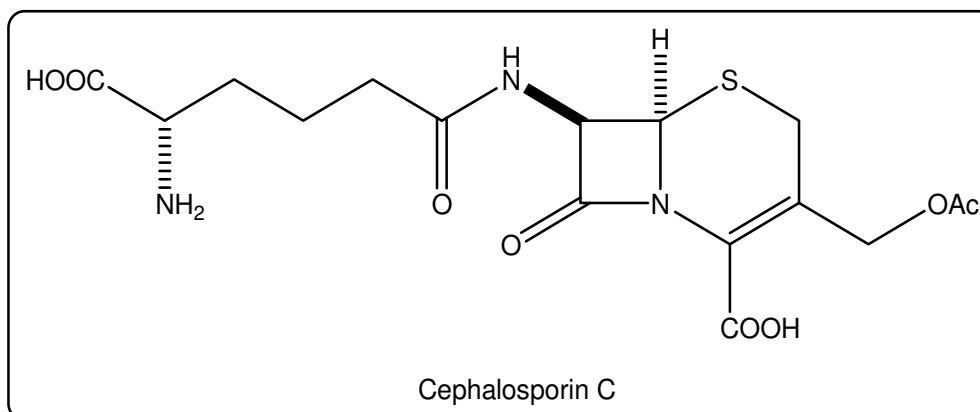
Some secondary metabolites can stimulate spore formation and inhibit or stimulate germination. Since formation of secondary metabolites and spores are regulated by similar factors, this phenomenon can ensure secondary metabolites production during sporulation. Thus, the secondary metabolites can slow down germination until a less competitive environment and more favourable conditions for growth exist, protect the dormant or initiated spore from consumption by amoebae or cleanse the immediate environment of competing microorganisms during germination (Demain, 2000).

1.2.1 Sponge-Associated Fungi

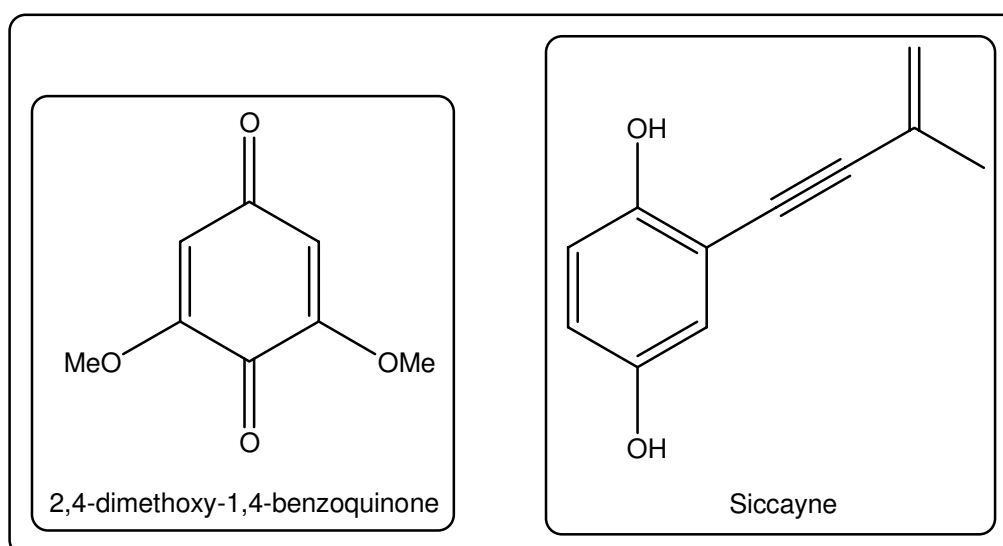
The marine environment became a focus of natural products drug discovery because of its relatively untapped biodiversity compared to terrestrial habitats. Marine plants, animals, and microbes produce secondary metabolites that have a promising potential as new drugs

for the treatment of cancer, infectious diseases, and inflammation (Faulkner, 1998). Furthermore, it possesses a unique feature of chemical structures which could not be found in terrestrial metabolites (Larsen et al., 2005). However, the major problem is that most promising pharmacologically active marine natural products can only be isolated in an extremely low yield. In addition, the limited amounts of biomass of most marine organisms, especially invertebrates, in nature usually causes the supply problems of the promising compounds for drug development and sustainable production (Proksch et al., 2003). Thus, most of natural products or its derivatives that are being used as medicines in the market were isolated from terrestrial organisms which can either be fermented (in the case of microorganisms) or be produced by agriculture (in the case of medicinal plants).

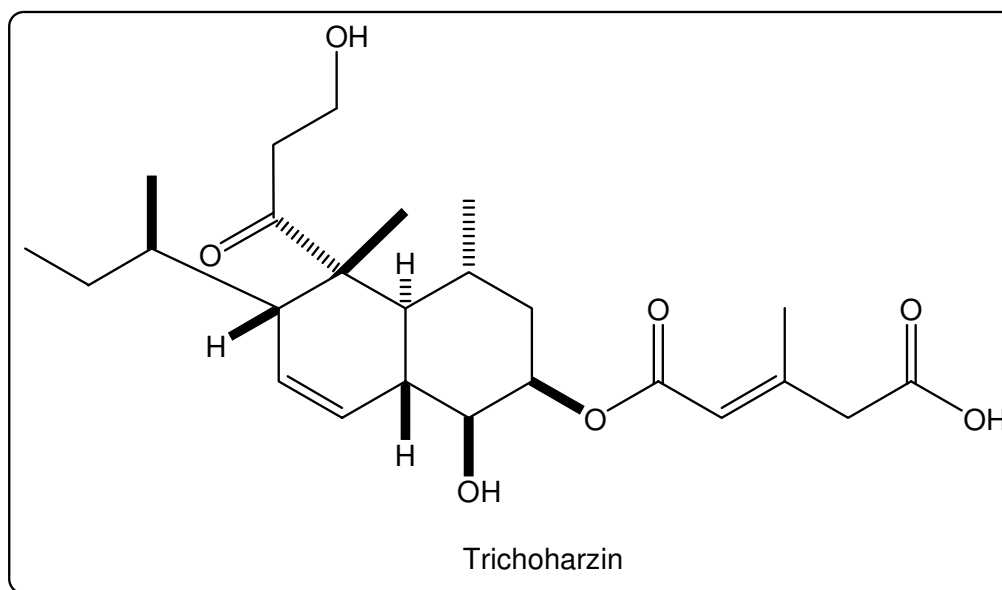
The exploration of microorganisms living inside invertebrates is one of the most exciting strategies to solve the pressing supply issue inherent to marine drug discovery. Marine microorganisms including fungi, have shown to be potential sources of pharmacologically active metabolites because of their capability to adapt and survive in the marine environment, and to produce unique secondary metabolites (Bugni and Ireland, 2004). The first chemical investigation of marine-derived fungi was carried out by Giuseppe Brotzu in 1945. He found that a fungus (later identified as *Cephalosporium acremonium*) isolated from seawater near a sewage outlet off the Sardinian coast exhibited pronounced antibacterial activities (Demain and Elander, 1999). Ten years later Newton and Abraham discovered that the β -lactame cephalosporin C was responsible for the antibacterial activity of this fungus (Newton and Abraham, 1955). Cephalosporin C shows structural similarity to the penicillins (which were already marketed at that time), but differs from the latter by the cephalosporane (instead of the penicillane) backbone. Nowadays, semisynthetic cephalosporine derivatives have by far outnumbered medicinally applied penicillines, especially in the clinical use.



After the discovery of cephalosporin C, the detailed studies of secondary metabolites from marine-derived fungi were still scarce until 1975, when the second secondary metabolite of marine-derived fungi, 2,6-dimethoxy-1,4-benzoquinone, was successfully identified in a culture of *Dendryphiella salina* (Fukuzumi, et al., 1975). Six years later, siccayne was isolated from *Halocyphina vilosa* and identified as the second antibiotic from marine-derived fungi (Kupta et al., 1981). Starting from 1980's, marine derived fungi have been systematically studied with regard to their potential to produce novel bioactive secondary metabolites, yielding up to now more than 300 structure in more than 200 publications (Bugni and Ireland, 2004 ; Ebel, 2006)

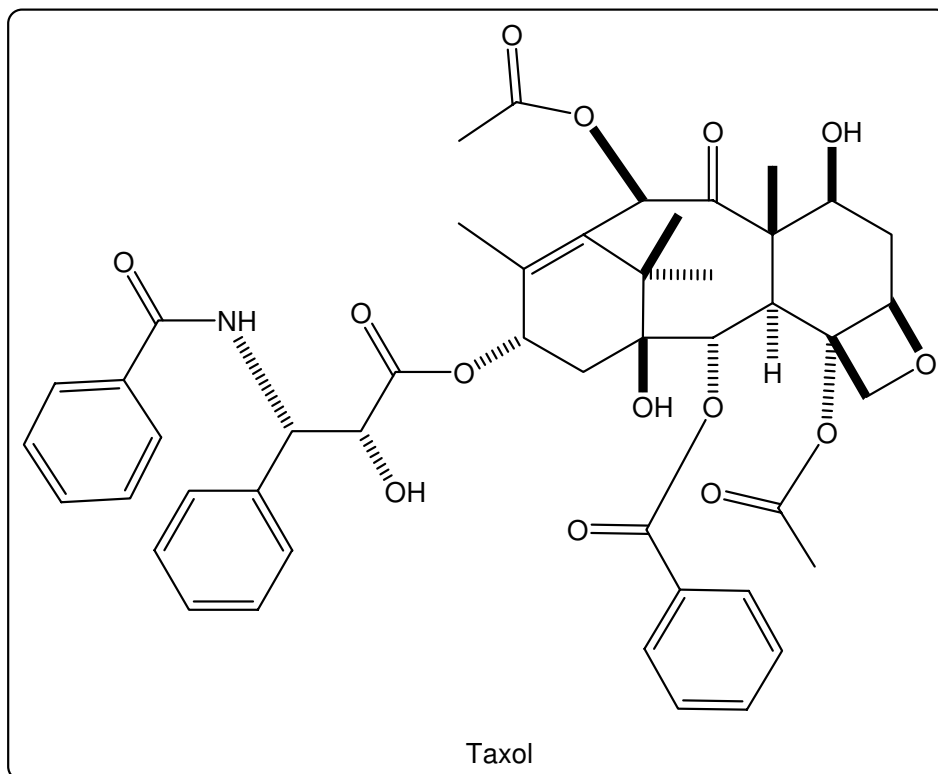


In particular, sponge-associated fungi have yielded novel metabolites with potent antibacterial and anticancer activities (Jensen, 2000) which have not been previously reported from terrestrial strains of the same species (Hiort et al., 2004). Trichoharzin, a compound isolated from *Trichoderma harzianum* associated with the sponge *Mycale cecilia*, was the first novel metabolite from sponge-associated fungi (Kobayashi et al., 1993), while gymnastatins A, B and C were the first novel cytotoxic metabolites from sponge-associated fungi (Amagata et al., 1998)



1.2.2 Terrestrial Endophytic Fungi

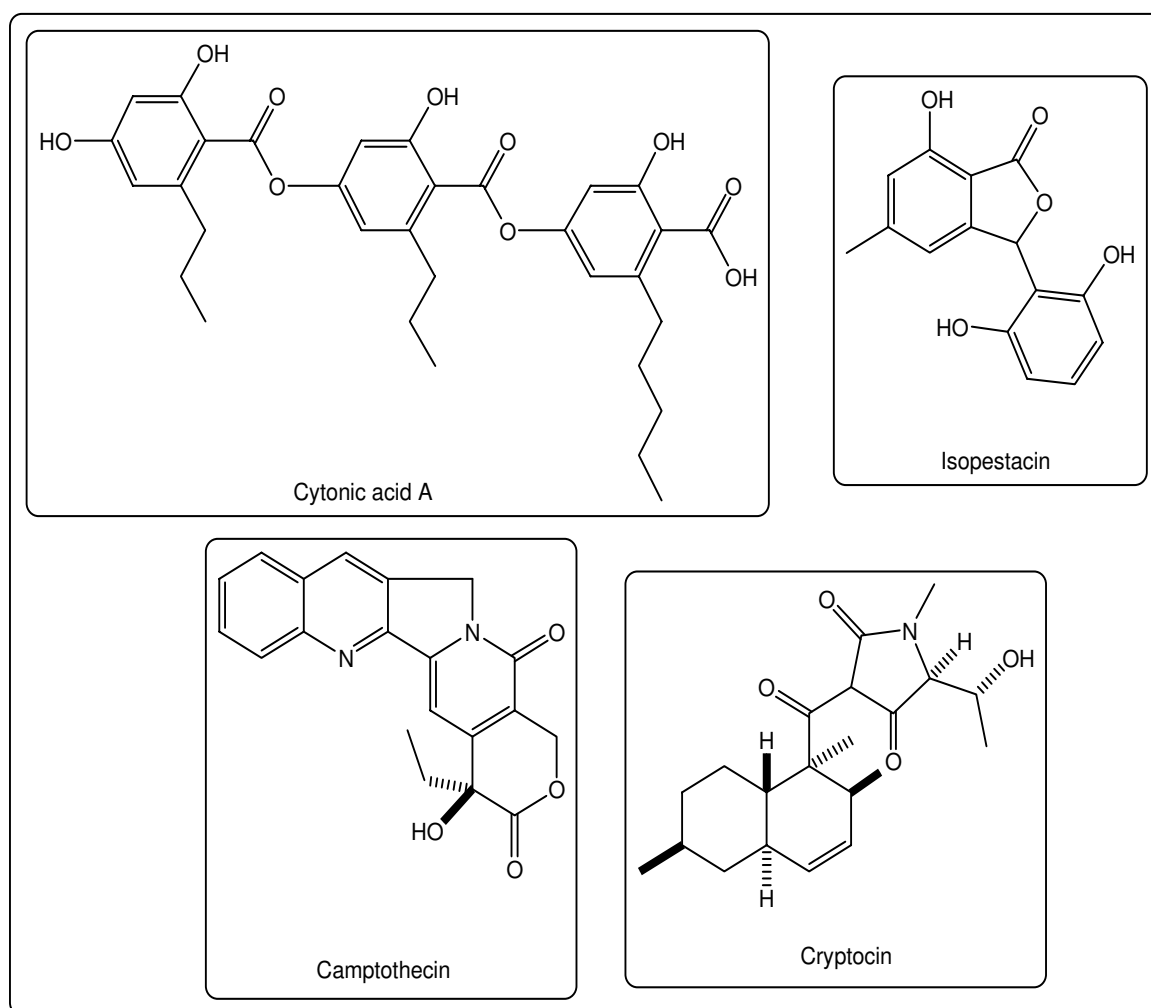
“An endophyte is a bacterial (including actinomycete) or fungal microorganism, which spends the whole or part of its life cycle colonizing inter- and/or intra-cellularly inside the healthy tissues of the host plant” (Tan and Zou, 2001). Since the relationship between the endophyte and its host plant may range from symbiotic to bordering on pathogenic, some secondary metabolites involved in the host-endophyte relationships may also be produced by the endophytes during the colonization. As a direct result of the role of these secondary metabolites in the nature, they may show to have applicability in medicine, agriculture and industry (Strobel, 2002).



Almost all vascular plant species examined to date were found to harbour endophytes. Commonly, several to hundreds of endophyte species can be isolated from a single plant, among them, at least one species showing host specificity. Since the environmental conditions under which the host is growing also affect the endophyte population, the endophyte profile may be more diverse in plants obtained from tropical as compared to temperate regions (Tan and Zou, 2001).

The intensive chemical study of endophytic fungi was begun after the invention of taxol (paclitaxel), a billion dollar anticancer drug which was isolated for the first time from *Taxus brevifolia* (Wani et al., 1971). More than 20 years later, Strobel isolated a novel taxol producing endophytic fungus, *Taxomyces andreanae*, from *Taxus brevifolia* (Strobel et al., 1993). In the following years, further endophytic fungi such as *Pestalotiopsis microspora* (Strobel et al., 1996), *Seimatoantlerium tepuiense* (Strobel et al., 1999), *Periconia* sp (Li et al., 1998), have also been reported to be producers of taxol or its derivatives.

While the initial chemical studies were mainly concerned with taxol, it was soon discovered that endophytic fungi are producers of interesting secondary metabolites by themselves, which are normally not structurally related to natural products produced by their host plants. Interesting examples include cryptocin (Li et al., 2000), isopestacin (Strobel et al., 2002), and cytonic acid A (Guo et al., 2000) were reported to be active as antifungal, antioxidant, and antiviral, respectively. However, very recently a report appeared in the literature that another cytotoxic plant alkaloid, camptothecin (which was originally described from *Camptotheca acuminata* (Wall et al., 1966) and is commercially exploited as an anticancer agent) is also produced by an endophytic fungus. Thus, it can be concluded that endophytic fungi besides marine derived fungi represent an interesting source of new lead structures for pharmaceutical and agrochemical applications.



1.3 Aims and Scopes of the Study

The aim of the study was isolation of secondary active metabolites from tropical sponge-associated and endophytic fungi and the preliminary identification of their pharmaceutical potential. Three sponge associated fungi, *Aspergillus niger*, *Penicillium citreonigrum* and one unidentified fungus, and two terrestrial endophytic fungi, *Pestalotiopsis longisetula* and *Chaetomium globosum*, were subjected as biological sources of the study.

In order to isolate the secondary metabolites, the fungi were grown in a static Wickerham medium at room temperature. For sponge associated fungi, artificial salt water was added into the media until a final concentration 24.4 g/L. After three weeks of inoculation, the fungi were then harvested and subsequently extracted with some organic solvents. Ethyl acetate fraction of raw extracts was then separated using some chromatography techniques and their fractions were analysed using HPLC and/or GC for their purity and LC-MS for their molecular weight. The pure compounds were submitted to the different techniques of NMR for structure elucidation.

The pure compounds were subjected to some bioassays for their pharmaceutical potential. Antimicrobial assays were performed using *Eschericia coli* and *Bacillus subtilis*. Meanwhile, the isolated compounds were applied to *Clasdosporium herbarum* and *Cladosporium cucumerinum* in antifungal assay. The cytotoxicity assays were performed using some cancer and animal cell lines. Some pure compounds have been also been subjected to protein-kinases assays.

At the end of the study, some fermentation experiments were done to identify the effects of culture condition on the metabolite productions. *P. citreonigrum* was grown in different type of medium, salt concentration, pH, time of fermentation and the presence of elicitors to observe its metabolites profile.

2 MATERIAL AND METHODS

2.1 Materials

2.1.1 Fungal Origin

Table 2.1 shows the origin of the fungi used as raw materials in this study. Three of them are sponge associated fungi, *Aspergillus niger*, *Penicillium citreonigrum* and the unidentified fungal. Meanwhile, *Pestalotiopsis longisetula* and *Chaetomium globosum* are terrestrial endophytic fungi.

Table 2.1. The origin of the fungi

No.	Code	Fungal species	Host	Location	Note
1.	E99-3/341	<i>Aspergillus niger</i> van Tieghem	<i>Axinella damicornis</i>	Elba Island, 1999	-
2.	PAI 1/1 C	<i>Penicillium citreonigrum</i>	<i>Pseudocertina purpurea</i>	Bali Barat National Park, Indonesia, 1996	-
3.	AGBE	<i>Pestalotiopsis longisetula</i>	<i>Aglaia odorata</i>	Green House, University of Düsseldorf, 2002	Collected by Dr..F. Teuscher
4.	AGB2M GR	<i>Chaetomium globosum</i>	<i>Aglaia odorata</i>	Green House, University of Düsseldorf, 2002	Collected by Dr. F. Teuscher
5.	B 24	Unidentified fungus	Undidentified sponge	Kep. Seribu (SeribuIslands), Indonesia, 2002	Collected by Dr. A. Supriyono and Subintoro

2.1.2 Media

2.1.2.1 Medium for Isolation of Plant Endophytic Fungi

- Agar-agar 15.0 g
- Dried Plant Materials (leafs) 15.0 g
- Chloramphenicol 0.2 g
- Distilled water To make 1000 mL
- pH 7.4 – 7.8

(adjusted with NaOH)

2.1.2.2 GPYNS Medium for Isolation of Sponge Associated Fungi

- Agar-agar 16.0 g
- Artificial Sea Salt 24.4 g
- Yeast extract 1.0 g
- Glucose 1.0 g
- Ammonium nitrat 1.0 g
- Pepton 0.5 g
- Distilled water To make 1000 mL
- pH 7.4 – 7.8 (adjusted with NaOH)

To prevent bacterial contamination, Chloramphenicol (0.2 g) was added in to the medium before autoclaving. Alternatively, Streptomycin Sulfat (0.1 g) and Penicillin G (0.1 g), can also be added after autoclaving.

2.1.2.3 Wickerham Medium for Liquid Culture

- Yeast extract 3.0 g
- Malt extract 3.0 g
- Peptone 5.0 g

- Glucose monohydrate 20.0 g
- Distilled water To make 1000 mL
- pH 7.2 – 7.4 (adjusted with NaOH)

For sponge associated fungi, artificial sea salt was added to a final concentration 24.4. g/L.

2.1.2.4 Malt Agar (MA) Medium

MA medium was used for short term storage of fungal culture or fresh seeding for preparation of the liquid culture.

- Agar-agar 15.0 g
- Malt extract 15.0 g
- Distilled water To make 1000 mL
- pH 7.4 – 7.8 (adjusted with NaOH)

For sponge associated fungi, artificial sea salt was added to a final concentration 24.4. g/L.

2.1.2.5 Rice Media

- Rice 90 g
- Deionized water 100 mL

Water was added into the rice and it was kept overnight before sterilization.

2.1.2.6 Modified Abe Medium

Modified Abe medium was according to Vinokura (Vinokura, et al.,2004), however, with addition of yeast extract.

- Mannitol 50 g
- Yeast extract 5.0 g

- Succinic acid 5.4 g
- MgSO₄. 7H₂O 0.3 g
- KH₂PO₄ 1.0 g
- Distilled water To make 1000 mL
- pH 7.4 – 7.8 (adjusted with NaOH)

A sterile solution of trace elements containing FeSO₄. 7H₂O, ZnSO₄. 7 H₂O , MnSO₄. 5H₂O, CuSO₄. 5H₂O, was added into the medium with a final concentration 5.0, 4.4, 1.7, and 3.3 mg/L, respectively.

2.1.2.7 Modified Potatoes Dextrose Agar (PDA) Medium

Modified PDA medium was according to Ge, et.al. (Ge, J., et al.,2004), however, with addition of yeast extract and lack of agar..

- Infusion from Potatoes (see below) 1 L
- Yeast extract 5.0 g
- Dextrose 20 g

Potatoes infusion :

Potatoes (200 g) was first washed and cut into small pieces, boiled in a 1000 mL distilled water for 1 hour, and filtered to get the infusion potato

2.1.2.8 White Bean (*Phaseolus vulgaris L*) Medium

White bean (100 g) was boiled for 1 hour and then washed many times with tap water until the skin completely removed. A 100 mL distilled water was added just before sterilization.

2.1.2.9 Modified Czypek Yeast Agar (CYA) Medium

CYA medium according to Malmstrom (Malmstrom et al.,2000), however, without agar.

- Sucrose 30 g

- Yeast extract 5.0 g
- NaNO₃ 3 g
- K₂HPO₄ 1 g
- MgSO₄. 7H₂O 0.5 g
- KCl 0.5 g
- FeSO₄. 7H₂O 0.01 g
- Distilled water To make 1000 mL

2.1.2.10 Luria Bertoni (LB) Medium

The medium was used to conduct antibacterial assays.

- Peptone 10.0 g
- Yeast extract 5.0 g
- NaCl 10.0 g
- Distilled water To make 1000 mL
- pH 7.0 (adjusted with NaOH)

To prepare the agar plates, 15 g agar was added into 1L broth media.

2.1.2.11 Yeast Medium

The medium was used to perform bioassays using *Saccharomyces cerevisiae*.

- Yeast extract 3.0 g
- Malt extract 3.0 g
- Peptone 5.0 g
- Glucose 10.0 g
- Distilled water To make 1000 mL

To prepare the agar plates, 15 g agar was added into 1L broth media.

2.1.2.12 Fungal Medium for Bioassays

- Mannitose 50.0 g
- Saccharose 50.0 g
- Succinic acid 5.4 g
- Yeast extract 3.0 g
- KH_2PO_4 0.1 g
- MgSO_4 0.3 g
- FeSO_4 10.0 mg
- ZnSO_4 10.0 mg
- Distilled water To make 1000 mL
- pH 5.4 (adjusted with NaOH)

2.1.2.13 Potatoes Dextrose Agar (PDA) Medium for Bioassays

- Infusion from Potatoes (see below) 1 L
- Dextrose 20.0 g
- Agar 15.0 g

Potatoes infusion :

Potatoes (200 g) was first washed and cut into small pieces. It was then boiled in a 1000 mL distilled water for 1 hour and filtered to get the infusion potatoes.

2.1.3 Chemicals

2.1.3.1 Technical Grades Solvent for Separation

- Methanol
- Dichloromethane
- Ethylacetate

- n-Hexane
- Cyclohexane
- n-Butanol

2.1.3.2 Solvents for HPLC and LC/MS

- Acetonitril LiChroSolv HPLC grade, Merck
- Methanol LiChroSolv HPLC grade, Merck
- Nanopure water

2.1.3.3 Solvents for NMR

- DMSO-d₆ euriso-top
- CD₃OD euriso-top
- CDCl₃ euriso-top

2.1.3.4 Chemicals for Media

- Agar- agar Galke
- Glucose Caelo
- Yeast extract Sigma
- Malt extract Merck
- Sea salt Biomarine
- NaCl Merck
- Pepton BD
- Trypton Sigma

2.2 Methods

2.2.1 Collection and Isolation of Fungi

2.2.1.1 Isolation of Terrestrial Endophytic Fungi

A piece of plant was washed with sterilized demineralised water and then rinsed in a 70 % ethanol for 1-2 minutes. The plant piece was then taken out from the ethanol solution and dried under a laminar flow hood. With a sterile knife blade, the plant was cut and the outer tissues were removed. The inside tissue was immediately placed onto the MA media containing plant material and antibiotic (see section 2.1.2.1). After several days of inoculation, the hyphal tips of growing fungi were then subsequently transferred onto new MA medium (see section 2.1.2.4) to obtain the pure culture of fungi.

2.2.1.2 Isolation of Sponge Associated Fungi

A piece of sponge was washed with sterilized artificial sea water and then rinsed in a 70 % ethanol for 1-2 minutes. The piece of sponge was then taken out from the ethanol solution and cut to obtain the inside tissue of sponge. The inside tissue was immediately transferred onto the MA media containing artificial sea salt and antibiotics (see section 2.1.2.2). (These steps of work were performed on the sampling area because the sponge tissue should be in fresh condition). After some days, a single fungal colony was then subsequently transferred onto MA medium containing artificial sea salt (see section 2.1.2.4) to obtain the pure culture of fungi.

2.2.2 Fungal Identification and Taxonomy

2.2.2.1 Morphological Characteristic Identification

The identification of fungal culture using morphological characteristics was performed at Centraalbureau voor Schimmelcultures (CBS), Utrecht, Netherlands.

2.2.2.2 Fungal Identification using Molecular Biology Approach

Fungal identification using molecular biology approach was done by others PhD students (Apotheker Arnulf Diesel and Ine Dewi Indriani) at the Institute of Pharmaceutical Biology and Biotechnology, University of Düsseldorf.

Briefly, the identification of fungi through this technique is outlined below :

- Fungal DNA Isolation

Fungal DNA isolation and purification was performed using DNeasy Plant Mini Kit from Qiagen Company.

Dried (lyophilized) mycelial was pulverised and disrupted with a help of glass beads. The cell lysis was carried out by addition of lysis Buffer AP-1 and RNase-A solution and then followed by incubation of the mixture in 65°C. The remaining detergent, protein and polysaccharide was precipitated by addition of Buffer AP-2 to the lysate. The lysate was then applied to the Qias shredder™ Mini Spin Column and centrifugated to remove the cell debris and other remaining precipitates. The lysate was then transferred to a new tube.

An adequate volume of ethanolic Buffer AP3/E was added to the lysate and the mixture was then applied to DNeasy Mini Spin Column. After centrifugation, the filtrate was discarded. The column was washed by addition of ethanolic Buffer AW and followed by centrifugation. Another Buffer AW was added to the column for the second time and then centrifuged at maximum speed to dry the membrane in the column from residual ethanol.

Fungal DNA, which is incorporated to the membrane, was eluted by addition of Buffer AE directly to the membrane in the DNeasy column. The column was then incubated at room temperature for 5 minutes and then centrifuged to collect the filtrate. The filtrate is fungal DNA dissolved in Buffer AE.

- DNA Amplification

The isolated DNA was then amplified by the method called Polymerase Chain Reaction (PCR). The PCR was carried out using and HotstarTaq Master Mix Kit from Qiagen Company. The Master Mix contains HotStarTaq[®]DNA Polymerase, PCR buffer (with MgCl₂) and dNTPs.

ITS1 (with base sequences TCCGTAGGTGAACCTGCGG) and ITS4 (with base sequences TCCTCCGCTTATTGATATGC), as primers, were mixed with HotstarTaq Master Mix Kit and DNA template. The mixture was then applied to the thermal cycler using the programmed PCR cycle as outlined below :

- Initial activation step in 95°C for 15 minutes to activate HotStarTaq[®]DNA Polymerase
- Cycling steps which were repeated 35 times :
 - Denaturing : 1 minute at 95°C
 - Annealing : 1 minute at 56°C
 - Extension : 1 minute at 72°C
- Final extension for 10 minutes in 72°C

- Purification of PCR Products and DNA Sequencing

The PCR product was purified using 2% Agarose-Gel-Electrophoresis at 75 V for 60 minute in TBE buffer. The agarose gel was then stained using 1 % ethidium bromide. A 500 bp stained DNA fragment was then excised from the agarose gel.

The next step of PCR products purification was performed using Perfectprep[®]Gel Cleanup Kit from Eppendorf company. The binding buffer was mixed to the PCR products and incubated at 50°C for 10 minutes in an eppendorf thermomixer at 1000 rpm. The mixture was mixed with a volume of isopropanol and then centrifuged. The filtrate was discarded and the column was washed with wash buffer twice followed by centrifugation.

Amplified fungal DNA (the PCR product), which is incorporated to the column, was eluted by addition of elution buffer or molecular biology grade water to the centre of the column. The column was then centrifuged to collect the filtrate. The filtrate is fungal DNA dissolved in elution buffer.

The amplified fungal DNA was then submitted for sequencing and the base sequences was compared to the data in Genebank with a help of Blast-Algorithmus. By this method, a fungus is identified by its DNA sequence.

2.2.2.3 Taxonomy

The taxonomy classification of fungal strain, based on morphological characteristics (de Hoog et. al., 2000), used in this study are shown in Table 2.2.

Table 2.2. Taxonomy classification of fungal strains

	Strain 1	Strain 2	Strain 3	Strain 4*
Kingdom	Fungi	Fungi	Fungi	Fungi
Phylum	Ascomycota	Ascomycota	Ascomycota	Ascomycota
Class	Eucomycetes	Eucomycetes	Eucomycetes	Anamorps member of Ascomycetes
Order	Eurotiales	Eurotiales	Sordariales	
Family	Trichocomaceae	Trichocomaceae	Chaetomiaceae	Amphisphaeriaceae
Genus	<i>Aspergillus</i>	<i>Penicillium</i>	<i>Chaetomium</i>	<i>Pestalotiopsis</i>
Species	<i>A. niger</i>	<i>P. citreonigrum</i>	<i>C. globosum</i>	<i>P. longisetula</i>

*) www.botany.utoronto.ca/ResearchLabs/Mallochlab/Malloch/Moulds/Pestalotiopsis

2.2.3 Fungal Cultivation

2.2.3.1 Fungal Culture for short Term Storage

The fungi were grown onto MA media under room temperature for several days. Since the fungal hyphae almost covered the whole surface of MA medium, the cultures were then kept in 4°C for maximum 6 months before re-inoculation onto new MA media.

2.2.3.2 Fungal Culture for isolation of Secondary Metabolites

The fresh fungal culture on MA media, normally in the log phase of growth, was transferred into a 1 L Erlenmeyer flask containing 300 mL of Wickerham media. The culture was then incubated in a room temperature for three weeks. A large scale of cultivation (roundabout 10 L culture medium) was carried out using 30 Erlenmeyer flasks.

2.2.4 Fungal Extraction

The extraction scheme of the fungal cultures is described in Figure 2.1. This method was used to collect fungal extracts containing both extracellular (excreted into the medium) and intracellular metabolites. A 250 ml Ethylacetate was added into each fungal culture in an erlenmeyer flask and the mixture was kept overnight to ensure that the fungal cell died. The mixture was then applied to Ultraturrax for 10 minutes (for cell destruction) and followed by filtration using Büchner vacuum. The extracted mycelium (cell debris) was thrown away and the filtrate containing ethyl acetate phase and medium (water phase) was collected for further processes.

The ethylacetate phase was then separated from water phase (medium) using separation funnel. To remove the remaining salts and other polar constituents, the ethyl acetate phase was washed with water two times. Just after evaporation, the ethyl acetate extracts was diluted in 90 % Methanol and extracted with n-hexane to remove fatty acids and other non-polar constituents. At the same time, the water phase (medium) was extracted with water-saturated n-Butanol to collect the polar constituents.

Another method, as described in Figure 2.2, was also used in this study. This method was used to get the information of individual extracellular and intracellular metabolites profiles. Just before addition of organic solvents, the mycelium and medium were separated in a clean bench. Methanol and ethyl acetate were added into the mycelium and medium, respectively. They were then kept overnight. The mycelium was then disrupted with Ultraturrax and subsequently extracted with ethyl acetate and n-hexane. In parallel, the medium was also directly washed with water and followed by extraction with n-Hexane.

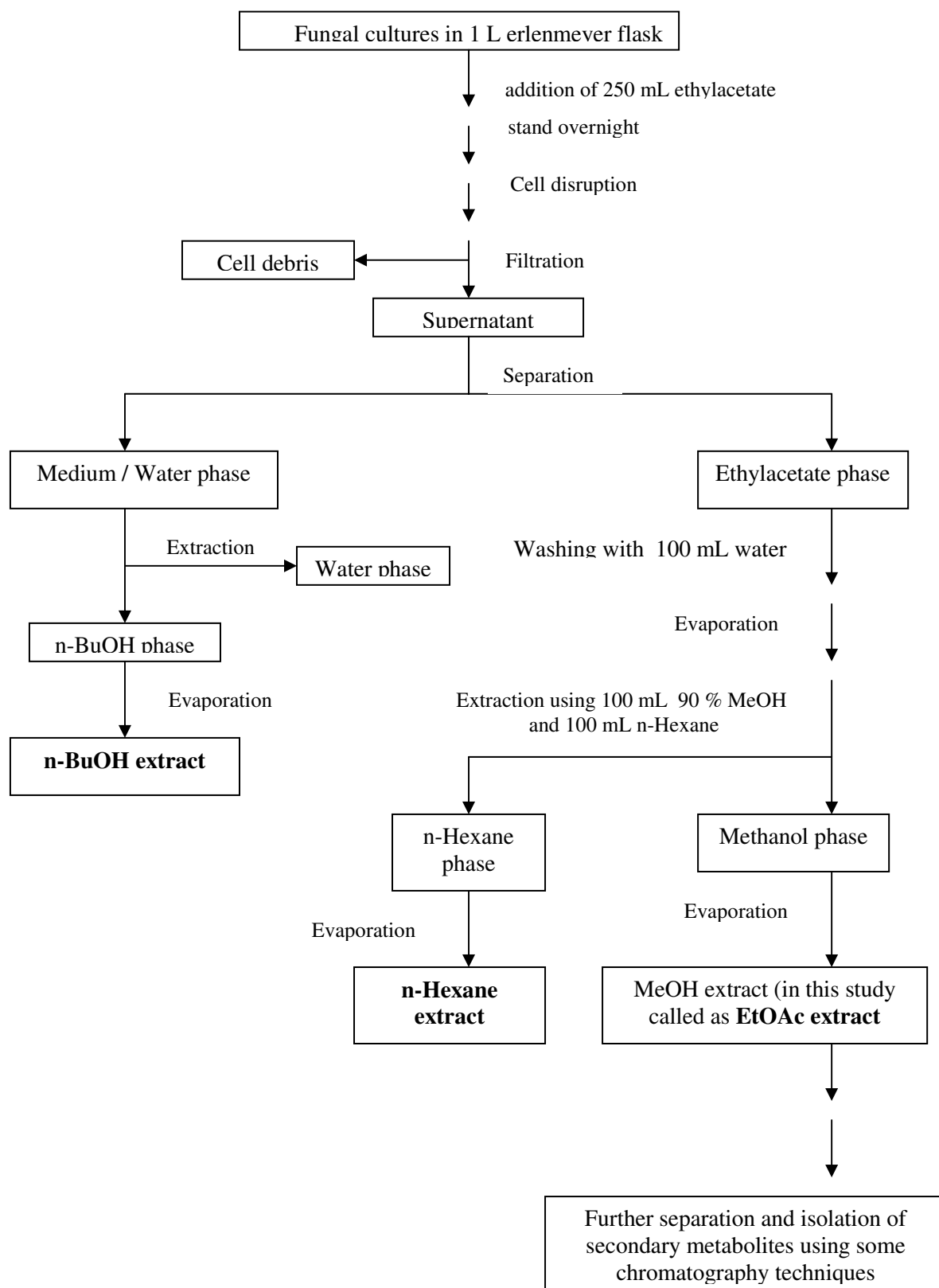


Figure 2.1 Scheme of Fungal Extraction (Method 1)

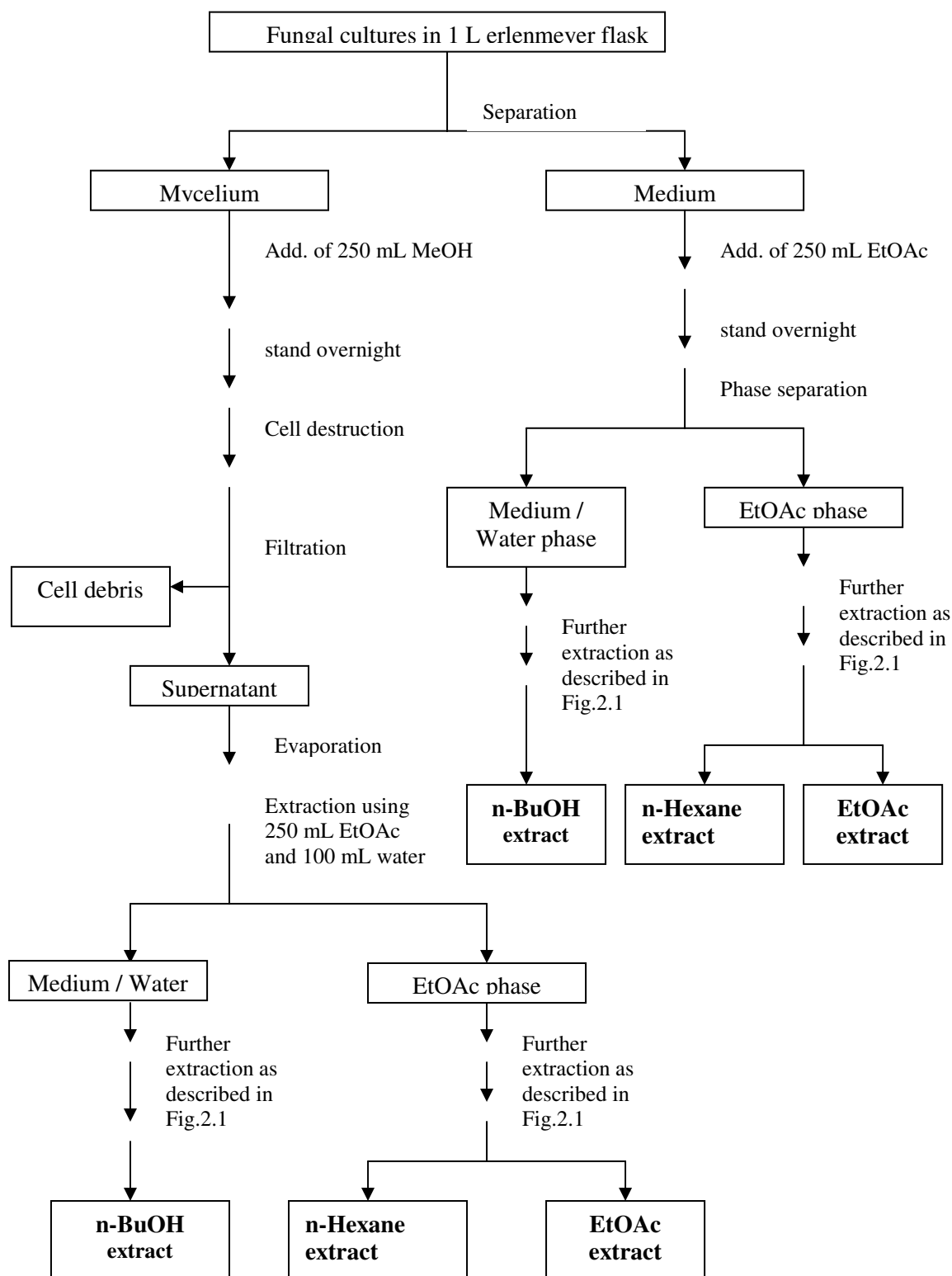


Figure 2.2 Scheme of Fungal Extraction (Method 2)

2.2.4.1 Solvent-Solvent Extraction

Solvent-solvent extraction is a widely employed technique to separate organic compounds from a mixture. It involves the separation of compound in two immiscible solvents. Since the technique is based upon an unequal distribution of solutes between two solvents with a different polarity, the solutes will be more soluble in one solvent compared to the other. The distribution of a component A between two phases can be expressed as distribution coefficient (K) :

$$K = \frac{[A]_{\text{top phase}}}{[A]_{\text{lower phase}}}$$

where, [A] is the concentration of solute A.

The following general principles should be considered in choosing a solvent for the system :

- the solvents involved in the extraction must be immiscible
- the solvents must not react to the components that will be separated
- the solvents should be easy to be removed by evaporation after the process

In this study, the solvent extraction was the first step in the whole separation process. It was meant to “clean” the ethyl acetate extract from salts and other undesirable polar constituents by water-ethylacetate extraction. Subsequently, the methanol-n-hexane extraction was applied to remove fatty acids and other undesirable non polar components.

2.2.5 Isolation, Purification and Identification of Secondary Metabolites

In this study, ethyl acetate extract were selected for further metabolites purification and isolation because of the following reasons :

- It contains more metabolites compared to n- butanol and n-hexane extract
- Its metabolites are easier to be separated and isolated using known and available chromatography techniques than n-butanol and n-hexane extracts

- Some preliminary bioassays indicated that ethyl acetate extract is more active than n-butanol and n-hexane extracts

The isolation and purification of secondary metabolites was performed using some chromatography techniques. The techniques used in the isolation depended on the amount and metabolites profiles of the extracts. Figure 2.3, 2.4 and 2.5 show the details of schematic isolation of secondary metabolites from *A. niger*, *P. citreonigrum* and *P. longisetula* cf.

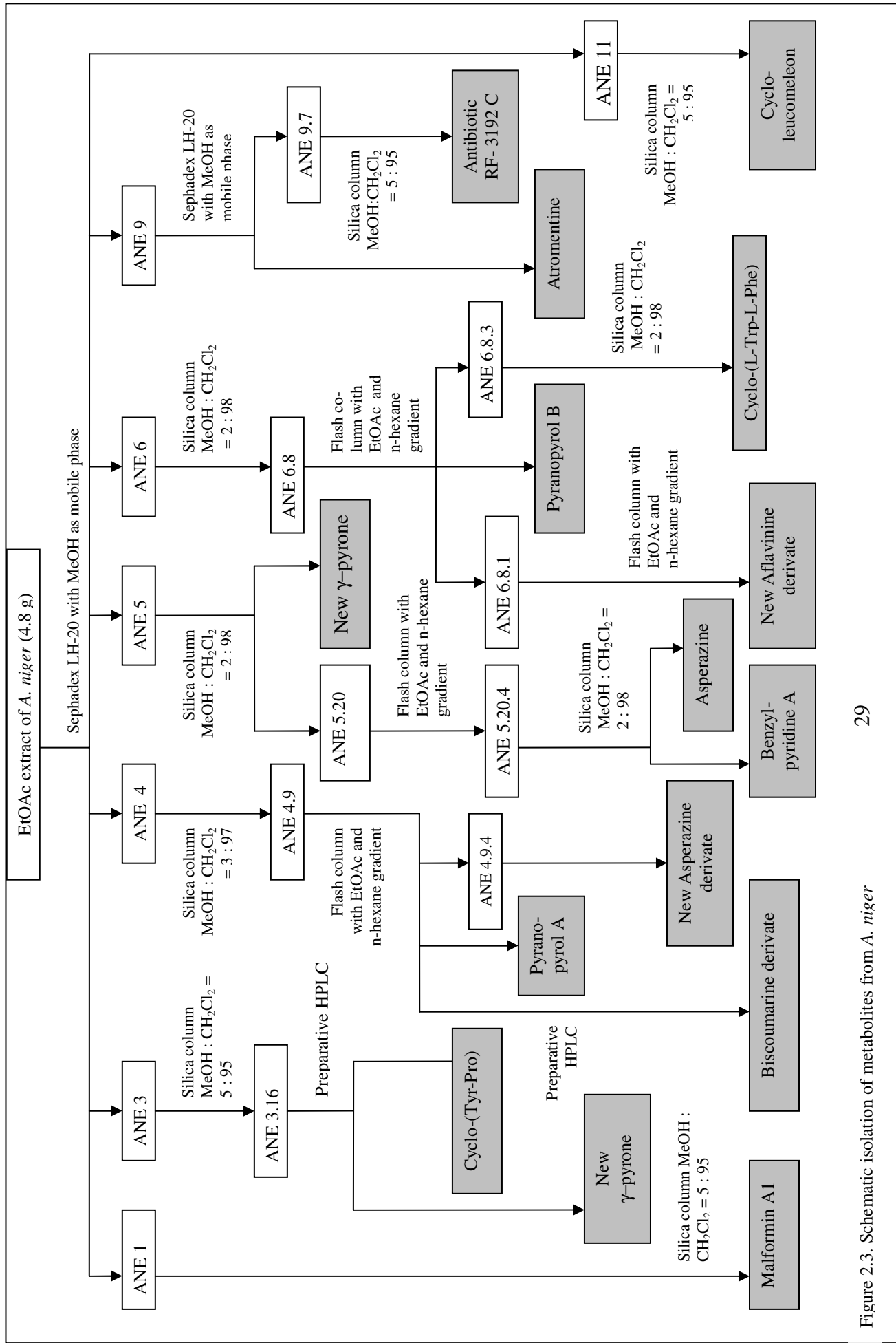


Figure 2.3. Schematic isolation of metabolites from *A. niger*

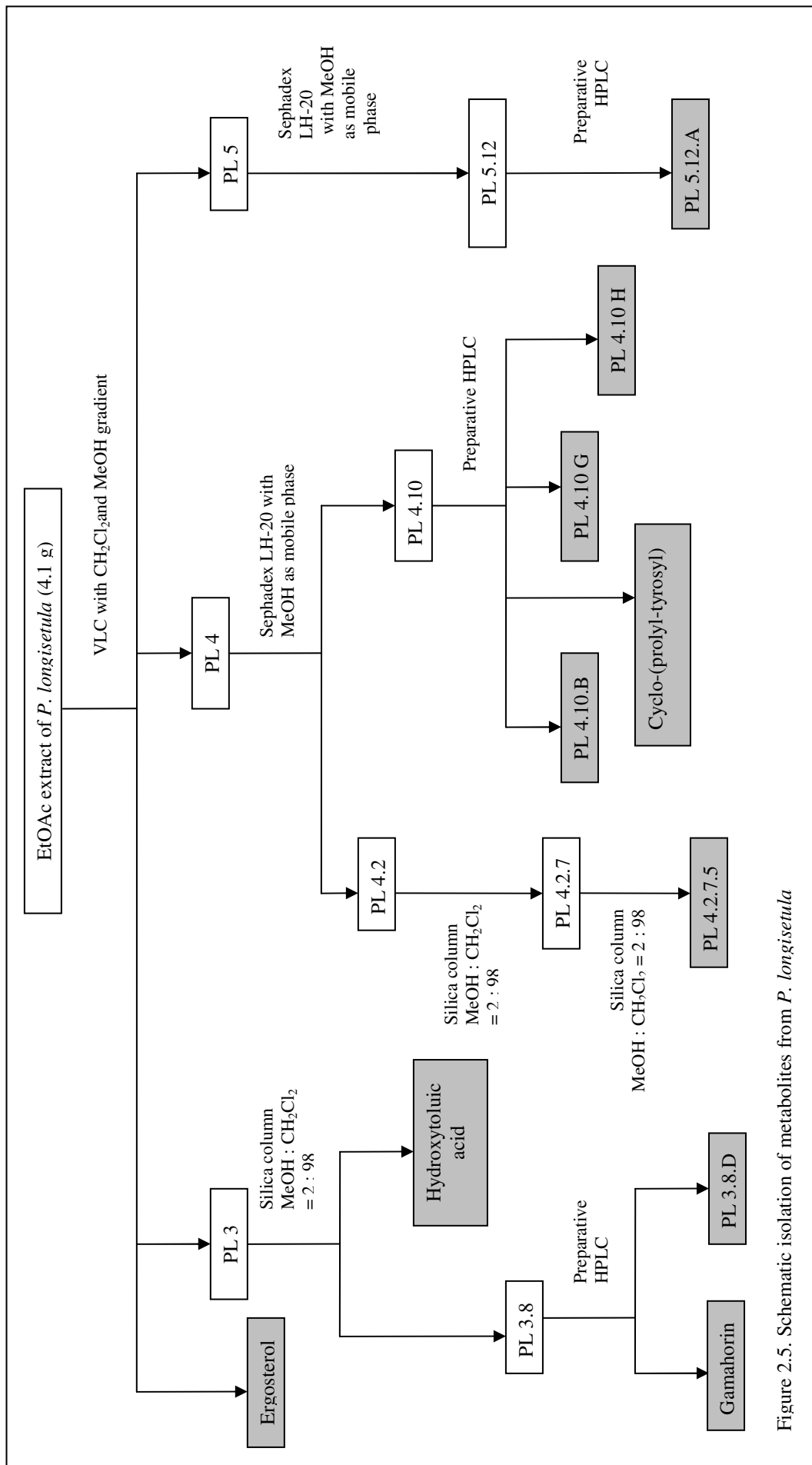
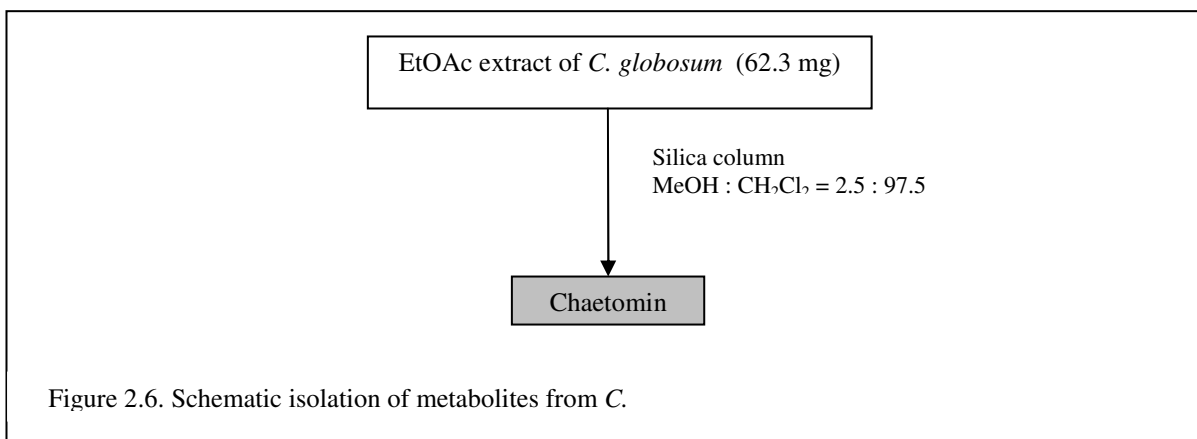


Figure 2.5. Schematic isolation of metabolites from *P. longisetula*



2.2.5.1 Chromatography

In chromatography, chemical components of a mixture are carried by a mobile phase through a stationary phase. The mixture is first placed in the stationary phase and the mobile phase is allowed to pass through the system. The chemical separation in a mixture is based on the selective interaction, such as surface absorption and relative solubility, of the components with both the stationary and mobile phase.

Three different type of chromatography, based on the physical property of stationary and mobile phase, used in this study include the following :

- a. Thin Layer Chromatography
- b. Column Chromatography
- c. Gas Chromatography

2.2.5.1.1 Thin Layer Chromatography

TLC is a simple and quick chromatography to analyze the components of the mixtures and to determine the purity of a substance. It is also usually used to determine the best solvent system for column chromatography. Sometimes TLC, called as preparative TLC, is also subjected to separate and purify the components in the mixtures.

TLC plate is a sheet of glass, metal or plastic (usually polyester) which is coated with a thin layer of stationary phase (usually silica, SiO₂, and alumina, Al₂O₃, in about 250 μm

thick). The samples are loaded close to the one edge of the plate. Then the plate is “developed” by immersing the loaded edge in a mobile phase. The mobile phase, usually the mixture of two or more solvents, migrates through the plate (stationary phase) causing the components of the mixture to distribute between the stationary and the mobile phase. Then the process is terminated just before the mobile phase reached the opposite edge of the plate. Development is done in a solvent vapour-saturated chamber. After the separation, the separated components of the mixture appear as spots or bands on the plate (chromatogram). Sometimes any strongly coloured bands are visible on the plate. The colourless bands can be visualized by spraying some dying agents, such as anisaldehyde, on the plate to make coloured spots. Fluorescent components can be visualized under ultraviolet light. If the spots absorb UV light but do not fluoresce, the spots will appear dark on a fluorescent background because silica gel may have a fluorescent dye.

The ratio of the distance reached by a particular spots (components) to the distance reached by the mobile phase front is the R_f or retardation factor. It is characteristic value of that component under the certain conditions used. In determining the solvent system for a column chromatography, the ideal system is one that gives the R_f of round about 0.25 for desired components

2.2.5.1.2 Column Chromatography

Column chromatography, sometimes also called liquid chromatography, is used to separate, purify and isolate the components of the mixture. The stationary phase is packed in an inert plastic or glass column. The ideal system of mobile phase, usually a mixture of two or more solvents, is determined by TLC. The mobile phase is passed through the column by either external pressure or gravity. The type of interaction between the chemical components, stationary phase, and mobile phase is depended on the stationary phase being applied.

2.2.5.1.2.1 Silica Column

In column chromatography, also called liquid chromatography, a vertical glass column is packed by stationary phase, SiO_2 , and the mobile phase usually the mixture of organic

solvents which is added to the top of the column. The separation based on polar interaction of the components to the mobile and stationary phase. This technique is ideally used to separate and purify the components in the range of semi-polar to non polar. The long of the column and interval drops (related to the rate of the eluent through the column) is depended on the amount of the sample and the number of components to be separated.

The sample or the mixture to be separated is loaded on the top of the column. The mobile phase (the eluent) flows down and brings the mixture through the column by a gravity force with a fix rate. The components are distributed along the column and the coloured components can be watched during the separation as coloured bands on the column. The drops on the bottom of the column were collected using fraction collector and the fractions were analyzed using TLC. The process continues until the whole components are eluted and collected and takes may overnight. Alternatively, the flow can be stopped during the process and the column can be packed out. Then the coloured bands were cut out and re-dissolved in an ideal solvent to recover the separated components.

2.2.5.1.2.2 Reverse Phase (RP) Column

Liquid chromatography with the stationary phase more polar than mobile phase is called 'normal phase'. 'Reverse phase', however, refers to liquid chromatography with the mobile phase more polar than stationary phase. The protocol of RP column are very similar to silica column, but the column was packed by RP-18 as stationary phase and the mobile phase used was normally water and methanol or a mixture of both of them (sometimes acetonitrile is also used instead of methanol). This technique is ideally used to separate and purify the polar components of the mixture which dissolve only, for example, in water.

2.2.5.1.2.3 Sephadex Column

The protocol of Sephadex column is similar to silica and RP column. The column was packed by Sephadex LH-20 as a stationary phase and the mobile phase varies from a polar to non-polar organic solvent or the mixture of them. The best system of mobile phase is one that can dilute all the components to be separated. The mixture flows down, along

together with the eluent, through the column forced by the gravity. The components are separated and distributed on the stationary phase according to their molecular size. Since the stationary phase consist of porous beads, the larger molecules will be excluded from the beads and eluted first. The smaller molecules will be eluted later because they enter the porous of the beads and stay inside until they find the certain size of pores to exit from the beads.

2.2.5.1.2.4 Flash Chromatography

Flash chromatography is a preparative column chromatography based on optimised pre-packed column and an air pressure driven eluent at a high flow rate. It is a simply and quickly technique and widely used to separate a variety organic compounds. Normally, the column is a dry Silica Gel G pre-packed at a height of 18 cm and vertically clamped and assembled in the system. The column is filled and saturated with the desired mobile phase just prior to sample loading on the top of the column. The mobile phase, an isocratic or gradient solvent, is then pumped through the column with the help of air pressure and brings the sample to be separated in the columns. This technique is only considered a low to medium pressure technique and applied to the samples from a few milligram to some gram of sample.

2.2.5.1.2.5 Vacuum Liquid Chromatography (VLC)

Like a normal silica column, VLC column was packed with SiO_2 as a stationary phase. The mobile phase, however, was quickly passed through the column by a vacuum condition, instead of gravity force. This technique was normally used to separate a high amount raw extract in a short time.

The lower part of the vertical column is connected to the vacuum pump to generate a vacuum condition. The sample was loaded on the top of the column and then, together with the mobile phase, quickly passed through the column by vacuum condition. The mobile phase was normally changed (gradient elution) from less to more polar condition by the step.

2.2.5.1.2.6 Semi Preparative HPLC

Theoretically, the separation of the mixtures in a column chromatography is much more effective when the stationary phase is a very thin layer on the surface of very small and very uniform spherical beads. This condition, however, is very sensitive to the flow of mobile phase. To solve this problem, a pressure must be applied to the mobile phase in order to get a desired flow. For example, a pressure of about 2000 psi must be reached to flow 1 – 3 mL/minute of mobile phase. A reciprocating piston pump is used in the most HPLC system to get this condition. But it is also possible to use a cylinder of compressed gas or diaphragm pump.

A typical HPLC column which is packed by octadecylsilyl (C18-Si-) groups bonded to 5 μ m silica beads in a stainless steel tubing was used in this experiment. The column with 8.00 mm ID was used to flow the solvent with a rate of 5 mL/minute. The column with 4.00 mm ID and 143 mm long, however, was used to flow the solvent by 1 mL/minute.

The mobile phase is normally a polar solvent or a mixture of polar solvents, for example water (nanopure water) with methanol or acetonitrile. The composition of mobile phase is programmed to change continuously (gradient elution) from more to less polar condition. Sometimes, 0.01 % trifluoroacetic acid was used, instead of water, to get a better resolution of separation.

The dissolved gas may create the bubbles as the mobile phase leaves the column because the pressure suddenly drops. In this case, the mobile phase should be degased by ultrasonic treatment before use. Alternatively, it can be also boiled or applied to the vacuum to remove the gases.

A few microliters of sample solution was applied into a sample loop on an injector. When the injector is operated, the sample loop is suddenly switched into the flow of mobile phase just before it reaches the column.

As the mobile phase leaves the column, it immediately passes into a detector which is used to determine the presence of components. The UV detector was used in this study because

it quite sensitive for the molecules which absorb ultraviolet light. Furthermore, the wavelength can be set to the absorption maximum for a particular molecule interests, or to a short wavelength where most molecules absorb.

An on-line chromato-integrator is connected to the detector in order to monitor the presence of the components leaving the column after separation. The peaks of chromatogram expresses the number of components eluted by the system and the peaks area is equal to the UV absorbance of a particular compound (component). By monitoring the chromatogram, the individual peak or fraction was collected in an individual sample collector.

The HPLC system used in this study is described as follows :

Pump : LaChrom L-7100, Merck/Hitachi
Detector : LaChrom L-7400, Merck/Hitachi
Printer : Chromato-Integrator D-2000, Merck/Hitachi
Column : Eurospher 100-C18, Knauer
Pre-column : Eurospher 100-C18, Knauer

2.2.5.1.2.7 Analytical HPLC

The principle of analytical HPLC is similar to the semi-preparative HPLC. The semi preparative HPLC is used to separate and to isolate the components of the mixture. The analytical HPLC, however, is used only to identify and, sometimes, to determine the concentration of the components of the mixture.

Unless stated different, the most gradient elution of mobile phase (as a standard program) used in this study is described in Table 2.3 and the water (as nanopure water) was adjusted to pH 2 with Phosporic acid (H_3PO_4). If the standard gradient elution could not separate the components properly, the program was changed to the one suitable to the samples.

Table 2.3. A standard gradient elution of mobile phase in HPLC

Time (minutes)	% Methanol	% Water
0	10	90
5	10	90
35	100	0
45	100	0
46	10	90
60	10	90

The specification of the parts in HPLC system is described as follows :

Pump	: P 580, dionex
Programme	: Chromeleon version 6.3
Autosampler	: ASI 100T, Dionex , with an injection volume of 20 μ L
Column	: Eurospher 100 C-18, Knauer (bonded 5 μ m silica beads ; 4 mm ID ; 125 mm long)
Column oven	: STH 585, Dionex
Detector	: UVD 340 S - Photo Diode Array Detector, Dionex

Unfortunately, the UVD 340 S detects only the compounds which absorb UV light. Other compounds which do not absorb UV light were analyzed using TLC sprayed with dying agent, such as anisaldehyde, and/or submitted to gas chromatography.

2.2.5.1.3 Gas Chromatography

In gas chromatography, the mobile phase is gases continuously flow through the column packed by stationary phase. These carrier gases include helium, argon and nitrogen which are chemically inert.

Based on the stationary phase used in the system, gas chromatography is divided into two different types :

- Gas solid chromatography, one with stationary phase as a solid that has a large surface area
- Gas-liquid chromatography, one with stationary phase as liquid, normally a high boiling liquid, that is immobilized onto a solid support surface by absorption or chemical bonding

The sample to be analyzed is loaded into the beginning of the column. The components of the mixture were then distributed by the mobile phase to the stationary phase by condensation or absorption on the stationary phase.

Gas chromatography is used only to detect, identify or analyze the compounds and components of the mixture and the compounds or the components must have sufficient volatility and thermal stability.

In this study, Agilent 6850 Series GC was used to determine the molecular weight of the compounds which do not absorb UV light.

2.2.5.2 Determination of Maximum UV Absorption

The absorption of UV or visible radiation corresponds to the excitation of outer electrons in the molecules. In many organic molecules, most absorption is based on transition of n or π electrons to the π^* excited form. Experimentally, these transitions fall in spectrum of region 200 – 700 nm. Consequently, these transitions need an unsaturated group (called as chromophores) of the molecules to provide π electrons.

In this study, determination of maximum UV absorption was done with the help of the UVD 340 S – Photo Diode Array Detector integrated to analytical HPLC (see 2.2.5.1.2.7).

2.2.5.3 Determination of Molecular Weight

2.2.5.3.1 Mass Spectrometry

Mass spectrometer is an analytical instrument used to determine the molecular weight of a compound. Basically, mass spectrometer is divided into three parts, ionisation source, analyser and detector, that should be maintained under high vacuum condition in order to maintain the ions travel through the instrument without any hindrance from air molecules. Once a sample is injected into the ionisation source, the molecules are then ionized. The ions are then passed and extracted into the analyser. In the analyser, the ions were separated according to their mass (m) to charge (z) ratio (m/z). Once the separated ions flow into the detector, the signals are then transmitted to the data system where the mass spectrum is recorded.

There are many different method of ionisation used in mass spectrometry and the method to be used is depend on the type of sample to be analysed. Some known ionisation methods include :

- Electron Impact (EI)
- Electro-Spray Ionisation (ESI)
- Fast Atom Bombardment (FAB)
- Chemical Ionisation (CI)
- Atmospheric Pressure Chemical Ionisation (APCI)
- Matrix Assisted Laser Desorption Ionisation (MALDI)
- Field Desorption / Field Ionisation (FD/FI)
- Thermo-Spray Ionisation (TSI)

The mass spectrum shows a plot the relative intensity *vs* mass to charge ratio (m/z) and gives the information about molecular weight and relative abundance of the components in the sample. The most intense peak in the spectrum is called the base peak and others are reported relative to the base peak intensity. The fragments which are formed follow the simple and predictable chemical pathways and reflect the most stable ions or radicals. The highest molecular weight peak observed in a spectrum represents the typical parent

molecule. Generally, small peaks are also observed above the calculated molecular weight due to the natural isotopic abundance of ^{13}C and ^1H , etc.

In this study, only the first three ionisation methods were used to determine the molecular weight of obtained pure secondary metabolites.

2.2.5.3.1.1 Electron Impact (EI) Mass Spectrometry

Electron impacts generate a molecular ion M^+ (radical cation) by collision an electron with the sample in gas phase. The sample is firstly vaporised and then directly injected into a high vacuum chamber where the sample is ionised by bombarding with neutral molecules having energy 70 eV and accelerated in a 8 kV electric field. The ionisation is then accelerated by vacuum condition through a magnet field and then sorted on the basis of mass to charge ratio in a continue changing of magnetic field.

Since the samples (molecules) must be volatile and thermally stable thus the measurement of EI-MS is limited to low molecular weight compounds of approximately 600 Da or less. Some classes of compounds are not ideal for this measurement because it forms only molecular ion M^+ . But the molecular structure information can be deduced from the spectra due to an extensive fragmentation is occurred in the analysis.

The determination of molecular weight using this method was conducted by Dr. Keck and Dr. Tommes at the Institute of Inorganic Chemistry, University of Düsseldorf. The instrument used was Mass spectrometer type Finnegan MAT 8200.

2.2.5.3.1.2 Fast Atom Bombardment (FAB) Spectrometry

In this method, a non volatile or thermally fragile organic sample which is dissolved in a matrix solution, such as glycerine, is bombarded by a focus beam of neutral atoms, such as Ar, Xe and Cs, to generate ions. The energetic beam of fast atoms is delivered by FAB gun which is located externally to the ion source. The atom beam hits the sample on the target and then the emerging secondary ions are accelerated by 2 kV – 30 kV electrical fields and focussed towards the analyzer by use the ion source optics.

Like EI-MS, the measurement of FAB-MS was also conducted at the Institute of Inorganic Chemistry, University of Düsseldorf.

2.2.5.3.1.3 ElectroSpray Impact (ESI) Mass Spectrometry

In this method, the ionisation process is carried out at atmospheric pressure (API) by spraying sample solution out of a small needle (capillary), to which a strong electric field is applied. This process produce highly charged droplets, and then the solvent is evaporated leaving the highly charged molecules (sample ions) in the gas phase. Then the sample ions pass through sampling cone into an intermediate vacuum region, and through a small aperture into the analyser of the mass spectrometer, which is held under high vacuum.

ESI is known as soft ionisation method because the sample is ionised by the addition or removal of a proton with a very little extra energy to cause fragmentation of sample ions. Sample (M) with the molecular weight greater than ca.1200 Da give rise to charged molecular-related ions such as $(M+H)^+$ in positive ionisation mode and $(M-H)^-$ in negative ionisation mode. In positive ionisation mode, a trace of formic acid is added to aid protonation of sample molecules, meanwhile, in negative ionisation mode a trace of ammonia solution or a volatile amine is added to aid deprotonation of the sample molecule. Instead of the sample molecule being ionised by the addition of a proton H^+ , some molecules have been ionised by the addition of a sodium cation Na^+ thus $(M+Na)^+$ common appears in the positive ionisation mode.

In this study, determination of molecular weight using ESI-MS was performed in a combination of liquid chromatography (LC) in LC/MS (see section 2.2.5.3.2)

2.2.5.3.2 LC/MS

Liquid Chromatography/Mass Spectrometry (LCMS) is widely used in drug metabolites analysis since most the metabolites are either chemically or thermally labile, and usually the purification and isolation involves some sort of liquid chromatography. Thus this

technique allows the determination of molecular weight of a compound not only as a pure substance but also as a mixture of compounds.

The LC/MS system used in this study was a combination of High Pressure Liquid Chromatography (HPLC) and MS. The sample was injected to the HPLC system for the fractionation and the fractions were then flows in to the ionisation chamber in the MS system. Although the instrument can also be used to ionise the sample using APCI method, but the most measurement in this study used ESI as an ionisation method.

In HPLC system, nanopure water (containing 0.1 % formic acid) and methanol (and/or acetonitrile) were used as mobile phase. It flows in a rate 0.4 ml/minute according to a standard gradient elution as described in Table 2.4.

Table 2.4. Standard gradient elution of mobile phase in LC/MS

Time (minutes)	% Methanol	% Water
0	10	90
2	10	90
35	100	0
45	100	0
47	10	90
60	10	90

The specification of the parts in LC/MS is described as follows :

HPLC system : HP 1100, Agilent
MS system : Finnigan LCQ^{Deca}, Thermoquest
Ion Source : ESI and APCI, Thermoquest
Pump : Edwards 30, BOC
Injector : G 1313 A ALS 1100, Agilent
Column : Knauer Eurospher 100 ; C-18A
Detector : G 1315 B DAD 1100, Agilent
Programme : Xcalibur, Version 1.3

2.2.6 Structure Elucidation of Pure Secondary Metabolites

After determination of molecular weight, then immediately the pure compounds were submitted to Nuclear Magnetic Resonance (NMR) measurement for structure elucidation.

2.2.6.1 NMR Measurements

Nuclear Magnetic Resonance (NMR) technique is based upon the magnetic property of atom's nucleus and often used to obtain structural information about a molecule. Nuclei with an odd mass (atomic number), such as ^1H and ^{13}C , have a nuclear spin that produces a small magnetic field when the atom is introduced to an external magnetic field.

The amount of samples depend on the molecular weight of the compound and the type of expected NMR experiments. Just before submitting to the NMR measurement, the sample was dried in a freeze drier for at least 24 hours. The sample was then dissolved in an adequate NMR solvent and degassed by ultrasonic treatment for some minutes. The solvents used in the experiment are the deuterated solvents, such as $\text{DMSO-}d_6$, CD_3OD , and CDCl_3 . The sample should also a free particles solution in a 15 cm sample tube.

The most NMR measurements were conducted by Dr. Peter and his colleges at the Institute of Inorganic Chemistry, University Düsseldorf. The instrument used was NMR Bruker type DRX 500. Some measurements were also performed at Gessellschaft Biotechnologie Forschung (GBF), Braunschweig, by Dr. V. Wray using NMR Bruker type AM-300, ARX-400 and DMX-600.

2.2.6.1.1 One Dimensional NMR

2.2.6.1.1.1 Proton (^1H) NMR

The measurement of ^1H NMR is a fundamental analysis for the structure elucidation. One the sample was identified as a pure compound, it was then sent to ^1H NMR measurement and decided about the necessary to get two dimensional NMR measurement. Sometimes,

one spectrum of ^1H NMR is enough to describe the structure of a compound, especially the known compounds.

- A spectrum of ^1H NMR gives the information of :
- the number of hydrogen atom, which is indicated by the peak integration
- the type of the hydrogen atoms (related to the functional groups), which is indicated by chemical shifts (δ),
- the type of correlation between one hydrogen atom to the other, which is indicated by coupling constant (J)
- the number of coupled neighbouring hydrogen atoms, which is indicated by splitting pattern

in a molecule.

2.2.6.1.1.2 Carbon (^{13}C) NMR

Differs to ^1H NMR experiment, the ^{13}C NMR measurement needs more amount of sample. This fact due to the ratio of ^{13}C to ^{12}C isotopes abundance in the nature is less than the ratio of ^1H to ^2H isotopes.

The spectrum of ^{13}C NMR gives the information of :

- the number of carbon atoms in a molecule
- the type of carbon atom (correlates to functional groups), which is indicated by the chemical shift (δ), in a molecule

In ^{13}C NMR spectrum, the peak integration does not directly represent the exact number of particular carbon atoms. In addition to, this experiment does not give information of carbon multiplicity

2.2.6.1.1.3 DEPT

Distortionless Enhancement by Polarisation Transfer (DEPT) experiment is used to enhance the sensitivity of ^{13}C NMR experiment. This experiment is started by proton

excitation and followed by transferring to the magnetisation of carbon atoms (called as polarisation transfer process). The ^1H - ^{13}C polarisation transfer increase the sensitivity by up to a factor 4.

The amplitude and sign of the carbon resonance is altered by the feature editing according to the number of directly attached protons, resulting CH signal multiplicity to identify the primary, secondary, tertiary and quaternary carbon atoms. In the experiment, different final proton pulse angles, resulting different signs carbon resonance (see Table 2.5).

Table 2.5. The relationships of CH multiplicity and the amplitude of carbon resonance in different proton pulse angles experiment

Carbon type (C-H multiplicity)	DEPT-45	DEPT-90	DEPT-135
Quaternary, R_4C (singlet)	0	0	0
Tertiary, R_3CH (doublet)	+	+	+
Secondary, R_2CH_2 (triplet)	+	0	-
Primary, RCH_3 (quartet)	+	0	+

In this study, the DEPT-135 was performed to assign and elucidate the structure of pure isolated secondary metabolites.

2.2.6.1.2 Two Dimensional NMR

Two dimensional NMR spectra provide more information about molecule than one dimensional NMR spectra. This experiment is applied especially to a molecule which is too complicated to be elucidated only by one dimensional NMR.

In one dimensional NMR, the signal is recorded as a function of one time variable thus the spectrum is plots of intensity vs frequency. Meanwhile, two dimensional NMR is recorded as a function of two time variables, t_1 and t_2 , thus the intensity is plotted as a function of two frequencies, F_1 and F_2 .

The F_1 and F_2 coordinates of the peaks correspond to those found in a normal one dimensional spectrum. In a one dimensional NMR, the couplings are expressed as the multiplicity in the spectrum. In two dimensional spectrum, however, the idea of multiplicity is expanded somewhat so that the multiplicity is expressed as a correlation of the two frequency F_1 and F_2 .

2.2.6.1.2.1 COSY NMR

Correlation Spectroscopy (COSY) NMR correlates the ^1H shifts of the coupling protons of a molecule. It means COSY experiment is used to determine the connectivity in a molecule by determining the protons which are coupled one to another. The proton shifts are plotted on both frequency axes in the two-dimensional experiment resulting a diagram with square symmetry. In COSY spectrum, the F_1 and F_2 coordinates of the peaks in two dimensional spectra also correspond to those found in normal one dimensional (^1H) NMR spectrum. Thus a COSY spectrum gives information about H-H connectivities in geminal, vicinal and w-relationships of a molecule.

The interpretation of COSY spectrum is limited by overlapping signals which are not separated by this experiment if the relevant protons coupled to one another.

2.2.6.1.2.2 HMQC NMR

Heteronuclear Multiple Quantum Correlation (HMQC) spectrum gives information about the correlation between ^1H to their directly attached heteronuclei (^{13}C). This technique provide a convenient way to identify diastereotopic geminal protons (which are sometimes difficult to be distinguished in COSY) since only these will produce two correlations to the same carbon.

2.2.6.1.2.3 HMBC NMR

Heteronuclear Multiple Bond Correlation (HMBC) experiment correlates ^{13}C shifts in one dimension with the ^1H shifts in the other via two or three bonds CH coupling. The coupling more than three bonds are usually small (exceptions include those across unsaturation bonds). The technique is valuable to detect quaternary carbon which is impossible to be obtained in ^{13}C NMR experiments due to low amount of material available. Sometimes, a direct CH correlation also is also observed in this experiment.

2.2.6.1.2.4 ROESY NMR

Like NOESY (Nuclear Overhauser Enhancement Spectroscopy), ROESY (Rotating Frame Overhauser Enhancement Spectroscopy) experiment uses through space phenomenon to study the three dimensional structure and conformation of molecule by measuring NOEs (Nuclear Overhauser Effects) in the rotating frame. NOE is a spin relaxation phenomenon which depends on molecular motion and, especially, molecular tumbling rates. Since the effects is a distance dependence effects, only protons which are close in space (4-5 Å) give rise to such changes.

In a solution, small molecules (<1000 Da) tumble rapidly and produce weak, positive proton NOEs that grow slowly. In contrast, large molecules (>3000 Da) tumble slowly and produce large, negative proton NOEs that grow quickly. Meanwhile, mid-sized molecules (1000 – 3000 Da) tumble at intermediate rate that have close to zero proton NOEs and thus NOESY can not be used to observed the mid size molecules. For this reason, the ROESY experiment is applied to the mid size molecule for mapping NOE correlations between protons by changing the motional properties under different physical conditions.

In this study, the ROESY experiments were only applied to new metabolites and conducted at GBF by Dr. V. Wray using 600 MHz NMR.

2.2.6.2 X-Ray Crystallography

The understanding of three dimensional structure and conformation using ROESY experiments seems to be more obvious when many methyl group (CH₃), instead of hydrogen atom, directly attach to asymmetrical carbon atoms. In this case, X-ray crystallography is performed to confirm the results of ROESY experiments.

X-ray crystallography is a technique in crystallography used to study the crystal structure through X-ray diffraction. When a crystalline lattice is bombarded by an X-ray beam, the beam is then scattered in definite manner. The scattering pattern is characterized by the atomic structure of the lattice. This phenomenon, called as X-ray diffraction, occurs when the wavelength of X-rays and the distances between the atoms in the lattice have the same order of magnitude. Then the spacing in the lattice can be determined using Bragg's Law :

$$n\lambda = 2 d \sin (\theta)$$

where :

n is an integer

λ is the wavelength of X-ray

d is the spacing between planes in the atomic lattice

θ is the angle between the incident ray and scattering planes

The intensities of X-ray diffraction is measured and computed using Fourier analysis to get 3 dimensional structure of the compound. Normally, the X-ray diffraction is carried out using single crystals of the compound, but if it not available and difficult to be obtained, microcrystalline powdered samples may also be used although this requires different equipment and is much less straightforward.

In this study, two single crystals of meroterpenoids were submitted to X-ray crystallography. The measurement was conducted by Prof. W. Frank at the Institute of Inorganic Chemistry, The University of Dusseldorf. The single crystals were obtained

using re-crystallisation of the compounds in some organic solvents. It was also tried to get the crystal by derivation of the compounds using p-bromobenzoylchloride.

2.2.7 Derivatization of Isolated Compounds

2.2.7.1 p-Bromobenzoate Esters (Hu, et al.,2001)

Esterification of meroterpenoids with p-bromobenzoylchloride was aimed to obtain a single crystal of meroterpenoids for X-ray crystallography.

An excess p-bromobenzoylchloride (12 μmol) was added to meroterpenoid (10 μmol) and dissolved in 100 μl CH_2Cl_2 . Dimethylaminopyridine (DMAP, 1 μmol) and pyridine (1 μmol) were added to the mixture and stirred at room temperature for 24 hours. The mixture was separated using chromatography techniques to isolate the p-bromobenzoate esters of meroterpenoids.

2.2.7.2 Marfey Analysis (Marvey, 1984)

In this study, Marfey analysis was performed to determine absolute configuration of amino acids in Asperazine and its new derivative, malformin and other peptides.

Marfey reagent (FDAA = 1-Fluor-dinitrophenyl-5-L-alanin) was used as a reagent for derivatization of a D- and L-amino acids in the mixture. The derivative products can be quantitated using HPLC and/or LC/MS

A 50 μl of 50 mM standard amino acids in H_2O and 100 μl of 1 % Marfey reagent in acetone were mixed in an eppendorf tube. A 20 μl of 1M NaHCO_3 was added to the mixture and heated over 40°C for one hour. The reaction was then stopped by addition of 10 μl of 2 M HCl. The product was then dried and re-dissolved in MeOH for LC/MS measurement.

The samples (0.5 – 1 mg) were first hydrolysed with 1 – 2 ml 6N-HCl at 110°C for 24 hours under nitrogen atmosphere. The product, containing a mixture of free amino acids,

was then dried and re-dissolved in water for further reaction as applied to standard amino acids.

2.2.8 Optical Rotation

When a polarized light is passed through a chiral molecule, the direction of polarization can be changed. This phenomenon is called optical rotation or optical activity. The measurement of this change in polarization orientation is called polarimetry and the instrument used to measure this phenomenon is called a polarimeter.

This measurement is used to study the structure of anisotropic compounds and check the purity of chiral mixtures. If the sample contains only one enantiomer of its chiral molecule, the sample is said to be optically pure. An enantiomer is called as a levorotatory (l) or (-) enantiomer if it rotates light to the left (counterclockwise). Meanwhile, if an enantiomer rotates light to the right (clockwise), it is said to be as a dextrorotary (d) or (+) enantiomer.

Since the degree of optical rotation depends on the number of optically active species (chiral) in which the light passes, thus the measurement of optical rotation depends on concentration (c) and light path length (l) of the sample. The specific rotation, $[\alpha]$, expresses the optical rotation degree after correction of concentration and path length, thus the specific rotation is a specific quantity for a chiral molecule at certain temperature T and wavelength λ .

$$[\alpha]_{\lambda}^T = 100\alpha / c.l$$

where :

$[\alpha]_{\lambda}^T$ is specific rotation at certain temperature T and wavelength λ

l is optical path length in dm

λ is wavelength

T is temperature

α is measured optical rotation degree at certain temperature T and wavelength λ
c is concentration in g/100 ml

In this study, the measurement of optical rotation was conducted using Perkin Elmer Polarimeter 341 LC using Sodium-D-lamp at wavelength of 589 nm. Unless otherwise stated, the measurement was performed at 20°C using 1 dm length of cuvette and concentration of 0.1 g/100 ml samples. Thus the result is expressed as :

$[\alpha]_D^{20}$ value (c 0.1. Solvent)

2.2.9 Bioactivity

2.2.9.1 General Cytotoxicity Assay using *Artemia salina*

General toxicity assay, called as brine shrimp assay, using *A. salina* was performed as a preliminary assay to identify the toxicity of a compound. In this study, the assay was normally applied to raw extracts.

The test used newly hatched brine shrimp in saline water. A small amount of the dried shrimp eggs was hatched and aerated in a 1000 mL artificial sea water (by dissolving 33 g artificial sea salt in 1000 mL water) for 48 hours.

Crude extracts (samples) were dissolved in an appropriate amount of solvent in different concentration. The sample were transferred to the test tubes and mixed with a small amount of DMSO. After addition of some amount artificial sea water, twenty newly hatched brine shrimps were the added to the mixture. The volume was then adjusted to a final volume 5 ml by addition of artificial sea water. After 24 hours, the effects of samples on brine shrimps can be observed by counting the survived and death brine shrimps.

2.2.9.2 Anti-bacterial and Anti-fungal Assays

The antimicrobial and antifungal assays was performed using *Escherichia coli* (gram negative bacterium), *Bacillus subtilis* (gram positive bacterium), and *Sacharomyces cerevisiae* (yeast) and two fungal strain *Cladosporium herbarum* and *C. cucumerinum*. The method, called agar diffusion assays, was used to detect the capability of a substance to inhibit the growth of microorganisms by measuring the diameter of inhibition zone around a tested compound on agar plate.

2.2.9.2.1 Anti-bacterial Assays

The assay was performed using *E. coli* and *B. subtilis*. A 100 – 200 µl of bacterial liquid culture, in an exponential growth phase, was spread on to the surface of Luria Bertoni (LB) agar plate (see section 2.1.2.10). Immediately, 10 – 20 µl of tested compounds (with a concentration 1 mg/ml) are loaded onto the disc paper (5 mm diameter, Oxid Ltd) and then transferred onto the surface of LB media. The culture was then incubated at 37°C for one or two days (depend on the microbial culture being used). The growth inhibition was then measured and compared to Penicillin G, streptomycin and Gentamycin as positive controls.

The same technique was also applied to the assay using *S. cerevisiae* in a yeast medium (see section 2.1.2.11) and incubation at room temperature.

2.2.9.2.2 Anti-fungal Assays

Mycellium of *C. cucumerinum* and *C. herbarum* (after growing the fungi for about one month) were put into a fresh fungal medium (see section 2.1.1.12) and destroyed using “ultraturax.”. The cell debris (extracted mycellium) was removed by vacuum filtration and the filtrate (medium containing fungal spore) was then used for the next steps of the assay.

A 100 ml of fungal spore was spread out onto the surface of potatoes dextrose agar medium (PDA, see section 2.1.2.13). Immediately, 10 – 20 µl of tested compounds (with a concentration 1 mg/ml) are loaded onto the disc paper (5 mm diameter, Oxid Ltd) and then

transferred onto the surface of the PDA medium. The fungal culture was then incubated at room temperature for several days and the inhibition growth was measured around the disks. The result was then compared to positive control (nystatin).

2.2.9.3 Cytotoxicity Assays

The cytotoxicity assays is used to identify the toxicity of a compound to the cell lines by inhibiting the proliferation of the cells. The assay normally uses human cancer or animal cell lines. In this study, the cytotoxicity assays were performed using PC-12 (rat adrenal pheochromocytoma), Hela (human cervix carcinoma) and L-5178-Y (mouse T-cell lymphoma) and carried out by Prof. W.E.G. Müller at the Institute of Physiological Chemistry, University of Mainz, Germany.

The test compounds, dissolved in DMSO or EGGME, were loaded into a 96- well ELISA plate. The RPMI media, supplemented with 10% fetal bovine serum, was then added to the test compounds. The cells, in an exponential growth phase, were transferred to the RPMI media containing tested substances and incubated in a humidified incubator at 37°C and 5 % CO₂. After incubation of a certain time (depend on the cells line being applied), the cells (normally adhered to the plate) were harvested and washed with a buffer solution. The number of living cells was then identified by a method called MTT assay. Such amount of yellow MTT (3-(4,5-Dimethylthiazol-2-yl)-2,5-diphenyltertrazolium bromide) was incorporated to the cells and oxidized to purple formazan which can be measured by spectrophotometer. The oxidation takes place when only mitochondrial reductase are actives, thus the intensity of purple formazan is directly related to the number of viable cells. Alternatively, the number of viable cells can also be determined using radioactive (methyl-³H)-thymidine.

2.2.9.4 Protein Kinase Assays

Protein kinase enzymes are integral components of numerous signal transduction pathways involved in the regulation of cell growth, differentiation, and response to changes in the extracellular environment. Consequently, kinases are major targets for potentially developing novel drugs to treat diseases such as cancer and various inflammatory

disorders. Based on the amino acids that is phosphorylated in target protein, protein kinases are divided into two classes : serine/threonine kinases and tyrosine kinases.

In this study, the assays was conducted at ProQinase GmbH, Freiburg, Germany. A proprietary protein kinase assay (³³PanQinase[®] Activity Assay) was used to measure the kinase activity of the 24 protein kinases. Briefly, the assay is described as follows (as issued by ProQinase GmbH) :

1. A reaction cocktail was performed in 96-well FlashPlates[™] from Perkin Elmer. The reaction cocktail was containing : assays buffer, ATP solution (in H₂O), test compound (in DMSO) and substrate /enzyme solution (premixed). Table 2.6 shows the kinase and the substrates used in the assay.
2. The assay for all enzyme contained HEPES-NaOH, pH 7.5, MgCl₂, MnCl₂, Na-orthovanadate, DTT, PEG₂₀₀₀, and [γ -³³P]-ATP.
3. The reaction cocktails were then incubated at 30°C for 80 minutes.
4. The reaction was stopped with 2 % (v/v) H₃PO₄ and plates were then aspirated and washed two times with 0.9 % (w/v) NaCl or H₂O.
5. The incorporation of ³³Pi was determined with a microplate scintillation counter (Microbeta Trilux, Wallac).

Table 2.6. List of Protein kinase and their substrate ^{*)}

Family	Kinases	Substrate	Oncologically relevant mechanisms	Diseases
Serine/threonine kinases	AKT1/PKB alpha	GCS3(14-27)	Apoptosis	Gastric cancer (Staal, 1987)
	ARK5	Autophos.	Apoptosis	Colorectal cancer (Kusakai et al., 2004)
	Aurora A	tetra(LRRWWSLG)	Proliferation	Pancreatic cancers (Li et al., 2003A).
	Aurora B	tetra(LRRWWSLG)	Proliferation	Breast cancer (Keen and Taylor, 2004)
	CDK2/Cyclin A	Histone H1	Proliferation	Pancreatic cancer (Iseki et al., 1998)
	CDK4/Cyclin D1	Rb-CTF	Proliferation	Breast cancer (Yu et al., 2006)
	CK2-alpha1	p53-CTM	Proliferation	Rhabdomyosarcoma (Izeradjene et al., 2004)
	COT	Autophos.	Proliferation	Breast cancer (Sourvinos, 1999)
	PLK-1	Casein	Proliferation	Prostate cancer

					(Weichert et al., 2004)
	B-RAF-VE	MEK1-KM		Proliferation	Thyroid cancer (Ouyang et al., 2006)
	SAK	Autophos.		Proliferation	Colorectal cancer (Macmillan et al., 2001)
Receptor tyrosine kinase	EGFR	Poly(Glu,Tyr) _{4:1}		Proliferation	Glioblastoma multiforme (National Cancer Institute, 2005)
	EPHB4	Poly(Glu,Tyr) _{4:1}		Angiogenesis	Prostate cancer (Xia et al.,2005)
	ERBB2	Poly(Glu,Tyr) _{4:1}		Proliferation	Gastric carcinomas (Lee et al., 2005).
	FLT3	Poly (Ala,Glu,Lys,tyr) _{6:2:4:1}		Proliferation	Leukemia (Menezes et al., 2005)
	IGF1-R	Poly(Glu,Tyr) _{4:1}		Apoptosis	Breast cancer (Zhang and Yee, 2000)
	INS-R	Poly (Ala,Glu,Lys,tyr) _{6:2:4:1}		“counter kinase”	Ovarian cancer (Kalli et al., 2002)
	MET	Poly (Ala,Glu,Lys,tyr) _{6:2:4:1}		Metastasis	Lung cancer (Qiao, 2002)

	PDGFR- beta	Poly (Ala,Glu,Lys,tyr) _{6:2:4:1}	Proliferation	Prostate cancer (Hofer et al., 2004)
	TIE-2	Poly(Glu,Tyr) _{4:1}	Angiogenesis	Rheumatoid arthritis (DeBusk et al., 2003)
	VEGF-R2	Poly(Glu,Tyr) _{4:1}	Angiogenesis	Pancreatic cancers (Li et al., 2003A).
	VEGF-R3	Poly(Glu,Tyr) _{4:1}	Angiogenesis	Breast cancer (Garces et al., 2006)
Soluble tyrosine kinase	FAK	Poly(Glu,Tyr) _{4:1}	Metastasis	Breast cancer (Schmit et al., 2005)
	SRC	Poly(Glu,Tyr) _{4:1}	Metastasis	Colon cancer (Dehm et al., 2001)

*) The assays was performed by ProQinase GmbH, Freiburg, Germany

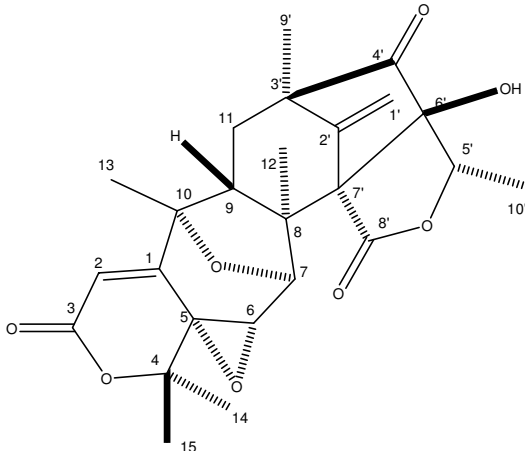
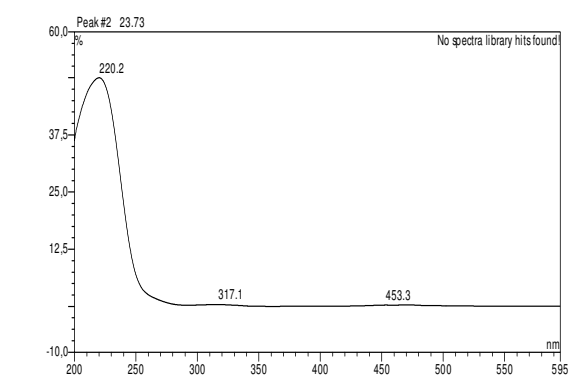
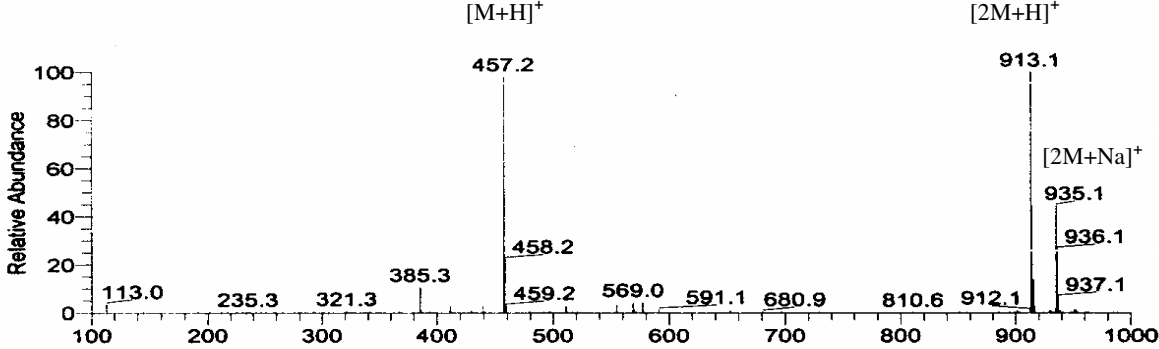
3 RESULTS

3.1 Secondary Metabolites from Sponge Associated Fungi

3.1.1 Secondary Metabolites from *Penicillium citreonigrum*

3.1.1.1 New Neoaustin-type Meroterpenes

3.1.1.1.1 Citreonigrin A

Citreonigrin A	
Biological Source	: <i>P. citreonigrum</i>
Sample code	: PC 3.3.6.11
Amount	: 24.98 mg
Molecular Formula	: C ₂₅ H ₂₈ O ₈
Molecular Weight	: 456 g/mol
Solubility	: CH ₃ OH
Physical Description	: White crystals (CH ₂ Cl ₂ /n-Hexane)
Optical rotation	: $[\alpha]_D^{20}$ -6 (c 0.1 in CH ₃ OH)
HPLC Retention Time (R _t)	: 23.75 (Standard gradient)
Structure	UV Spectrum
	
(+) ESI-MS	
	

Citreonigrin A was isolated as a pale yellow solid in CH₃OH and as colorless crystals after re-crystallisation in CH₂Cl₂/n-Hexane. This compound exhibited a pseudomolecular ion in the positive mode ESI-MS at m/z 457 [M + H]⁺.

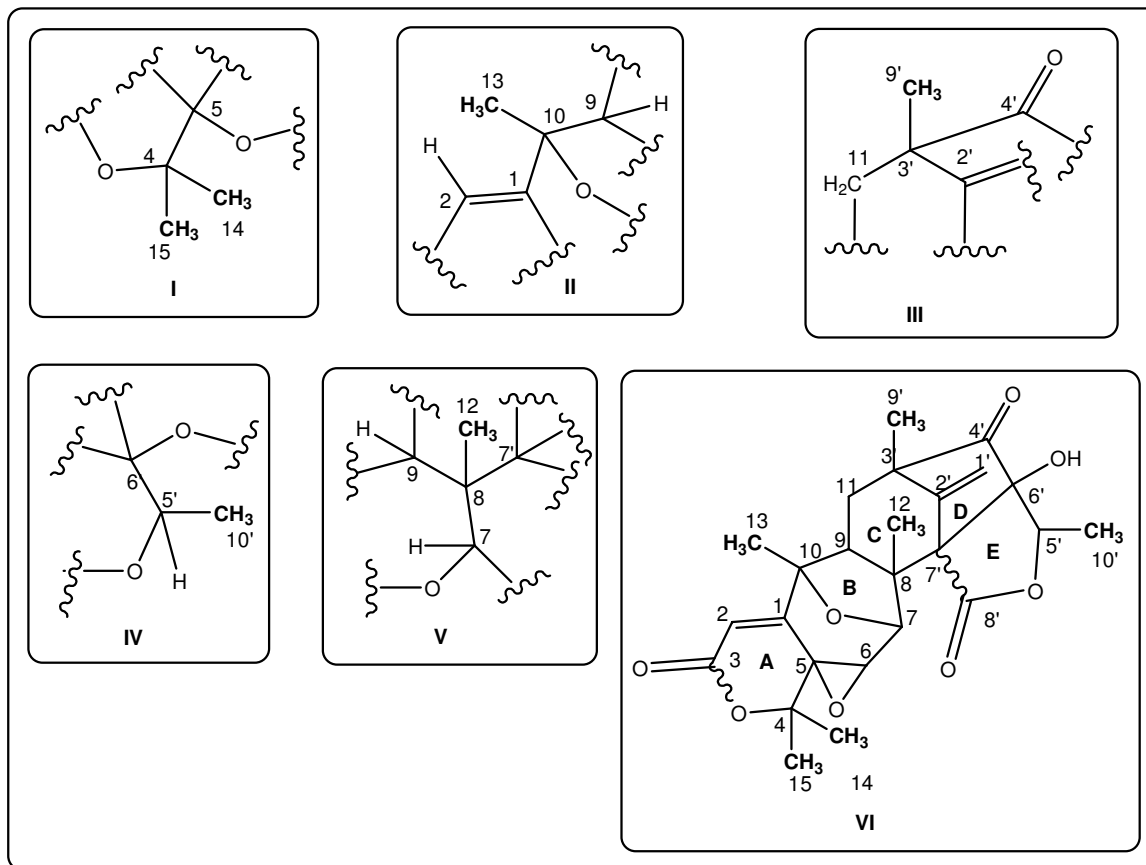


Figure 3.1.1.1.1 Partial structures of citreonigrin A based on the correlations of methyl protons in the HMBC spectrum

Analysis of the ¹H and ¹³C-NMR data for citreonigrin A revealed the presence of one hydroxyl and six methyl groups. Two of the methyl groups were found to be geminal based on HMBC analysis. In addition, three protons attached to different oxygenated carbons and three olefinic protons were also detected in the ¹H-NMR spectrum. Two of the olefinic protons were then assigned to an exo-methylene group (H-1A' and H-1'B). Among the protons attached to oxygenated carbons, one (H-5') was found to be directly coupled to a methyl group (H₃-10'), while the two remaining ones (H-6 and H-7) were adjacent to each other based on the COSY spectrum and by their coupling constant. The only remaining proton signals were assigned to a methine group (H-9) attached to a methylene function (H₂-11) as indicated by corresponding correlations in the COSY spectrum.

Based on the correlations of the methyl protons in the HMBC spectrum, it was possible to establish partial structures (see figure 3.1.1.1.1). The correlation of the two geminal methyl groups (H₃-14 and H₃-15) to two oxygenated carbons at δ 56.0 (C-5) and 77.5 (C-4) gave partial structure I. Meanwhile, substructure II was drawn up from the correlations of H₃-13 to the neighbouring carbons (C-1, C-9, and C-10), including a $^4J_{CH}$ correlation through a double bond to C-2. The HMBC correlations of H₃-9' to the methylene carbon (C-11), a keto function (C-4') and a quaternary olefinic carbon (C-2') at δ 37.0, 214.2 and 148.5, respectively, would give substructure III. Furthermore, the correlations of H₃-10' and H₃-12 to the respective neighboring carbons (C-7, C-7', C-8, C-9 and C5', C6', respectively) resulted in partial structures IV and V, respectively).

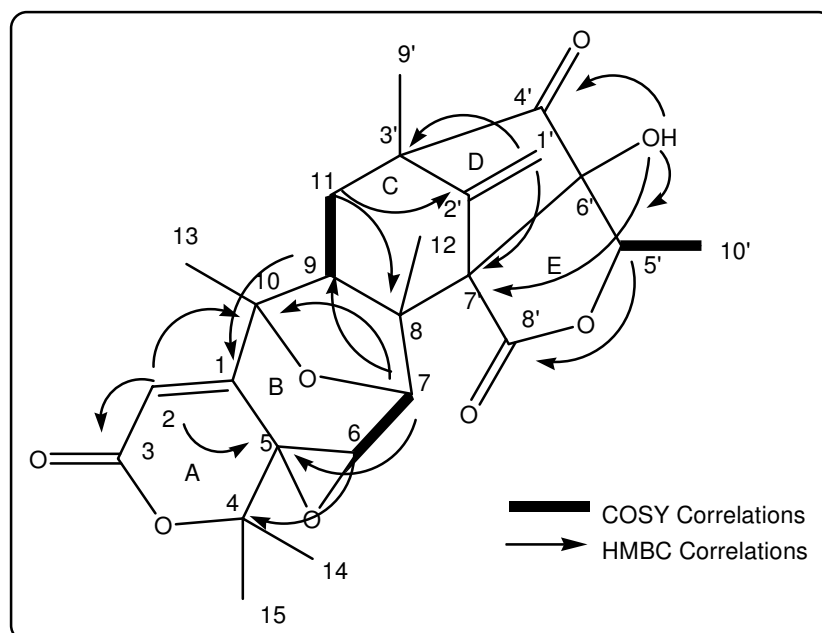


Figure 3.1.1.1.1.2 COSY (at 300 MHz) and diagnostic HMBC correlations of Citreonigrin A in DMSO-d₆

The connectivity of the substructures I – IV was established by further careful consideration of HMBC and COSY correlations. The link between II and V through C-9 was already evident by HMBC correlations of both H₃-13 and H₃-12 to this carbon, while the position of H-6 next to H-7 was evident from the COSY spectrum. Most importantly, a $^3J_{CH}$ between H-7 and C-10 clearly revealed the presence of an oxygen bridge between these positions. Crosspeaks between H-7 and C-5 as well as H-6 and C-4 allowed to further place substructure I, with the unusual upfield chemical shifts for C-6 (δ 53.6) and C-5 (δ 56.0) indicating that both carbons were incorporated into an epoxide function. Furthermore, the chemical shifts for C-1 (δ 154.5) and C-2 (δ 114.5) strongly suggested

that both were part of an α,β -unsaturated carbonyl ester (C-3, δ 162.8), leaving C-4 (δ 77.5) as the most plausible position for the ester alcohol. However, the closure of ring A was only postulated in the terminal steps of the structure elucidation of citreonigrin A when the remaining degrees of unsaturation were taken into account (see below).

The HMBC correlations of 6'-OH to C-4', C-5' and C-7' proved extremely diagnostic to confirm the connections of substructures III, IV, and V, while rings C and D could be closed by interpreting $^3J_{CH}$ correlations of H-9 (to C-7') in conjunction with H₂-11 (to C-8, C-10, and C-2'). Finally, an important $^3J_{CH}$ correlation of H-5' to C-8' (δ 172.1) suggested the presence of the five-membered lactone ring E, since the two remaining degrees of unsaturations not yet accounted for required a total ring count of 7.

For the same reason, the presence of the the six-membered ring α,β -unsaturated lactone ring A was postulated. Based on these considerations, the planar structure VI was deduced for citreonigrin A, but it has to be noted that there was no direct spectroscopical evidence for the connections between C-7'/C-8' and C-3/O/C-4, respectively (figure 3.1.1.1.2).

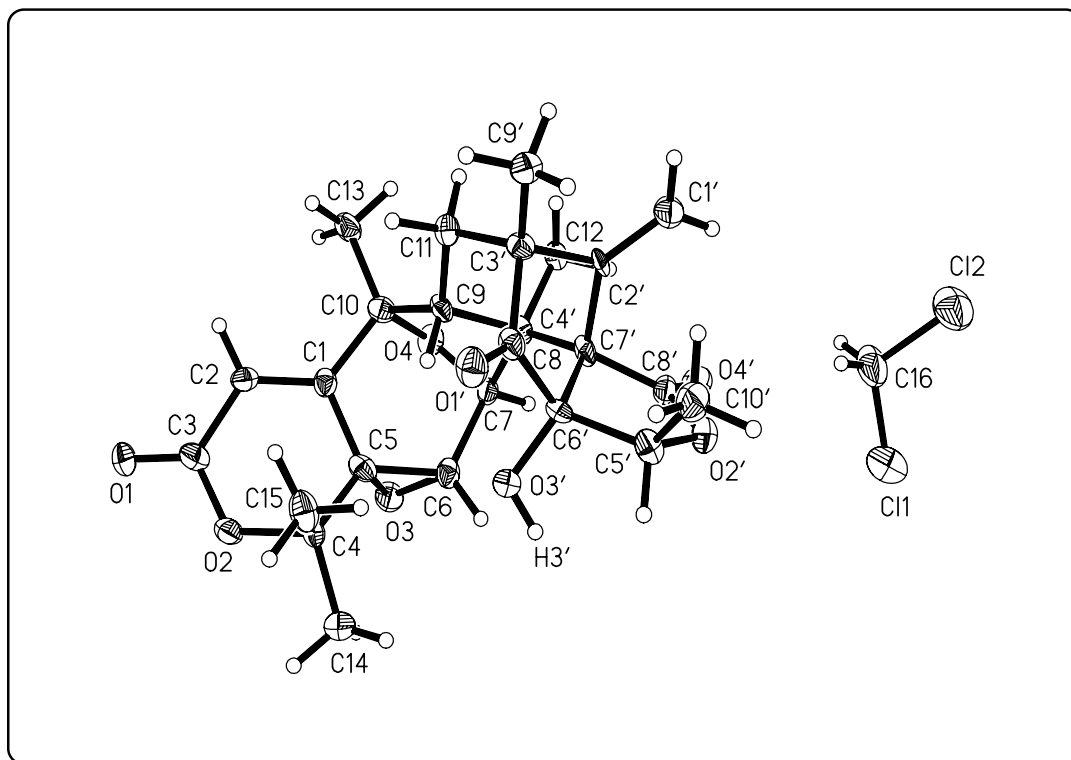


Figure 3.1.1.1.3 X-ray structure of citreonigrin A

The proposed structure for citreonigrin A was unequivocally proved by a single X-ray crystallography analysis, also allowing to establish the relative stereochemistry at its 10 chiral centers. Recrystallization of citreonigrin A from CH₂Cl₂ / n-hexane gave an orthorhombic crystal with the space group P2₁2₁2₁, and 0.5 x 0.05 x 0.025 mm³ in size. The crystal had a volume at 2531.0 (6) Å³ and unit cell dimension of a = 12.8647 (16) Å, b = 12.8336 (18) Å and c = 15.330 (2) Å. Furthermore, the determination of absolute configuration of the stereocenters in the molecule was performed with the help of CH₂Cl₂ molecules which was trapped in the crystal (figure 3.1.1.1.13).

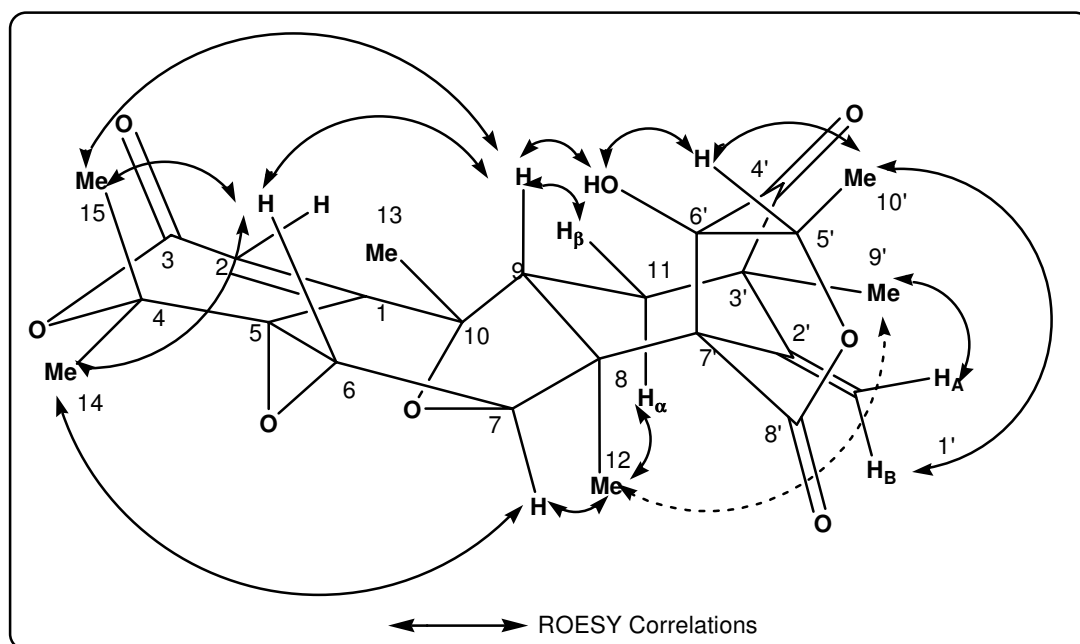


Figure 3.1.1.1.1.4 Stereo drawing of citreonigrin A showing the observed ROESY correlations in DMSO-d₆

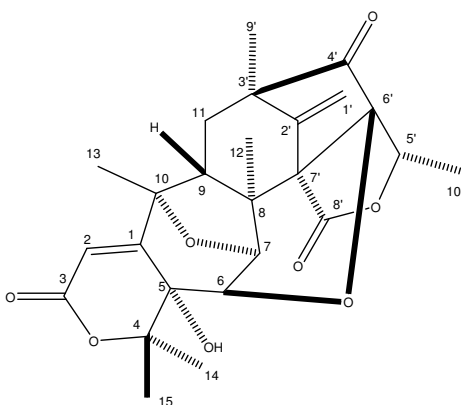
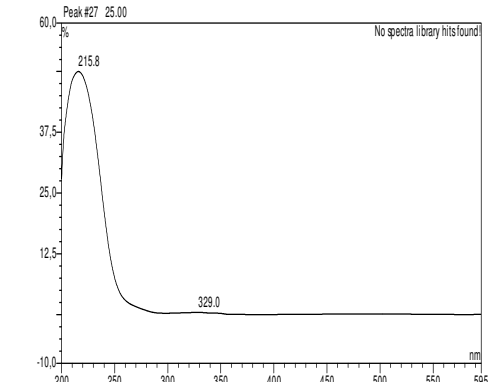
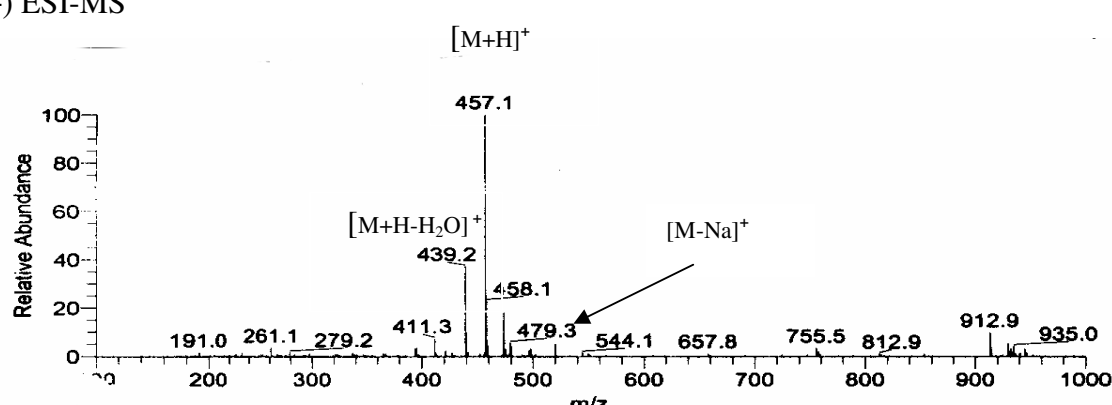
Once the X-ray structure was at hand, a 2D- ROESY spectrum was measured and carefully interpreted, so citreonigrin A could serve as a model to establish the relative stereochemistries of the further meroterpenoids isolated during this study. Key correlations were observed between H₃-12 and H₃-9', as well as H-7. In addition, the correlation of H-7 with H-11 α suggested the α -position of H₃-12 and H₃-9', while, the ROESY correlation of H-7 with H₃-14 allowed to assign the two geminal methyl groups. Consequently, the β -position of H-9 was confirmed by the strong correlations of H-9 with H-11 β and H₃-15. Furthermore, correlations of H-5 with 6'-OH followed by the correlations 6'-OH/H-9, and H₃-15/H-6 indicated that these protons were present in a close proximity on the β -face of the molecule (figure 3.1.1.1.1.4). Finally, the assignment of the exomethylene protons was achieved by NOEs of H-1'A and H₃-9', as well as H-1'B and H₃-10'.

Table 3.1.1.1.1.1 NMR data of Citreonigrin A in DMSO-d₆ at 600 MHz (¹H) and 100 MHz (¹³C)

Position	¹ H δ (ppm) <i>J</i> _{H-H} (Hz)	¹³ C δ (ppm)	HMBC (H to C)	ROESY
1		154.5		
2	5.93 s	114.5	3, 5, 10	11A, 13, 14
3		162.8		
4		77.5		
5		56.0		
6	3.67 d (0.9)	53.6	4, 5, 7	7, 9, 15
7	4.20 d (0.9)	77.5	5, 6, 9, 10	6, 12, 14
8		49.8		
9	2.49 ^h	45.5	1, 10, 11, 12, 13, 7'	11A, 15
10		75.9		
11	Aβ 1.85° Bα 1.85°	37.0	8, 9, 11, 12, 2', 3', 9' 8, 9, 11, 12, 2', 3', 9'	12, 13 12, 13
12	1.47 s	22.3	7, 8, 9, 7'	7, 11B, 13
13	1.20 s	15.7	1, 9, 10	11A, 12, 15
14	1.41 s	24.4	4, 5, 15	6, 7, 6'-OH
15	1.14 s	20.4	4, 5, 14	7, 13
1'	A 5.35 s B 5.13 s	111.3	11, 2', 3', 4', 7' 11, 2', 3', 7'	12, 9' 12, 10'
2'		148.5		
3'		54.8		
4'		214.2		
5'	4.45 q (7.2)	83.4	6', 8', 10'	10'
6'		88.1		
7'		65.1		
8'		172.1		
9'	1.18 s	15.8	11, 2', 3', 4'	11A/B, 1'A
10'	1.11 d (7.2)	17.7	5', 6'	5'
6'-OH	7.56 s		4', 5', 6', 7'	6, 7, 9, 14, 5'

^h hidden under residual solvent or water signal, ^o mutually overlapped

3.1.1.1.2 Citreonigrin B

Citreonigrin B	
Synonym(s)	: -
Biological Source	: <i>P. citreonigrum</i>
Sample code	: PC 3.3.6.6.3.H
Amount	: 29.0 mg
Molecular Formula	: C ₂₅ H ₂₈ O ₈
Molecular Weight	: 456 g/mol
Solubility	: CH ₃ OH, CH ₂ Cl ₂
Physical Description	: White powders
Optical rotation	: $[\alpha]_D^{20} +8^\circ$ (c 0.1 in CH ₃ OH)
HPLC Retention Time (R _t)	: 24.99 min (Standard gradient)
Structure	
UV Spectrum	
(+) ESI-MS	

Analysis of the NMR data of citreonigrin B indicated that this compound was closely related to citreonigrin A. The ¹H-NMR spectrum still indicated the presence of six methyl

groups, one exomethylene, one olefinic proton, three protons attached to different oxygenated carbons, one methylene, one methine and one hydroxyl group. As in the case of citreonigrin A, one methyl group (H₃-10') was present as a doublet and coupled to H-5'.

The close relationship between citreonigrin A and B was not only verified by NMR data, but also by the UV absorption pattern of citreonigrin B (λ_{max} at 215.8 nm) which was almost identical to that of citreonigrin A (λ_{max} at 220.2 nm). Furthermore, citreonigrin B showed a pseudomolecular ion peak at m/z 457.1 [M + H]⁺ in the positive mode ESI-MS, thus, indicating molecular weight of 456 g/mol.

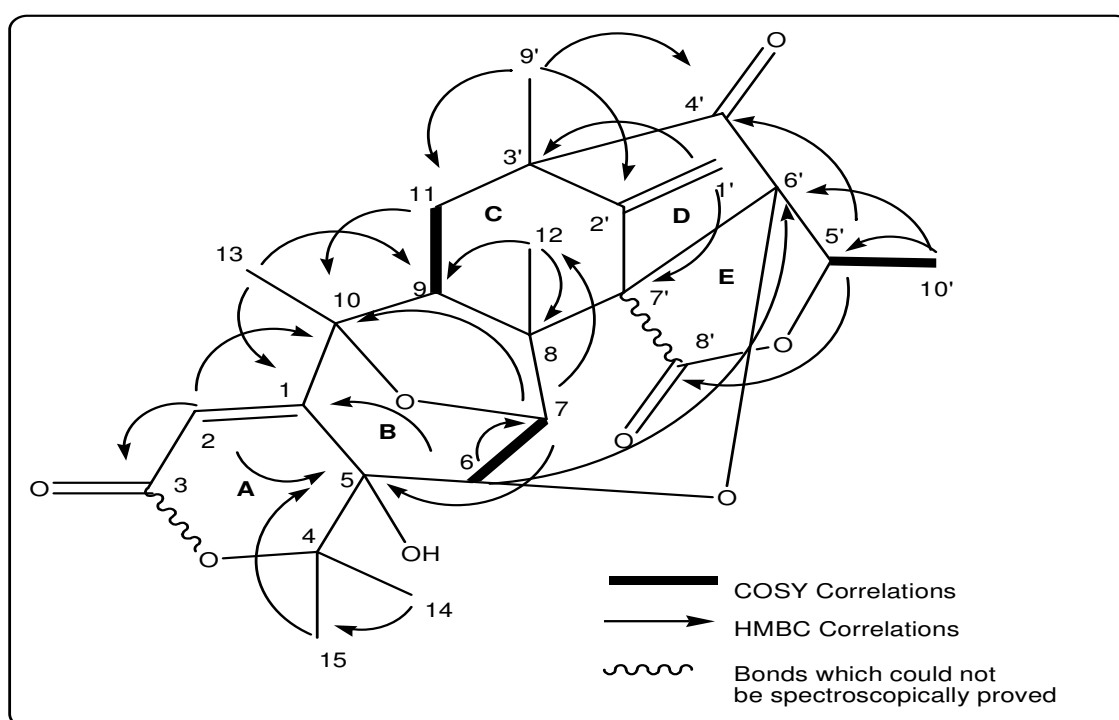


Figure 3.1.1.1.2.1. COSY (at 300 MHz) and some important HMBC correlations detected for Citreonigrin B in DMSO-d₆

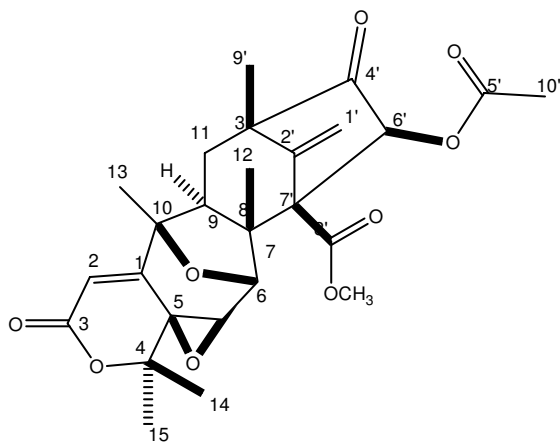
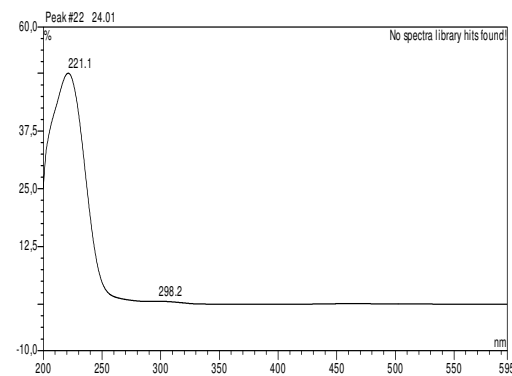
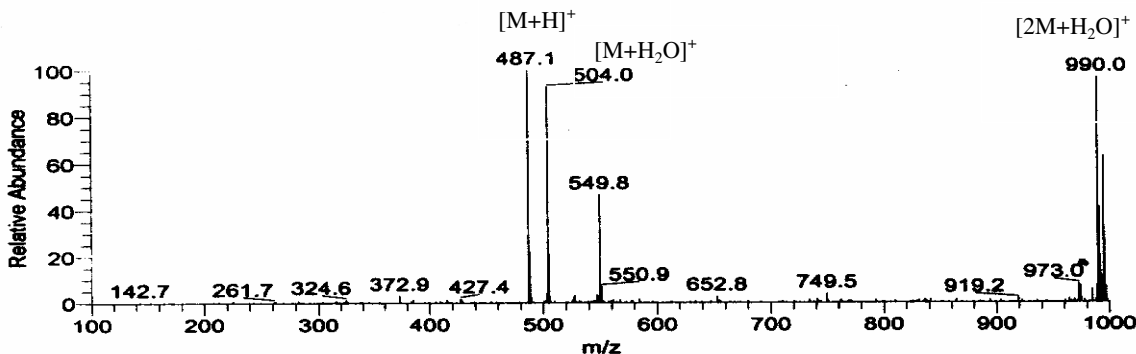
The larger coupling constant between H-6 and H-7 (7.9 Hz) and the downfield shift of C-5 (δ 72.7), however, indicated that citreonigrin B lacked the epoxide group at C-5/C-6 which present in citreonigrin A. Instead, a new oxygen bridge between C-6 and C-6' was confirmed by a long range correlation of H-6 to C-6' in the HMBC spectrum, while, the oxygen bridge between C-7 and C-10 was still existent. The long range correlations of 5-OH to C-1 and C-4 in the HMBC spectrum confirmed the position of the OH group in citreonigrin B which was attached to C-5, instead of C-6' in citreonigrin A. As described in

Table 3.1.1.1.2.1 NMR data of Citreonigrin B in DMSO-d₆ at 600 MHz (¹H) and 100 MHz (¹³C)

Position	¹ H δ (ppm) <i>J</i> _{H-H} (Hz)	¹³ C δ (ppm)	HMBC (H to C)	ROESY
1		160.5		
2	5.64 s	110.5	3, 5, 10	13, 14, 15
3		163.3		
4		85.8		
5		72.7		
6	4.53 d (7.9)	74.6	1, 5, 7, 8, 6'	5-OH, 7, 9, 14, 5'
7	4.35 d (7.9)	72.8	5, 6, 9, 10, 12	5-OH, 6, 12
8		43.1		
9	2.50 dd (13.9; 3.4)	49.5	1, 8, 10, 13, 3'	2; 5-OH, 6, 13, 14, 9'
10		77.3		
11	Aβ 2.11 dd (11.7; 3.4) Bα 1.92 dd (13.9; 11.7)	37.2	8, 9, 2', 3', 9' 9, 2', 3', 4'	2, 9, 12, 13, 9' 12, 13, 1'A, 9'
12	1.39 s	13.5	7, 8	9, 11A, 11B
13	1.32 s	16.0	1; 2, 9, 10	9, 11A, 11B
14	1.42 s	21.3	4, 5, 15	9
15	1.44 s	25.6	4, 5, 14	9
1'	A 5.36 s B 5.21 s	110.4	8, 11, 2', 3', 4', 7' 8, 11, 2', 3', 4', 7'	11B, 12, 9', 10' 12, 9', 10'
2'		145.6		
3'		57.6		
4'		211.1		
5'	4.66 q (7.4)	82.1	4', 6', 8', 10'	6, 7, 14, 1'B, 10'
6'		87.5		
7'		57.0		
8'		170.4		
9'	1.17 s	15.4	9, 11, 2', 3', 4'	9, 11A, 11B
10'	0.99 d (7.4)	17.7	5', 6'	1'A, 1'B, 5'
5-OH	5.44 s		1, 4	6, 7, 13, 14, 9'

3.1.1.2 New Austinoneol-type Meroterpenes

3.1.1.2.1 Citreonigrin C

Citreonigrin C	
Synonym(s)	: -
Biological Source	: <i>P. citreonigrum</i>
Sample code	: PC 3.3.6.6.3.X
Amount	: 6.68 mg
Molecular Formula	: C ₂₆ H ₃₀ O ₉
Molecular Weight	: 486 g/mol
Solubility	: CH ₃ OH (sl), CH ₂ Cl ₂
Physical Description	: White powders
Optical rotation	: $[\alpha]_D^{20} + 246$ (c 0.1 in CH ₂ Cl ₂) $[\alpha]_D^{20} + 20$ (c 0.01 in CH ₂ Cl ₂)
HPLC Retention Time (R _t)	: 23.99 min. (Standard gradient)
Structure	UV Spectrum
	
(+) ESI-MS	
	

In this study, citreonigrin C was the only meroterpene which was isolated as white powders, slightly soluble in CH₃OH and highly soluble in CH₂Cl₂ and CHCl₃. The UV absorption pattern (λ_{max} 221.1 nm) of this compound indicated that citreonigrin C was structurally related to citreonigrin A and B. However, positive mode ESI-MS measurement of this compound showed a pseudomolecular ion at m/z 487.1 [M + H]⁺, thirty mass unit higher than that of citreonigrin A and B.

In general, ¹H-NMR spectrum of this compound was almost similar to that of citreonigrin A and B, however, an extra methoxy group was detected as a part of the structure citreonigrin C. Moreover, a doublet methyl was not longer present and detected for this compound, instead, a singlet methyl (H₃-10') in a lower field was assigned to be attached to an *sp*-2 carbon. In addition, the presence of hydroxyl group was not detected and assigned to be incorporated in the citreonigrin C.

The structure elucidation of citreonigrin C was begun by the establishment of some partial structures (Figure 3.1.1.2.1.1) obtained by the HMBC correlations of the methyl protons. As like as citreonigrin A, the partial structure I – IV were also observed and identified in the HMBC spectrum of citreonigrin C. However, two others partial structures, V and VI, which were not observed in HMBC spectrum of citreonigrin A and B, but they were identified in the HMBC spectrum of citreonigrin C. The correlation of H₃-10' to a carbonyl carbon at δ 168.9 ppm (C-5') and methoxy protons (H₃-OMe) to a carbonyl carbon at δ 169.8 ppm (C-8') resulted in partial structure V and VI, respectively.

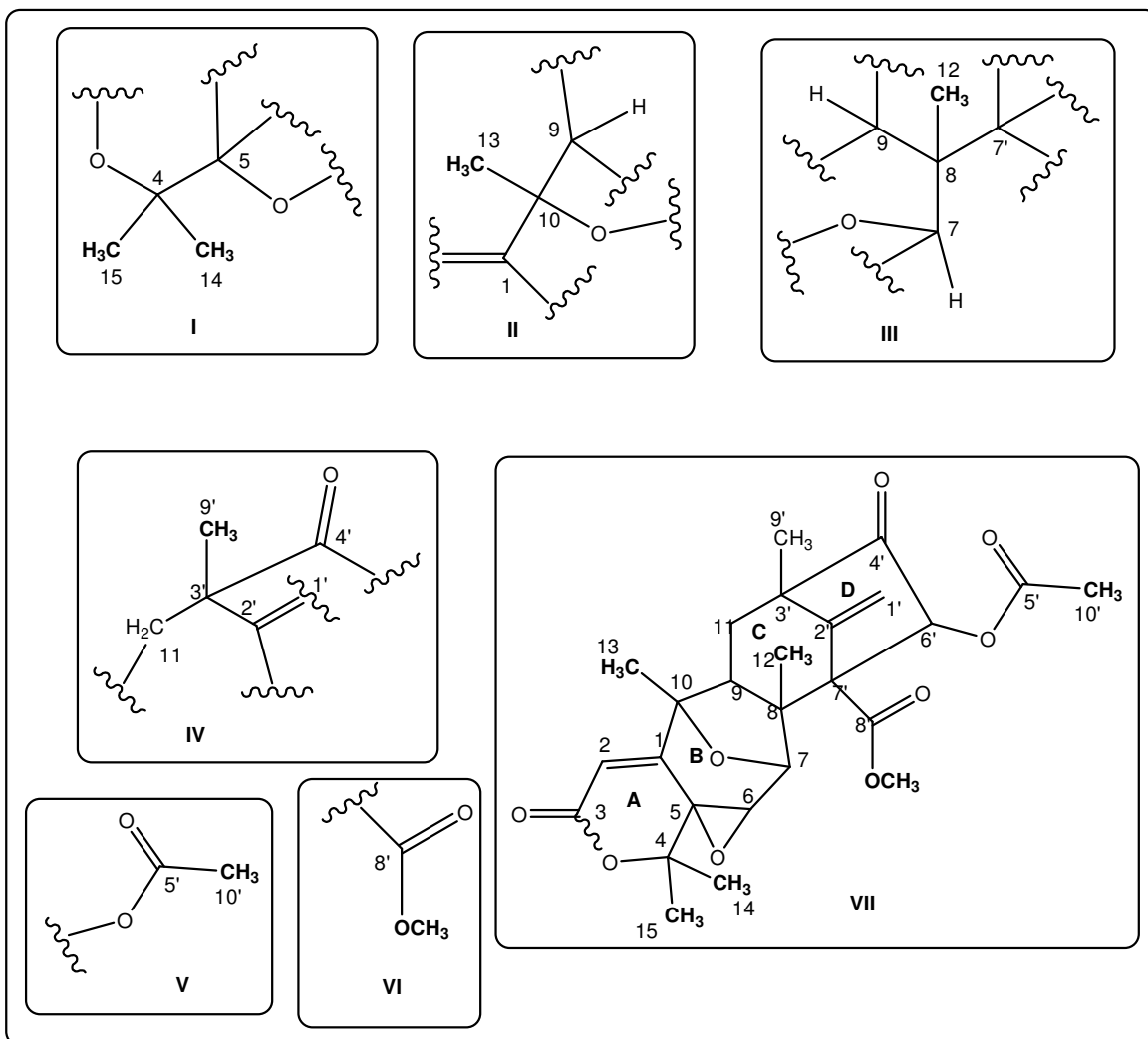


Figure 3.1.1.2.1.1 Partial structures of citreonigrin C based on the correlations of methyl protons in the HMBC spectrum

The connectivity of the substructures I – VI was established not only by further HMBC correlations, but also by the presence of spin systems identified in COSY spectrum (Figure 3.1.1.2.1.2). The substructure I was connected to substructure II by HMBC correlation of H-2 to C-5, while the HMBC correlations of H-9 to C-1 and C-10 allowed the linkage between substructure II and III. The position of H₂-11 (substructure IV) next to H-9 (substructure III) was evident by the observed spin systems between H-9 and H-11 α ($^3J_{HH}$ 4.6 Hz), as well as H-9 and H-11 β ($^3J_{HH}$ 4.6 Hz) in COSY spectrum. Finally, the key correlations of H-6 to C-4', C-5', C-7', C-8' and C-8 in HMBC spectrum joined the substructure III, IV, V, and VI to form the northern part molecule.

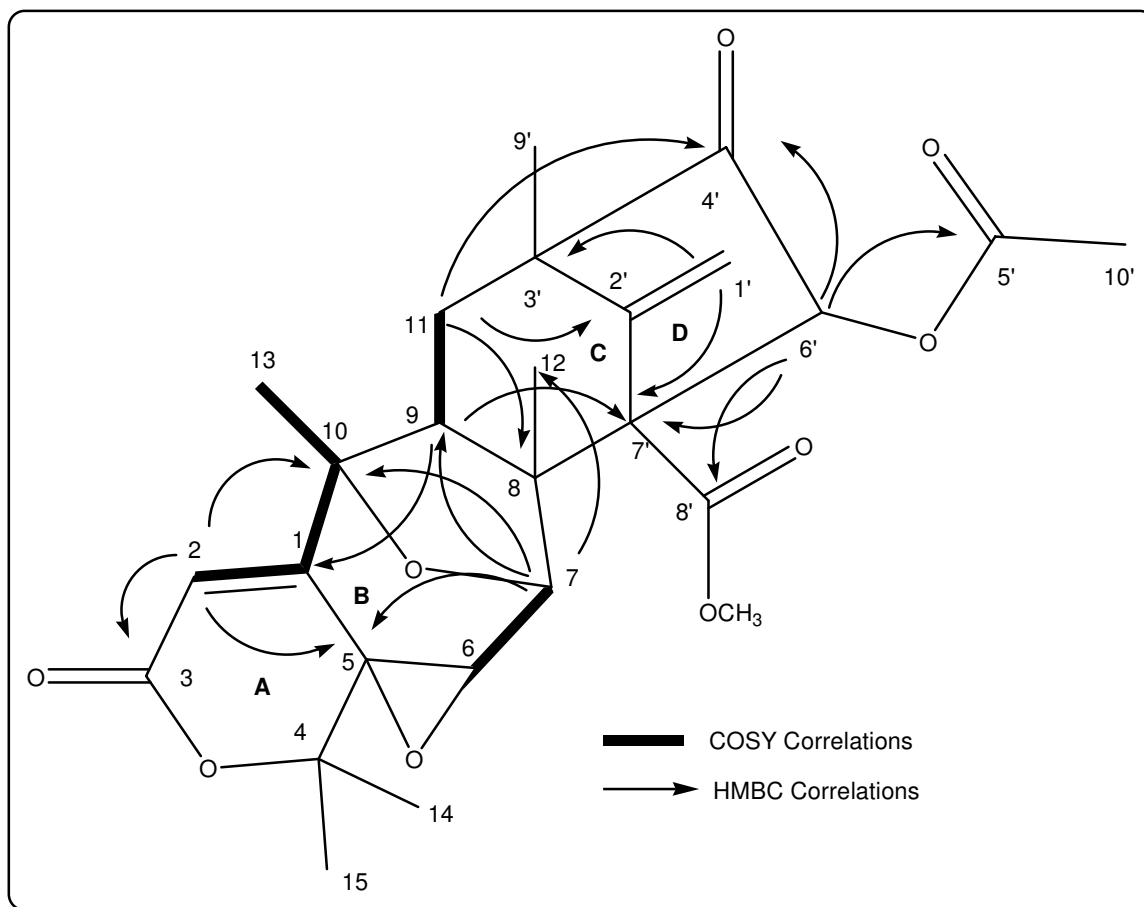


Figure 3.1.1.2.1.2. COSY (at 300 MHz) and diagnostic HMBC correlations of citreonigrin C in DMSO- d_6

The position of olefinic proton (H-2) and the presence of a carboxyl group next to C-2 were confirmed by HMBC correlations of H-2 to C-3 (δ 162.0 ppm) and C-5 (δ 55.9 ppm). Although the presence of an α - β -unsaturated δ -lactone (A ring) was proposed for citreonigrin C (structure VII), there was no direct evidence for the connectivity between C-3 and C-4. Nevertheless, the presence of this type of planar substructure has been also introduced and identified in citreonigrin A and B.

As like as citreonigrin A, the unusual upfield chemical shifts of C-5 (δ 55.9 ppm) and C-6 (δ 51.9 ppm) suggested the presence of an epoxide ring between these two carbon atoms. In addition, the presence of epoxide functional group was also indirectly supported by a small coupling constant ($^3J_{HH}$ 0.9 Hz) between H-6 and H-7. In the mean time, the presence of oxygen bridge between C-7 and C-10 was confirmed by HMBC correlation of H-7 to C-10, while, the assignment of H-1'A (δ 5.67 ppm) and H-1'B (δ 5.36 ppm) was

determined by not only by their correlations to C-2', C-3' and C-7' , but also by their direct correlations in HMBC spectrum.

The establishment of relative configuration in citreonigrin C was performed using ROESY experiment and the comparison of its optical rotation to other isolated and known meroterpenoids, especially citreonigrin A. The different optical rotation value between citreonigrin C (positive value) and citreonigrin A (negative value) suggested that the epoxide ring and oxygen bridge of citreonigrin C are located at *exo*-face in the seven membered ring system, compared to that of citreonigrin A which are located at the *endo*-face. Consequently, based on the molecular model, the position of H-6 and H-7 are also *exo*-face in the ring system.

The β -configuration of Me-12 and carbomethoxy group at C-7' were verified by ROESY correlations of H₃-12 with H-7, as well as correlation of H₃-12 with H₃-OMe group. The α -orientation of H-9, however, was determined by ROESY correlation of H-9 and H₃-15. However, it was difficult to determine the configuration of C-11 because both H-11A and H-11B showed the same correlations in ROESY. But the coupling constant of H-9 to H-11B ($^3J_{HH}$ 13.8 Hz) suggested the axial position of H-11B from H-9, thus H-11B is located at the β -position of the ring system. Furthermore, the coupling constant of H-9 to H-11A ($^3J_{HH}$ 4.6 Hz) indicated that equatorial position of H-11A from H-9, thus H-11A is located at α -position of the cyclohexane ring.

Furthermore, the relative stereochemistry of C-6' was established by the consecutive ROESY correlations of H-6' with H-6, H-9 and H₃-15, consecutively. These correlations indicated that the carbynolic hydrogen H-6' is located at the *exo*-face in the bicyclo[3.2.1]octane while the acetyl group is located at the *endo*-face. The complete assignment of stereocenters in the molecule is described in Fig. 3.1.1.2.1.3.

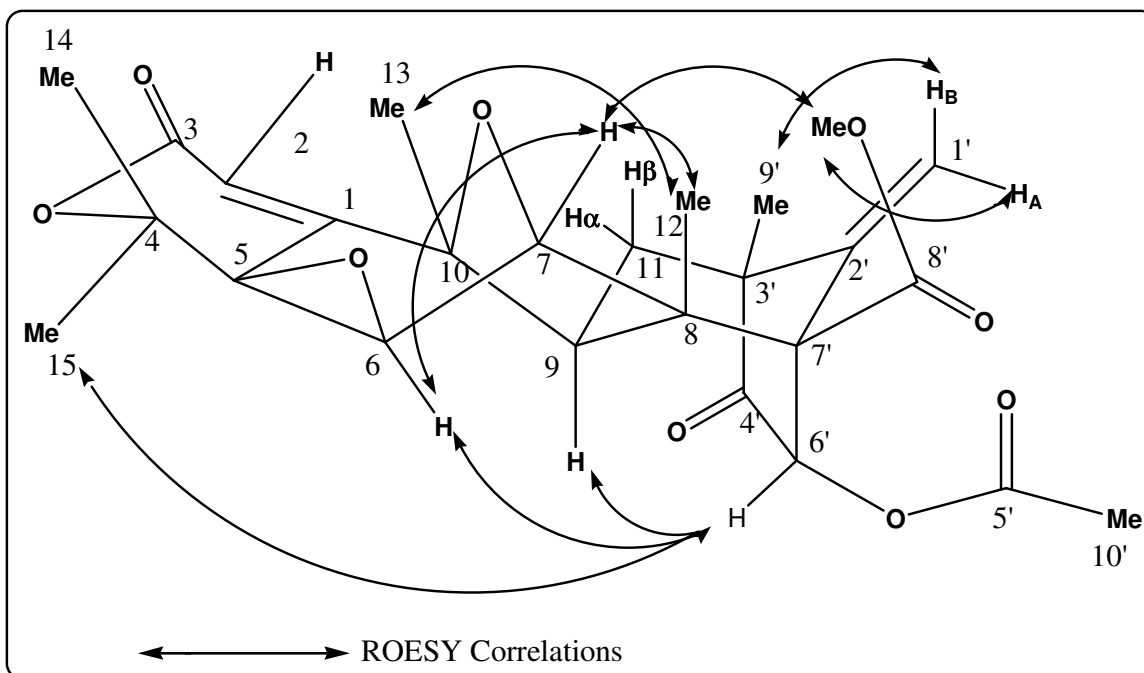


Figure 3.1.1.2.1.3 Selected ROESY correlation of Citreonigrin C in DMSO-d₆

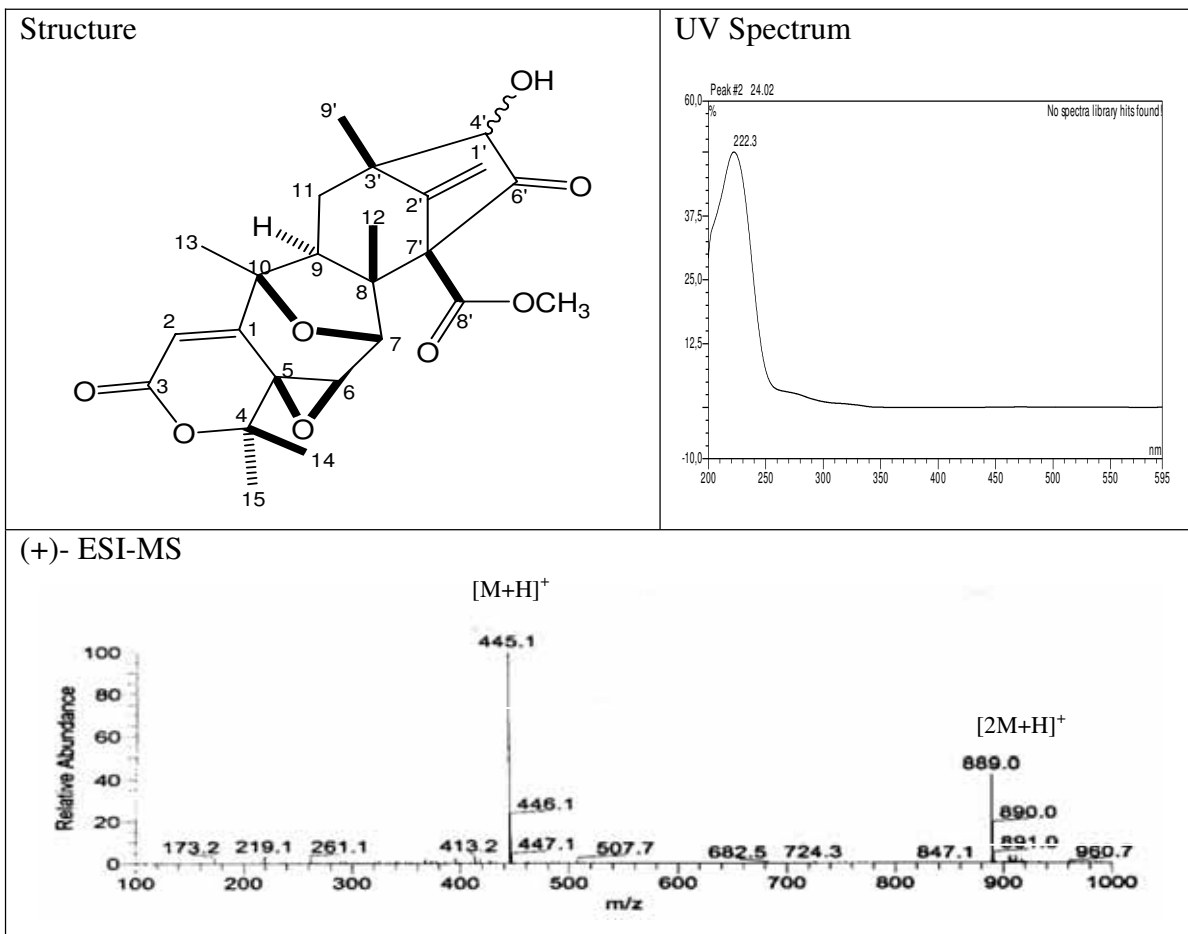
Table 3.1.1.2.1.1 NMR data of Citreonigrin C in DMSO-d₆ at 600 MHz (¹H) and 100 MHz (¹³C)

Position	¹ H δ (ppm) <i>J</i> _{H-H} (Hz)	¹³ C δ (ppm)	HMBC (H to C)	ROESY
1		162.0		
2	6.02 s	115.1	3, 5, 10	-
3		162.0		
4		82.4		
5		55.9		
6	3.64 d (0.9)	51.9	5, 7	9, 14, 15, 10'
7	4.36 s	79.5	5, 6, 9, 10, 12	6, 12, 8'-OCH ₃
8		50.3		
9	2.20 dd (13.8; 4.6)	46.0	1, 8, 10, 11, 12, 13, 7'	6, 11A, 11B, 12, 13, 15
10		75.8		
11	Aα 1.87 dd (11.9; 4.6) Bβ 1.80 dd (13.8; 11.9)	36.3	8, 9, 2', 3', 4', 9' 8, 9, 2', 3', 4', 9'	9, 11B, 12, 13, 9' 9, 11A, 12, 13, 9'
12	1.33 s	24.0	7, 8, 9, 7'	13
13	1.22 s	15.7	1, 9, 10	
14	1.27 s	21.4	4, 5, 15	15

15	1.48 s	24.6	4, 5, 14	14
1'	A 5.67 s B 5.36 s	111.9	11, 2', 3', 7' 11, 2', 3', 4', 6', 7'	9, 11A, 12, 13, 15, 1'B, 8'-OCH ₃ 11B, 12, 13, 1'A, 9'
2'		145.8		
3'		51.8		
4'		209.4		
5'		168.9		
6'	5.72 s	78.7	8, 4', 5', 7', 8'	6, 9, 14, 15, 8'-OCH ₃ , 10'
7'		62.7		
8'		169.8		
9'	1.18 s	16.3	11, 2', 3', 4'	14
10'	2.24 s	20.7	5', 6'	6, 14, 15, 8'-OCH ₃
8'-OCH ₃	3.75 s	52.5	8'	12, 10'

3.1.1.2.2 Citreonigrin D

Citreonigrin D	
Synonym(s)	: -
Biological Source	: <i>P. citreonigrum</i>
Sample code	: PC 3.3.6.9.D
Amount	: 5.0 mg
Molecular Formula	: C ₂₄ H ₂₈ O ₈
Molecular Weight	: 444 g/mol
Solubility	: CH ₃ OH
Physical Description	: Yellowish brown solids
Optical rotation	: $[\alpha]_D^{20} + 14^\circ$ (c, 0.1 in CH ₃ OH)
HPLC Retention Time (R _t)	: 24.04 min. (Standard gradient)



Citreonigrin D was isolated as a yellowish brown solid in CH₃OH. This compound revealed a pseudomolecular ion at m/z 445.1 [M+H]⁺. Analysis of 1D and 2D NMR suggested that the citreonigrin D was structurally related to citreonigrin C. However, ¹H-NMR spectrum of citreonigrin D showed the presence only five methyls and one hydroxyl group, compared to six methyls and the absence of hydroxyl group in citreonigrin C.

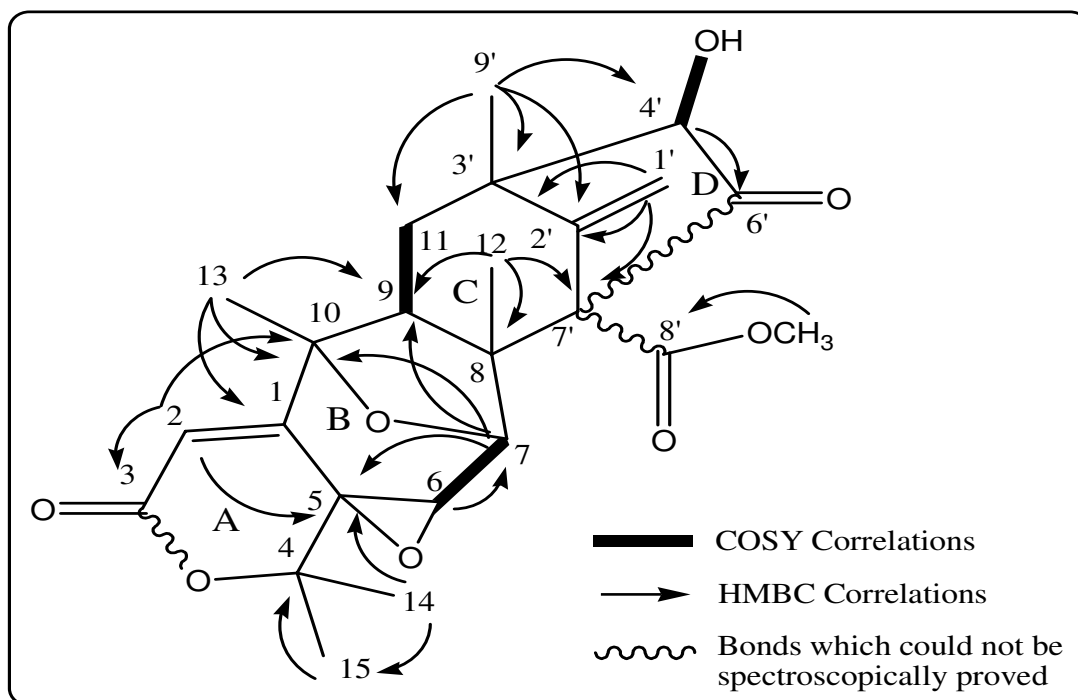


Figure 3.1.1.2.2.1. COSY (at 500 MHz) and HMBC correlations of Citreonigrin D in DMSO- d_6

The presence of OH group at C-4' (80.2 ppm), instead of keto in citreonigrin C, was confirmed not only by a COSY correlation of OH to H-4', but also by HMBC correlations of H-4' to C-11, C-6' and C-9'. In addition, an HMBC correlation of H₃-9' to C-4' supported the assignment. The presence of C-6' keto carbonyl, which was normally an oxygenated carbon in citreonigrin A, B, and C, was confirmed by an HMBC correlation of H-4' to C-6'. As shown by HMBC and COSY correlations in Fig. 3.1.1.1.7, the rest part of the molecule was identical to citreonigrin C.

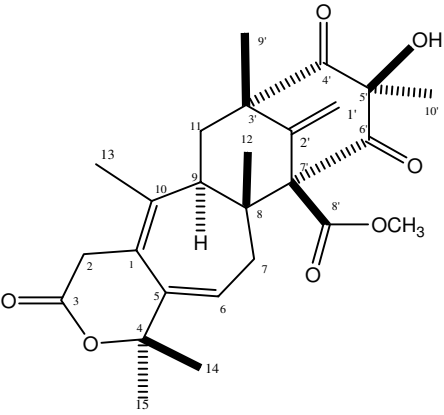
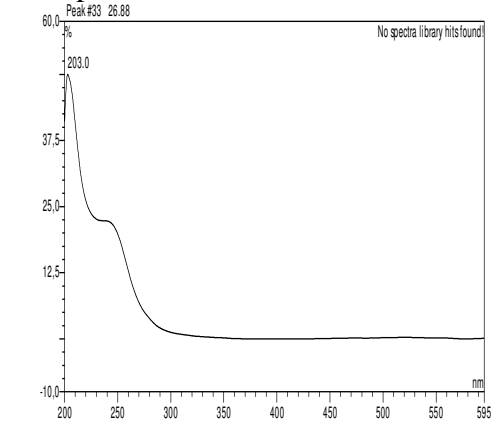
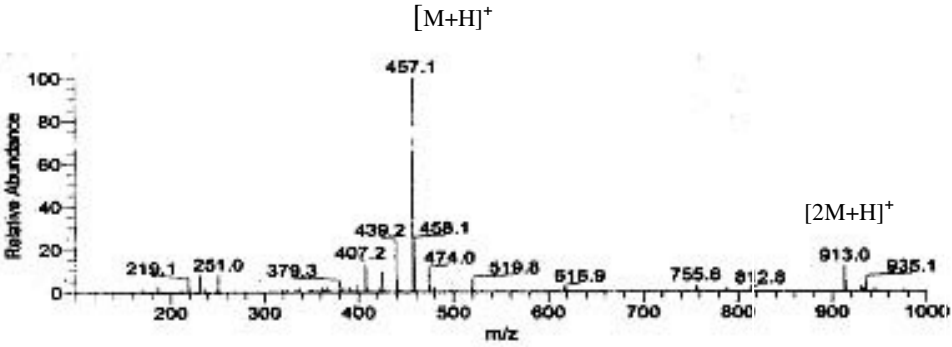
Although the ROESY data was not available for citreonigrin D, the relative stereochemistry of the stereocenters in this compound was assumed to be similar to the previous compounds, especially the southern part of molecule. However, because of no ROESY data available, the relative configuration of C-4' could not be established in this study.

Table 3.1.1.2..2.1 NMR data of Citreonigrin D in DMSO-d₆ at 500 MHz (¹H) and 125 MHz (¹³C)

Position	¹ H δ (ppm) <i>J</i> _{H-H} (Hz)	¹³ C δ (ppm)	HMBC (H to C)
1		154.0	
2	6.05 s	114.8	3, 5, 10
3		162.7	
4		82.6	
5		55.8	
6	3.35 s	50.5	7
7	4.52 s	79.7	5, 9, 10
8		46.6	
9	2.16 dd (12.6; 3.8)	45.5	
10		76.4	
11	Aα 1.74 dd (9.3; 3.8) Bβ 1.54 dd (12.6; 9.3)	28.5	
12	1.17 s	16.2	8, 9, 7'
13	1.22 s	21.0	1, 9, 10
14	1.15 s	25.8	4, 5, 15
15	1.45 s	21.1	4, 5, 14
1'	A 5.35 s B 5.12 s	111.4	2', 3', 7'
2'		147.5	
3'		48.6	
4'	3.55 d (5.4)	80.2	11, 6', 9'
6'		211.5	
7'		69.7	
8'		168.3	
9'	1.22 s	20.4	11, 2', 3', 4'
4'-OH	6.54 d (5.4)		
8'-OCH ₃	3.83 s	52.5	8'

3.1.1.3 New Preaustinoïd A-type Meroterpenes

3.1.1.3.1 Citreonigrin E

Citreonigrin E	
Synonym(s)	: -
Biological Source	: <i>P. citreonigrum</i>
Sample code	: PC 3.3.6.6.3.J
Amount	: 19.6 mg
Molecular Formula	: C ₂₆ H ₃₂ O ₇
Molecular Weight	: 46 g/mol
Solubility	: CH ₃ OH, CH ₂ Cl ₂
Physical Description	: White crystals (Acetone/water)
Optical rotation	: [α] _D ²⁰ +56° (c, 0.1 in CH ₃ OH)
HPLC Retention Time (R _t)	: 26.89 min. (Standard gradient)
Structure	UV Spectrum
	
(+) ESI-MS	
	

Citreonigrin E was isolated as pale yellow solids in CH₃OH and white crystals after recrystallisation with acetone/water. It gave a pseudomolecular ion peak at *m/z* 457.1 (M + H)⁺ in the positive mode ESI-MS. Based on the analysis 1D and 2D NMR data (see table 3.1.1.3.1.1), its structure was quite different to the previous four isolated meroterpenes with regard to, mainly, the partial structure of 3-hydroxy-3-methyl-2,4-dioxo at bicyclo [3.3.1] nonane system in the northern part of molecule. This fact was also supported by the different between UV absorption pattern of citreonigrin E and that of the four previous meroterpenes.

Carbon NMR data of citreonigrin E indicated the presence of six olefinic (*sp*²) carbons at δ 125.7, 140.1, 128.4, 135.5, 111.3 and 144.0 ppm for C-1, C-5, C-6, C-10, C-1' and C-2', respectively. Furthermore, it has two keto carbonyls at δ 208.9 ppm (C-4') and δ 205.3 ppm (C-6'). Interestingly, the presence of six diastereotopic methylene protons in this compound were observed in the ¹H-NMR spectrum and confirmed by HMQC experiment. However, it was quite different to citreonigrin A, B, C, and D which have only four olefinic carbons, two methylene protons and one keto carbonyls.

Based on the HMBC correlations of the methyl protons in the molecule, some substructures were then set up to elucidate the complete structure of citreonigrin E (figure 3.1.1.3.1.1). Substructure I was built based on the correlations of H₃-14 and H₃-15 to C-4, C-5 and C-6. The correlations of H₃-13 to C-1, C-5, C-9 and C-10 resulted in substructure II. The ³*J*_{HC} correlations of H₃-12 to C-8, C-9, and C-7', and H₃-9' to C-2' and C-4' gave the substructures III and V, respectively. The presence of two keto carbonyls in the substructure VI were confirmed by the correlations of H₃-10' to C-4' and C-6'. Finally, the substructure IV was formed by a single correlation of H₃-OMe to C-8'.

The connectivities between substructures in the molecule resulted in the proposed structure of citreonigrin E (VII). As like as the previous isolated meroterpenes, the connectivity between C-3 and C-4 through an oxygen atom could not be directly proved directly from the NMR experiment. Nevertheless, the correlations of the methylene protons (H₂-2) to C-3 (a carbonyl atom at δ 169.2 ppm) and C-5 (δ 140.1 ppm) would assume the formation of a planar unsaturated δ -lactone ring (ring A). The same problem was also occurred to assign the position of carbomethoxy group at C-7'.

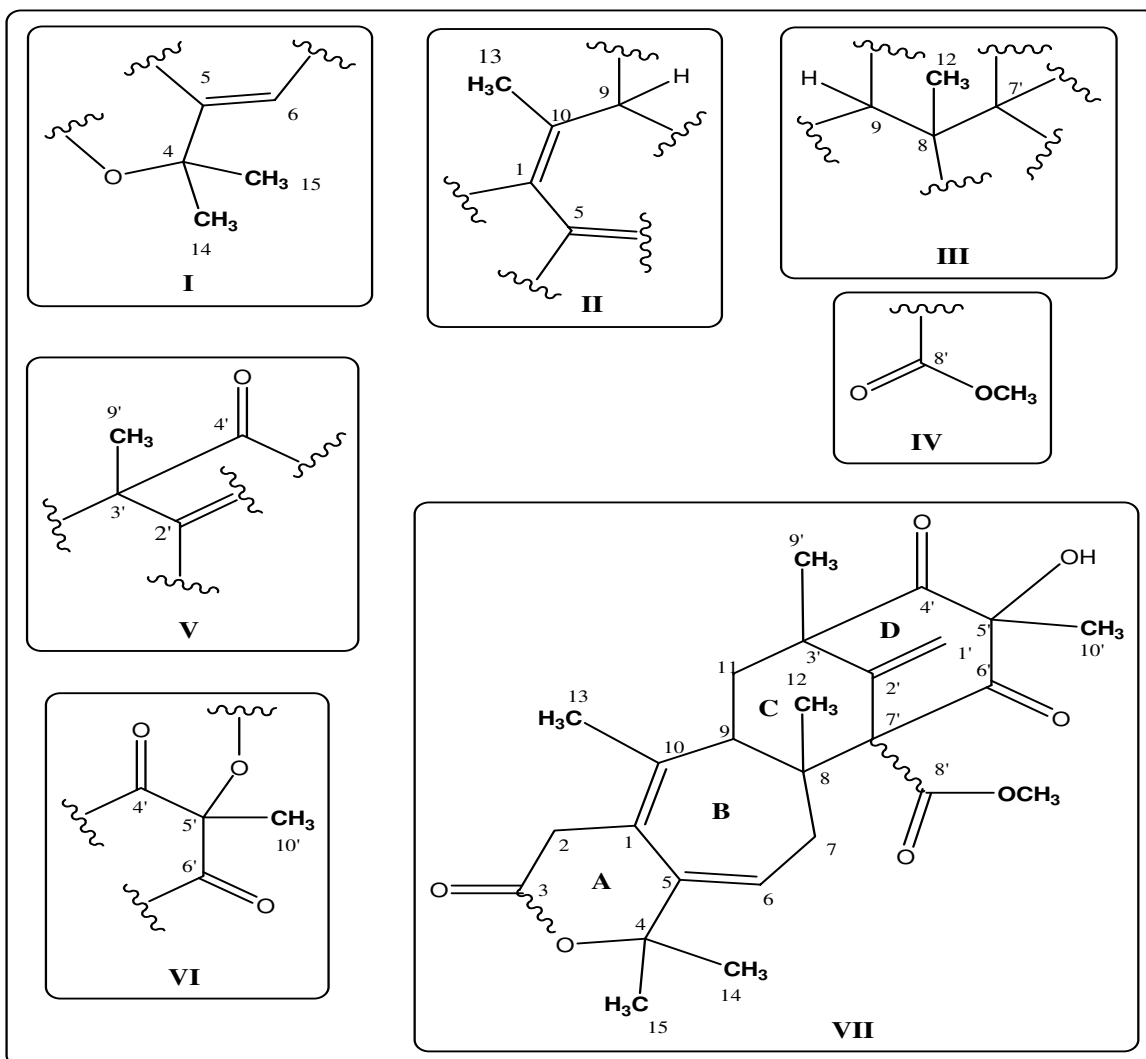


Figure 3.1.1.3.1.1 Partial structures of citreonigrin C based on the correlations of methyl protons in the HMBC spectrum

The direct connectivity between substructure I and II was evident by the correlations of H₃-10, H₃-14 and H₃-15 to C-5. Substructures II and III was directly linked by a correlations of H₃-12 and H₃-10 to C-9 (δ 44.4 ppm) in HMBC spectrum. Meanwhile, indirect connectivity between substructures I and III through C-6 and C-7 was proved by the HMBC correlations H₂-7 to C-5, C-6, C-8 and C-9, as well as H-6 to C-4 and C-8. In the mean time, the position of H₂-7 next to H-6 was proved by a spin system formed by these protons in the COSY experiment. The connectivity between substructures I, II, and III resulted in the southern part of citreonigrin C molecule containing a cycloheptadiene

partial structure which was not observed in the citreonigrin A, B, C, and D. The presence of a conjugated double bond was also detected by the presence of $^4J_{HC}$ from H₃-10 to C-5, as well as H₃-14 and H₃-15 to C-6.

The presence of a bicyclo [3.3.1]nonane system in the northern part of molecule was formed by the connectivity between substructure III, V and VI. The direct link between substructures V and VI was confirmed by HMBC correlations of H₃-9' and H₃-10' to C-4'. The position of exomethylene group (H₂-1') was assigned by HMBC correlations of H₂-1' to C-2', C-3' and C-7'. Furthermore, rare $^4J_{HC}$ correlations of H-1'B to C-6' and C-8 helped the connectivity amongst substructure III, V, VI to form the northern part molecule of citreonigrin E. The position of OH group at C-5', however, could not directly determined by HMBC experiment. Its position was identified by a ROESY correlation to H₃-10' (Fig. 3.1.1.1.9) and the chemical shifts of C-5' at δ 77.2 ppm. Figure 3.1.1.3.1.2 shows some diagnostic HMBC correlations and observed COSY spin systems of citreonigrin E.

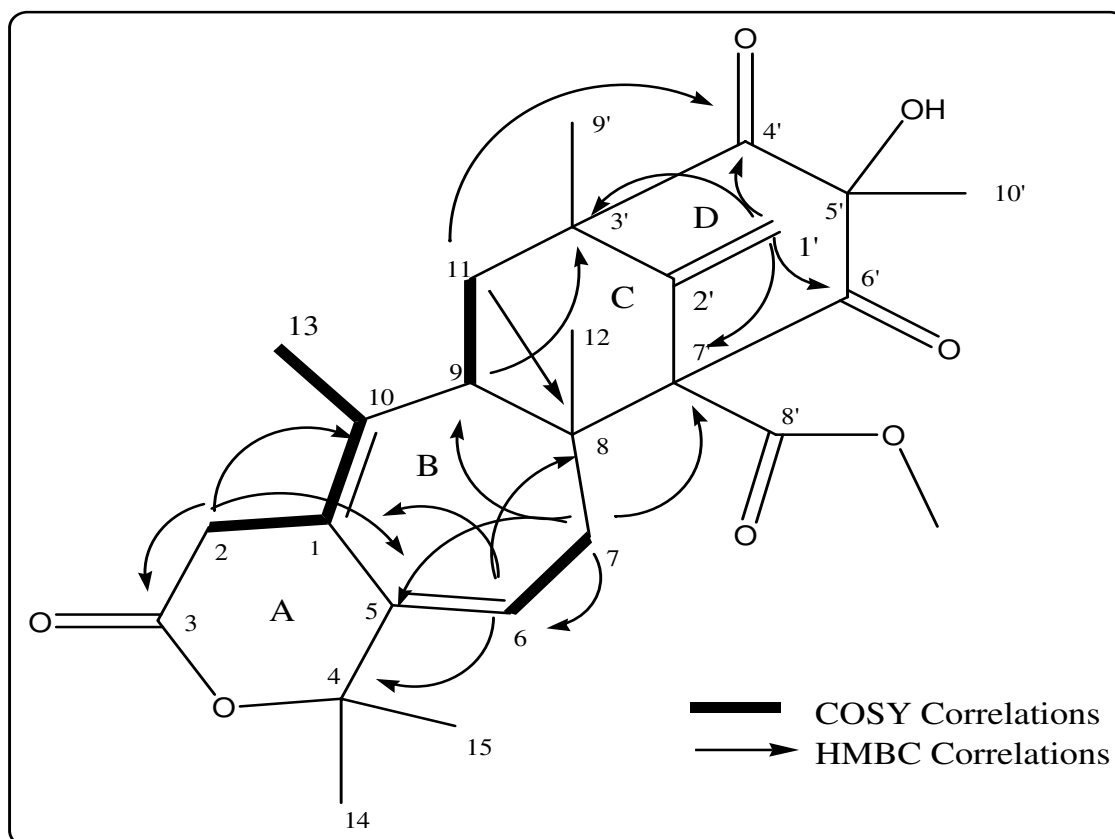


Figure 3.1.1.3.1.2 COSY (at 300 MHz) and diagnostic HMBC correlations of Citreonigrin E in DMSO-d₆

A single X-ray crystallography was performed to prove the proposed structure of citreonigrin E and establish the relative stereochemistry at its 6 chiral centers (Figure 3.1.1.3.1.3). Once X-ray model has obtained, the ROESY experiment was performed to confirmed the relative stereochemistry of the stereocenters in the molecule.

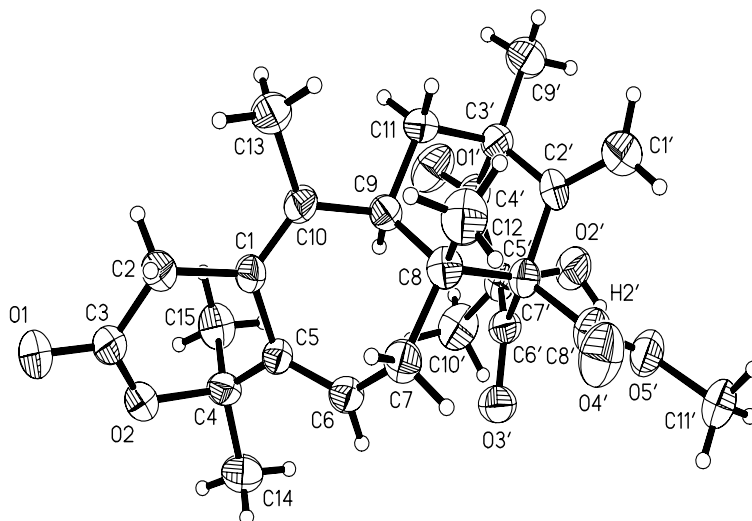


Figure 3.1.1.3.1.3 X-ray crystallography of citreonigrin E

Strong ROESY correlations of H₃-12 with H₃-9' and H-11β, as well as ROESY correlations of H₃-OCH₃ with H₃-12 and H₃-9' verified the β-configuration of Me-12, Me-9', and carbomethoxy group at C-8, C-3', and C-7', respectively. However, it was difficult to determine the relative configuration of H-9 because of its overlapping with H-11α and H-7B. Nevertheless, H-9 was determined to be located in α-configuration in X-ray experiment and its comparison to the previous compounds.

The relative configuration of C-7 was determined by the ROESY correlations of H-7A with H-6, H₃-14 and H₃-OCH₃, consecutively. These correlations indicated that H-7A was located at the pseudo-equatorial, meanwhile, H-7B was located at the pseudo-axial. On the other side, the relative stereochemistry of C-5' was determined by correlations of H₃-10' with H₃-9 and supported by the correlation of 5'-OH with H₃-OCH₃, which turned to the correlation of H₃-OCH₃/ H-12.

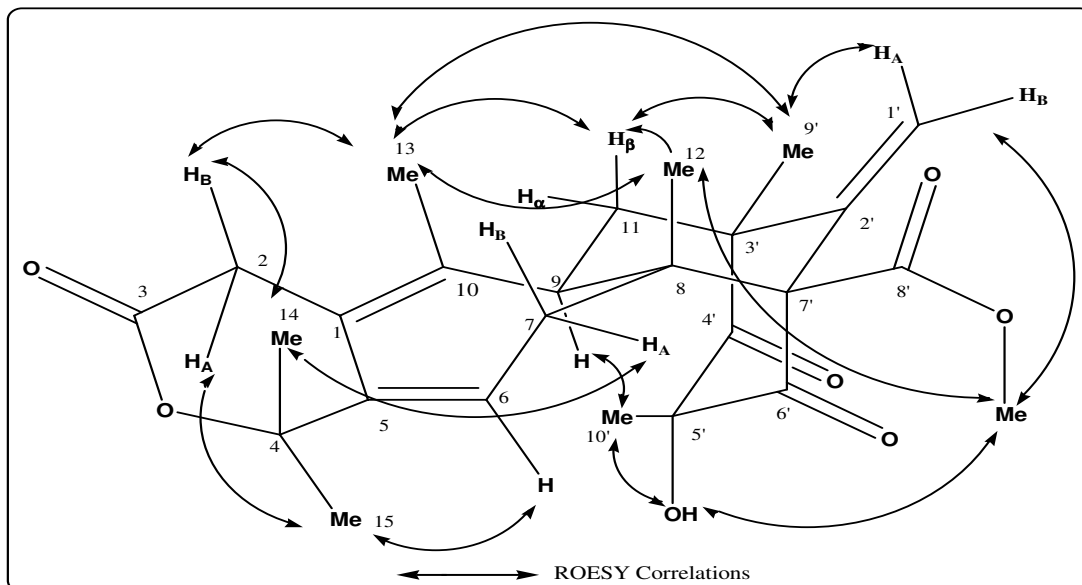


Figure 3.1.1.3.1.4 Selected ROESY correlations of citreonigrin E in DMSO-d₆

Table 3.1.1.1.5 NMR data of Citreonigrin E in DMSO-d₆ at 600 MHz (¹H) and 75 MHz (¹³C)

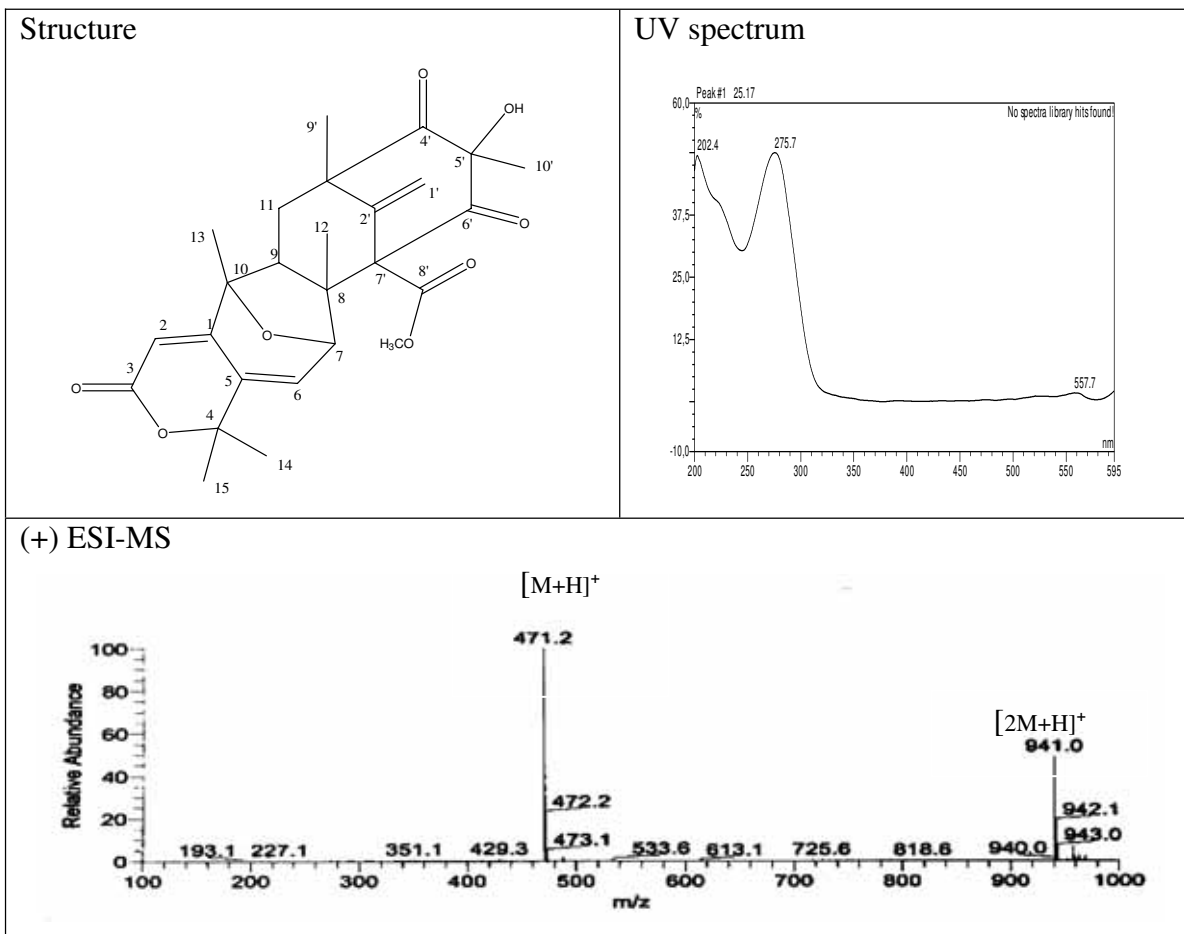
Position	¹ H δ (ppm) <i>J</i> _{H-H} (Hz)	¹³ C δ (ppm)	HMBC (H to C)	ROESY
1		125.7		
2	A 3.47 d (21.1) B 3.30 d (21.1)	33.7	1, 2, 3, 5, 10 1, 3, 10	13, 15 13, 14
3		169.2		
4		81.0		
5		140.1		
6	5.74 dd (8.2; 5.3)	128.4	4, 6, 7, 8	7A, 14, 15
7	A 2.90 dd (13.9; 8.2) B 1.70 dd ^o	36.0	5; 6; 7, 8, 9; 12, 7' 5; 6; 8, 9; 12, 7'	6, 11B, 12, 8'-OCH ₃ too complex ^o
8		67.0		
9	1.70 dd ^o	44.4	8; 12, 3', 7'	too complex ^o
10		135.5		
11	Aβ 1.88 dd (14.8; 12.6) Bα 1.70 dd ^o	41.5	8, 9; 2', 3', 4'	12, 13, 9' too complex ^o
12	1.21 s	19.6	9, 12, 7'	7A, 11A, 1'A, 1'B
13	1.63 s	15.0	1, 5, 9, 10, 13	2A, 2B, 11A, 12
14	1.41 s	26.2	4, 5, 6, 14, 15	7A, 15
15	1.20 s	28.7	4, 5, 6, 14, 15	6, 14

1'	A 5.24 s B 4.70 s	111.3	<u>1'</u> , 8, 11, 2', 3', 4', 7' <u>1'</u> , 8, 11, 2', 3', 6', 7'	11A, 12, 1'B, 8'-OCH ₃ , 9' 12, 1'A, 8'-OCH ₃ , 9'
2'		144.0		
3'		50.2		
4'		208.9		
5'		77.2		
6'		205.3		
7'		70.7		
8'		169.7		
9'	1.37 s	21.6	2', 3', 4', <u>9'</u>	11A, 1'A, 1'B
10'	1.18 s	15.6	4', 5', 6', <u>10'</u>	5'-OH
5'-OH	6.55 s			8'-OCH ₃ , 10'
8'-OCH ₃	3.63.s	51.8	8', 8'- <u>O</u> CH ₃	5'-OH, 6, 7A, 12, 1'A, 1'B

^o mutually overlapped

3.1.1.3.2 PC 3.3.6.8.4.F

PC 3.3.6.8.4.F	
Synonym(s)	:
Biological Source	: <i>P. citreonigrum</i>
Sample code	: PC 3.3.6.8.4.F
Amount	: 0.4 mg
Molecular Formula	: C ₂₆ H ₃₀ O ₈
Molecular Weight	: 470 g/mol
Solubility	: CH ₃ OH
Physical Description	: White powders
HPLC Retention Time (R _t)	: 25. 17 min (Standard gradient)



The analysis of NMR data indicated that PC 3.3.6.8.4.F was structurally related to citreonigrin E. PC 3.3.6.8.4.F was isolated only in a small amount as white powders and revealed a pseudomolecular ion at m/z 471.2 $[M+H]^+$ in the positive mode ESI-MS. It indicated that PC 3.3.6.8.4.F has 14 mass units higher compared to citreonigrin E which implied that this compound contained an additional oxygen atom by replacing two olefinic protons as seen in the ^1H -NMR spectrum.

Like citreonigrin E, PC 3.3.6.8.4.F contained a partial structure of 3-hydroxy-3-methyl-2,4-dioxo and 8-methylene at bicyclo [3.3.1]nonane system in the northern part of molecule. However, this compound differed to citreonigrin E with regard to the position of two double bonds and the presence of oxygen bridge in the southern part of molecule. The presence of olefinic proton (H-2) at δ 5.60 ppm was confirmed by its correlation to C-3 (δ 163.5 ppm), C-5 (δ 132.0 ppm) and C-10 (δ 77.0 ppm) in HMBC experiment. Other olefinic proton (H-6) at δ 6.23 ppm was assigned by its HMBC correlations to C-1 (δ 156.5 ppm) and C-4 (δ 81.5 ppm). The presence of two oxygenated carbon at δ 77.0 ppm (C-10)

and δ 79.0 ppm (C-7) and observed HMBC correlation of H-7 to C-10 suggested the presence of oxygen bridge between C-7 and C-10 to form a substructure of 8-OxaBicyclo[3.2.1]Octa-2-ene system.

Since the compound was isolated only in a small amount, however, the presence of one olefinic carbon (C-2) could not be spectroscopically confirmed in this study. The same problem was also faced to justified the position of H-7 and H-6 Like the previous meroterpenes in this study, the connectivities between C-3 and C-4 through an oxygen atom, as well as C-7'/C-8' bond could not be proved for this compound. Nevertheless, general HMBC correlations (figure 3.1.1.3.2.1) revealed the close relationships between PC 3.3.6.8.4.F and citreonigrin E. Thus, although there was no ROESY data available for this compound, it was also assumed that relative stereochemistry of the stereocenters in PC 3.3.6.8.4.F was similar to that found in citreonigrin E.

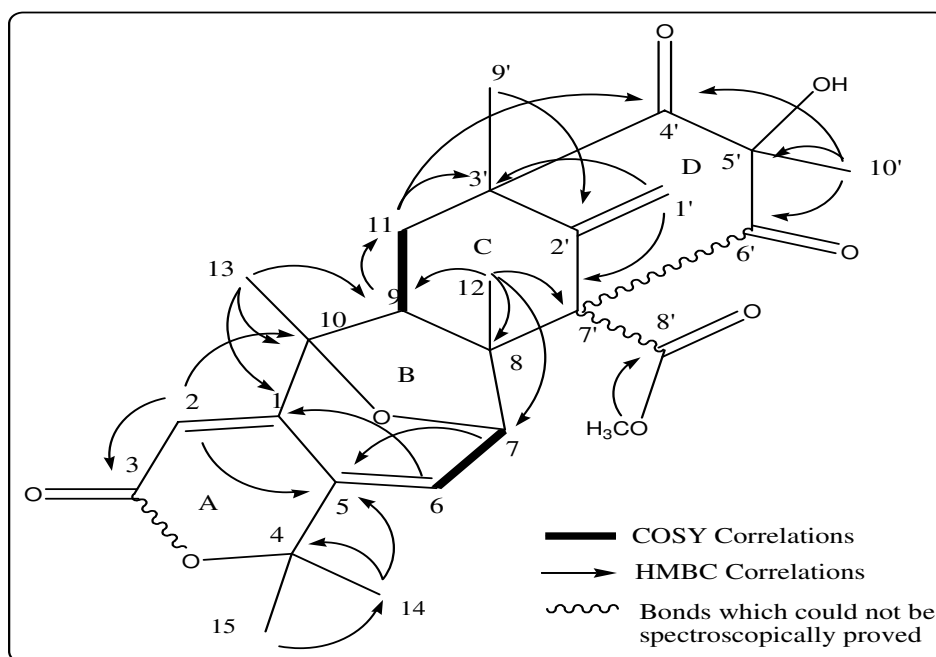


Figure 3.1.1.1.12. COSY (at 300 MHz) and HMBC correlations of PC 3.3.6.8.4.F in DMSO-d₆

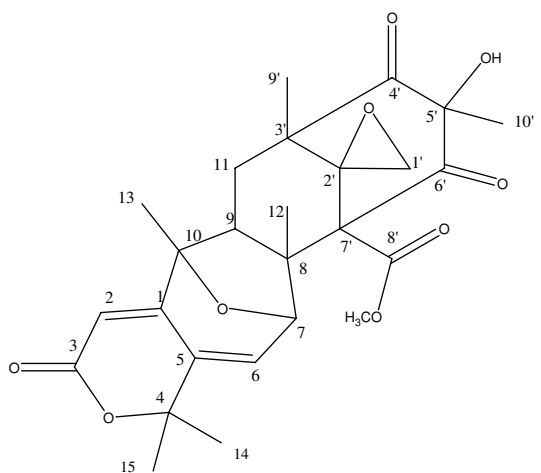
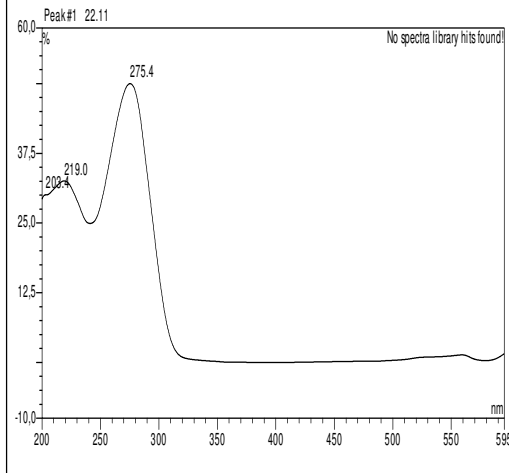
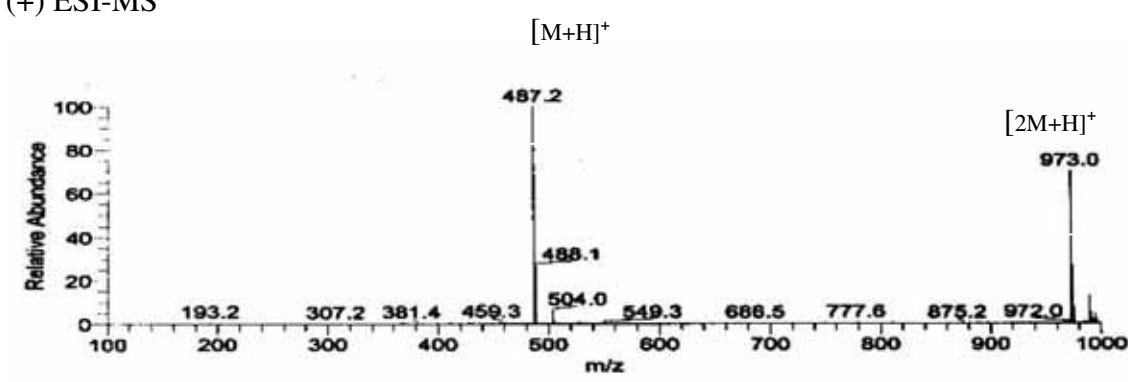
Table 3.1.1.1.6. NMR data of PC 3.3.6.8.4.F in DMSO-d₆ at 600 MHz (¹H) and 150 MHz (¹³C)

Position	¹ H δ (ppm) J_{H-H} (Hz)	¹³ C ^a δ (ppm)	HMBC H to C
1		156.5	
2	5.60 d (1.4)	?	3, 5, 10
3		163.5	

4		81.5	
5		132.0	
6	6.23 dd (5.1 ; 1.4)	106.0	1,4
7	4.81 d (5.1)	79.0	5,8,9,10,12
8		54.0	
9	1.99 dd (12.3 ; 3.6)	48.0	11
10		77.0	
11	A 1.80 dd (14.2 ; 12.3) B 1.18 dd (14.2 ; 3.6)	38.0	3', 4'
12	1.29 s	20.5	7,8,9,7'
13	1.28 s	15.5	1,9,10
14	1.39 s	30.5	4,5
15	1.47 s	26.5	4,5,14
1'	A 5.43 s B 5.20 s	115.0	3', 7' 2', 3', 7'
2'		142.0	
3'		51.0	
4'		208.9	
5'		78.0	
6'		204.0	
7'		71.0	
8'		169.0	
9'	1.37 s	20.5	11, 3', 4'
10'	1.04 s	15.8	4', 5', 6'
8'-OMe	3.75 s	52.0	8'
5'-OH	6.65 s		4', 5', 6'

^a Based on HMBC correlations

3.1.1.3.3 PC 3.3.6.8.4.A

PC 3.3.6.8.4.A	
Synonym(s)	:
Biological Source	: <i>P. citreonigrum</i>
Sample code	: PC 3.3.6.8.4.A
Amount	: 0.6 mg
Molecular Formula	: C ₂₆ H ₃₀ O ₉
Molecular Weight	: 486 g/mol
Solubility	: CH ₃ OH
Physical Description	: White powders
HPLC Retention Time (R _t)	: 22.08 min. (Standard gradient)
Structure	UV Absorption
	
(+) ESI-MS	
	

PC 3.3.6.8.4.A, as like as PC 3.3.6.8.4.F, was also isolated as a small amount of white powders from ethyl acetate extract of *P. citreonigrum*. The analysis of NMR data and UV

absorption pattern of this compound (λ_{\max} 219.0 and 275.4 nm) suggested that it was structurally related to PC 3.3.6.8.4.F. Furthermore, the positive mode ESI-MS experiment of this compound revealed a pseudomolecular ion peak at m/z 487.2 ($M + H$)⁺ which was 16 mass unit higher than that of PC 3.3.6.8.4.F and additionally suggested the presence of an extra oxygen atom in the molecule.

Analysis 1D and 2D NMR data indicated that the southern part molecule of this compound (ring A and B) was similar to that of PC 3.3.6.8.4.A. In the northern part, however, PC 3.3.6.8.4.A differed to PC 3.3.6.8.4.F with regard the absence of exomethylene function in the bicyclo [3.3.1]nonane system. The chemical shifts of C-2' at δ 59.5 ppm not only confirmed the absence of exomethylene function at this position, but also suggested the presence epoxide function between C-2' and C-1'. In addition, the chemical shifts of two extra methylene protons (H₂-1' at δ 3.06 and 2.67 ppm) and their coupling of ² J_{H-H} 3.1 Hz also suggested the presence of epoxide function at this position. Unfortunately, this assignment could not be directly evident by HMBC correlation.

Since the compound was isolated only in a small amount, the presence of some carbons, such as C-2, C-3, C-6, etc., could not be spectroscopically defined. Thus, this problem was also happened to evident some bonds in the molecule. Nevertheless, the observed HMBC and COSY correlations (figure 3.1.1.3.1.1) suggested the proposed structure which was closely related to PC 3.3.6.8.4.F and citreonigrin E. Thus, although the ROESY experiment was not performed to this compound, the relative configuration of the stereocenters in the molecule was assumed to be identical to that of citreonigrin E.

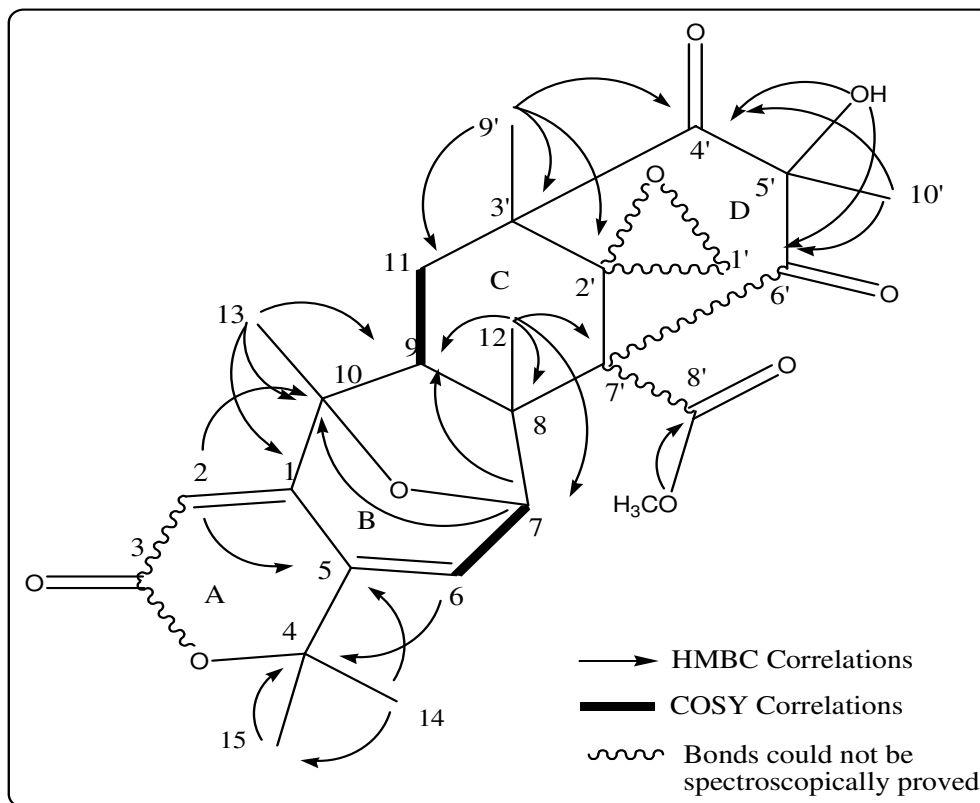


Figure 3.1.1.1.13. COSY (at 500 MHz) and some important HMBC correlations of PC 3.3.6.8.4.A in DMSO- d_6

Table 3.1.1.1.7 NMR data of PC 3.3.6.8.4.A in DMSO- d_6 at 600 MHz (^1H) and 150 MHz (^{13}C)

Position	^1H δ (ppm) $J_{\text{H-H}}$ (Hz)	$^{13}\text{C}^a$ δ (ppm)	HMBC H to C
1		156.5	
2	5.65 s	?	5,10
3		?	
4		82.0	
5		132.0	
6	6.19 d (5.0)	?	4
7	4.80 d (5.0)	80.5	9,10
8		57.0	
9	1.97 dd (12.6 ; 3.5)	48.5	
10		78.5	
11	A 2.07 dd (13.9 ; 12.6) B 1.24 dd (13.9 ; 3.5)	34.5	
12	1.46 s	?	7,8,9,7'

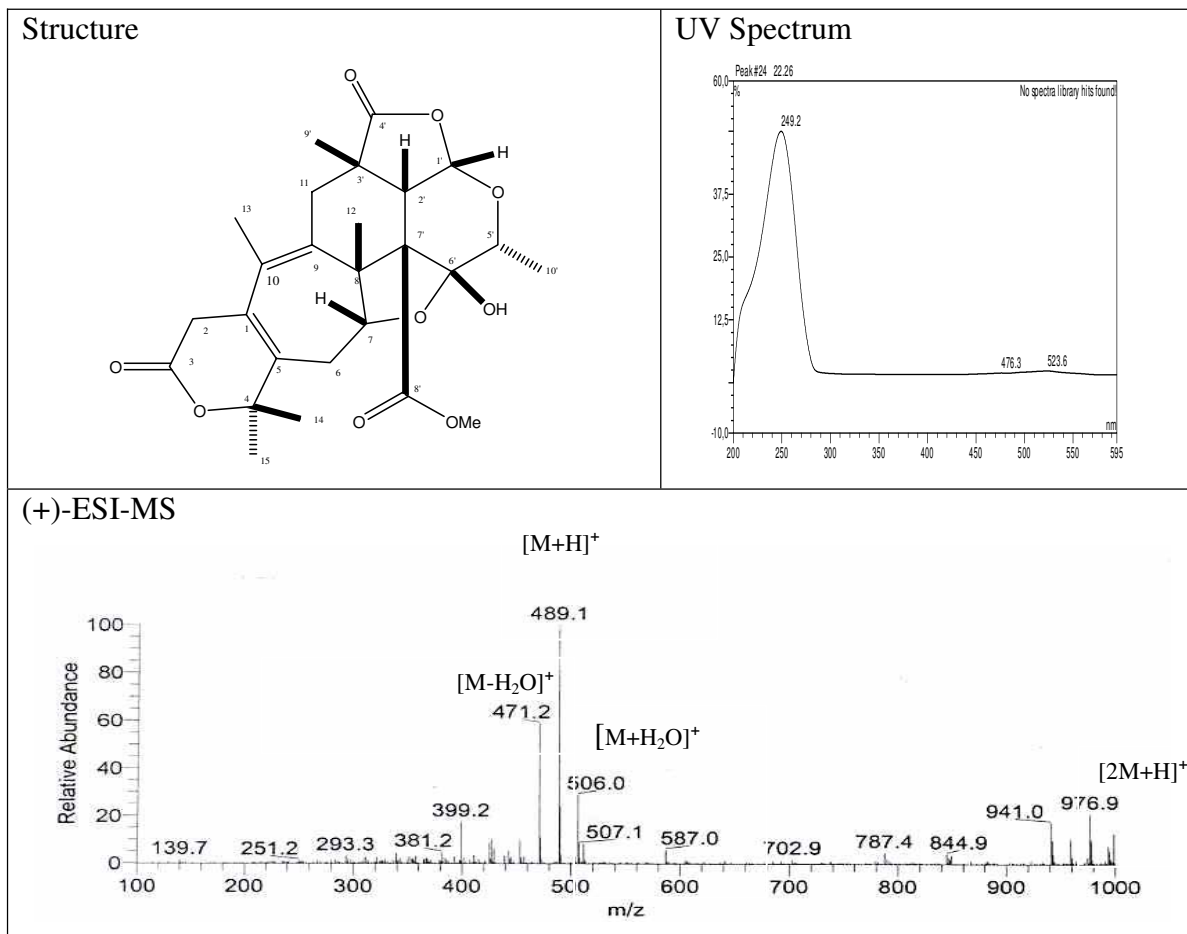
13	1.33 s	?	1,9,10
14	1.52 s	26.0	4,5,15
15	1.36 s	32.0	4,5,14
1'	A 3.06 d (3.1) B 2.67 d (3.1)	?	
2'		59.5	
3'		52.0	
4'		210.5	
5'		78.0	
6'		205.5	
7'		68.5	
8'		168.0	
9'	1.03 s	30.5	11,2',3',4'
10'	1.07 s	?	4',6'
8'-OMe	3.64 s	?	8'
5'-OH	6.41 s		4',6'

^a Based on HMBC correlations

3.1.1.4 New Paraherquonin-type Meroterpenes

3.1.1.4.1 Citreonigrin G

Citreonigrin G	
Synonym(s)	: -
Biological Source	: <i>P. citreonigrum</i>
Sample code	: PC 3.3.6.6.3.D
Amount	: 6.75 mg
Molecular Formula	: C ₂₆ H ₃₂ O ₉
Molecular Weight	: 488 g/mol
Solubility	: CH ₃ OH
Physical Description	: Pale yellow solids
Optical rotation	: [α] _D ²⁰ -6 (c 0.1, CH ₃ OH)
HPLC Retention Time (R _t)	: 22.26 min (Standard gradient)



Citreonigrin G was isolated as pale yellow solids from ethyl acetate extract of *P. citreonigrum*. The positive mode of ESI-MS data of this compound revealed a pseudomolecular ion peak at m/z 489.1 $[M+H]^+$. The maximum of UV absorption at 249.2 and 1D-NMR spectroscopic data indicated the structure of citreonigrin G was quite different to the previous isolated meroterpenes.

The proton NMR spectrum of this compound, as like as the previous isolated meroterpenes, still showed the presence of six methyls, six methylene protons and one methoxy group. This compound, however, revealed the presence of more methyne protons at δ 6.11 ppm (H-1'), 3.99 ppm (H-5'), 3.82 ppm (H-7) and 3.12 ppm (H-2') and the absence of olefinic proton. Meanwhile, the ^{13}C -NMR and DEPT spectra still showed the presence of four quaternary olefinic carbons at C-1 (δ 126.5 ppm), C-5 (δ 131.6 ppm), C-9 (δ 134.7 ppm) and C-10 (δ 127.0 ppm). In addition, the presence of one quaternary (C-6') and one tertiary (C-1') hemi-acetal carbons at δ 100.2 ppm and δ 97.9 ppm, respectively, were also detected by ^{13}C NMR and DEPT spectra of this compound.

Based on the correlations of methyl proton in HMBC spectrum, some substructures were set up and described as shown in figure 3.1.1.4.1.1. The substructure I was formed by the correlations of H₃-14 and H₃-15 to C-4, C-5 and C-6. The correlations of H₃-13 to C-1, C-8, C-9 and C-10 would give the substructure II. The presence of H₃-12 was confirmed by its HMBC correlations to C-7, C-8, C-9, and C-7' in substructure III. The correlations of H₃-9' to C-11, C-2', C-3' and C-4', and the correlations H₃-10' to C5 and C6 resulted in substructure IV and V, respectively.

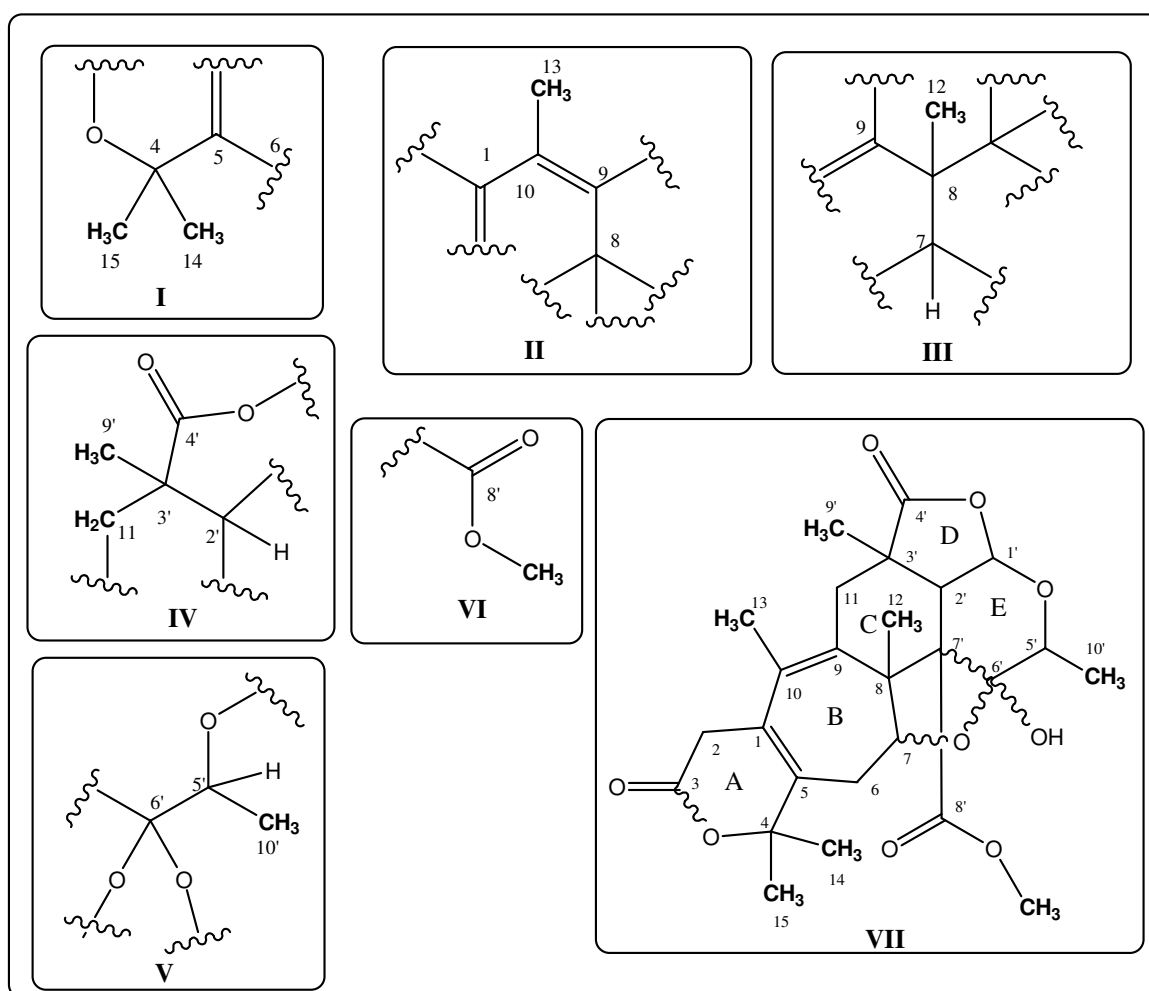


Figure 3.1.1.4.1.1. Partial structures of citreonigrin G based on the correlations of methyl protons in the HMBC spectrum

The connectivity amongst the substructures to form the proposed structure VII was confirmed by HMBC and COSY correlations as summarized in table 3.1.1.4.1.1 and figure 3.1.1.4.1.2. As shown in the structure VII, the presence of unsaturated δ -lactone ring was

evident by HMBC correlations H₂-2, H₃-14, H₃-15 to C-5, an olefinic carbon at δ 131.6 ppm. Although the ester bond could not be spectroscopically proved, it was assumed that this part of structure was planar. The position of H-7 (δ 3.82 ppm) adjacent to H₂-6 was proved by the spin system formed by these protons in the COSY spectrum. The correlation of H₃-12 to C-7 and followed by the correlation H-7 to C-5 linked the substructure I and III. HMBC correlation of H₃-12 and H₃-13 to an olefinic carbon at δ 134.7 ppm (C-9) suggested not only the connectivity of between substructure II and III, but also the position one of the two double bonds in the heptadiene system. The chemical shifts of C-1 and C-5 at δ 126.5 and 131.6 ppm, respectively, suggested the position of another double bond which linked the substructure I and II in the southern part of molecule.

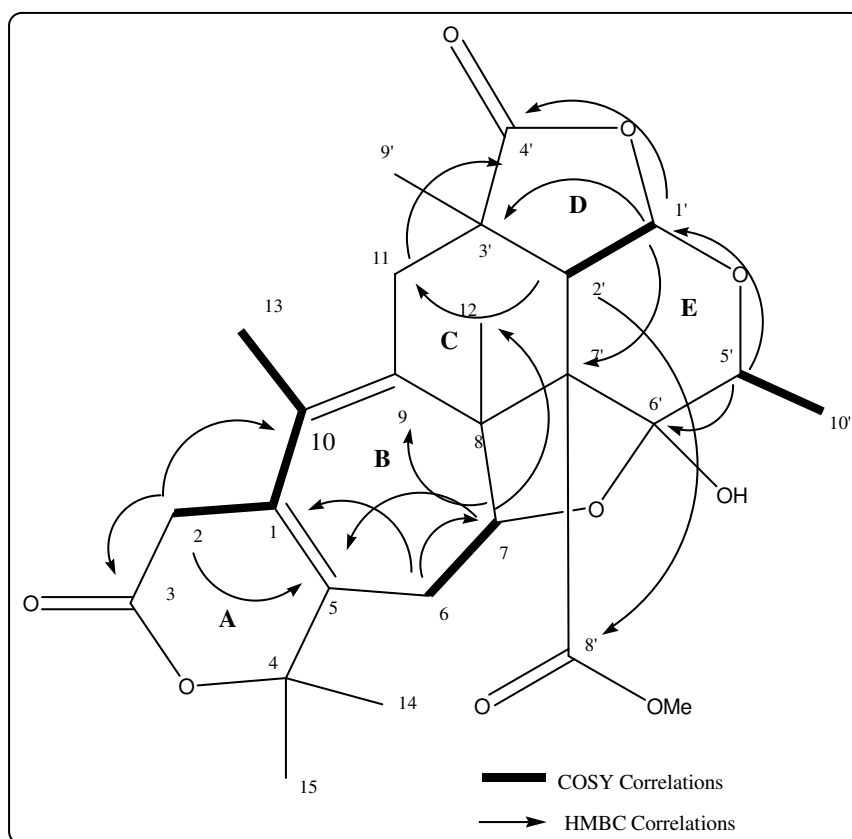


Figure 3.1.1.4.1.2. COSY (at 300 MHz) and diagnostic HMBC correlations of Citreonigrin G in DMSO-d₆

In the northern part of molecule, however, the assignment was not as easy as that in the southern part molecule. The connectivity between substructure IV and V through C-1 was proved by HMBC correlations of H-1' to C-4' at δ 177.2 ppm and C-5' at δ 70.7 ppm. In

the mean time, HMBC correlation of H₂-11 to C-10, C-8, C-2' and C-4' not only confirmed the assignment H₂-11 at δ 2.73 and 2.35 ppm but also proved the link between substructures II and IV through C-11.

The presence of E ring system was confirmed by the HMBC and COSY correlations of three methyne protons, i.e., H-1', H-2' and H-5', incorporated in the system. The presence of a methyne proton (H-2') at δ 3.12 ppm was confirmed not only by its COSY correlation to H-1' (δ 6.11 ppm), but also by its HMBC correlation to C-8, C-8', C-1' and C-4'. Consequently, a quartet proton (H-5') at δ 3.99 ppm coupled to a doublet methyl (H₃-10') at δ 1.20 ppm by forming an observed spin system in the COSY spectrum and correlated to two hemi-acetal carbons, C-1' (δ 97.9 ppm) and C-6' (δ 100.2 ppm) in HMBC spectrum.

Unfortunately, the presence of C-6'/C-7' bond could not be evident in this study because neither key correlation of H-2'/C-6' nor H-5'/C-7' was observed in the HMBC spectrum. In addition, the HMBC experiment could also not prove the presence of an oxygen bridge between C-7 and C-6', as well as, the position of 6'-OH in the molecule. The presence of the oxygen bridge was assumed only by the chemical shifts of two carbons and the planarity of this substructure. Meanwhile, the position of 6'-OH was confirmed not only by the chemical shifts of C-6' at δ 100.2 ppm but also by ROESY experiment which showed the correlation of 6'-OH with H-5' and H₃-10'.

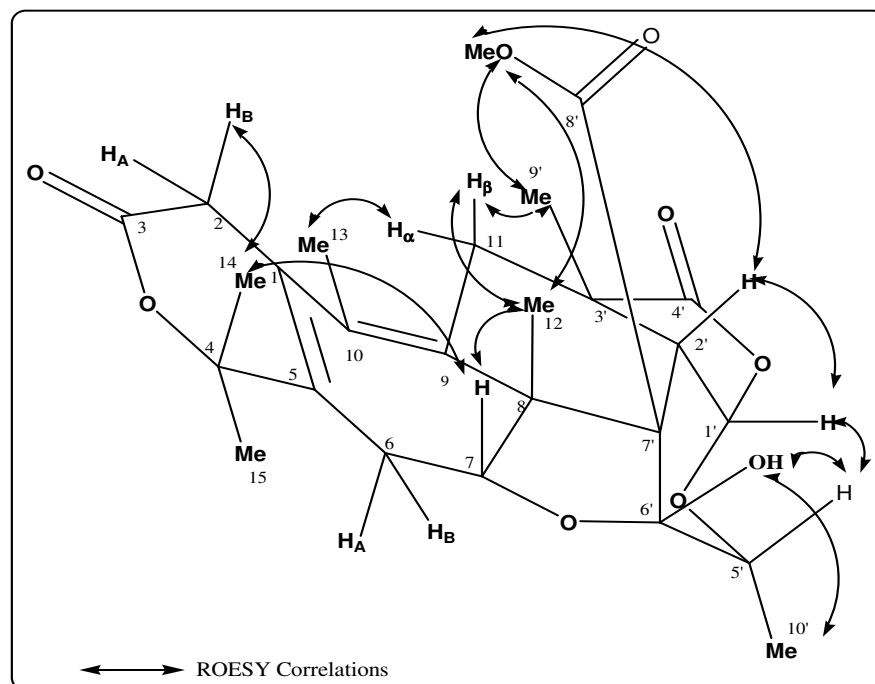


Figure 3.1.1.4.1.3. Stereo drawing of Citreonigrin G showing the observed ROESY correlation in DMSO-d₆

The establishment of relative stereochemistry of the eight stereocenters in citreonigrin G was established therefore by a ROESY experiment (Fig. 3.1.1.4.1.3). The strong correlations of H₃-12 with H-11 β , H₃-OCH₃, H-7 and H-2' suggested the β -position of Me-12, carbomethoxy group, H-7 and H-2'. The close proximity of H-2', H-1', H-5' and 6'-OH was determined by ROESY correlations of H-2'/H-1', H-1'/H-5', H-1'/H₃-9' and H-5'/6'-OH, consecutively. In the mean time, relative configuration of C-11 was confirmed by the correlation of H₃-9'/H-11 β , as well as the correlation of H₃-13/H-11 α .

Table 3.1.1.4.1.1. NMR data of Citreonigrin G in DMSO-d₆ at 600 MHz (¹H) and 75 MHz (¹³C)

Position	¹ H δ (ppm) J_{H-H} (Hz)	¹³ C δ (ppm)	HMBC (H to C)	ROESY
1		126.5		
2	A 3.54 d (20.0) B 2.98 d (20.0)	34.5	1, 3, 5 1, 3, 5	2B, 6B, 13, 15, 9' 6B, 13, 15, 9'
3		170.1		
4		83.7		
5		131.6		
6	A 2.90 dd (19.3; 6.2)	33.5		6B, 13, 15, 9'

	B 2.27 dd (19.3; 9.5)		1, 7	13, 15, 9'
7	3.82 dd (9.5; 6.2)	79.9	5, 9, 12	6A, 6B, 12, 13, 15, 10'
8		49.2		
9		134.7		
10		127.0		
11	A α 2.73 d (13.5) B β 2.35 d (13.5)	33.3	8, 9, 10, 2', 3', 4', 9' 9, 10, 2', 3', 4'	11B, 13, 9' 12, 9'
12	1.38 s	12.5	7, 8, 9, 7'	
13	1.82 s	18.3	1, 8, 9, 10	12, 14
14	1.44 s	25.4	4, 5, 15	
15	1.46 s	26.5	4, 5, 14	
1'	6.11 d (6.8)	97.9	2', 3', 4', 7'	7, 5', 9'
2'	3.12 d (6.8)	45.4	8, 1', 3', 4', 7', 8', 9'	11B, 12, 9'
3'		45.6		
4'		177.2		
5'	3.99 q (6.3)	70.7	1', 6', 10'	7, 10', 8'-OCH ₃
6'		100.2		
7'		62.5		
8'		173.4		
9'	1.27 s	25.7	11, 2', 3', 4'	11B, 1'
10'	1.20 d (6.3)	13.4	5', 6'	6'-OH
6'-OH	6.16 s			12, 5', 8'-OCH ₃ , 10'
8'-OCH ₃	3.68 s	52.2	8'	12, 9'

3.1.1.4.2 Citreonigrin I

Citreonigrin I	
Synonym(s)	: -
Biological Source	: <i>P. citreonigrum</i>
Sample code	: PC 3.3.6.8.6.D
Amount	: 5.95 mg
Molecular Formula	: C ₂₄ H ₂₈ O ₇
Molecular Weight	: 428 g/mol
Solubility	: CH ₃ OH
Physical Description	: Pale yellow solids
Optical rotation	: $[\alpha]_D^{20}$ -35 (c, 0.1 in CH ₃ OH)
HPLC Retention Time (R _t)	: 23.77 min (Standard gradient)
Structure	UV spectrum
(+) ESI-MS	

Analysis of NMR data supported by the UV pattern of citreonigrin I (λ_{\max} 222.5 nm,) suggested the close relationships between the structure of citreonigrin I and citreonigrin G.

Positive mode ESI-MS experiment of citreonigrin I showed a pseudomolecular ion at m/z 429.4 $[M+H]^+$ which indicated that its molecular weight was 60 mass unit higher than that of citreonigrin G. Since the $^1\text{H-NMR}$ spectrum did not show the presence of any methoxy group, the difference between this compound and citreonigrin G was only the absence of a carbomethoxy group attached to C-7'.

As like as citreonigrin G, the $^1\text{H-NMR}$ spectrum of this compound still showed the presence of five singlet methyls, one doublet methyl, one hydroxy group, six methylene protons and the absence of an olefinic proton. Based on $^{13}\text{C-NMR}$ data, however, this compound revealed the presence of six quaternary olefinic carbons, instead of four that in citreonigrin G. As confirmed in the $^1\text{H-NMR}$ spectrum, the higher number of olefinic carbons resulted in the elimination of one methyne proton and the carbomethoxy group. Compared to citreonigrin G which has two hemi-acetal carbons, $^{13}\text{C-NMR}$ spectrum of citreonigrin I showed the presence of only one hemi-acetal carbon.

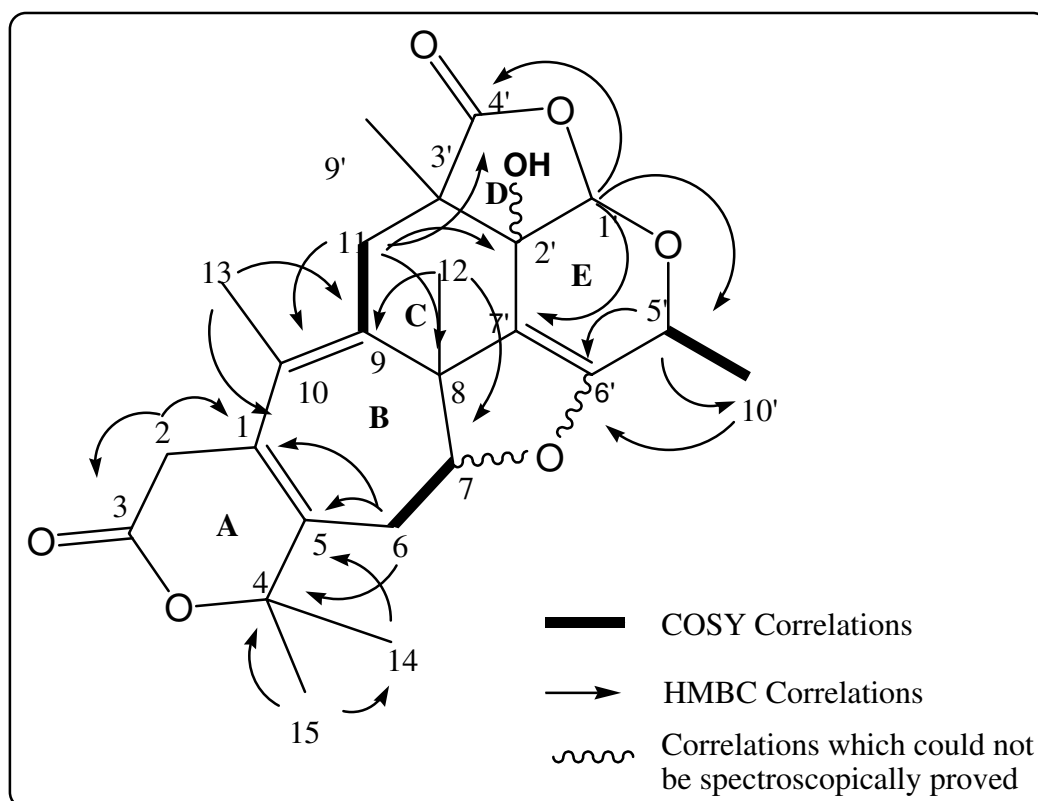
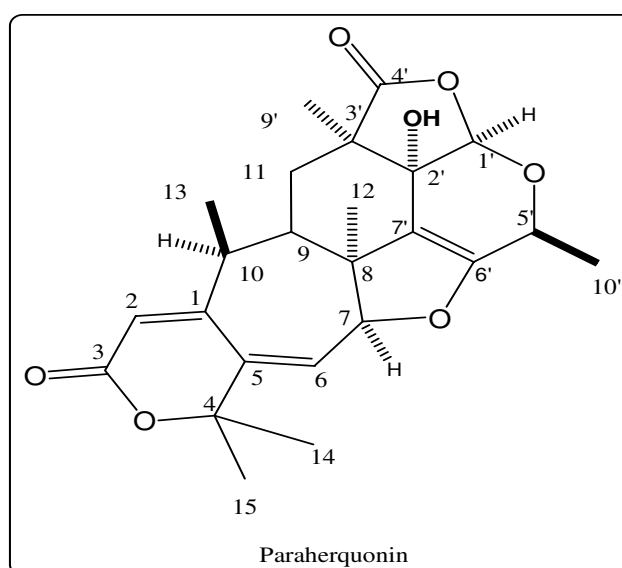


Figure 3.1.1.4.2.1 COSY (at 500 MHz) and some important HMBC correlations of Citreonigrin I in DMSO-d_6

In general, HMBC and COSY correlations in the southern part of citreonigrin I molecule (figure 3.1.1.4.2.1) were found still to be similar to that in citreonigrin G. In the northern part, however, the absence of carbomethoxy group would result in some bonds rearrangement and atoms replacement in the molecule. The presence an extra double bond between C-6' and C-7' was confirmed by HMBC correlation of H-1'/ C-7', H₃-12/C-7' , H₃-10'/C-6', and H-5'/C-6'. However, the position of H-6' adjacent to C-7' could not be spectroscopically proved due to the absence of expected H-5'/C-7' HMBC correlation.

Meanwhile, the presence of 2'-OH, instead of a methyne proton in citreonigrin G, was only confirmed by the chemical shifts of C-2' (δ 71.0 ppm). Unfortunately, the position of hydroxyl group at C-2' itself could not be directly proved in HMBC spectrum. Nevertheless, this type of substructure has been reported and found to be similar to that of paraherquonin (Okuyama, *et al.*, 1983). The different between paraherquonin and citreonigrin I was only the position of two double bonds in the southern part of molecule.

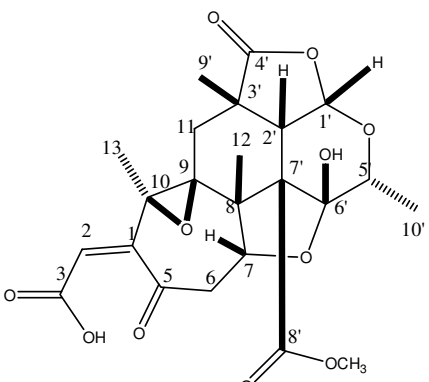
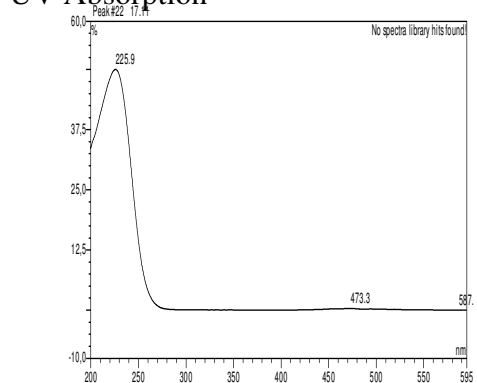
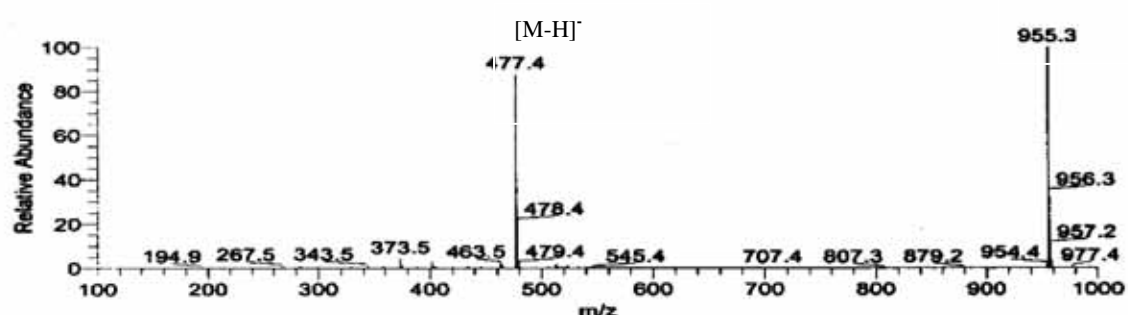


Since the ROESY experiment was not performed to this compound, the establishment of relative configuration of the stereocenters in the molecule was determined by the comparison of optical rotation value and biogenetically relationships between this compound to other isolated meroterpenes, especially citreonigrin G.

Table 3.1.1.1.11 NMR data of Citreonigrin I in DMSO-d₆ at 500 MHz (¹H) and 125 MHz (¹³C)

Position	¹ H δ (ppm) <i>J</i> _{H-H} (Hz)	¹³ C δ (ppm)	HMBC (H to C)
1		128.6	
2	A 3.50 d (20.5) B 2.89 d (20.5)	31.7	1, 3 1, 3
3		168.9	
4		84.1	
5		128.2	
6	A 2.28 dd (12.6; 2.6) B 2.14 dd (12.6; 12.3)	31.2	1, 4, 5
7	4.31 dd (12.3; 4.6)	92.8	
8		51.1	
9		137.6	
10		126.1	
11	A 2.85 d (16.4) B 2.14 dd (16.4)	30.8	8, 9, 10, 2', 3', 4' 8, 9, 10, 2', 3', 4'
12	1.24 s	30.3	7, 8, 9, 7'
13	1.74 bs	16.9	1, 9, 10
14	1.56 s	26.7	4, 5, 15
15	1.43 s	26.9	4, 5, 14
1'	5.84 s	101.1	2', 4', 5', 7'
2'		71.0	
3'		49.5	
4'		175.4	
5'	4.55 q (7.0)	66.1	1', 6', 10'
6'		151.8	
7'		105.1	
9'	1.18 s	18.7	11, 2', 3', 4'
10'	1.27 d (7.0)	20.5	5', 6'
2'-OH	6.04 s		

3.1.1.4.3 PC 3.3.6.6.3.A

PC 3.3.6.6.3.A	
Synonym(s)	:
Biological Source	: <i>P. citreonigrum</i>
Sample code	: PC 3.3.6.6.3.A
Amount	: 1.17 mg
Molecular Formula	: C ₂₃ H ₂₆ O ₁₁
Molecular Weight	: 478 g/mol
Solubility	: CH ₃ OH
Physical Description	: Pale yellow solids
Optical rotation	: $[\alpha]_D^{20} + 18^\circ$ (c, 0.1 in CH ₃ OH)
HPLC Retention Time (R _t)	: 17.10 min. (Standard gradient)
Structure	UV Absorption
	
(-)-ESI-MS	[2M-H] ⁻
	

PC 3.3.6.6.3.A was the most polar isolated meroterpenoid in this study. The negative mode of ESI-MS showed a pseudomolecular ion at m/z 477.4 $[M-H]^-$. It was isolated as small amount of pale yellow solids and the only isolated meroterpenoid which could not

detected in the positive mode of ESI-MS. The UV pattern (λ_{\max} 225.9 nm) suggested the close relationships to citreonigrin G and I.

As like as citreonigrin G, $^1\text{H-NMR}$ spectrum of this compound still showed the presence of five singlet methyls, one doublet methyl, one methoxy group, one hydroxy, and four methyne protons. In contrast, $^{13}\text{C-NMR}$ spectrum indicated the presence of only two olefinic carbons and extra two oxygenated carbons at δ 69.6 ppm (C-9) and δ 60.8 ppm (C-10). Furthermore, the presence of one olefinic proton at δ 6.45 ppm (C-2) in the $^1\text{H-NMR}$ spectrum differed this compound to citreonigrin G and I.

Analysis and comparison of the NMR data indicated that PC 3.3.6.6.3.A did not contain the δ -lactone ring which always present in other meroterpenes. Instead, the presence of an additional carboxyl keto at C-5 (δ 210.0 ppm) and a free unsaturated carboxylic acid moiety at C-1 was derived from 1D and 2D-NMR data analysis. The presence of free unsaturated carboxylic acid was confirmed by a correlation of 2'-OH (δ 8.14 ppm) to an olefinic carbon at δ 123.0 ppm (C-2') in HMQC spectrum. The presence of H-2 as an olefinic proton was verified by its HMBC correlation to C-1 (δ 168.2 ppm) and C-10 (δ 60.8 ppm) and its direct correlation to C-2 in HMQC spectrum.

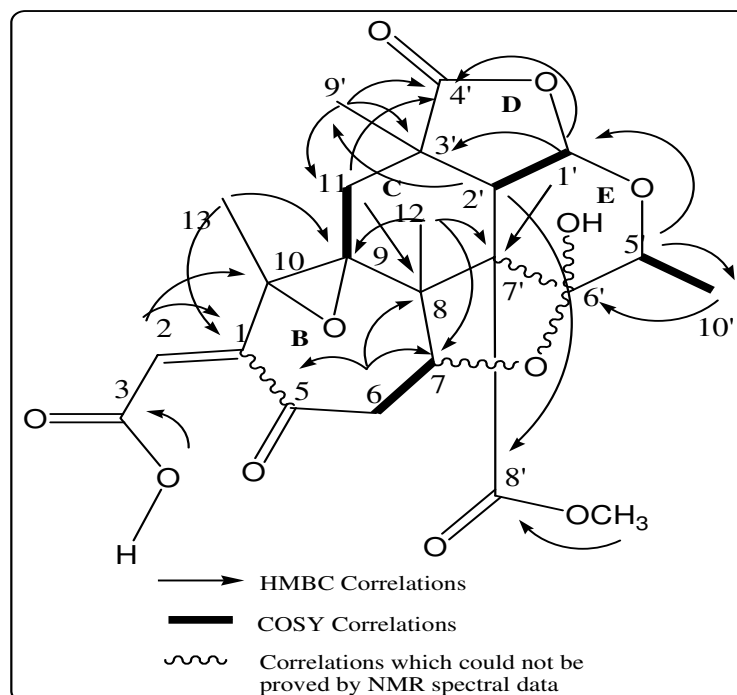


Figure 3.1.1.4.3.1. COSY (at 300 MHz) and some important HMBC correlations of PC 3.3.6.6.3.A in DMSO- d_6

A weak HMBC correlation of H-6A (δ 2.34 ppm) to a carbonyl keto (δ 210.0 ppm) confirmed the presence of a keto functional group at C-5. Unfortunately, HMBC spectrum showed neither the expected correlations of H-2/C-5 nor H-7/C-5 to support this assignment, thus the presence of keto functional group at C-5 was not strongly supported by NMR spectral data. At the other side of molecule, the presence of an epoxide ring between C-9 (δ 69.6 ppm) and C-10 (δ 60.8 ppm), instead of a double bond at citreonigrin G and I, was identified in this compound. In general, the rest HMBC and COSY correlations (figure 3.1.1.4.3.1) indicated that the rest part of PC 3.3.6.6.3.A molecule was identical to that of citreonigrin G.

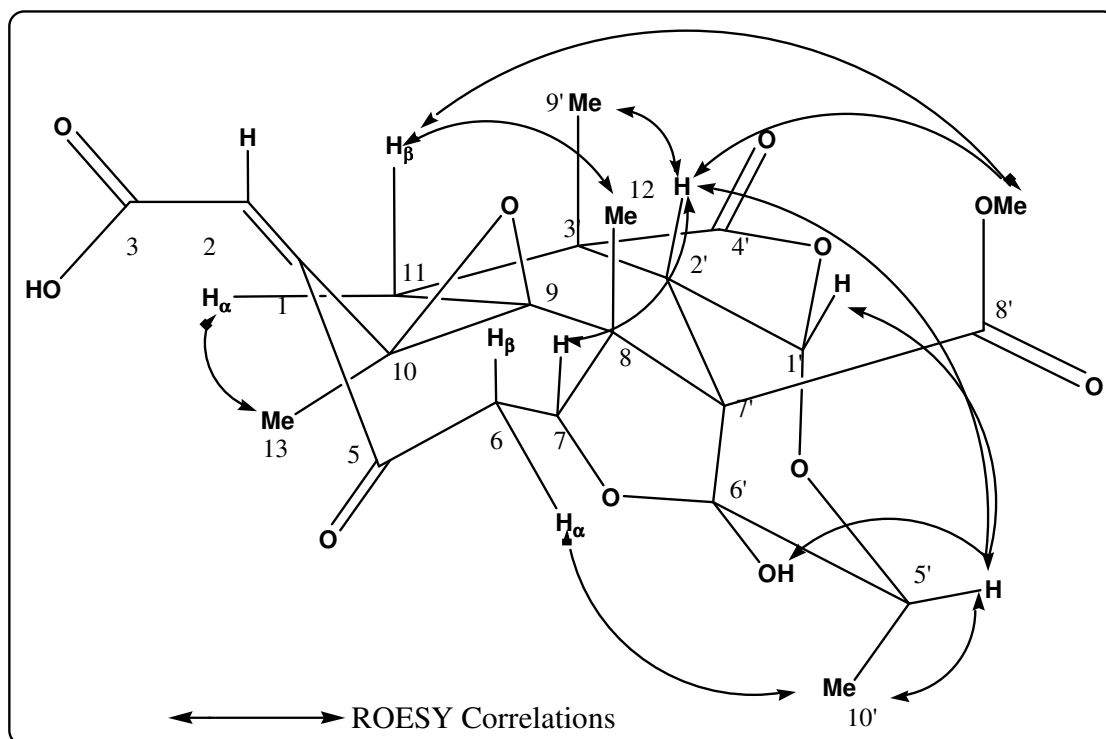


Figure 3.1.1.4.3.2. Stereo drawing of PC 3.3.6.6.3.A showing the observed ROESY correlation in DMSO- d_6

Relative configuration of the stereocenters in PC 3.3.6.6.3.A were assigned using ROESY experiment (figure 3.1.1.4.3.2). The correlations of H-5'/OH-6' and H-5'/H-2' which turn to H-5'/H₃-9' and H-5'/H₃-12 indicated the β -orientation of OH-6', H-5', H-2', Me-9' and Me-12 in the molecule. Relative configuration of C-6 and C-7 were verified by the correlations of H-6A/H₃-10 and H-7/H-2', respectively. The β -configuration of

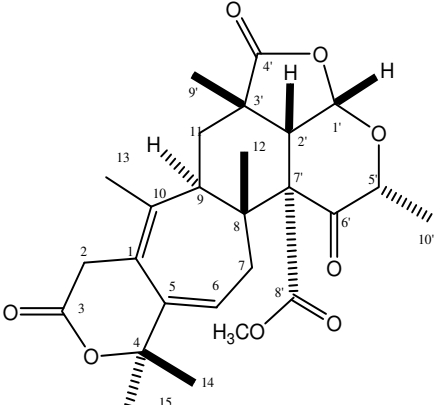
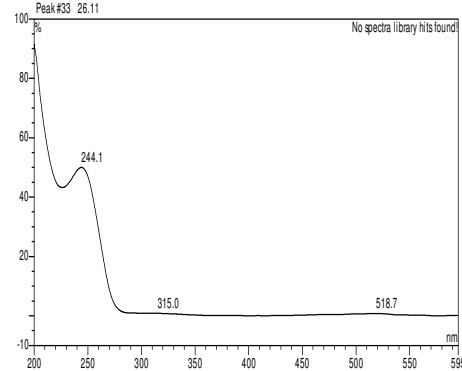
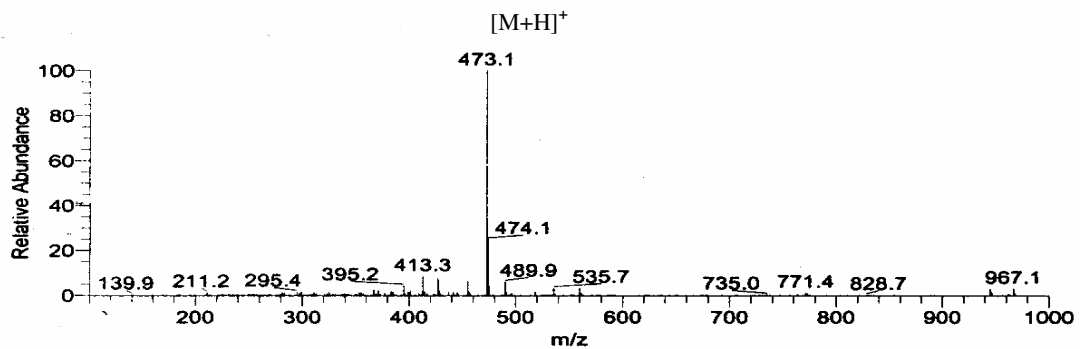
carbotheoxy group was determined the correlation of H-11 β /H₃-OCH₃, as well as H-2'/H₃-OCH₃. In general, relative stereochemistry of the rest stereocenters in PC 3.3.6.6.3.A were identical to that found citreonigrin G.

Table 3.1.1.4.3.1 NMR data of PC 3.3.6.6.3.A in DMSO-d₆ at 600 MHz (¹H) and 75 MHz (¹³C)

Position	¹ H δ (ppm) J_{H-H} (Hz)	¹³ C* δ (ppm)	HMBC (H to C)	ROESY
1		168.2		
2	6.45 s	123.0	1,10	12,13
3		165.0		
5		210.0		
6	A α 2.34 dd (13.4 ; 2.5) B β 1.70 dd (13.4 ; 12.6)	26.5	5,7,8 7,8	6B,10' 12
7	4.40 dd (12.6 ; 2.5)	70.3		6A,2',5',12,10'
8		49.0		
9		69.6		
10		60.8		
11	A β 1.99 d (14.3) B α 1.87 d (14.3)	32.4	2',3',4',9' 8,9,10,2',3',4'	12,9' 13,9'
12	0.93 s	19.5	7,8,9,7'	
13	1.55 s	20.5	1,9,10	
1'	5.70 d (7.9)	98.5	2',3',4',5',7'	2',5'
2'	3.30 ^h	42.6	8,11,3',7',8',9'	11A,9'
3'		42.6		
4'		179.1		
5'	3.67 q (6.0)	75.5	1',10'	2',10',6'-OH
6'		100.2		
7'		62.5		
8'		173.5		
9'	1.42 s	26.5	11,2',3',4'	
10'	1.25 d (6.0)	13.6	5',6'	
8'-OCH ₃	3.72 s	52.4	8'	2',11A,12,9'
OH-6'	6.19 s			
OH-2	8.45 s		1 (in HMQC)	

^h hidden under residual solvent or water signal

3.1.1.4.4 Citreonigrin F

Citreonigrin F	
Synonym(s)	: -
Biological Source	: <i>P.citreonigrum</i>
Sample code	: PC 3.3.6.6.3.I
Amount	: 2.56 mg
Molecular Formula	: C ₂₆ H ₃₂ O ₈
Molecular Weight	: 472 mg/mol
Solubility	: CH ₃ OH
Physical Description	: Pale yellow solid
Optical rotation	: $[\alpha]_D^{20} +42^\circ$ (c, 0.1 in CH ₃ OH)
HPLC Retention Time (R _t)	: 26.10 min (Standard gradient)
Structure	UV Spectrum
	
(+)-ESI-MS 	

Citreonigrin F was isolated from ethyl acetate extract of *P. citreonigrum* and gave a pseudomolecular ion at m/z 473.1 in the positive mode ESI-MS. Although the UV

absorption pattern (λ_{max} 244.1 nm) of this compound was quite different to citreonigrin G and I, the analysis NMR data still indicated the presence of A, B, C, D and E ring systems like in citreonigrin G and I. It differs to citreonigrin G with regard to the position of two double bonds in the B ring system and the presence of an additional carbonyl keto, instead of a hemi-acetal carbon, in the E ring system.

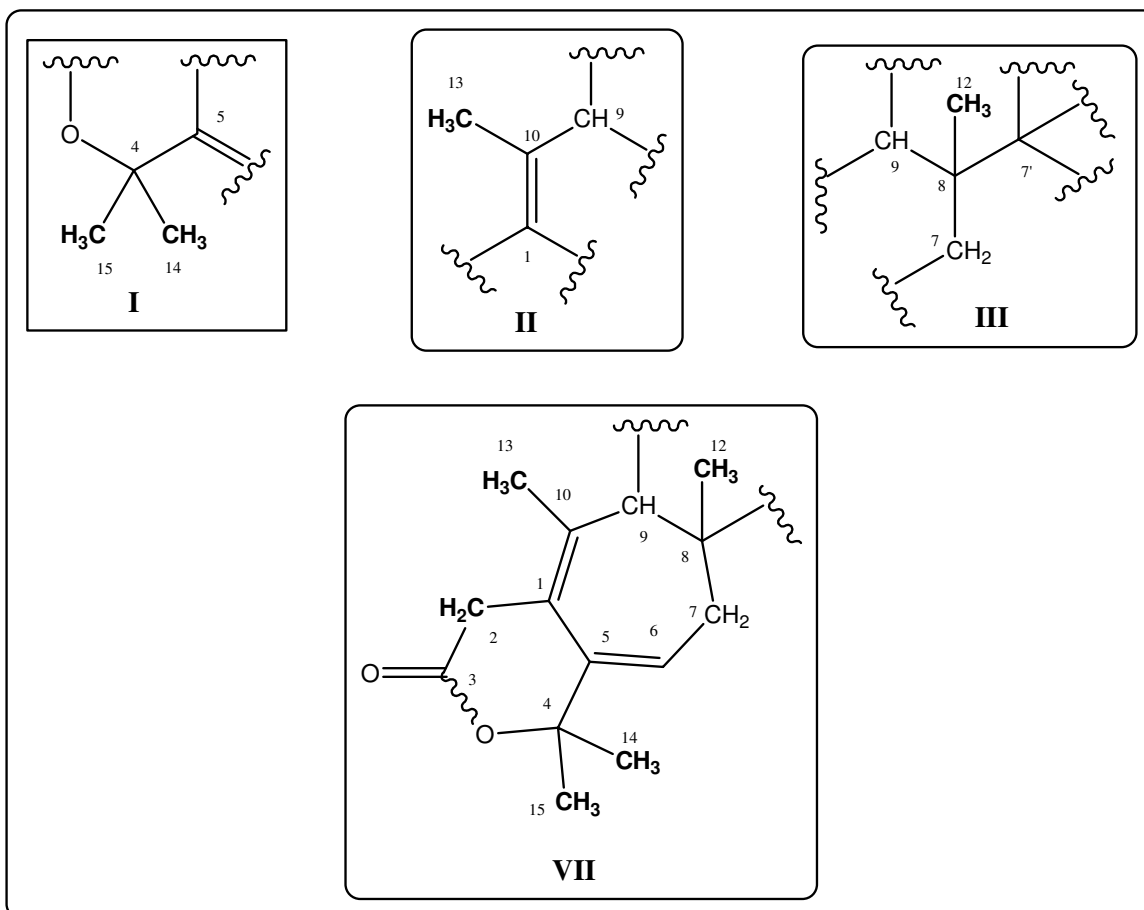


Figure 3.1.1.4.4.1. Partial structures in the southern part molecule of citreonigrin F based on the correlations of methyl protons in the HMBC spectrum

The connectivity between substructure I, II and III in the molecule (figure 3.1.1.4.4.1) resulted in the southern part molecule of citreonigrin F (VII) which was similar to that found in citreonigrin E. Substructure I was formed by the HMBC correlations of H₃-14 (δ 1.55 ppm) and H₃-15 (δ 1.40 ppm) to C-4 (δ 81.6 ppm) and C-5 (δ 136.4). The correlations of H₃-13 and H₃-12 to the corresponding neighbour carbons resulted in substructure II and III, respectively.

The substructure I was connected to the substructure II with the helps of HMBC correlations of H₂-2 (δ 3.60 and 3.33 ppm) to C-1 (δ 126.6 ppm) and C-10 (δ 135.7 ppm), as well as HMBC correlation of H-6 (δ 6.30 ppm) to C-1 (δ 126.6 ppm). The presence of δ -lactone ring was confirmed by HMBC correlation of H-2 to a carbonyl carbon (C-3, δ 169.5 ppm). Then, HMBC connections of H₂-7 (δ 2.46 and 1.59 ppm) to C-5 (δ 136.4 ppm) and COSY correlations of H₂-7 and H-6 confirmed the connectivity between substructure I and substructure III. Finally, the correlations of both H₃-12 and H₃-13 to C-9 connected the substructure III and II. The rest HMBC and COSY correlations of the southern part molecule were shown in figure 4.1.1.4.4.4.

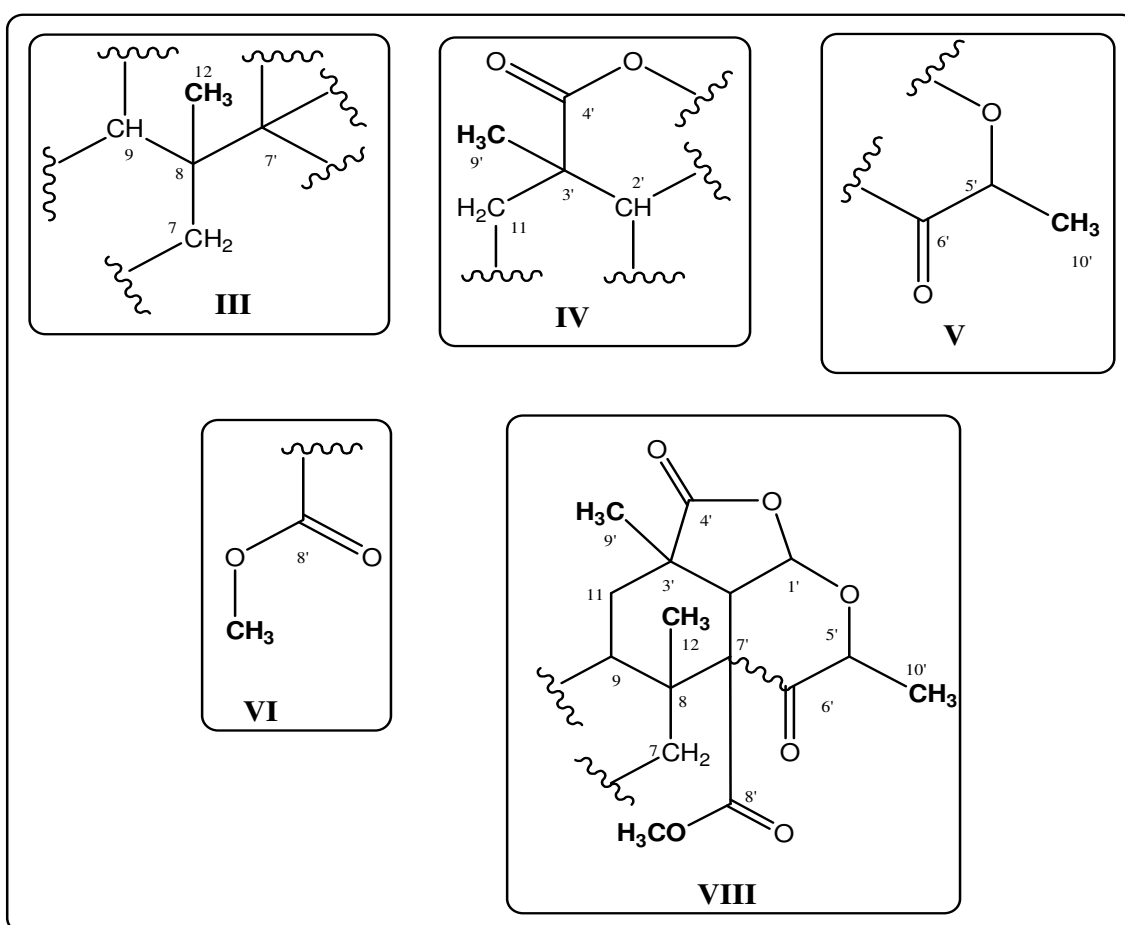


Figure 3.1.1.4.2. Partial structures in the northern part molecule of citreonigrin F based on the correlations of methyl protons in the HMBC spectrum

In the northern part of molecule, the presence of substructures III, IV and VI which were formed by the correlations of H₃-12, H₃-9' and H₃-OCH₃ to the corresponding neighbour carbons, respectively, were observed in the HMBC spectrum of this compound. As like as in citreonigrin G, the connectivity between substructure III and IV was identified by the

HMBC correlations of H₂-11/C-9 and the spin system formed by H₂-11 and H-9 in COSY spectrum. HMBC correlations of H-1' to C-3', C-4' and C-7' would give the formation of C and D ring system. This assignment was also supported by the correlation of H-1' with H-2' in COSY experiment and HMBC correlations of H-2' to the correspond neighbour carbons. As like as in citreonigrin G, the position of carbomethoxy group at C-7' was confirmed by HMBC correlations of H₃-OCH₃ and H-2' to C-8'.

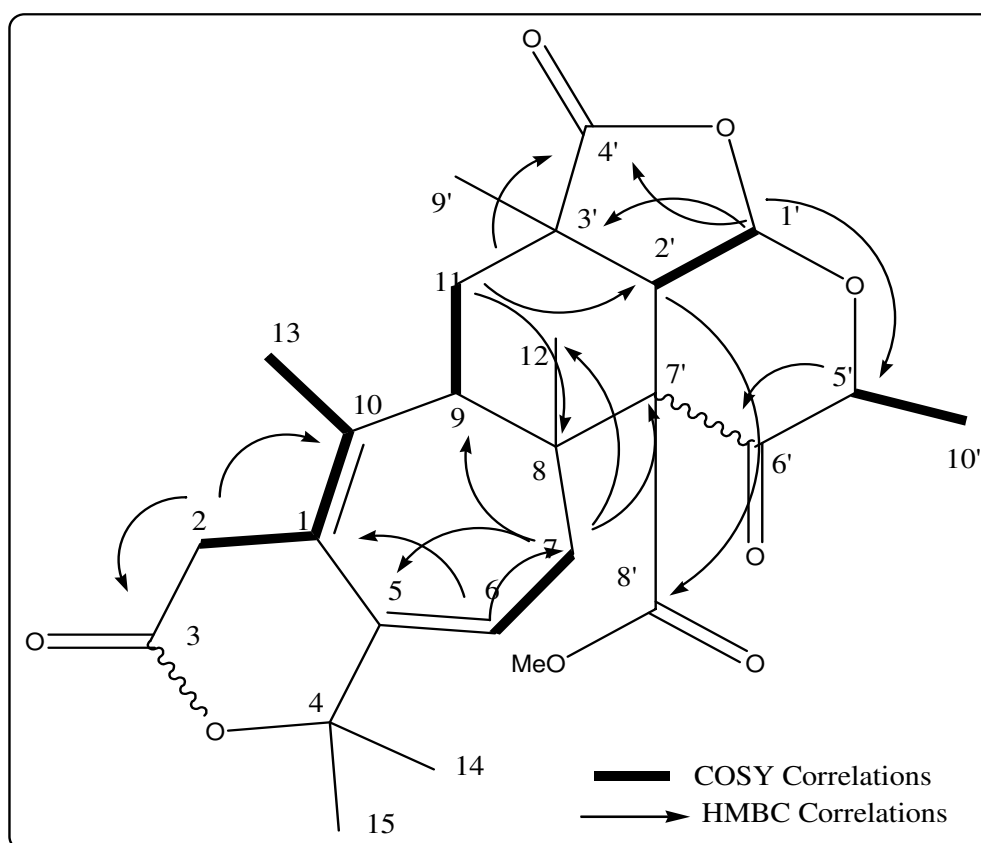


Figure 3.1.1.4.4.4. COSY (at 300 MHz) and diagnostic iHMBC correlations of Citreonigrin F in DMSO-d₆

However, HMBC correlation of H₃-10' to a keto carbonyl (C-6', δ 205.5 ppm), resulted in substructure V, one which has not been identified in the previous meroterpenoids. Compared to citreonigrin G, the presence of keto carbonyl at C-6', instead of an hemi acetal carbon, in citreonigrin F resulted in the elimination of the oxygen bridge as observed in citreonigrin G and I. Although the connectivity between C-6' and C-7' could not be confirmed by the performed spectroscopy experiment, HMBC correlations of H-5' to C-1' and C-6', which was also supported by correlation of H-1' to C-7' rised the formation of E ring system in molecule. The rest HMBC and COSY correlations showing the connectivity

in the northern part molecule, as well as the connectivity between the northern part and the southern part molecule are shown in figure 3.1.1.4.4.4.

The relative configuration of asymmetrical carbons in citreonigrin F was deduced from ROESY experiment. Strong correlations of H-1'/H-5' and H-1'/H-2', as well as H-1'/H₃-12 and H-1'/H₃-9' suggested the β-position of Me-12, Me-9', H-2', H-1' and H-5'. The α-position of H-9, however, was verified not only by the observed correlation of H-11α to H-9 in ROESY spectrum, but also by the coupling constants of H-9/H-11α ($^3J_{HH}$ 4.3 Hz) and H-9/H-11β ($^3J_{HH}$ 14.2 Hz). At the other part of molecule, relative configuration of C-7 was determined by the correlations of H-7B to H₃-12 and H-7A to H-6, thus H-7B and H-7A were located at the pseudo-axial and pseudo-equatorial of the ring system, respectively. Since H₃-10' and H₃-OCH₃ did not show any correlations to other protons, it was assumed that Me-10' and carbomethoxy group were located in the α-orientation. The complete assignment of ROESY spectrum is described in Fig. 3.1.1.4.4.5.

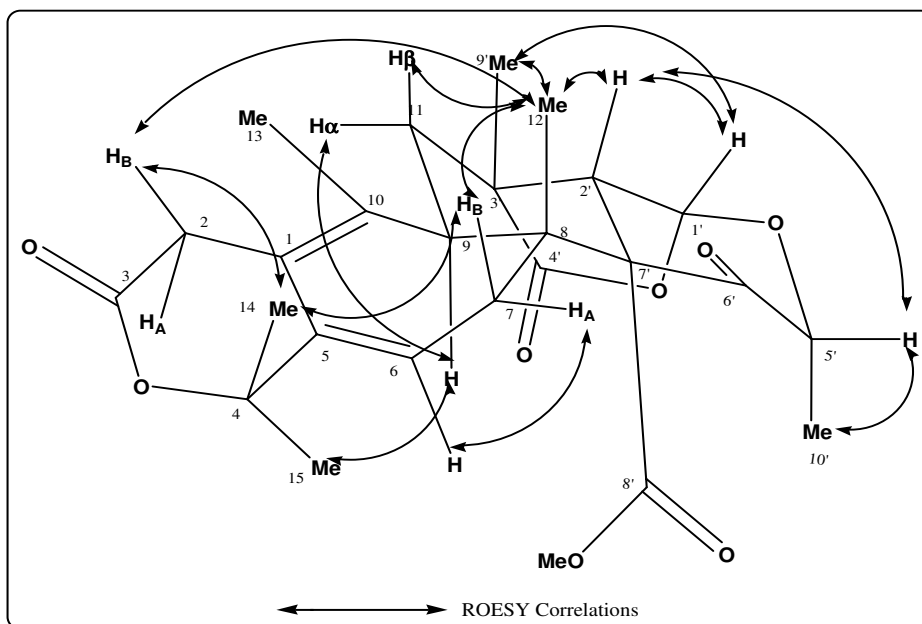


Figure 3.1.1.4.4.4. Stereo drawing of Citreonigrin F showing the observed ROESY correlation in DMSO-d₆

Table 3.1.1.4.4.1. NMR data of Citreonigrin F in DMSO-d₆ at 600 MHz (¹H) and 75 MHz (¹³C)

Position	¹ H δ (ppm) <i>J</i> _{H-H} (Hz)	¹³ C δ (ppm)	HMBC (H to C)	ROESY
1		126.6		
2	A 3.60 d (19.3) B 3.33 d (19.3)	34.5	1, 3, 10 1, 3, 10	13, 15 13, 15
3		169.5		
4		81.6		
5		136.4		
6	6.03 dd (8.0; 5.2)	128.2	1, 4, 7	7A, 14, 15
7	A 2.46 dd (13.6; 8.0) B 1.59 dd (13.6; 5.2)	35.3	5, 6, 8, 9, 12, 7' 5, 7'	7B, 12 7A, 12
8		56.4		
9	2.61 dd (14.2; 4.3)	38.4		11Aα, 13, 15
10		135.7		
11	Aα 1.82 dd (10.5; 4.3) Bβ 1.71 dd (14.2; 10.5)	29.5	8, 9, 3', 4', 7' 9, 3', 4', 9'	11Bβ, 9' 11Aα, 12, 9'
12	0.75 s	20.8	7, 8, 9, 7'	2B, 13, 2', 10'
13	1.76 s	15.6	1, 9, 10	
14	1.55 s	25.0	4, 5, 15	14
15	1.40 s	28.7	4, 5, 14	
1'	6.37 d (5.3)	99.1	2', 4', 5', 7'	2', 9'
2'	3.81 d (5.3)	51.5	2, 1', 3', 4', 7', 8'	12, 9'
3'		43.0		
4'		175.9		
5'	4.64 q (6.5)	74.9	1', 6', 10'	2', 10'
6'		205.5		
7'		62.4		
8'		169.3		
9'	1.35 s	26.3	11, 2', 3', 4'	
10'	1.27 d (6.5)	19.2	5', 6'	11Aα, 5'
8'-OCH ₃	3.82 s	53.3	8'	

3.1.1.4.5 Citreonigrin H

Citreonigrin H	
Synonym(s)	: -
Biological Source	: <i>P. citreonigrum</i>
Sample code	: PC 3.3.6.6.3.G
Amount	: 5.65 mg
Molecular Formula	: C ₂₆ H ₃₂ O ₈
Molecular Weight	: 472 g/mol
Solubility	: CH ₃ OH
Physical Description	: Pale yellow solid
Optical rotation	: $[\alpha]_D^{20} +74^\circ$ (c, 0.1 in CH ₃ OH)
HPLC Retention Time (R _t)	: 24.58 min (Standard gradient)
Structure	UV Spectrum
(+) ESI-MS	

Citreonigrin H was isolated as pale yellow solid from the ethyl acetate extract of *P. citreonigrum* after separation using VLC, sephadex, subsequent silica column and HPLC preparative. This compound showed a pseudomolecular ion at m/z 473.1 $[M+H]^+$ in the positive mode of ESI-MS which were similar to that shown by citreonigrin F. In addition, UV absorption pattern (λ max 243.7 nm) which was almost similar to that of citreonigrin F supported this assignment.

Like citreonigrin F, $^1\text{H-NMR}$ spectrum of citreonigrin H showed one olefinic proton, six methylene protons, one methoxy and four methyne protons. One methyne proton (H-9, δ 2.20 ppm) coupled to H₂-11 (δ 1.87 and 1.63 ppm) to form a spin system in COSY spectra. Differ to citreonigrin F, however, $^1\text{H-NMR}$ spectrum of citreonigrin H did not show the presence of a doublet methyl, thus the six methyls present in the compound appeared as singlets.

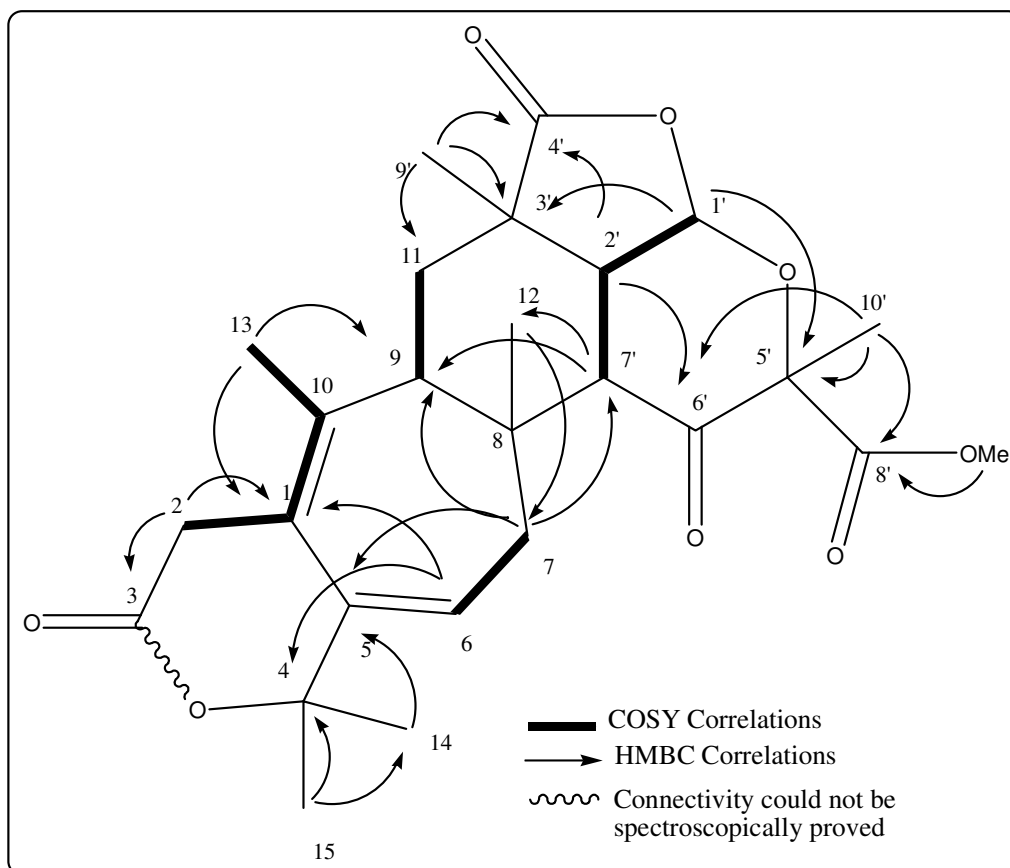


Figure 3.1.1.4.5.1. COSY (at 300 MHz) and some important HMBC correlations of citreonigrin H in DMSO-d₆

Further NMR data analysis indicated that the carbomethoxy group attached to C-5' in the E ring system of this molecule. This assignment was confirmed not only by HMBC correlation of H₃-10' (δ 1.48 ppm) to C-8' (δ 169.8 ppm), but also by the correlation of H₃-OCH₃ (δ 3.55 ppm) to C-8'. Instead, the presence of a methyne proton at C-7' (H-7', δ 2.88 ppm) was confirmed by its coupling to H-2' (δ 3.28 ppm) as shown in COSY spectrum. As shown by the rest HMBC and COSY correlations (figure 3.1.1.4.5.1.), the rest part of this molecule was assigned to be identical to that in citreonigrin F.

ROESY experiment was performed to determine the stereochemistry of the stereo centers in the molecule. Based on the ROESY correlations (figure 3.1.1.4.5.2), relative configuration of the most stereocenters in this molecule was similar to that of citreonigrin F. The close proximity amongst Me-12, H-2', H-1' was confirmed by ROESY correlations of H₃-12/H-2' and H-2'/H-1'. Although the orientation of Me-9' could not be confirmed by this experiment, it was assumed that it must be present in the close proximity to Me-12 as assigned in other meroterpenes, especially citreonigrin F. The β -position of Me-10' was determined by a strong correlation of H-1' and H₃-10', and thus the carbomethoxy group attached to C-5 in the α -orientation. Finally, the stereochemistry of C-7' was determined by a correlation of H-7' to H-1'.

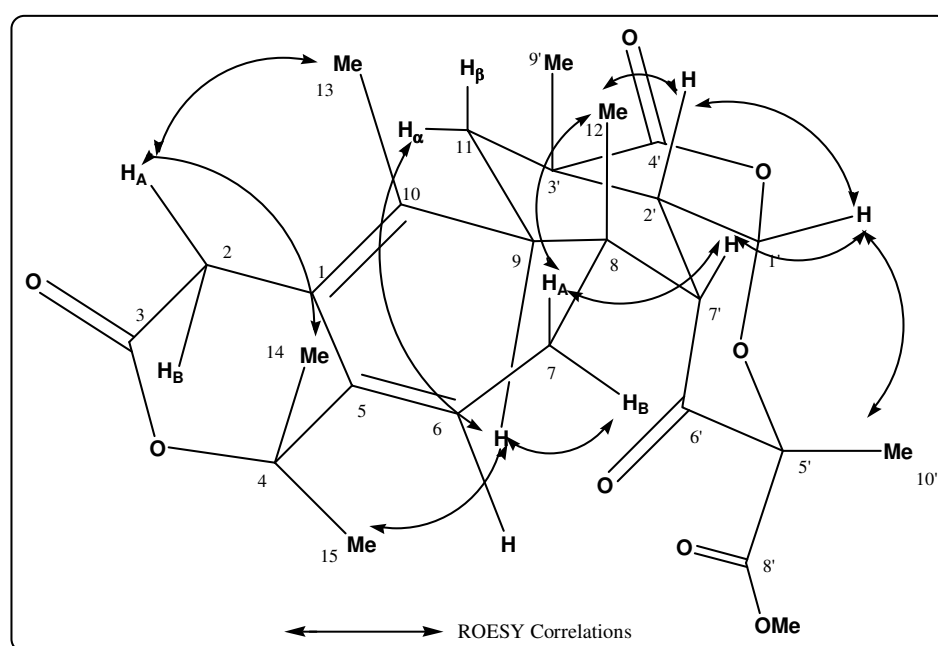


Figure 3.1.1.1.16. Stereo drawing of Citreonigrin H showing the observed ROESY correlation in DMSO-d₆

Table 3.1.1.1.10 NMR data of Citreonigrin H in DMSO-d₆ at 600 MHz (¹H) and 75 MHz (¹³C)

Position	¹ H δ (ppm) <i>J</i> _{H-H} (Hz)	¹³ C δ (ppm)	HMBC (H to C)	ROESY
1		125.3		
2	A 3.55 ^o B 3.30 ^h	33.9	1,3 1,3	13, 15 13
3		169.4		
4		81.5		
5		138.5		
6	6.22 dd (7.6; 5.3)	127.8	1, 4	2A, 7A, 11, 14, 15, 8'-OCH ₃ , 10'
7	A 2.46 dd (13.2; 7.6) B 1.62 dd (13.2; 5.3)	37.6	5, 6, 8, 9 5, 6, 8	11B, 12
8		54.0		
9	2.20 dd (13.3; 1.6)	41.9		7B, 11A, 14, 9', 10'
10		136.5		
11	Aα 1.87 bd (13.0) Bβ 1.63 dd (13.3; 13.0)	29.4		15
12	0.96 s	24.4	7, 8, 9, 7'	
13	1.75 s	14.9	1, 9, 10	12, 14, 10'
14	1.46 s	28.7	4, 5, 15	
15	1.27 s	26.0	4, 5, 14	
1'	6.13 d (7.2)	96.5	3'	2', 7', 10'
2'	3.28 dd (10.0; 7.2)	41.5	1', 3', 4', 6', 8', 9'	12, 13, 14, 15, 7'
3'		45.0		
4'		171.3		
5'		78.6		
6'		208.4		
7'	2.88 d (10.0)	48.8	8, 9, 3'	7A, 12
8'		169.8		
9'	1.34 s	30.0	9, 11, 2', 3', 4'	
10'	1.48 s	24.9	5', 6', 8'	12, 9'
8'-OCH ₃	3.55 s ^o	52.6	8'	13, 15, 2', 10'

^h hidden under residual solvent or water signal, ^o mutually overlapped

3.1.1.5 Others New Meroterpenes

3.1.1.5.1 PC 3.3.6.6.3.B

PC 3.3.6.6.3.B	
Synonym(s)	: -
Biological Source	: <i>P. citreonigrum</i>
Sample code	: PC 3.3.6.6.3.B
Amount	: 2.1 mg
Molecular Formula	: C ₂₆ H ₃₂ O ₉
Molecular Weight	: 488 g/mol
Solubility	: CH ₃ OH
Physical Description	: Pale yellow solid
Optical rotation	: $[\alpha]_D^{20} +42$ (c, 0.1 in CH ₃ OH)
HPLC Retention Time (R _t)	: 21.19 min (Standard gradient)
Structure	UV Spectrum
(-) ESI-MS	

PC 3.3.6.6.3.B was isolated as pale yellow solids in CH₃OH and showed a unique UV absorption pattern (λ_{max} 213.5 and 281.3 nm) which was not shown by any other isolated meroterpenes. As like as other isolated meroterpenes, ¹H-NMR spectrum still showed the presence of six methyls and one methoxy group. The presence two olefinic, four methylene, and three methyne protons were also detected, supported by interpretation of 2D-NMR data, in the ¹H-NMR spectrum. Although ¹H-NMR spectrum did not show the presence of OH group, the chemical shifts of C-10 at δ 87.7 ppm indirectly confirmed the presence of OH-10.

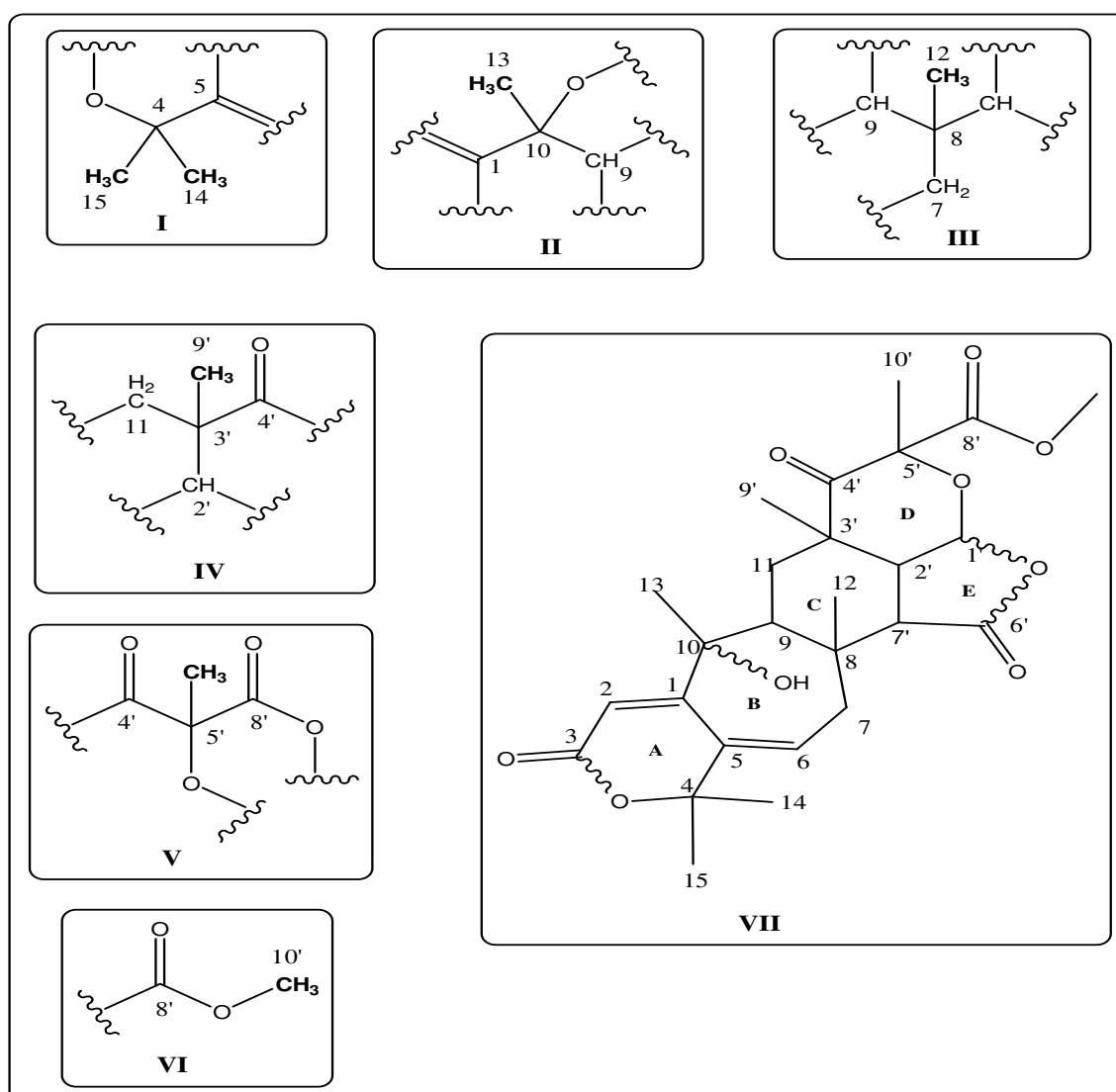


Figure 3.1.1.5.1.1. Partial structures in the northern part molecule of citreonigrin F based on the correlations of methyl protons in the HMBC spectrum

Although the connectivity between C-3 and C-4 could not be confirmed using spectroscopically proved, the presence of an unsaturated δ -lactone (A ring system) was confirmed by HMBC correlations of H-2, an olefinic singlet at δ 5.73 ppm, to a carbonyl carbon at δ 162.0 ppm (C-3) and an olefinic carbon at δ 134.4 ppm (C-5). The connectivities between substructures I, II and III would give the formation of the seven membered ring (B ring) system in the northern part molecule. Both HMBC correlation of H₃-12/C-9 and H₃-13/C-9 linked the substructure II and III. The presence of a double bond in the B ring system was identified by not only chemical shifts of C-5 (δ 134.4 ppm) but also by the one at C-6 (δ 130.5 ppm). Moreover, this assignment was supported by HMBC correlations of H-7B/C-5 and H-6/C-1, as well as the coupling between H-6 (δ 6.20 ppm) and H₂-7 (δ 3.51 and 2.18 ppm) detected as a spin system in COSY. The last correlations also connected the substructure I and III.

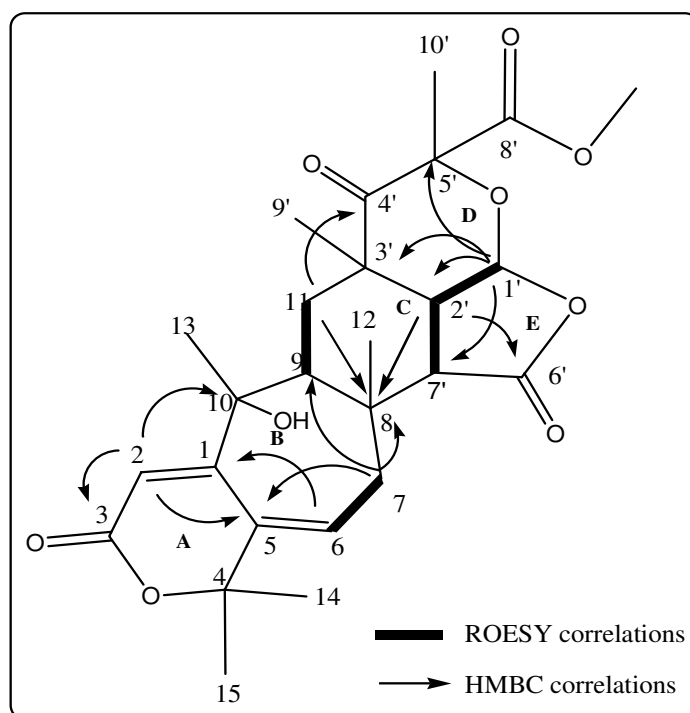


Figure 3.1.1.5.1.2 COSY (at 600 MHz) and diagnostic HMBC correlations of PC 3.3.6.6.3.B in DMSO- d_6

In the northern part, the presence of C ring system and the correlations involved in the formation of C ring system were similar to that found in citreonigrin F and H. Meanwhile, the correlation of H₃-10' (δ 1.55 ppm) and H₃-9' (δ 1.34 ppm) to C-4' (δ 207.5 ppm) and supported by the correlations of H-1'/C-5' and H-1'/C-3' confirmed the presence of D ring system as a pyrone function in the molecule. However, in other isolated meroterpenes, such as citreonigrin F and H, the D ring system was present as a γ -lactone ring. As described in substructure VI, the correlation of H₃-OCH₃ (δ 3.60 ppm) to C-8' (δ 170.0 ppm), as well as the correlation of H₃-10'/C-8' confirmed the position of carbomethoxy group at C-5'. The COSY spin system formed by the couplings amongst H-1' (δ 6.10 ppm), H-2' (δ 3.30 ppm) and H-7' (δ 2.54 ppm) and supported by HMBC correlations of H-2' to a carbonyl carbon (C-6', δ 171.0 ppm), as well as H-1' to C-7' (δ 53.0 ppm) confirmed the presence of a γ -lactone (E ring) system in the molecule.

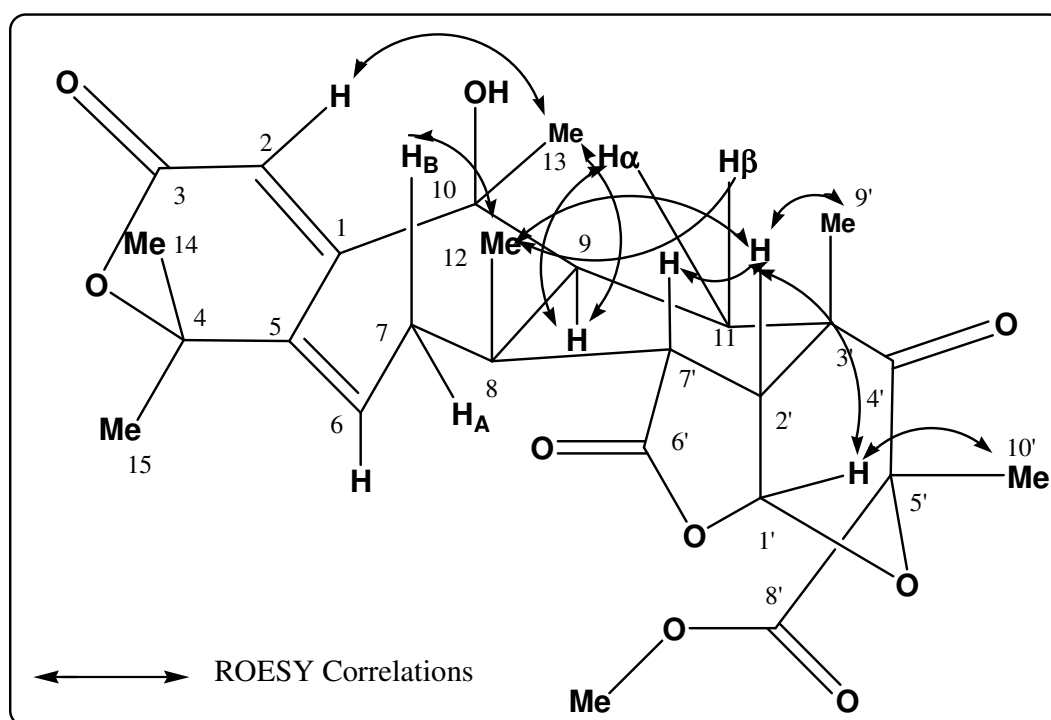


Figure 3.1.1.5.1.3. Stereo drawing of PC 3.3.6.6.3.B showing the observed ROESY correlation in DMSO-d₆

The configurations of the stereocenters in the molecule were deduced from ROESY data analysis. The correlations of H₃-9' with H-2', as well as correlation of H₃-12/H-7' were the keys in determination of β -position of Me-12, H-7', H-2' and Me-9'. Furthermore, the correlation of H₃-10'/H-1' which turned to correlation of H-1'/H-2' confirmed the relative

configuration of C-1' and C-5' in the molecule. On the other side, the α -position of H-9 was determined by the correlations of H-9 with H-11 α . The position of Me-13 which was located at the pseudo axial of seven membered ring system was confirmed by the correlations of H₃-13 with H-9. Meanwhile, the correlations of H-7B with H₃-12 confirmed the configuration of C-7. Figure 3.1.1.5.1.3 shows the complete assignments of ROESY correlations in PC 3.3.6.6.3.B.

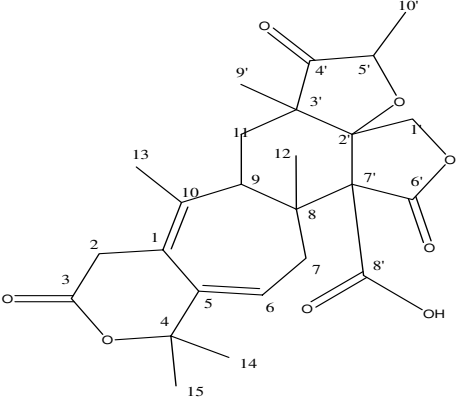
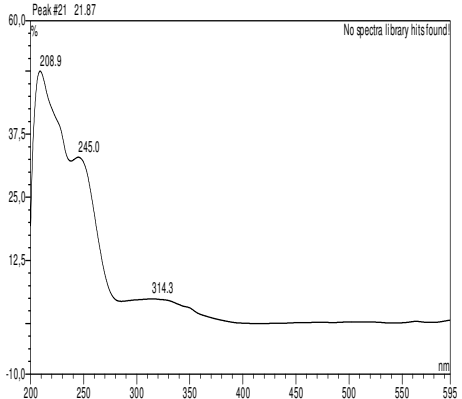
Table 3.1.1.5.1.1 NMR data of PC 3.3.6.6.3.B in DMSO-d₆ at 600 MHz (¹H) and 150 MHz (¹³C)

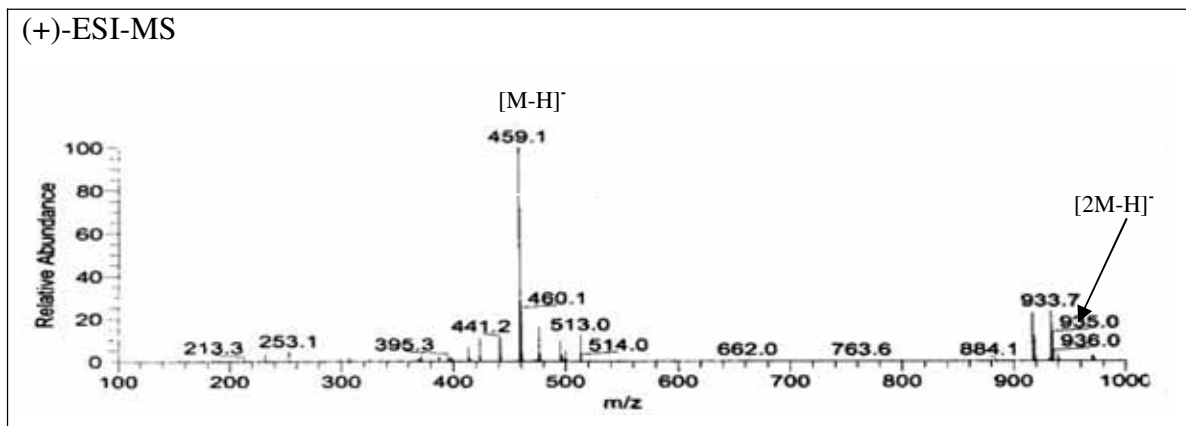
Position	¹ H δ (ppm) J_{H-H} (Hz)	¹³ C ^a δ (ppm)	HMBC H to C	ROESY H to H
1		158.5		
2	5.90 s		3, 5, 10, 4'	7B, 13
3		162.0		
4		83.5		
5		134.4		
6	6.20 ^o	130.5	1,4,8	7A, 7B, 14, 15
7	A 3.51 ^h B 2.18 dd (17.6 ; 8.5)	39.0	5, 6,8,9	7B 12
8		37.0		
9	2.60 dd (14.2 ; 7.9)	47.5	7,8,3',4',7'	11A, 11B,13
10		87.7		
11	A α 1.29 dd (12.9 ; 7.9) B β 1.08 dd (14.2 ; 12.9)	45.5	8 9,2',4',9'	12
12	0.84 s	21.0	7,8,9,7'	2', 6'
13	1.55 s [#]	?	1,9,10,	9
14	1.45 s	27.0	4,5,15	14
15	1.55 s [#]	26.0	4,5,14	
1'	6.10 ^o	97.5	2'3'5'7'	7B, 2', 10'
2'	3.30 ^h	46.0	8,11,1', 3',6',7',9'	7'
3'		42.5		
4'		207.5		
5'		79.0		
6'		171.0		

7'	2.54 d (12.5)	53.0	8,2',3',6'	12
8'		170.0		
9'	1.34 s	30.0	11,2',3',4'	2'
10'	1.55 s [#]	?	4', 5', 8'	
OCH ₃	3.60 s	54.0	8'	
10-OH	?			

^a based on HMBC correlations ; ^h hidden under residual solvent or water signal ; ^{o,#} mutually overlapped.

3.1.1.5.2 PC 3.3.22.D

PC 3.3.22.D	
Synonym(s)	: -
Biological Source	: <i>P. citreonigrum</i>
Sample code	: PC 3.3.22.D
Amount	: 1.02 mg
Molecular Formula	: C ₂₅ H ₃₀ O ₈
Molecular Weight	: 458 g/mol
Solubility	: CH ₃ OH
Physical Description	: Pale yellow solids
Optical rotation	: $[\alpha]_D^{20} +4^\circ$ (c, 0.1 in CH ₃ OH)
HPLC Retention Time (R _t)	: 21.88 min (Standard gradient)
Structure	
UV Spectrum	



PC 3.3.22.D was isolated as a small amount of pale yellow solid from ethylacetate extract of *P. citreonigrum* after consecutive isolation using VLC, sephadex, silica column and HPLC preparative. It showed a pseudomolecular ion peak of $[M+H]^+$ at m/z 459.1 in the positive mode ESI-MS analysis. Proton NMR spectrum of PC 3.3.22.D indicated the presence of one olefinic, two methyne, and eight methylene protons. The spectrum also showed the presence of one OH-group, six methyls, and one methoxy group. One methyl at δ 1.24 ppm (H_3-10') appeared as a doublet and coupled to a methyne proton at δ 3.94 ppm ($H-5'$).

Further NMR analysis data suggested that the southern part molecule of this compound was similar to that found in citreonigrin E, F and H. Unfortunately, some connectivities in the δ -lactone ring (A ring system) could not be confirmed using the available spectroscopical techniques because of limited amount of compound. Nevertheless, the observed methyl correlations in HMBC spectrum indicated the connectivity which were also found in citreonigrin E, F and H (figure 3.1.1.5.2.1). In addition, the COSY correlations between olefinic proton $H-6$ (δ , 5.80 ppm) and H_2-7 (δ 2.68 and 1.47 ppm), as well as the A/B spin system assigned to the presence of H_2-2 (δ 3.53 and 3.30 ppm) supported this assignment.

In contrast, the northern part molecule of PC 3.3.22.D showed a unique substructure which has not been observed in any other isolated meroterpenes. A doublet methyl at δ 19.5 ppm ($H-10'$) which coupled to $H-5'$ (δ 3.94 ppm) correlated to a keto carbonyl ($C-4'$) at δ 210.0 ppm in HMBC spectrum. Consequently, correlation of H_3-9' (δ 1.12 ppm) to $C-4$ was also observed in HMBC spectrum. Although the connectivity between $C-2'$ and $C-5'$ could not

be confirmed in this experiment, the HMBC correlation of H3-9' to C-2' and the chemical shifts of C-2' (δ 87.0 ppm) and C-5' (δ 75.0 ppm) suggested the presence of a furon (D ring) system in the molecule.

As shown in COSY and HMQC spectrum, two protons at δ 4.69 and 4.34 ppm ($^2J_{HH}$ 11.0) were assigned as the methylene protons (H₂-1') of an oxygenated carbon C-1' (δ 73.0 ppm). Although some connectivities could not be proved by spectroscopical data, the presence of H₂-1' and the chemical shifts of C-1', C-2' and C-7' brought to the conclusion for the presence of a γ -lactone (E ring) system in molecule. Meanwhile, the presence of C ring system, as observed in citreonigrin F and H, in the northern part molecule was confirmed by HMBC correlations of H₃-9' to C-11 (δ 28.0 ppm), C-3' (δ 47.0 ppm) and C-2' (δ 87.0 ppm), as well as the presence of a spin system between H-9 (δ 37.5 ppm) and H₂-11 (δ 1.86 and 1.76 ppm) in COSY spectrum.

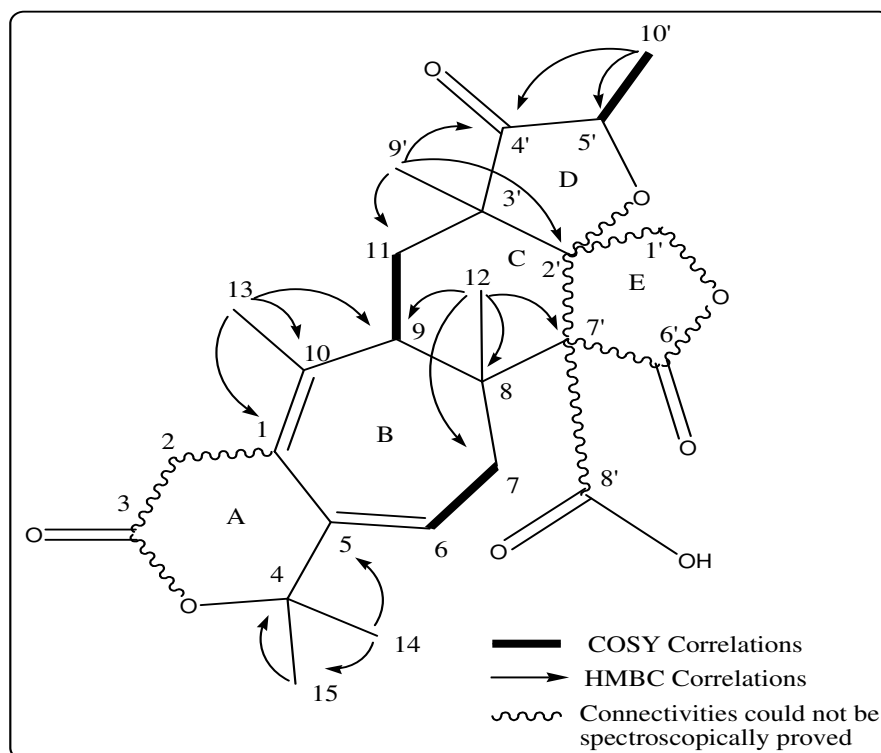


Figure 3.1.1.5.2.1 COSY (at 500 MHz) and some important HMBC correlations of PC 3.3.22.D in DMSO-d₆

Table 3.1.1.5.2.1. NMR data of PC 3.3.22.D in DMSO-d₆ at 500 MHz (¹H) and 125 MHz (¹³C)

Position	¹ H δ (ppm) <i>J</i> _{H-H} (Hz)	¹³ C δ (ppm)	HMBC H to C
1		136.0	
2	A 3.53 d (21.1) B 3.30 ^h	34.0	
3		?	
4		82.0	
5		140.0	
6	5.80 dd (7.8 ; 5.7)	123.0	
7	A 2.68 dd (14.1 ; 7.8) B 1.47 dd (14.1 ; 5.7)	35.0	
8		62.0	
9	3.13 bd (12.6)	37.5	
10		127.0	
11	A 1.86 dd (14.2 ; 3.9) B 1.76 dd (14.2 ; 12.6)	28.0	
12	0.88 s	20.5	7,8,9,7'
13	1.76 s	15.0	1,9,10
14	1.44 s	25.0	4,5,15
15	1.24 s	30.0	4,5,14
1'	A 4.69 d (11.0) B 4.34 d (11.0)	73.0	
2'		87.0	
3'		47.0	
4'		210.0	
5'	3.94 q (7.3)	75.0	
6'		?	
7'		59.0	
8'		?	
9'	1.12 s	21.5	11,2',3',4'
10'	1.24 d (7.3)	19.5	4',5'
8'-OH	?		

^h hidden under residual solvent or water signal ; ^a based on HMBC and HMQC correlations

3.1.1.6 Biological Activities of New Meroterpenes

The meroterpenoid compounds isolated from this study were then subjected to the some bioassays, i.e. antimicrobial, antifungal, cytotoxicity and pro-kinase assays.

A standard agar diffusion method was used to identify the antimicrobial and anti-fungal activities of the isolated compounds using *Bacillus subtilis* and *Cladosporium herbarum*, respectively. The samples were loaded in amount of 100 and 200 mg on agar containing microorganisms. The result was expressed as zone inhibition of microorganisms growth and compared to known antibiotic and antifungal substances.

Table. 3.1.1.6.1. Results of antimicrobial and antifungal assays^{a)} on the isolated meroterpenes.

Compound	Zone of inhibition (mm)			
	<i>B. subtilis</i>		<i>S. cerevisiae</i>	<i>C. herbarum</i>
	100 µg	200 µg		
Citreonigrin A	n.a	n.a	n.a	n.a
Citreonigrin B	n.a	10	n.a	n.a
Citreonigrin C	n.a	n.a	n.a	n.a
Citreonigrin D	n.a	n.a	n.a	n.a
Citreonigrin E	n.a	n.a	n.a	n.a
PC 3.3.6.8.4.F	n.t	n.t	n.t	n.t
PC 3.3.6.8.4.A	n.t	n.t	n.t	n.t
Citreonigrin F	n.a	n.a	n.a	n.a
Citreonigrin G	n.a	n.a	n.a	n.a
Citreonigrin H	n.a	n.a	n.a	n.a
Citreonigrin I	n.a	n.a	n.a	n.a
PC 3.3.6.6.3.A	n.t	n.t	n.t	n.t
PC 3.3.22.D	n.t	n.t	n.t	n.t
PC 3.3.6.6.3.B	n.t	n.t	n.t	n.t
Penicillin G	30 (10 µg) 35 (20 µg)		n.t	n.t
Streptomycin sulfat	12 mm (10 µg)		n.t	n.t

	15 mm (20 µg)		
Gentamicin	10 mm (20 µg)	n.t	n.t
Nystatin	-	8 mm (20 µg)	18 mm (10µg)

n.a : not active

n.t : not tested

Meanwhile, the cytotoxicity assays using some animal and cancer cell lines, for example PC-12, HeLa, and L5178Y cell lines, were also applied to the isolated meroterpenes (table 3.1.1.6.2). Unfortunately, only one of four selected meroterpenes showed a weak activity, meanwhile, the rests did not show any activities.

At the same time, the isolated compounds were also submitted to the protein-kinase assays. Twenty four protein kinases, for example AKT1, ARK5, FAK, etc., were applied to the compounds and the results are shown in table 3.1.1.6.2.

Table. 3.1.1.6.2. Results of the cytotoxicity^{a)} and protein kinase assays^{b)} obtained for the isolated meroterpenes

Compound	Cell growth (%) of test cell lines at the respective concentration of substances		IC ₅₀ (in g/mL) on various protein kinases
	L 5178Y	HeLa	
Citreonigrin A	n.t	n.t	n.a
Citreonigrin B	n.a	n.t	AKT1 (++) ; SRC (+) EPHB4 (+) ; IGF1-R (++) FAK (++) ; ARK5 (-)
Citreonigrin C	n.t	n.t	n.a
Citreonigrin D	n.t	n.t	n.a
Citreonigrin E	50 % (at 8.2 µg/mL)	n.t	n.a
PC 3.3.6.8.4.F	n.t	n.t	n.t
PC 3.3.6.8.4.A	n.t	n.t	n.t
Citreonigrin F	n.a	n.t	n.a
Citreonigrin G	n.a	n.t	n.a
Citreonigrin H	n.t	n.t	n.a
Citreonigrin I	n.t	n.t	n.a
PC 3.3.6.6.3.A	n.t	n.t	n.t
PC 3.3.22.D	n.t	n.t	n.t

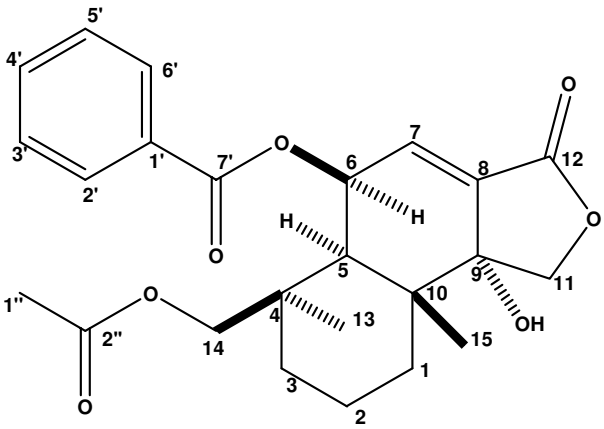
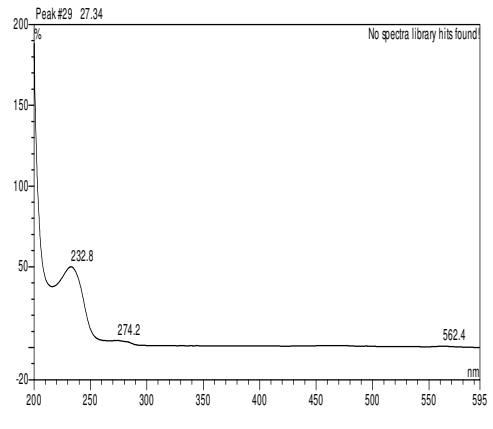
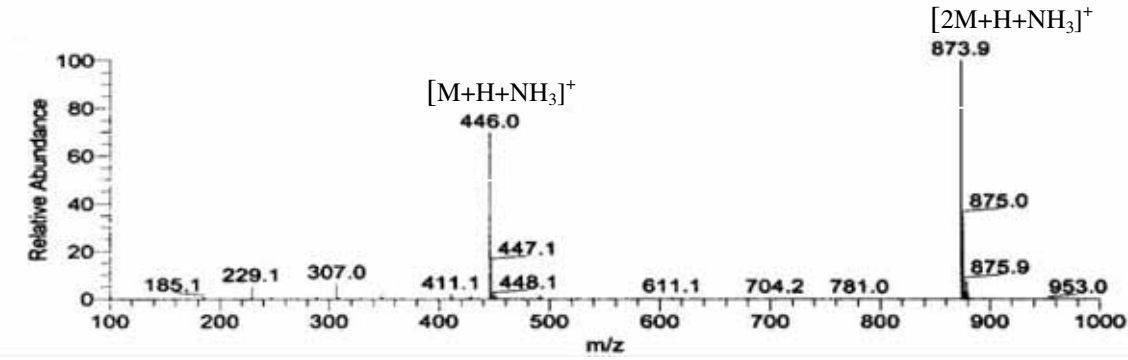
^{a)}The assays were conducted by Prof. W.E.G. Müller at the Institute of Physiological Chemistry, University of Mainz

^{b)}The assays were conducted by ProQinase GmbH, Freiburg

n.a = not active ; n.t = not tested ; (+) = active ; (++) = moderately active ; (-) = weakly active

3.1.1.7 New Sesquiterpene Lactones

3.1.1.7.1 Citredrimene A

Citredrimene A	
Synonym(s)	: 14-acetyl-6-benzoyl-9-hydroxy-7-drimen-12,11-olide ; 14-acetyl-6-benzoyl-9-hydroxycinnamolide
Biological Source	: <i>P. citreonigrum</i>
Sample code	: PC 3.3.6.8.7.H
Amount	: 1.17 mg
Molecular Formula	: C ₂₄ H ₂₈ O ₇
Molecular Weight	: 428 g/mol
Solubility	: CH ₃ OH, CH ₂ Cl ₂
Physical Description	: Pale yellow solid
Optical rotation	: $[\alpha]_D^{20}$ -80° (c 0.1 in CH ₃ OH)
HPLC Retention Time (R _t)	: 27.69 min (Standard gradient)
Structure	
UV Spectrum	
(+) ESI-MS	

Citreodrimene A was isolated as a small amount of pale yellow solids from the ethyl acetate extract *P. citreonigrum*. A molecular weight of 428 g/mol was assigned to this compound with the help of ESI-MS data analysis showing a pseudomolecular ion at m/z 446.0 $[M + H + NH_3]^+$ in the positive mode. The 1H NMR spectrum of this compound showed the presence of three methyls and one hydroxy group at δ 5.84. Moreover, five aromatic protons between δ 7.53 and δ 7.64, one olefinic proton at δ 6.64, and ten methylene protons lying between δ 0.98 and δ 4.58 were also detected in the spectrum.

As shown in the COSY spectrum, the connectivity between H_{2-1} , H_{2-2} and H_{2-3} was confirmed by the presence of a spin system which included these protons. Consecutively, the position of this three methylene groups in the A ring system was determined by the HMBC correlations of $H-3\alpha/C-5$ and $H-1\alpha/C-10$. Furthermore, HMBC correlations of $H_3-15/C-1$ and $H_3-13/C-3$ not only supported the assignment of the three methylene groups but also proved the position of CH_3-15 and CH_3-13 in the A ring, respectively. The exocyclic nature of H_2-14 was revealed by the HMBC correlations of H_3-13 to $C-14$ (δ 65.5) and $C-4$ (δ 36.5), as well as $H-5$ to $C-14$ and $C-13$.

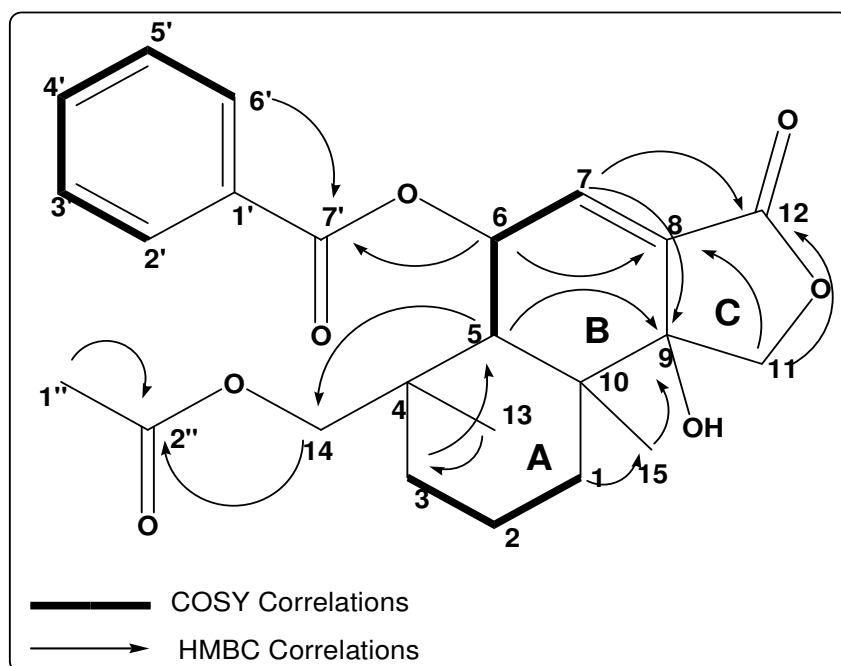


Figure 3.1.1.7.1.1. COSY (600 MHz) and some selected HMBC correlation of citreodrimene A in DMSO- d_6

In the B ring system, the presence of H-7 (δ 6.64) as an olefinic proton was confirmed by a direct correlation of this proton to an olefinic carbon at δ 130.5 (C-7) as well as HMBC correlations of H-7 to C-5 (δ 46.0), C-9 (δ 75.8) and C-12 (δ 168.0). The position of H-6 (δ 5.94) next to H-7 was evident by their mutual coupling constant ($^3J_{HH}$ 4.5 Hz) and their spin system in the COSY spectrum. Consequitively, the position of H-5 (δ 2.36) next to H-6 was verified by HMBC correlations of H-7/C-5 and H-6/C-5 as well as the coupling between H-6 and H-5 ($^3J_{HH}$ 4.0 Hz) as confirmed by the COSY spectrum. The connection of the B ring system to A ring at C-5 and C-10 was evident by the HMBC correlations of H-5 to C-4 as well as H-6/C-10 and H-1/C-10. Furthermore, the correlations of H₃-15 to C-9 (δ 75.8) and C-10 (δ 38.5) as well as H-5 to C-15 (δ 20.5) in the HMBC spectrum confirmed the position of H₃-15, attached at the crosspoint (C-10) of the two rings.

The presence of a γ -lactone ring in the molecule was revealed by HMBC correlation of H-11B to a carbonyl atom at δ 168.0 ppm (C-12). Moreover, the direct correlation of H₂-11 to an oxygenated carbon (C-11, δ 76.0 ppm) indicated the position of the ester alcohol in the C ring. The incorporation of C-8 (δ 132.5) and C-9 (δ 75.8) in to the γ -lactone ring as well as the linkage between rings B and C was evident not only by HMBC correlations of H-11B to C-8 (δ 132.5 ppm) and C-9 (δ 75.8 ppm), but also the correlation of H-6/C-8, H-7/C-9, and H-7/C-12.

The presence of the aromatic ring system in the molecule was confirmed by the presence of a distinctive doublet of doublets at δ 7.94 (H-2' and H-6') displaying an "ortho-like" coupling ($^3J_{HH}$ 8.5 Hz) to other two aromatic protons at δ 7.53 (H-3' and H-5') and a "meta-like" coupling ($^4J_{HH}$ 1.2 Hz) to another aromatic proton at δ 7.67 (H-4'). Furthermore, the corresponding spin system was discernible in the COSY spectrum. The HMBC correlations of H-2', H-6' and H-6 to a carbonyl atom at δ 164.5 (C-7') clearly indicated the position of the benzoyl group as attached to C-6 in the B ring system.

However, here was no direct spectroscopical evidence to prove the position of the hydroxyl group at C-9 (9-OH). Although the presence of the hydroxyl group was observed in the ¹H-NMR spectrum, its signal did not show any correlation in the HMBC spectrum. However, this assignment was verified by the chemical shifts of C-9 at δ 75.8 and the close spatial

proximity of OH-9 and H-5 shown by the ROESY experiment (see below). Meanwhile, the position of the acetyl group at C-14 was evident by the HMBC correlations of H₂-14 and H₃-1''' to carbonyl carbon at δ 170.0 (C-2'''), as well as the chemical shift of C-14 at δ 65.5. The important HMBC and COSY correlations are given in detail in figure 3.1.1.7.1.1..

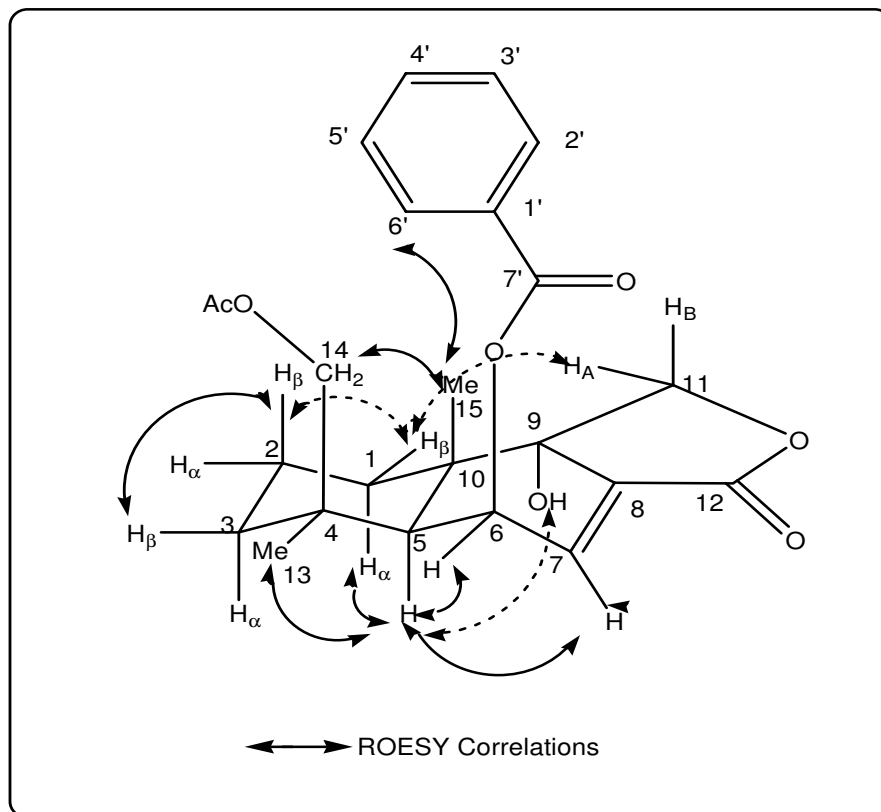


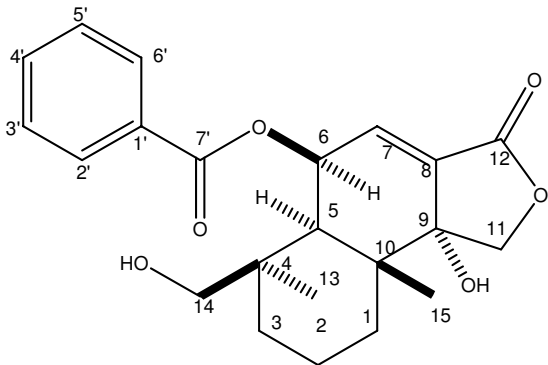
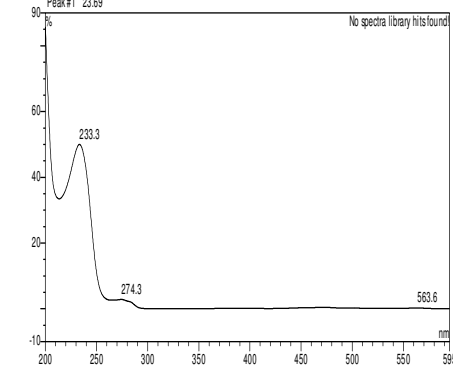
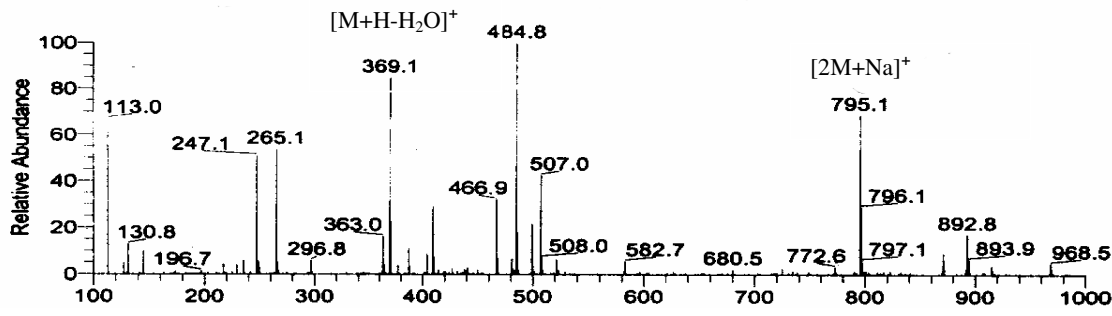
Figure 3.1.1.7.1.2. Stereo drawing of citreodrimene A showing the observed ROESY correlation in DMSO-d₆

A model of this compound was built based on ROESY correlations (see fig.3.1.1.7.1.2) to determine the relative configurations of the its five stereocenters. The most important correlations include H-5 with 9-OH, H-6, and H₃-13 on the one hand, and H₃-15 with H₂-14 and H₂-11 on the other hand. Further cross signals helped to assign also the relative stereochemistries of the diastereotopic methylene groups (see figure 3.1.1.7.1.2)

Table 3.1.1.7.1. 1 NMR data of citreodrimene A in DMSO-d₆ at 600 MHz (¹H) and 150 MHz (¹³C)

No.	¹ H δ (ppm), J (Hz)	¹³ C δ (ppm)	HMBC H to C	ROESY
1	Aα 2.08 dt (13.2 ; 4.4) Bβ 1.24 m	30.5	10,15	5 2A,11A,14A
2	Aβ 1.55 m Bα 1.49 m	17.5		1B,3A,11A
3	Aβ 1.85 m Bα 0.98 m	36.0	4 5	2A,11A
4	-	36.5		
5	2.36 d (4.5)	46.0	4,9,10,13,14,15	1A,6,7,13,9-OH
6	5.94 dd (4.5 ; 4.0)	65.0	5,7,8,10,7'	5,7,13
7	6.64 d (4.0)	130.5	5,9,12	5,6,11B,13
8	-	132.5		
9	-	75.8		
10	-	38.5		
11	A 4.58 d (11.2) B 4.12 d (11.2)	76.0	8,9,12	1B,2A,3A,15 7,13
12	-	168.0		
13	1.03 s	26.5	3,4,14	6,7
14	A 4.49 d (9.8) B 4.17 d (9.8)	65.5	4,13,2'' 4,13,2''	1B,15
15	1.24 s	20.5	1,9,10	11A,14A,2',6'
1'	-	129.4		
2'	7.94 dd (8.5 ; 1.2)	129.8	4',6',7'	15
3'	7.53 dt (8.2 ; 7.4)	129.0	1',4',5'	
4'	7.67 dt (7.4 ; 1.2)	134.0	2',6'	
5'	7.53 dt (8.2 ; 7.4)	129.0	1',2',4'	
6'	7.94 dd (8.5 ; 1.2)	129.8	2',4',7'	15
7'	-	164.5		
1''	1.88 s	20.5		
2''	-	170.0		
9-OH	5.84 s			5

3.1.1.7.2 Citreodrimene B

Citreodrimene B	
Synonym(s)	: 6-benzoyl-9,14-dihydroxy-7-drimen-12,11-olide 6-benzoyl-9,14-dihydroxycinnamolide
Biological Source	: <i>P. citreonigrum</i>
Sample code	: PC 3.3.8.6
Amount	: 17.17 mg
Molecular Formula	: C ₂₂ H ₂₆ O ₆
Molecular Weight	: 386 g/mol
Solubility	: Slightly soluble in CH ₃ OH
Physical Description	: White crystals
Optical rotation	: $[\alpha]_D^{20}$ -270° (c 0.1 in DMSO)
HPLC Retention Time (R _t)	: 23.71 min (Standard gradient)
Structure	
UV Spectrum	
(+) ESI-MS	

HMBC correlations of H₃-13 and H₃-15 to C-3 (δ 35.3) and C-1 (δ 31.8), respectively. The HMBC correlations of 14-OH to C-4 (δ 39.0) as well as C-14 (δ 62.7) confirmed the presence of the hydroxyl group at C-14 which was present as a side chain attached to the A ring of citrolide B. Meanwhile, as shown by the HMBC and COSY correlations (figure 3.1.1.7.2.1) the remaining part of citreodrimene B was shown to be similar to that found in citreodrimene A.

Although no ROESY experiment was carried out, it was assumed that the relative configuration of the stereocentres in citreodrimene B were identical to the ones observed for citreodrimene A, since the ¹H and ¹³C NMR chemical shifts attributed to the stereogenic centers were virtually identical. In addition, the sign of the optical rotation was identical in citreodrimene B and citreodrimene A, thus suggesting that both compounds also share the same absolute configuration.

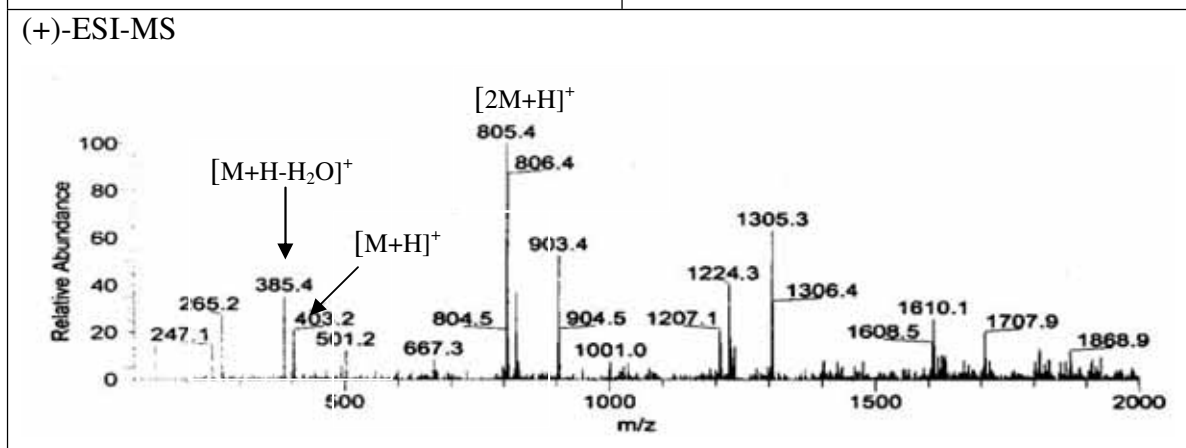
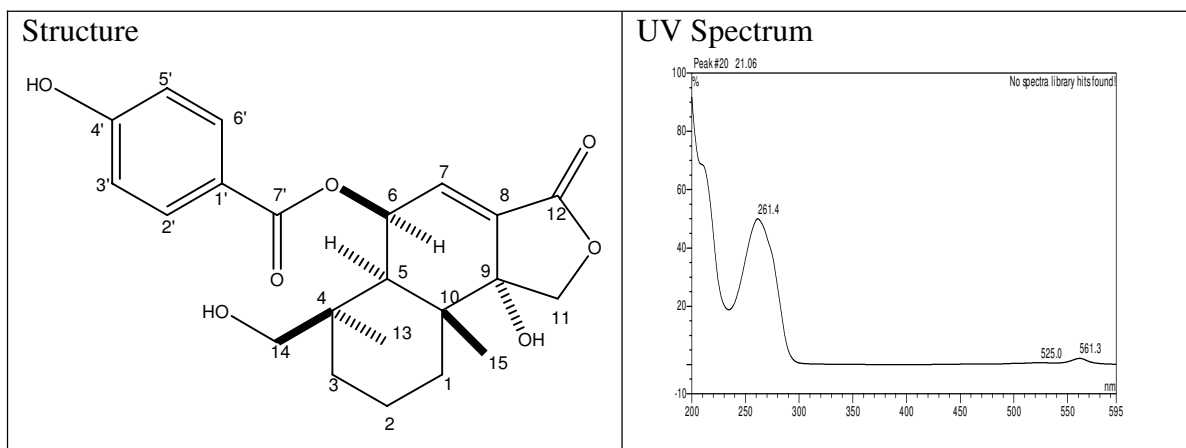
Table 3.1.1.7.2.1. NMR data of citreodrimene B in DMSO-d₆ at 500 MHz (¹H) and 125 MHz (¹³C)

No.	¹ H δ (ppm) <i>J</i> (Hz)	¹³ C δ (ppm)	HMBC H to C
1	A 2.07 dt (13.3 ; 2.8) B 1.23 dm (13.3)	31.8	
2	A 1.56 m B 1.42 m	17.2	
3	A 2.07 dm (12.9) B 0.78 dt (12.9 ; 2.20)	35.3	
4	-	39.0	
5	2.36 d (4.4)	45.8	4,9,10,13,14
6	5.93 dd (4.4 ; 4.1)	66.2	4,5,7,8,7'
7	6.60 d (4.1)	131.4	5,9,12
8	-	133.1	
9	-	75.6	
10	-	38.7	
11	A 4.47 d (9.8) B 4.17 d (9.8)	74.6	9 8,9,12
12	-	168.7	
13	0.95 s	27.0	3,4,5,14

14	A 3.91 dd (10.7 ; 5.7) B 3.28 dd (10.7 ; 5.7)	62.7	13 3,13
15	1.25 s	21.0	1,5,9,10
1'	-	129.3	
2'	7.95 dd (7.5 ; 1.3)	129.4	4',6',7'
3'	7.56 dd (7.9 ; 7.5)	128.9	1',5'
4'	7.68 dt (7.9 ; 1.3)	133.7	2',6'
5'	7.56 dd (7.9 ; 7.5)	128.9	1',3'
6'	7.95 dd (1.3 ; 7.5)	129.4	2',4',7'
7'	-	164.7	
9-OH	5.90 s	-	8,10,11
14-OH	4.28 t (5.7)	-	4,14

3.1.1.7.3 Citreodrimene C

Citreodrimene C	
Synonym(s)	: 6-(4-hydroxybenzoyl)-9,14-dihydroxy-7-drimen-12,11-olide 6-(4-hydroxybenzoyl)-9,14-dihydroxycinnamolide
Biological Source	: <i>P. citreonigrum</i>
Sample code	: PC 5.8.D
Amount	: 1.91 mg
Molecular Formula	: C ₂₂ H ₂₆ O ₇
Molecular Weight	: 402 g/mol
Solubility	: CH ₃ OH
Physical Description	: Brown solid
Optical rotation	: $[\alpha]_D^{20}$ -39° (c 0.1 in CH ₃ OH)
HPLC Retention Time (R _t)	: 21.06 min (Standard gradient)



The UV spectrum pattern of citreodrimene C (λ_{\max} 261.4 nm) indicated that this compound was structurally closely related to citreodrimene A and B. The molecular weight of 402 g/mol was derived from the positive mode ESI-MS experiment which showed a pseudomolecular ion at m/z 805.4 $[2M + H]^+$. Compared to citreodrimene B, the higher molecular weight of 16 mass units indicated the presence of an extra oxygen atom in citreodrimene C. This assumption was also corroborated by the presence of an extra hydroxyl group signal at δ 10.45 in the ^1H NMR spectrum.

As in the case of citreodrimene B, the ^1H -NMR spectrum showed the presence two methyl groups at δ 1.19 and 0.95, one olefinic proton at δ 6.54, two methines protons at δ 5.88 and 2.33, four methylene protons attached to oxygenated carbons, and six aliphatic methylene protons resonating between δ 2.07 and 0.76. However, the spectrum showed the presence of three hydroxyl groups δ 10.45, δ 5.75, and δ 4.27.

In the aromatic region the ^1H NMR spectrum showed the presence of only two distinctive doublets at δ 7.80 and δ 6.88 which coupled to each other as shown in the COSY spectrum. The integration of the peaks and the coupling constant of $^3J_{\text{HH}}$ 8.8 Hz suggested the presence of an AA'BB' spin system in the molecule. Compared to citreodrimene B which has a monosubstituted benzene ring, the aromatic part of PC citreodrimene C consisted a para-disubstituted benzene ring. This assumption was also supported by the strong HMBC correlations of H-2'/H-6' to an oxygenated aromatic carbon at δ 162.4, as well as the weak correlations of H-3'/H-5' to C-4'. In addition, the position of the ester functional group was determined by the HMBC correlations of H-2'/H-6' and H-6 to C-7' (δ 164.4) and supported by the chemical shift of C-1' at δ 119.8.

As indicated by the COSY and HMBC data analysis (figure 3.1.1.7.3.1), the remaining part of citreodrimene C molecule was found to be identical to that of citreodrimene B. Consequently, the relative and the absolute stereochemistry of its five stereocenters was assumed to correspond to those in citreodrimene B. This assumption was supported not only by the same sign of the optical rotation, but also by the close biosynthetic relationships of both compounds (see discussion).

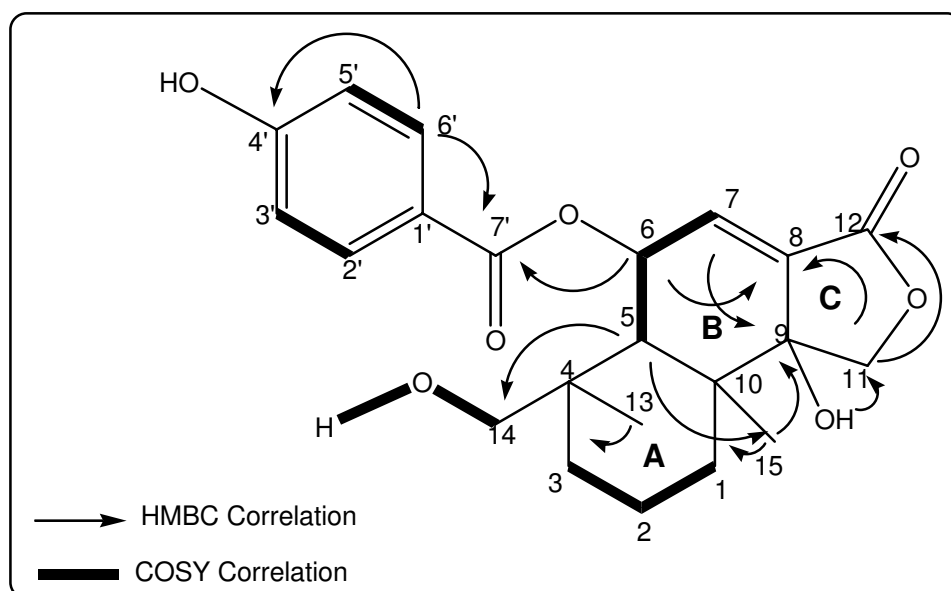
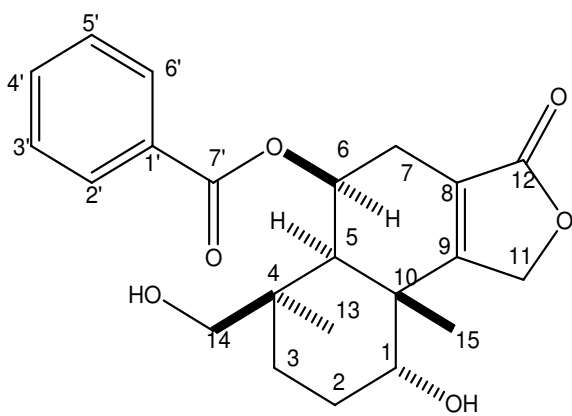
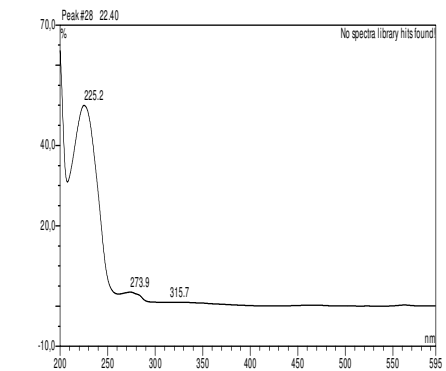
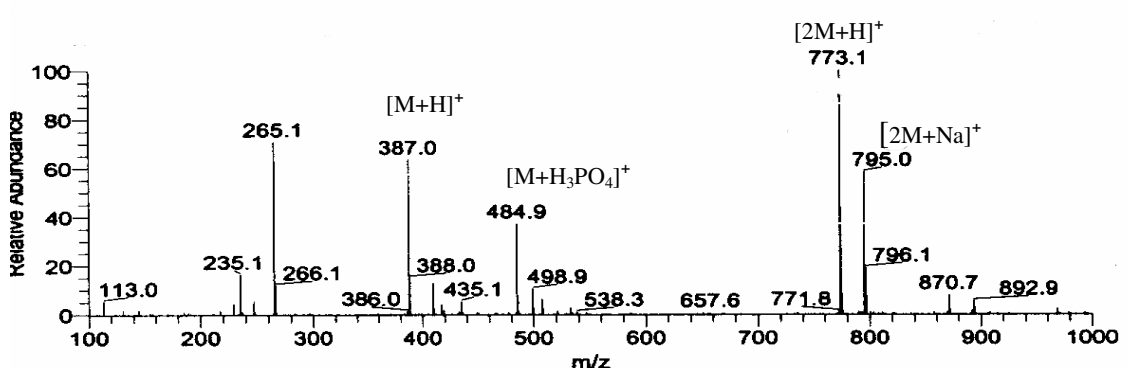


Figure 3.1.1.7.3.1 COSY (500 MHz) and some selected HMBC correlation of citreodrimene C in DMSO- d_6

Table 3.1.1.7.3.1. NMR data of citreodrimene C in DMSO-d₆ at 500 MHz (¹H) and 125 MHz (¹³C)

No.	¹ H δ (ppm) <i>J</i> (Hz)	¹³ C δ (ppm)	HMBC H to C
1	A 2.07 bd (12.9) B 1.22 bd (12.9)	31.7	
2	A 1.55 m B 1.40 m	17.2	
3	A 2.06 dt (13.3 ; 3.7) B 0.76 dt (13.3 ; 2.3)	35.2	
4	-	39.9	
5	2.33 d (4.4)	45.7	4,9,10,13,14,15
6	5.88 dd (4.4 ; 3.8)	65.5	4,7,8,10,7'
7	6.54 d (3.8)	131.7	9,12
8	-	132.9	
9	-	75.9	
10	-	39.7	
11	A 4.45 d (9.7) B 4.15 d (9.7)	74.6	8,9,12
12	-	168.7	
13	0.95 s	26.9	3,4,5,14
14	A 3.88 dd (10.7 ; 5.0) B 3.25 dd (10.7 ; 5.0)	62.7	
15	1.19 s	20.9	1,5,9,10
1'	-	119.8	
2'	7.80 d (8.8)	131.7	4',6',7'
3'	6.88 d (8.8)	115.6	1',4',5'
4'	-	162.4	
5'	6.88 d (8.8)	115.6	1',3',4'
6'	7.80 d (8.8)	131.7	2';4',7'
7'	-	164.4	-
9-OH	5.75 s	-	8,11
14-OH	4.27 t (5.0)	-	
4'-OH	10.45 bs	-	

3.1.1.7.4 Citreodrimene D

Citreodrimene D	
Synonym(s)	: 6-benzoyl-1,14-dihydroxy-8-drimen-12,11-olide
Biological Source	: <i>P. citreonigrum</i>
Sample code	: PC 3.3.14.G
Amount	: 2.51 mg
Molecular Formula	: C ₂₂ H ₂₆ O ₆
Molecular Weight	: 386 g/mol
Solubility	: CH ₃ OH
Physical Description	: Pale yellow solid
Optical rotation	: $[\alpha]_D^{20}$ -20 (<i>c</i> 0.1 in CH ₃ OH)
HPLC Retention Time (R _t)	: 22.37 min (standard gradient)
Structure :	UV Spectrum
	
(+) ESI-MS	
	

Citreodrimene D was isolated as a pale yellow solid from the ethyl acetate extract of *P. citreonigrum* after subsequently separation using VLC, Sephadex LH-20 and silica column chromatography followed by preparative HPLC. The positive mode ESI-MS

In the B ring system, the presence of H₂-7 was assigned not only by direct correlations of H-7A (δ 2.54) and H-7B (δ 2.29) to C-7 (δ 28.0), but also by HMBC correlations of H-7B to C-6 and C-9 (δ 169.8) as well as the correlation of H-5 to C-7. Moreover, these methylene protons coupled to H-6 (δ 5.89) which in turn was coupled to H-5 (δ 2.20) in the COSY spectrum.

Although the ¹H NMR spectrum did not show the presence of any olefinic protons, the presence of quarternary olefinic carbons at δ 169.8 and δ 119.9 was still detected in the ¹³C-NMR spectrum. The position of C-8 (δ 119.9) and C-9 (δ 169.8) in the molecule was assigned by the HMBC correlations of H-7B and H-11B to both carbons, as well as the HMBC correlations of H-5/C-9, H₃-15/C-9 and H-6/C-8. Furthermore, the homoallylic coupling between H₂-11 and H₂-7 in the COSY spectrum confirmed the presence of a double bond between C-8 and C-9. Thus, these findings confirmed the presence of an α,β -unsaturated γ -lactone (C ring) in the molecule.

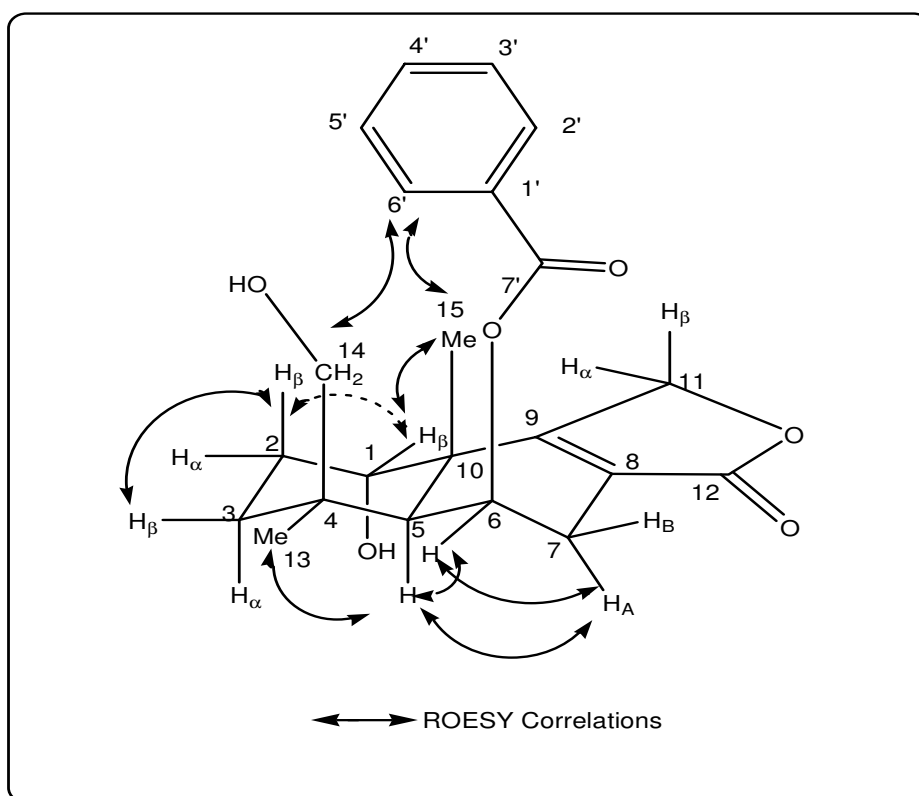


Figure .3.1.1.7.4.2. Spatial correlations of citreodrimene D observed in the ROESY experiment in DMSO-d₆

As in citreodrimene B, the presence of the benzoyl function was evident by the distinctive doublet of doublets at δ 7.97 (H-2'/ H-6') and δ 7.48 (H-3'/ H-5') as well as a doublet of triplets at δ 7.61 (H-4'). This assignment was also confirmed by the presence of a corresponding spin system in the COSY spectrum which involved these aromatic protons and HMBC correlations of H-2'/ H-6' to C-4' (δ 134.5) as well as H-3'/ H-5' to C-1' (δ 131.5). Finally, the position of the ester in the main skeleton was determined by the HMBC correlations of H-2'/H-6' and H-6 to a carbonyl carbon at δ 167.7 (C-7').

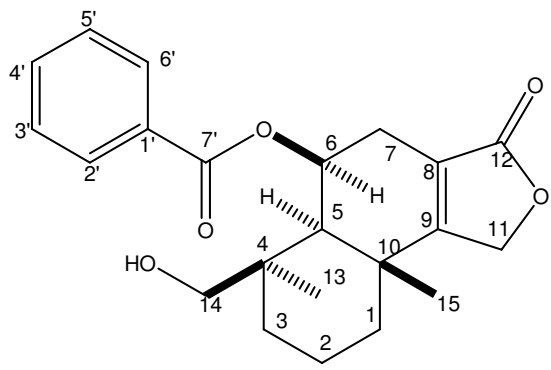
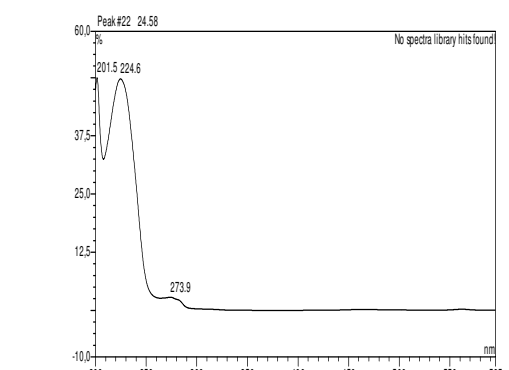
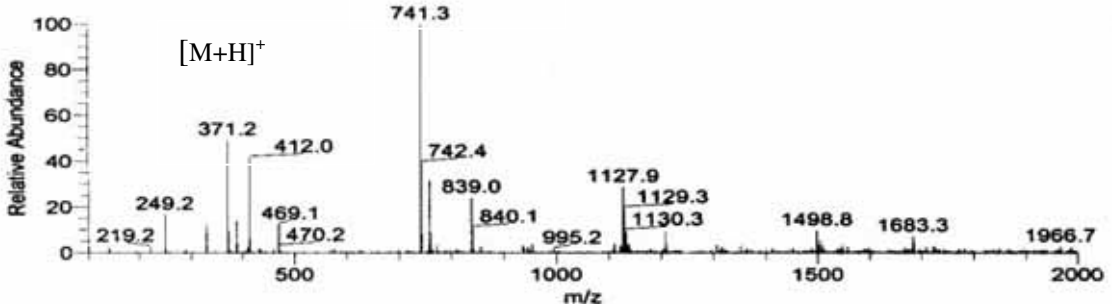
Based on the ROESY correlations, the relative configurations of C-4, C-5, C-6 and C-10 were found to be identical to that in the previous sesquiterpene lactones. In addition, the β -orientation of H-1 was determined the ROESY correlations of H-1 with H-2 β , H-3 β , H-15, and H-11 α . The close spatial proximity of H-7A, H-5 and H-6 was indicated by the ROESY correlations of H-7A with H-5, as well H-6. The complete ROESY correlations of citreodrimene D are shown in figure 3.1.1.7.4.3.

Table 3.1.1.7.4. 1. NMR data of citreodrimene D

Position	MeOD at 500 MHz (¹ H) and 125 MHz (¹³ C)		DMSO-d ₆ at 600 MHz (¹ H) and 150 MHz (¹³ C)				
	¹ H δ(ppm) J (Hz)	¹³ C δ(ppm)	HMBC H to C	¹ H δ(ppm) J (Hz)	¹³ C δ(ppm)	HMBC H to C	ROESY
1	3.85 bs	73.2		3.72 s	70.9	9	2A,3A,7B,11A,14A,15
2	Aβ 2.08 m	26.1		A 1.93 dt	24.8		1,3A,14A
	Bα 1.62 m			B 1.46 m			
3	Aβ 1.82 dt (13.2 ; 3.2)	29.1		1.72 dm	27.9		1,2A,14A
	Bα 1.60 m			1.44 dt			
4	-	40.6			40.0		
5	2.29 bs	47.8	4,10,14,15	2.20 s	45.7	1,3,4,6,7,9,10,13,14,15	6,7A,13
6	6.04 bd (5.1)	69.3	8,10,7'	5.89 d (5.6)	67.8	4,8,10,7	5,7A,7B,13,14B,2',6'
7	A 2.62 dm (18.3)	29.6		A 2.54 dm	28.0		5,6
	B 2.47 d (18.3)			B 2.29 d (20.0)			
8	-	122.4			119.9		
9	-	171.2			169.8		
10	-	43.1			41.4		
11	A+B 5.03 bs	70.8	9	Aα 5.05 dm	68.9	9	1,15
				Bβ 4.94 dd°			
12		176.6			173.6		
13	1.14 s	27.7	3,4,5	1.05 s	27.2	3,4,5,14	3B,5,6,14B
14	A 4.01 d (13.5)	64.7	3,4,13	A 3.80 d (13.0)	62.4	13	1,2A,3A,15,2',6'

	B 3.39 d (13.5)		3,13	B 3.18 d (13.0)		13	6,13,2',6'
15	1.65 s	24.2	1,5,9,10	1.55 s	23.1	1,5,9,10	1,11,14A,2',6'
1'	-	131.5			129.9		
2'	7.97 dd (8.1 ; 1.3)	130.5	4',6',7'	7.90 d (8.7)	129.0	4',6',7'	6,14A,14B,15
3'	7.48 dd (8.1 ;7.8)	129.8	1',5'	7.54 dd (8.7 ; 8.0)	128.8	1',5'	
4'	7.61 dt (7.8 ; 1.3)	134.5	2',6'	7.67 t (8.0)	133.4	2',3',5',6'	
5'	7.48 dd (8.1 ; 7.8)	129.8	1',3'	7.54 t (8.7 ; 8.0)	128.8	1',3'	
6'	7.97 dd (8.1 ; 1.3)	130.5	2',4',7'	7.90 d (8.7)	129.0	2',4',7'	6,14A,14B,15
7'	-	167.7			165.6		
OH-1				4.94 s°			
OH-14				4.30 bs			

3.1.1.7.5 Citreodrimene E

Citreodrimene E	
Synonym(s)	: 6-benzoyl-14-hydroxy-8-drimen-12,11-olide
Biological Source	: <i>P. citreonigrum</i>
Sample code	: PC 3.3.6.8.6.E
Amount	: 6.98 mg
Molecular Formula	: C ₂₂ H ₂₆ O ₅
Molecular Weight	: 370 g/mol
Solubility	: CH ₃ OH, CH ₂ Cl ₂
Physical Description	: Pale yellow solid
Optical rotation	: $[\alpha]_D^{20}$ -23 (c 0.1 in CH ₃ OH)
HPLC Retention Time (R _t)	: 24.60 min (Standard gradient)
Structure	UV Spectrum
	
(+) ESI-MS	
[2M+H] ⁺	
	

The UV spectrum pattern and NMR data analysis indicated that citreodrimene E was closely related to citreodrimene D. The pseudomolecular ion peak at m/z 371.2 $[M+H]^+$ which was shown by this compound in the positive mode ESI-MS suggested the molecular weight of 370 g/mol. Compared to citreodrimene D, the difference of 16 mass units lower suggested the lack of an oxygen atom in this molecule. This fact was also supported by the proton NMR spectrum which showed only one hydroxyl group.

As described above for citreodrimene D, the ^1H NMR spectrum of citreodrimene E showed the presence of five aromatic protons and four methylene protons attached to two different oxygenated carbons. The presence of two quaternary olefinic carbons was also observed in the ^{13}C -NMR data. However, the ^1H spectrum showed only one hydroxyl group, two methine protons and eight methylene protons appearing between δ 2.74 and δ 0.97.

In the A ring system, the HMBC and COSY correlations of this compound were different to the ones observed for citreodrimene D, but similar to those found in citreodrimene B and C. Three methylene groups, H_2 -1, H_2 -2 and H_2 -3, were observed in the ^1H NMR spectrum and were found to form a common spin system in the COSY spectrum. Furthermore, the HMBC correlations H_3 -15/ C -1, H_3 -13/ C -3, H -14A/ C -13, H -5/ C -4, and H -5/ C -10 revealed the nature pattern of the A ring system and its side chain as identical to that of citreodrimene B and C.

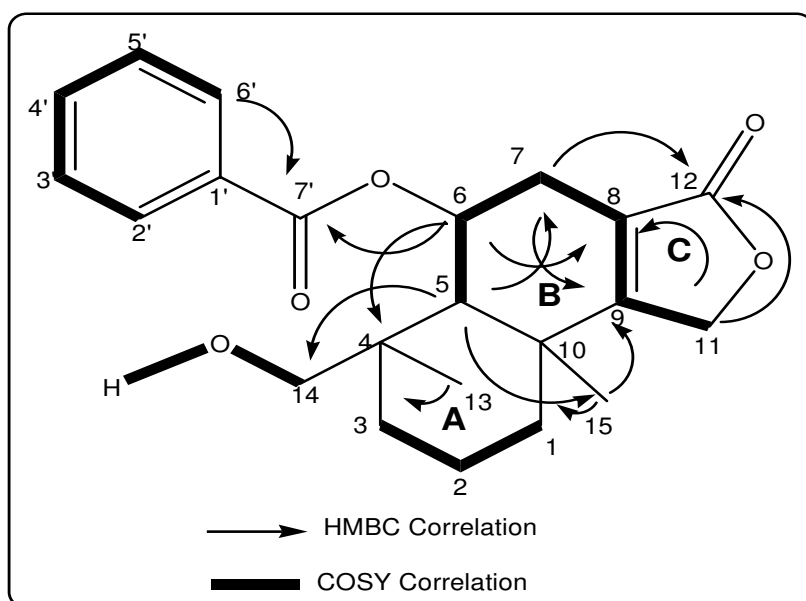


Figure 3.1.1.2.6. COSY (500 MHz) and selected HMBC correlations of citreodrimene E

The B and C ring systems of PC 3.3.6.8.6.E, however, were found to be identical to those in citreodrimene D. The presence of a double bond lying at the junction between ring B and C was confirmed by HMBC correlations including H-6/C-8, H₂-11/C-8, H₃-15/C-9 and H-7A/C-9 as well homoallylic coupling between H₂-11 and H₂-7 observed in the COSY spectrum.

Although no ROESY experiment was acquired, the relative and absolute stereochemistry of the stereocenters in the molecule was assumed to be identical to that found in citreodrimene D, since both compounds share the same sign of the optical rotation and display very similar chemical shifts in the spectra.

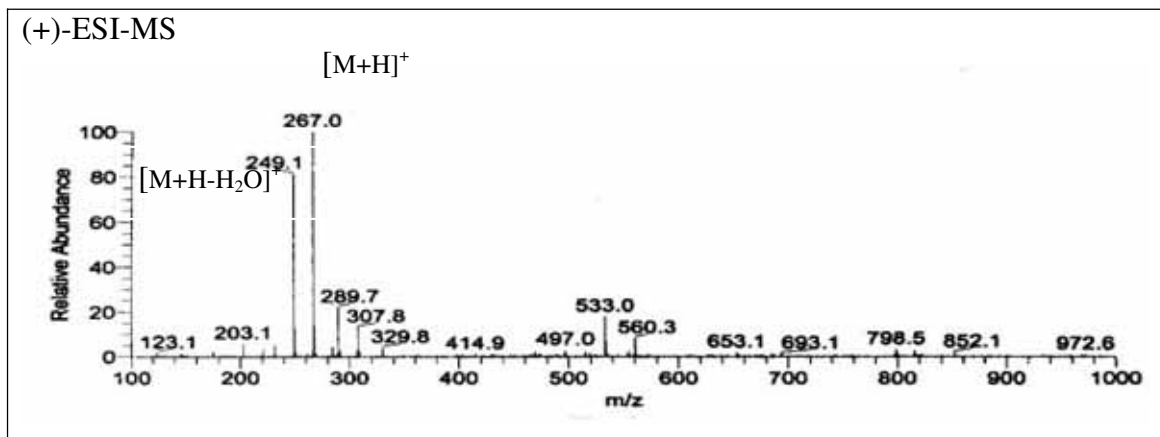
Table 3.1.1.7.5.1 NMR data of citreodrimene E in DMSO-d₆ at 500 MHz (¹H) and 125 MHz (¹³C)

No.	¹ H δ (ppm) J (Hz)	¹³ C δ (ppm)	HMBC H to C
1	A 1.73 bd (13.1) B 1.52 bd (13.1)	37.9	
2	A 1.75 m B 1.55 m	17.8	
3	A 2.05 bd (13.2) B 0.97 dt (13.2 ; 3.5)	34.9	
4	-	39.0	
5	1.78 s	52.6	4,6,10,13,14,15
6	5.92 d (5.4)	67.0	4,5,8,10,7'
7	A 2.74 dm (8.6) B 2.38 bd (8.6)	28.3	5,6 8,9,12
8	-	118.7	
9	-	170.5	
10	-	36.0	
11	A 5.09 dt (7.3 ; 2.6) B 4.92 dd (7.3 ; 2.2)	68.7	8;9;12 8;9;12
12	-	170.3	
13	1.06 s	27.1	3,4,5,14
14	A 3.87 dd (10.2 ; 4.1) B 3.23 bd (10.2)	62.5	13

15	1.63 s	22.9	1,5,9,10
1'	-	129.9	
2'	7.97 dd (8.2 ; 1.3)	129.1	4',6',7'
3'	7.60 dd (8.2 ; 7.4)	128.9	3',5'
4'	7.72 tt (7.4 ; 1.3)	133.5	2',6'
5'	7.60 dd (8.2 ; 7.4)	128.9	1',3'
6'	7.97 dd (8.2 ; 1.3)	129.1	2',4',7'
7'	-	165.6	
14-OH	4.39 bs	-	

3.1.1.7.6 Citreodrimene F

Citreodrimene F	
Synonym(s)	: 6,14-dihydroxy-7-drimen-12,11-olide 6,14-dihydroxycinnamolide
Biological Source	: <i>P. citreonigrum</i>
Sample code	: PC 3.3.12.E
Amount	: 6.43 mg
Molecular Formula	: C ₁₅ H ₂₂ O ₄
Molecular Weight	: 226 g/mol
Solubility	: CH ₃ OH
Physical Description	: Pale yellow solid
Optical rotation	: $[\alpha]_D^{20} -13$ (c 0.1 in CH ₃ OH)
HPLC Retention Time (R _t)	: 20.14 min (Standard gradient)
Structure	
UV Spectrum	



Citreodrimene F was isolated as pale yellow solids from the ethylacetate fraction of *P. citreonigrum*. This compound showed a pseudomolecular ion at m/z 267.0 $[M + H]^+$ in the ESI-MS positive mode which corresponds to a molecular weight of 266 g/mol. Compared to the other isolated sesquiterpene lactones, the ^1H NMR spectrum of this compound did not show the presence of any aromatic protons.

One and two dimensional NMR data indicated that the A ring system of this compound was found identical to that of citreodrimene B and C. The presence of three methylene groups, H₂-1, H₂-2 and H₂-3 forming a contiguous COSY spin system was also observed for this compound. The HMBC correlations H₃-15/C-1 and H₃-13/C-3 not only confirmed the presence of the three methylene groups, but also the position of H₃-15 and H₃-13 as side chains in the A ring system. Although the presence of 14-OH could not be spectroscopically proved, the chemical shifts of C-14 at δ 68.5, as well as the biosynthetic relationships between this compound and the other isolated sesquiterpene lactones suggested the attachment of the hydroxyl group to C-14. Moreover, the HMBC correlations H₂-14/C-5 assigned the position of this functional group in the A ring system.

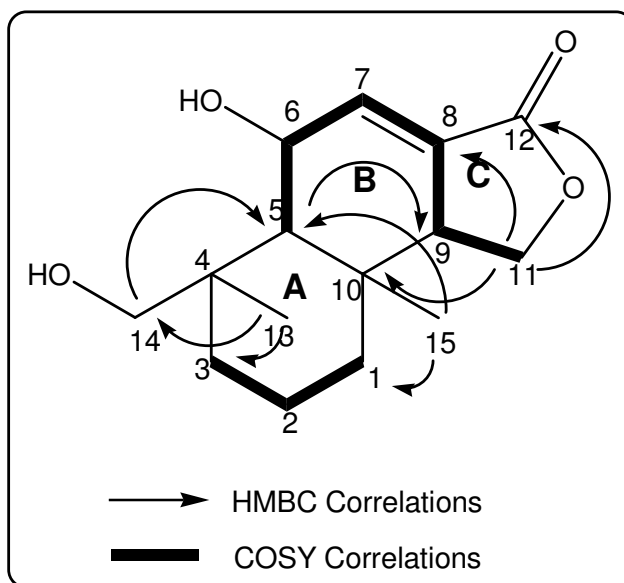


Figure 3.1.1.7.6.1. COSY (500 MHz) and selected HMBC correlations of citreodrimene F in DMSO- d_6

The HMBC and COSY correlations observed for the B and C ring system in citreodrimene F indicated that this part of molecule was quite different to that found in the other isolated sesquiterpene lactones. The ^1H NMR showed the presence of one olefinic, three methine and two methylene protons, as well as one hydroxyl group. As in other sesquiterpene lactones, the olefinic proton at δ 6.60 coupled to H-6 and further to H-5 in the COSY spectrum. Meanwhile, the methine proton at δ 2.75 (H-9) coupled to H₂-11 and H-7 in the COSY spectrum and correlated to C-7 and C-8 in the HMBC spectrum. An allylic ($^4J_{HH}$) coupling of 2.5 Hz between H-7 and H-9 suggested the presence of a double bond in between. Although the presence of 6-OH could not be confirmed by either HMBC or COSY correlations, the chemical shifts of C-6 (δ 64.5 in CD₃OD) as well as molecular weight calculation suggested the placement of hydroxyl group at C-6, thus indicating the absence of any ester substituent as observed for the previously described citreodrimanes. The remaining HMBC and COSY correlations of this compound are shown in figure 3.1.17.6.1.

The results of ROESY experiment suggested that the stereochemistry of this molecule was comparable to that of the previous sesquiterpene lactones. The ROESY correlation of H-5 with H-9 as well as H-6 and H₃-13 indicated the close spatial proximity between H-5, H-6, H-9, and H₃-13 on the α -face of the molecule. Consequently, 6-OH was present in β -orientation, together with H₃-15 and H₂-14 as shown by the ROESY correlations of H₃-15

with H₂-14. The remaining ROESY correlations are shown in figure 3.1.1.7.6.2, also establishing the orientation of methylene protons at H₂-1, H₂-2, H₂-3 and H₂-11.

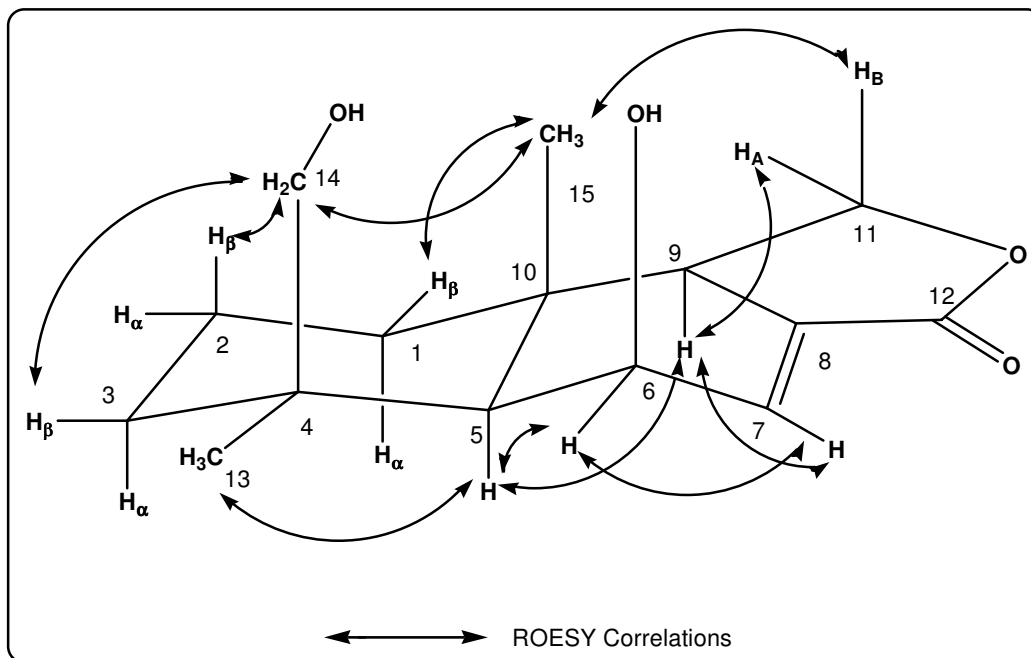


Figure 3.1.1.7.6.2. Spatial correlations of citreodrimene F based on the ROESY experiment in DMSO-d₆ (400 MHz)

Table 3.1.1.7.6. 1. NMR data of citreodrimene F

Position	in CD ₃ OD at 500 MHz (¹ H) and 125 MHz (¹³ C)		in DMSO-d ₆ at 400 MHz (¹ H) and 150 MHz (¹³ C)	
	¹ H δ (ppm) J (Hz)	¹³ C ^α δ (ppm)	¹ H δ (ppm) J (Hz)	¹³ C ^α δ (ppm)
1	Aβ 1.67 dm (12.6) Bα 1.33 m	43.0	1.55 m 1.15 m	42.0
2	Aβ 1.58 m Bα 1.42 m	19.5	1.45 m 1.25 m	?
3	Aβ 1.78 dm (14.6) Bα 1.25 m	41.0	1.80 bd (14.2) 1.05 m	? 5
4	-	39.5	-	39.0
5	1.45 d (4.1)	56.5	1.20 d (4.0)	56.0
6	4.63 dd (6.6 ; 4.1)	64.5	4.52 dd (6.5 ; 4.0)	? 4
7	6.74 dd (6.6 ; 2.8)	137.0	6.60 dd (6.5 ; 2.5)	137.0
8	-	128.0	-	128.0
9	2.85 ttt (9.1 ; 9.1 ; 2.8)	53.0	2.75 ttt (9.0 ; 9.0 ; 2.5)	53.0
10	-	35.0	-	34.0
11	A 4.48 t (9.1) B 4.13 t (9.1)	69.5	4.40 t (9.0) 4.05°	68.0
12	-	173.5	-	170.0
13	1.13 s	27.0	1.10 s	27.0
14	A 4.26 d (11.8)	68.5	4.05°	68.5

	B 3.46 d (11.8)		3,4,5,13	3.48 d (11.5)		5	2A,3A,15
15	1.06 s	16.5	1,5,9,10	0.90 s	17.0	1,5,9,10	1A,11A,11B, 14A,14B
6-OH				?			
14-OH				?			

^a Based on HMBC spectrum

^o Mutually overlapped

3.1.1.8 Biological Activity of New sesquiterpene Lactones

The isolated sesquiterpene lactones were tested for their biological activities. Table 3.1.1.8.1 shows the results of antimicrobial and antifungal assays. It can be concluded that citreodrimenes A - F did not show any activities in anti-fungal assays and only one of them (citreodrimene A) showed a weak antimicrobial activity toward *Bacillus subtilis*.

Table. 3.1.1.8.1 Results of antimicrobial and antifungal assays obtained for citreodrimenes A - F.

Compound	Zone of inhibition (mm)			
	<i>B. subtilis</i>		<i>S. cerevisiae</i>	<i>C. herbarum</i>
	100 µg	200 µg		
Citreodrimene A	9	n.t	n.a	n.a
Citreodrimene B	n.a	n.t	n.a	n.a
Citreodrimene C	n.a	n.t	n.a	n.a
Citreodrimene D	n.a	n.t	n.a	n.a
Citreodrimene F	n.a	n.t	n.a	n.a
Citreodrimene G	n.a	n.t	n.a	n.a
Penicillin G	30 (10 µg) 35 (20 µg)		n.t	n.t
Streptomycin sulfat	12 mm (10 µg) 15 mm (20 µg)		n.t	n.t
Gentamicin	10 mm (20 µg)		n.t	n.t
Nystatin	-		8 mm (20 µg)	18 mm (10µg)

n.a : not active

n.t : not tested

Meanwhile, table 3.1.1.8.2 shows the results of the cytotoxicity and protein-kinase assays. Three of the isolated sesquiterpene lactones, citreodrimene A,B and C, proved active against some cell lines when it subjected to cytotoxicity assays. On the other hand, citreodrimene D showed the activities on some protein-kinases assays.

Table. 3.1.1.8.2. Results of the cytotoxicity^{a)} and protein kinase assays^{b)} obtained for citreodrimenes A - F.

Compound	Cell growth (%) of test cell lines at the respective concentration of substances			IC ₅₀ (in g/mL) on various protein kinases
	L 5178Y	HeLa	PC 12	
Citreodrimene A	50 % (at 1.1 µg/mL)	50 % (at 1.78 µg/mL)	n.t	n.t
Citreodrimene B	50 % (at 0.48 µg/mL)	80 % (at 0.3 µg/mL)	34 % (at 1 µg/mL)	n.a
Citreodrimene C	50 % (at 1.5 µg/mL)	50 % (at 7.6 µg/mL)	n.t	n.a
Citreodrimene D	n.a	n.t	n.t	FAK (+) EPHB4 (+) ERBB2 (++) EGF-R (+-) VEGF-R3 (++) MET (-) SAK (-)
Citreodrimene E	n.a	n.t	n.t	n.a
Citreodrimene F	n.a	n.t	n.t	n.t

^{a)}The assays were conducted by Prof. W.E.G. Müller at the Institute of Physiological Chemistry.

University of Mainz

^{b)}The assays were conducted by Pro-Qinase GmbH, Freiburg

n.a = not active n.t = not tested

(+) = active (++) = moderately active (-) = weakly active

3.1.1.9 New Vermistatine Derivate

(PC 3.3.6.6.5.E)	
Synonym(s)	: 14,15-dihydrovermistatin
Biological Source	: <i>P. citreonigrum</i>
Sample code	: PC 3.3.6.6.5.E
Amount	: 5.8 mg
Molecular Formula	: C ₁₈ H ₁₈ O ₆
Molecular Weight	: 330 g/mol
Solubility	: CH ₃ OH
Physical Description	: Yellow solid
Optical rotation	: $[\alpha]_D^{20}$ -20 (c 0.2 in CHCl ₃)
HPLC Retention Time (R _t)	: 24.70 min (Standard gradient)
Structure	UV Spectrum
(+) ESI-MS	

PC 3.3.6.5.E obtained from the ethylacetate extract of *P. citreonigrum* over subsequent separations using VLC, Sephadex LH-20, silica column chromatography and preparative HPLC as yellowish white crystals. The molecular weight of 330 g/mol was deduced from

ESI-MS data which showed a pseudomolecular ion at m/z 331.2 $[M + H]^+$ in the positive mode. The molecular formula of this compound was assigned as $C_{18}H_{18}O_6$ by analysis of NMR data and the available molecular weight. Moreover, the UV spectrum indicated that this compound was structurally closely related to vermistatin, a known cytotoxic fungal metabolite which was also isolated in this study.

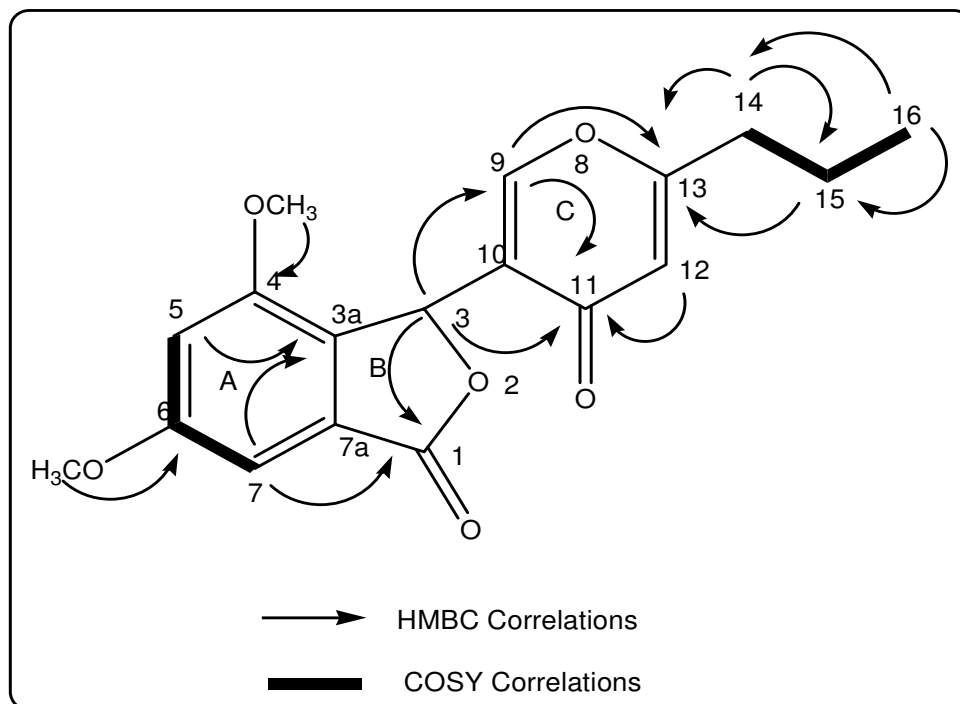


Figure 3.1.1.9.1. COSY (500 MHz) and some selected HMBC correlation of PC 3.3.6.6.5.E in $CDCl_3$

The 1H NMR spectrum of this compound showed the presence of four aromatic protons, one methyl and two methoxy groups. Furthermore, two distinctive methylene group were also identified in the spectrum. Further data analysis indicated that two aromatic protons at δ 6.68 (H-5) and δ 6.98 (H-7) showed a meta-coupling ($^4J_{HH}$ 1.8 Hz) to each other, which was confirmed in the COSY spectrum. The HMBC correlations of 4-OCH₃ (δ 3.79) and H-5 (δ 6.68) to C-4 (δ 153.5), as well as the HMBC correlations of 6-OCH₃ (δ 3.88), H-5 (δ 6.68) and H-7 (δ 6.98) to C-6 (δ 163.4) enabled assignment not only of the positions of H-7 and H-5, but also the two methoxy groups as substituents in the A ring system. Furthermore, the HMBC correlation of H-7 to a carbonyl carbon at δ 172.8 assigned not only the position of H-7 in the A ring system, but also the presence of a γ -lactone (B ring)

system in the molecule. The latter assignment was also supported by the HMBC correlations of the only methine proton (H-3, δ 6.46) to C-1, as well as the chemical shifts of C-3 (δ 73.5), the only methine carbon in the molecule.

The γ -pyrone (C ring) system in the molecule was identified by the HMBC correlations of H-9 (δ 7.44) and H-12 (δ 6.20) to an unusual upfield keto carbonyl at δ 178.2 (C-11). Moreover, this assignment was also supported not only by the chemical shifts of C-9 (δ 154.5) and C-13 (δ 170.1), but also the correlations of H-9 and H-12 to C-13 in the HMBC spectrum and a direct correlation of H-9 to C-9 in the HMQC spectrum. The linkage of the A ring system to the γ -lactone (B ring) system was evident by the HMBC correlations of H-3 to C-9, C-10 and C-11, as well as H-9 to C-3.

The COSY correlations revealed the presence of a spin system in the aliphatic region belonging to a n-propyl chain which incorporated H₂-14 (δ 2.49), H₂-15 (δ 1.65) and H₃-16 (δ 0.97). This was also supported by the multiplicity of H₂-14 (triplet), H₂-15 (multiplet) and H₃-16 (triplet), as well as the HMBC correlations of H₂-15 and H₃-16 to C-4. Meanwhile, the attachment of this aliphatic chain to the C ring system was determined by the HMBC correlations of H₂-14 and H₂-15 to C-13 (figure 3.1.1.9.1).

Thus PC 3.3.6.5.E was found to differ from the known vermistatin only in the presence of a propyl unit as a side chain at C-13 instead of a 1-propenyl function. Similar to vermistatin, PC 3.3.6.6.5.E has only one stereocenter (C-3) and showed a negative value for the optical rotation. However, since in the original communication (Fuska et al., 1986) no attempt was made to elucidate the absolute configuration, the stereochemistry at C-3 in PC 3.3.6.6.5.E could not be determined.

As vermistatin, isolated from *P. vermiculatum*, has been reported to be active against leukaemia cell line (Fuska et al., 1979)

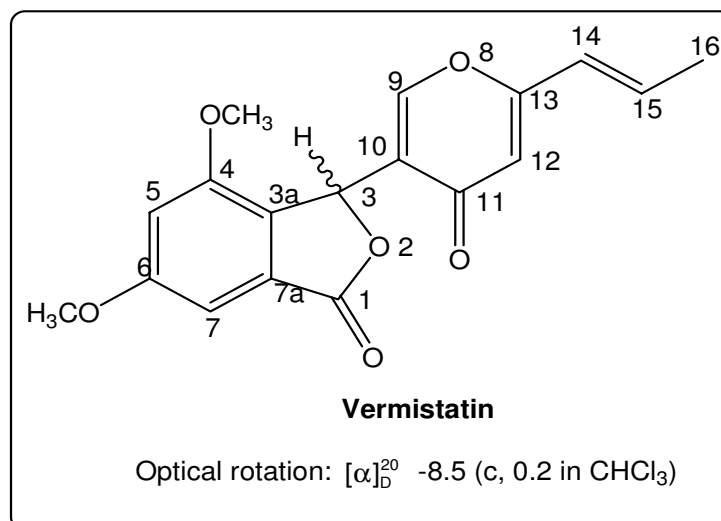


Figure 3.1.1.9.2. Vermistatin

As vermistatin isolated from *P. vermiculatum* has been reported as a fungal cytotoxic agent (Fuska et al., 1979), the new PC 3.3.6.6.5.E together with the isolated vermistatin were tested against different cell lines, but did not show any activity in the cytotoxicity assay using L-5178Y cell lines together. Moreover, PC 3.3.6.6.5.E also did not show any activity in antibacterial, antifungal and protein kinases assays. However, vermistatin showed only weak inhibitory activities against the protein kinases Aurora B, CDK4/cycD1, ERBB2, IGF1R, BRAV-VE, VEGFR-2, Aurora A and AKT1 (data provided by ProQinase GmbH, Freiburg)

Table 3.1.1.9.1 NMR data of Vermistatin and PC 3.3.6.6.5.E in CDCl_3 at 500 MHz (^1H) and 125 MHz (^{13}C)

Position	PC 3.3.6.6.5.E			Vermistatin		
	^1H δ (ppm) <i>J</i> (Hz)	^{13}C δ (ppm)	HMBC H to C	^1H δ (ppm) <i>J</i> (Hz)	^{13}C δ (ppm)	HMBC H to C
1		172.8			172.8	
2		-			-	
3	6.46 s	73.5	1,7a,9,10,11	6.46 s	73.5	1,7a,9,10,11
3a		128.0			128.0	
4		153.5			153.5	
5	6.68 d (1.8)	105.6	3a,6,7	6.68 d (1.8)	105.6	3a,6,7
6		163.4			163.4	
7	6.98 d (1.8)	99.5	1,3a,5,6	6.98 d (1.8)	99.5	1,3a,5,6
7a		128.0			128.0	

8		-			-	
9	7.44 s	154.5	3,10,11,13,	7.44 s	154.5	3,10,11,13,
10		125.8			125.8	
11		178.2			178.2	
12	6.20 s	114.5	10,11,13,	6.16 s	113.0	10,11,13,
13		170.1			162.6	
14	A/B 2.49 t (7.6)	35.6	13	6.06 dd (15.4 ; 1.5)	123.0	13
15	A/B 1.65 m	20.5	13, 14	6.60 dq (15.4 ; 6.8)	136.2	13
16	0.97 t (7.4)	13.5	14	1.92 dd (6.8 ; 1.5)	18.5	13,14,15
4-OCH ₃	3.79 s	56.0	4	3.79 s	56.0	4
6-OCH ₃	3.88 s	56.0	6	3.88 s	56.0	6

3.1.1.10 Known Isolated Metabolites from *P. citreonigrum*

In this study, some known metabolites were also isolated from ethyl acetate extract *P. citreonigrum*. Since they are only known metabolites, their structure elucidations are not discussed in detail in this report. Meanwhile, their activities in some bioassays are reported in section 3.3. The structure of the known compounds which have been isolated from *P.citreonigrum* are shown below.

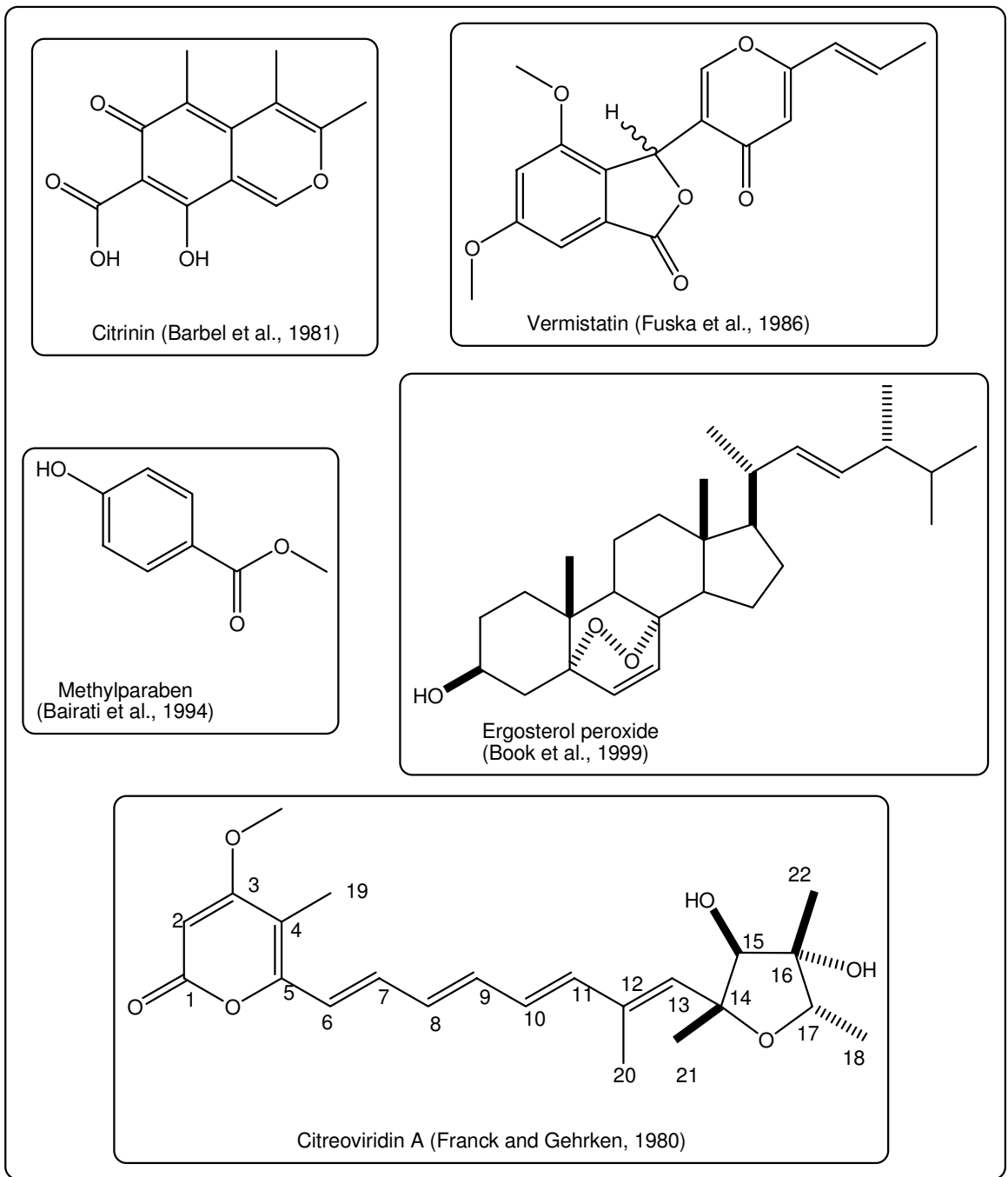
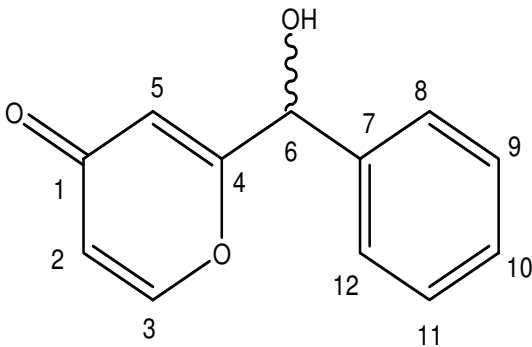
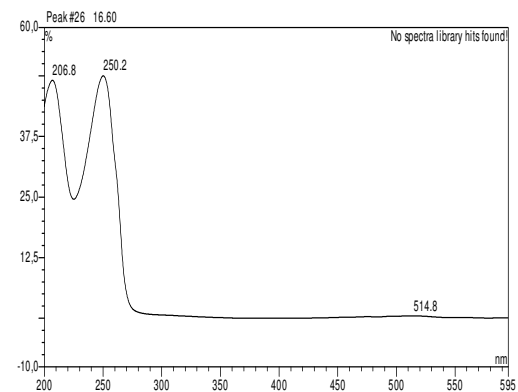
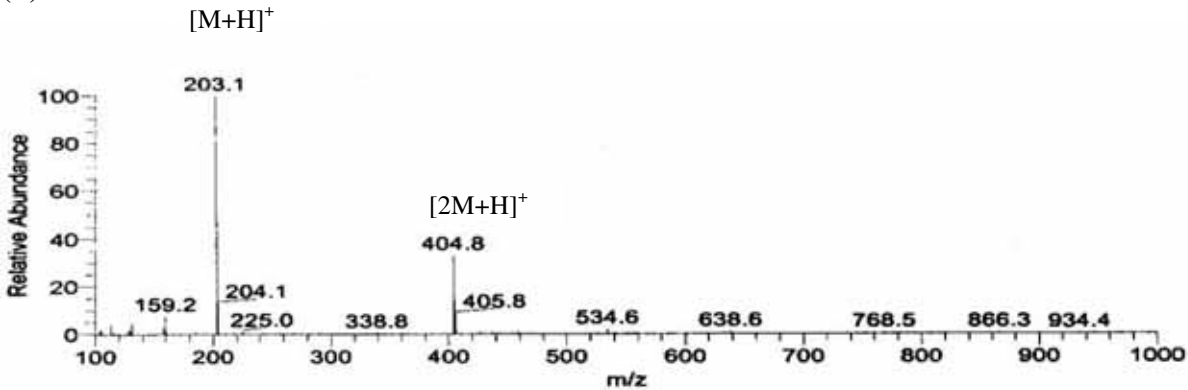


Figure 3.1.1.10.1 Known compounds which were also isolated from *P. citreonigrum* in this study.

3.1.2 New Secondary Metabolites from *Aspergillus niger*

3.1.2.1 2-(Hydroxy(phenyl)methyl)-4-pyrone

2-(Hydroxy(phenyl)methyl)-4-pyrone	
Synonym(s)	: 2-(Hydroxy(phenyl)methyl)-4H-pyron-4-one
Biological Source	: <i>A. niger</i>
Sample code	: ANE 3.16.E
Amount	: 1.49 mg
Molecular Formula	: C ₁₂ H ₁₀ O ₃
Molecular Weight	: 202 g/mol
Solubility	: CH ₃ OH
Physical Description	: Brown solid
Optical rotation	: $[\alpha]_D^{20} +28$ (c 0.1 in CH ₃ OH)
HPLC Retention Time (R _t)	: 16.62 min (Standard gradient)
Structure	UV Spectrum
	
(+)-ESI-MS	
	

This compound was isolated as a brown solid from ethyl acetate fraction of *A. niger*. It showed UV absorption maximum at λ_{\max} 206.8 and 250.2 nm. The molecular weight of

202 g/mol was deduced from the positive mode ESI-MS spectrum showing a pseudomolecular ion at m/z 203 $[M+H]^+$. Its ^1H NMR spectrum revealed five aromatic protons between δ 7.37 – 7.40, one singlet at δ 5.49, and further three protons in the aromatic region.

Five overlapped aromatic protons in the area between δ 7.37 – 7.40 which formed a COSY spin system indicated the presence of a monosubstituted phenyl group in the molecule. The singlet at δ 5.49 was assigned as H-6 attached to an oxygenated carbon at δ 73.4 (C-6) as shown in the HMQC spectrum. The presence of H-6 and its connectivity to the phenyl group was confirmed by HMBC correlations of H-6 to C-7 (δ 142.0), C-8 (δ 128.5) and C-12 (δ 128.5). Furthermore, the chemical shifts of C-6 at δ 73.4 also proved the presence of a hydroxyl group at this position (6-OH) which could not be detected because of the solvent used (CD_3OD) in the NMR measurement.

The presence of a γ -pyrone ring in the molecule was indicated by three protons at δ 6.19, 6.48 and 8.05 ppm, and their correlations by forming a spin system in the COSY spectrum. One of them at δ 6.19 (H-2) showed an ortho coupling ($^3J_{\text{HH}}$ 5.7 Hz) to the one at δ 8.05 (H-3) and a meta coupling ($^4J_{\text{HH}}$ 2.5 Hz) to the remaining one at δ 6.48 (H-5). This assignment was also supported by HMBC correlations of H-3 to C-1 (δ 182.5), C-2 (δ 117.2) and C-4 (δ 173.0). Consequently, the HMBC correlation of H-6 to C-4 as well as a small coupling between H-6 and H-5 as shown in the COSY spectrum (figure 3.1.2.1.1) assigned the linkage of C-6 to C-4 in the γ -pyrone ring system.

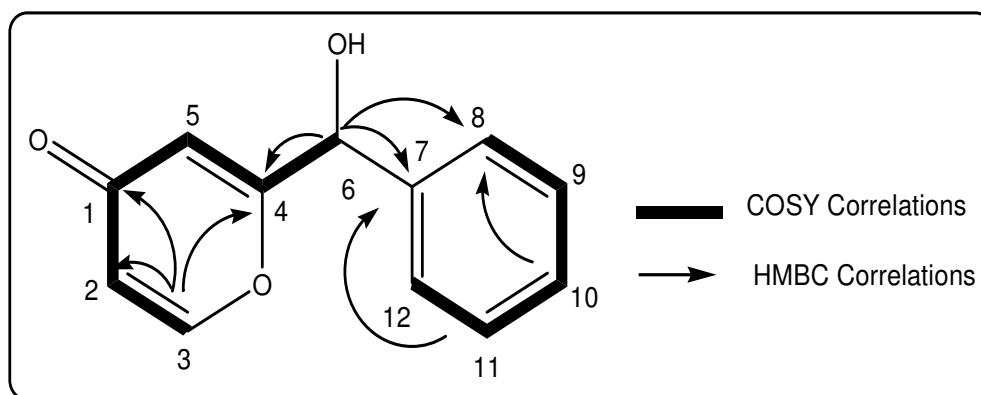


Figure 3.1.2.1.1. COSY (500 MHz) and some important HMBC correlation of 2-(hydroxy(phenyl)methyl)-4-pyrone in CD_3OD

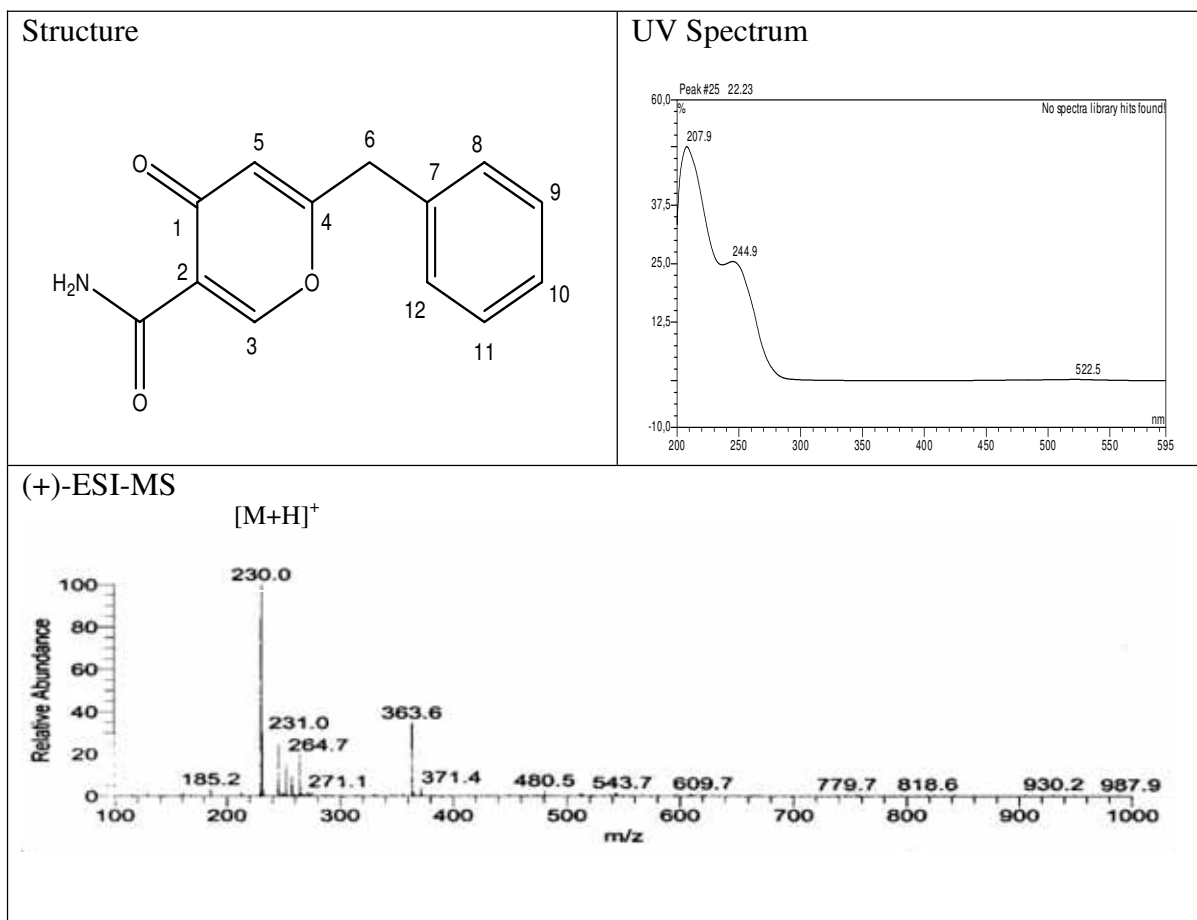
Table 3.1.2.1.1 NMR data of 2-(hydroxy(phenyl)methyl)-4-pyrone in CD₃OD at 500 MHz (¹H) and 125 MHz (¹³C)

Position	¹ H δ (ppm) <i>J</i> _{H-H} (Hz)	¹³ C δ (ppm)	HMBC (H to C)
1	-	182.5	
2	6.19 dd (5.7 ; 2.5)	117.2	
3	8.05 d (5.7)	157.0	1,2,4
4	-	173.0	
5	6.48 d (2.5)	113.5	
6	5.49 s	73.4	4,7,8,12
7	-	142.0	
8/12	7.37 m ^o	128.5	8,10,12
9/11	7.37 m ^o	129.0	9,11
10	7.40 m ^o	129.0	8,12

^o mutually overlapped

3.1.2.2 6-Benzyl-4-oxo-4H-pyran-3-carboxamide

6-Benzyl-4-oxo-4H-pyran-3-carboxamide	
Synonym(s)	: 6-Benzyl-4-oxo-4H-pyran-3-carboxamide
Biological Source	: <i>A. niger</i>
Sample code	: ANE 5.8
Amount	: 6.94 mg
Molecular Formula	: C ₁₃ H ₁₁ NO ₃
Molecular Weight	: 229 g/mol
Solubility	: CH ₃ OH
Physical Description	: Brown solid
HPLC Retention Time (R _t)	: 22.24 min (Standard gradient)



This compound was isolated as a brown solid from the ethylacetate fraction of *A. niger* after subsequent separation techniques using Sephadex LH-20, silica column chromatography and preparative HPLC. Similar to 2-(hydroxy(phenyl)methyl)-4-pyrone, the ^1H NMR spectrum of this compound also showed five overlapping aromatic protons between δ 7.22 and 7.25. However, the spectrum showed only two other singlets in the aromatic region and two protons at δ 3.95. The positive mode ESI-MS spectrum gave a pseudomolecular ion peak at m/z 230.0 $[\text{M}+\text{H}]^+$ which was consistent with a molecular weight of 229 g/mol. The odd value of molecular weight indicated the presence of a nitrogen atom as confirmed by spraying using Dragendorff reagent.

The monosubstituted phenyl group was indicated by the observed five overlapping aromatic protons between δ 7.22 and 7.25 ppm which coupled to each other by forming a COSY spin system. One singlet at δ 3.95 ppm which integrated for two protons belonged to a methylene group (H_2 -6) directly correlated to C-6 (δ 39.5) in the HMBC spectrum.

Moreover, the HMBC correlation of H₂-6 to C-7 (δ 137.5) and C-8/12 (δ 129.5) confirmed this assignment.

In remaining part of the molecule, two singlets at δ 6.30 and 8.78 were characteristic of a γ -pyrone ring. This assignment was confirmed by HMBC correlations of H-3 (δ 8.78) to a keto carbon at δ 179.3 (C-1), a quaternary aromatic carbon at δ 119.8 (C-2) and an oxygenated aromatic carbon at δ 171.0 (C-4) as well as the correlations of H-5 (δ 6.30) to C-2 and C-4. The connectivity of this γ -pyrone ring to the methylene function (H₂-6) was evident by HMBC correlations of H-5 to C-6 as well as H₂-6 to C-4 and C-5. Although the amide protons could not be detected in the ¹H NMR spectrum because of the protic solvent used, the HMBC correlation of H-3 (δ 8.78) to the carbonyl carbon at δ 165.4 (C-1') confirmed the presence of an amide function as a substituent in the γ -pyrone ring system. The remaining HMBC and COSY correlations of 6-benzyl-4-oxo-4H-pyran-3-carboxamide are described in detail in figure 3.1.2.2.1 and table 3.1.2.2.1.

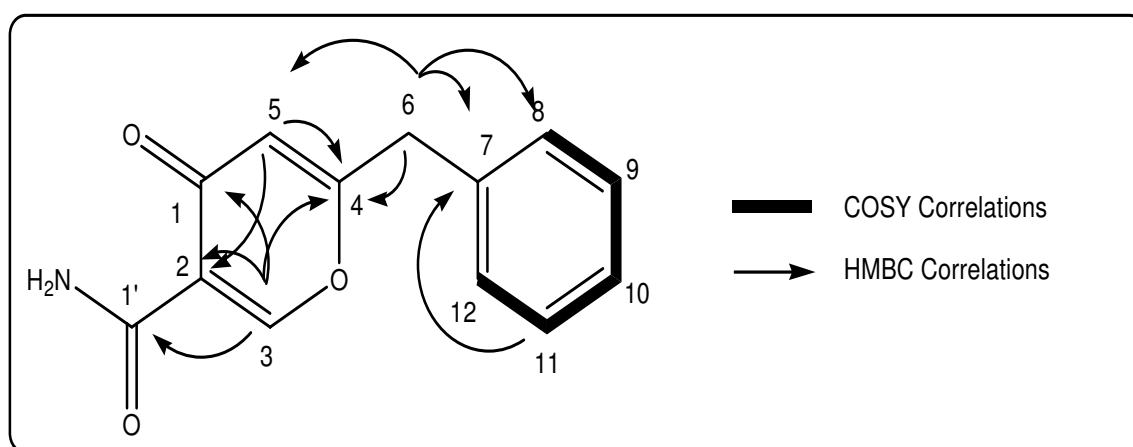


Figure 3.1.2.2.1. COSY (500 MHz) and selected HMBC correlations of 6-benzyl-4-oxo-4H-pyran-3-carboxamide in CD₃OD

Unfortunately, this compound did not show any biological activity in the antimicrobial, antifungal, cytotoxicity or protein kinase assays.

Table 3.1.2.2.1 NMR data of 6-benzyl-4-oxo-4H-pyran-3-carboxamide in CD₃OD at 500 MHz (¹H) and 125 MHz (¹³C)

Position	¹ H δ (ppm) <i>J</i> _{H-H} (Hz)	¹³ C δ (ppm)	HMBC (H to C)
1		179.3	
2		119.8	
3	8.78 s	162.8	1,2,4,1'
4		171.0	
5	6.30 s	115.6	2,4,6
6	(2H) 3.95 s	39.5	4,5, <u>6</u> ,7,8,12
7		137.5	
8/12	7.22 m ^o	129.5	6
9/11	7.25 m ^o	129.5	7
10	7.22 m ^o	129.0	
1'		165.4	

^o mutually overlapped

3.1.2.3 New Aflavinine Derivate

New Aflavinine Derivate	
Synonym(s)	: 19-Epi-21-hydroxy-10,23-dihydro- 24,25-dehydroaflavinine
Biological Source	: <i>A. niger</i>
Sample code	: ANE 6.8.1.1
Amount	: 1.70 mg
Molecular Formula	: C ₂₈ H ₃₉ NO ₂
Molecular Weight	: 421 g/mol
Solubility	: CH ₃ OH, CH ₂ Cl ₂
Physical Description	: Yellowish brown solid
Optical rotation	: $[\alpha]_D^{20} -7$ (c 0.05 in CH ₃ OH)
HPLC Retention Time (R _t)	: 32.86 min (Standard gradient)
Structure	
UV Spectrum	
(+) ESI-MS	

ANE 6.8.1.1 was purified from the ethyl acetate fraction of *A. niger* as a yellowish brown solid with UV absorbance at λ_{\max} 229.6, 282.8 and 283.3 nm. The ¹H NMR spectrum

showed four methyls, two hydroxyls, five aromatic protons and one NH-group. The presence of protons belong to one exomethylene, seven methines, and five methylene groups was detected in the ^1H NMR spectrum after analysis of ^{13}C and 2D NMR data. The appearance of a pseudomolecular ion at m/z 422.2 $[\text{M} + \text{H}]^+$ in the positive mode ESI-MS suggested the molecular weight of 421 g/mol. The odd molecular weight, supported by dyeing using Dragendorff reagent, indicated the presence of a nitrogen atom in the molecule.

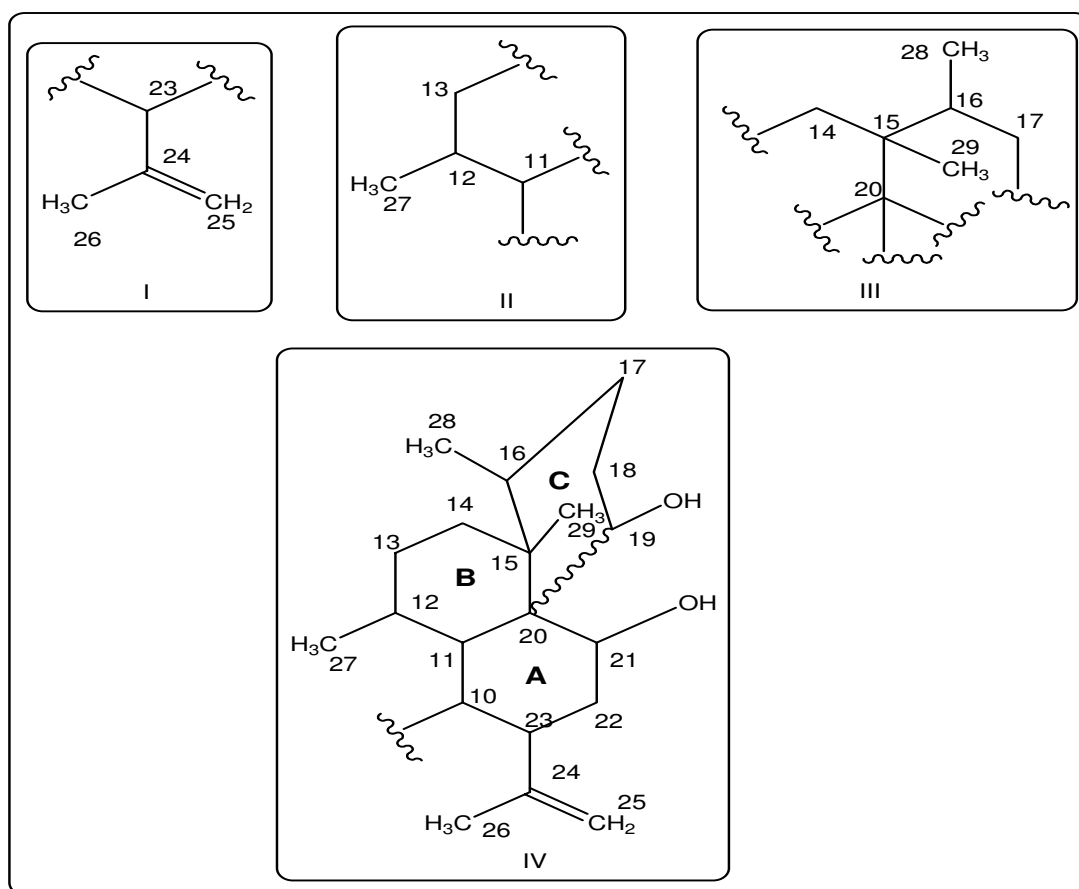


Figure 3.1.2.3.1 Partial structures of ANE 6.8.11 based on the correlations of methyl protons in the HMBC spectrum

Based on the HMBC correlations of the methyl protons in the molecule, it was possible to establish partial structures (see figure 3.1.2.3.1). The correlations of H_3 -26 to two olefinic carbons at δ 150.0 (C-24) and δ 110.4 (C-25) as well as a methine carbon at δ 38.5 (C-23) resulted in substructure I. In addition, a direct correlation of two olefinic protons at δ 4.81 and 4.61 to C-25 in the HMQC spectrum suggested the presence of an exomethylene function (H_2 -25) in this substructure. Meanwhile, the correlations of H_3 -27 to two methine carbon at δ 37.3 (C-11) and δ 28.4 (C-12) as well as one methylene carbon at δ 28.4 (C-13)

in the HMBC spectrum would give partial structure II. Furthermore, partial substructure III appeared as a result of HMBC correlations of two methyl groups (H₃-28 and H₃-29) to C-15 (δ 39.0) as well as the correlations H₃-29/C-14, H₃-29/C-20 and H₃-28/C-17.

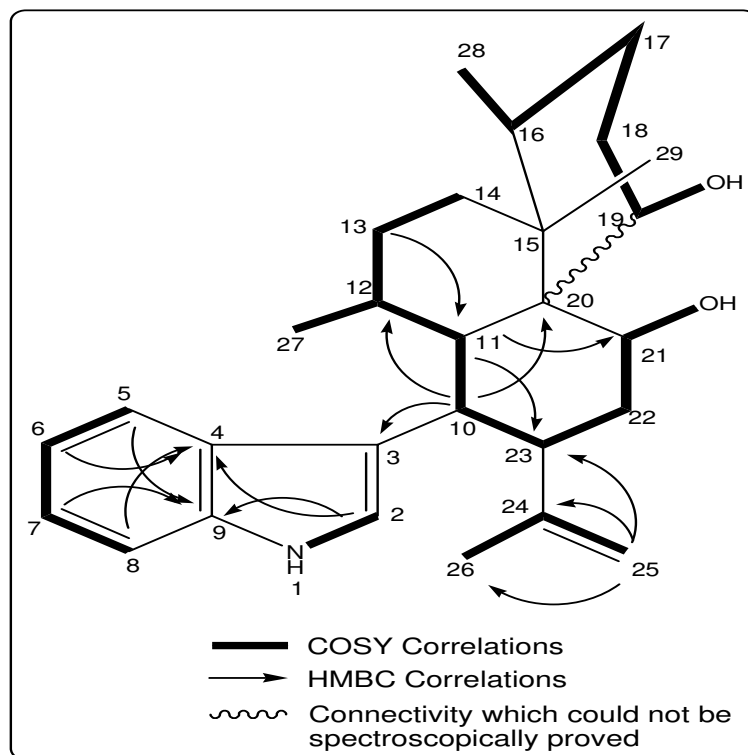


Figure 3.1.2.3.2 COSY (600 MHz) and some selected HMBC correlation of aflavinine derivate in DMSO

Further careful consideration of COSY and remaining HMBC correlations (figure 3.1.2.3.2) allowed the connectivity of substructures I – III. The link between I and II through C-10 was proved by the HMBC correlations of H-11 (δ 2.59) to C-10 (δ 34.0) and C-23 (δ 38.5) as well as the coupling amongst H-23 (δ 3.30), H-10 (δ 3.56) and H-11 (δ 2.59) as observed in the COSY spectrum. Moreover, the couplings between H₂-13 and H₂-14 in the COSY spectrum as well as the HMBC correlations of H-11 to C-20 suggested the connectivity of the substructures II and III.

The presence of rings A and B in this compound was evident not only by an observed complex spin system which included H₂-22, H-23, H-10, H-11, H-12, H₂-13 and H₂-14, but also by the HMBC correlations H₃-29/C-14 and H₃-29/C-20 in substructure III as well as the correlation H-11/C-21. Moreover, the presence of a hydroxyl group in ring A was confirmed not only by the chemical shift of C-21 (δ 68.6), but also the coupling ($^3J_{HH}$ 3.8 Hz) between H-21 (δ 4.55) and 21-OH (δ 4.37) as shown in the COSY spectrum. Another

COSY spin system in the aliphatic region was assigned as a part of ring C and involved H₃-28, H-16, H₂-17, H₂-18 and H-19. Meanwhile, the chemical shift of C-19 (δ 65.7) and the coupling of H-19 to a water exchangeable signal at δ 4.30 (19-OH) defined a further hydroxyl function at this position. However, although the linkage between C-19 and C-20 could not be proven by the performed spectroscopical methods, the chemical shifts of the two carbons allowed ring closure forming a stable six membered ring as a part of a diterpenoid moiety (substructure IV) in this molecule.

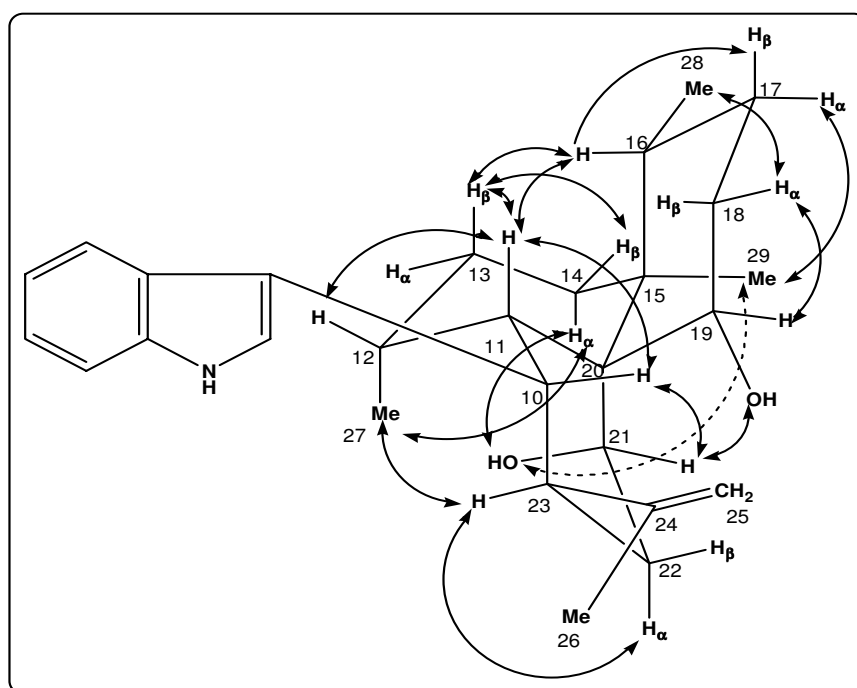


Figure 3.1.2.3.2. Stereo drawing of the new aflavinine deivate showing the observed ROESY correlations in DMSO-d₆

The relative configuration of the stereocenters in the molecule was established by a ROESY experiment. The close proximity of H-10, H-11, H-12 and H-16 in the β -face of the molecule was determined by the ROESY correlations of H-11 with H-10 as well as H-12 and H-16. In addition, the ROESY correlation of H-10 with H-21 assigned the relative configuration of C-21. On the other hand, the α -orientation of H₃-29 was established by the correlations of 21-OH with H₃-29. Moreover, the correlations of H₃-27 with H-23 helped to assign the orientation of H-23 in the α -face of the molecule. Meanwhile, the relative stereochemistry of C-19 was determined by the correlations of H-21 with 19-OH. The remaining ROESY correlations assigned to this compound are described in detail in figure 3.1.1.2.3.3 and table 3.1.1.2.3.1.

In the cytotoxicity assay using the L-5178Y cell line, this compound showed high activity with an ED₅₀ of 2.5 µg/mL. However, this compound could only inhibit the growth of the HeLa cell line by 17 % at a concentration of 3 µg/mL. In antimicrobial assays, ANE 6.8.1.1 showed a weak inhibitory activity in the assay using *B. subtilis* (11 and 12 mm inhibition zone diameter upon loading an amount of 100 and 200 µg, respectively).

Table 3.1.2.3.1 NMR data of the new aflavinine derivate in DMSO-d₆ at 600 MHz (¹H) and 150 MHz (¹³C)

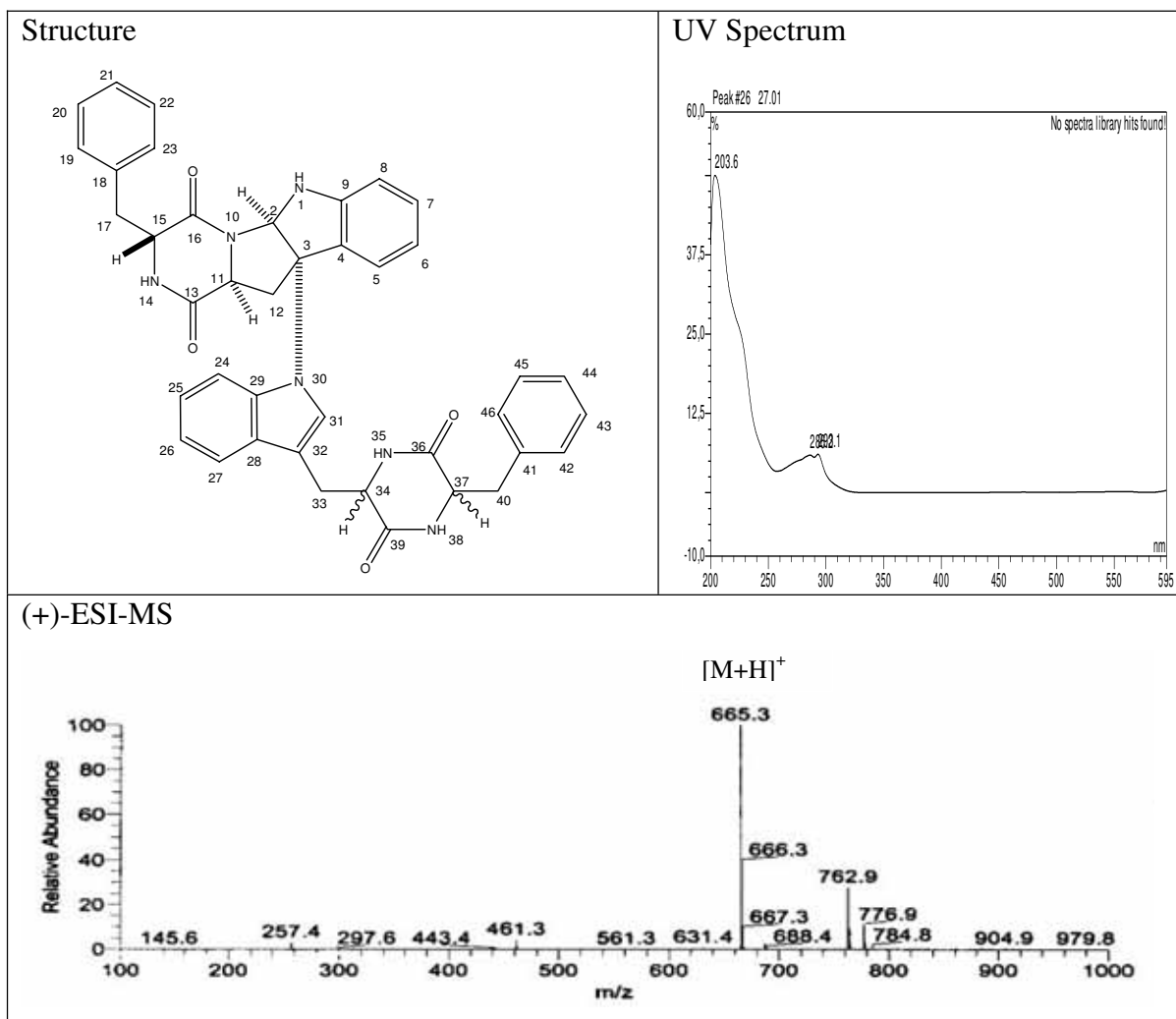
Position	¹ H δ (ppm) J _{H-H} (Hz)	¹³ C δ (ppm)	HMBC (H to C)	ROESY
1	10.65 s	-		2,8
2	7.06 s	123.3	3,4,9	1,10,12,23,25A,27
3	-	114.5		
4	-	127.5		
5	7.45 d (7.8)	116.9	7,9	6,7,10,11,16,18α
6	6.98 dd (7.8 ; 7.0)	117.9	4,8	5,8
7	7.05 dd (7.9 ; 7.0)	120.2	5,9	5,8
8	7.32 d (7.9)	111.0	4,6	1,6,7,16
9	-	136.0		
10	3.56 dd (12.9 ; 5.4)	34.0	3,11,20,23	2,5,11,21,25A,26
11	2.59 m	37.3	10,12,20,21,23	5,10,12,13α,13β,14β,16,21
12	1.17 m [#]	28.4		2,11,16
13	β1.57 m α0.71 m ⁺	28.4	11	11,14β,16,18α 11,14α,14β
14	α2.34 m β0.95 bd (13.9)	28.8		27,29,21-OH 11,13α,13β,
15	-	39.0		
16	2.05 m [§]	30.8		5,8,11,12,13β,17β,18β
17	α1.76 ddd (12.9 ; 12.6 ; 2.5) β1.17 m [#]	24.7		29 16,18β
18	α2.05 m [§] β1.68 dd (13.2 ; 2.2)	30.6		5,13β,19,28,21-OH 16,17β,21,19-OH

19	4.55 bs ^o	65.7		18 α ,22 α ,23,26,29
20	-	45.5		
21	4.55bs ^o	68.6		10,11,18 β ,22 β ,19-OH
22	β 2.14 ddd (13.9 ; 12.6 ; 2.3) α 1.41 m*	37.1		21 19,21-OH
23	3.30 ^h	38.5		2,19,26,27
24	-	150.0		
25	A 4.81 s B 4.61 s	110.4	23,26 23,26	2,10 26
26	1.40 s*	13.7	23,24,25	10,19,25B
27	1.33 d (7.2)	19.2	11,12,13	2,14 α ,23,29,21-OH
28	0.70 d (6.8) ⁺	15.4	15,17	18 α
29	1.05 s	16.6	14,15,20	14 α ,17 α ,19,27,21-OH
19-OH	4.30 d (4.4)			18 β ,21
21-OH	4.37 d (3.8)			14 α ,18 α ,22 α ,27,29

^h hidden under residual solvent or water signal ; ^{o,*,\$,+,#} mutually overlapped

3.1.2.4 New Asperazine Derivate

New Asperazine Derivate	
Synonym(s)	: -
Biological Source	: <i>A. niger</i>
Sample code	: ANE 4.9.4.D
Amount	: 4.56 mg
Molecular Formula	: C ₄₀ H ₃₆ N ₆ O ₄
Molecular Weight	: 464 g/mol
Solubility	: CH ₃ OH
Physical Description	: White crystals
Optical rotation	: $[\alpha]_D^{20} +69$ (c 0.01 in DMSO)
HPLC Retention Time (R _t)	: 27.02 min (Standard gradient)



The molecular weight of 664 g/mol was assigned on the basis of positive mode ESI-MS data showing a pseudomolecular ion at m/z 665.3 $[M+H]^+$. This compound was isolated as white crystals showing UV maxima at λ_{\max} 203.6, 288.3 and 289.1 nm. Interpretation of 1D and 2D NMR spectra (table 3.1.2.4.1) revealed the amino acid nature of this compound. As confirmed in the HMBC spectrum, four alpha protons resonating in the area between δ 3.41 and 4.10 ppm correlated to amide carbonyls. It was apparent that this compound was potentially related to asperazine (Varoglu et al., 1997), which was also isolated in this study, and WIN 64821 (Barrow et al., 1993), both resembling known diketopiperazines which were also described from *Aspergillus* spp. (figure 3.1.2.4.1).

The presence of a diketopiperazine moiety in the northern part of the molecule was evident by the HMBC correlation of a methine at δ 3.41 (H-11) to a carbonyl carbon at δ 168.6 (C-16) as well as the HMBC correlations of another methine proton at δ 3.28 (H-15) to the

second carbonyl at δ 168.2 (C-13). Consecutively, this assignment was supported by the presence of a water exchangeable signal at δ 7.96 (14-NH) which coupled to H-15 in the COSY spectrum and the HMBC correlations of 14-NH to the first carbonyl carbon (C-16) and the methine carbon at δ 56.5 (C-11). Meanwhile, the presence of another COSY spin system involving five aromatic protons at δ 7.11 – 7.19 (H-19 to H-23) as well as HMBC correlations of H-9 and H-23 to a methylene carbon at δ 39.0 (C-17) suggested the presence of a phenylalanine subunit as part of the diketopiperazine moiety in the northern part of the molecule.

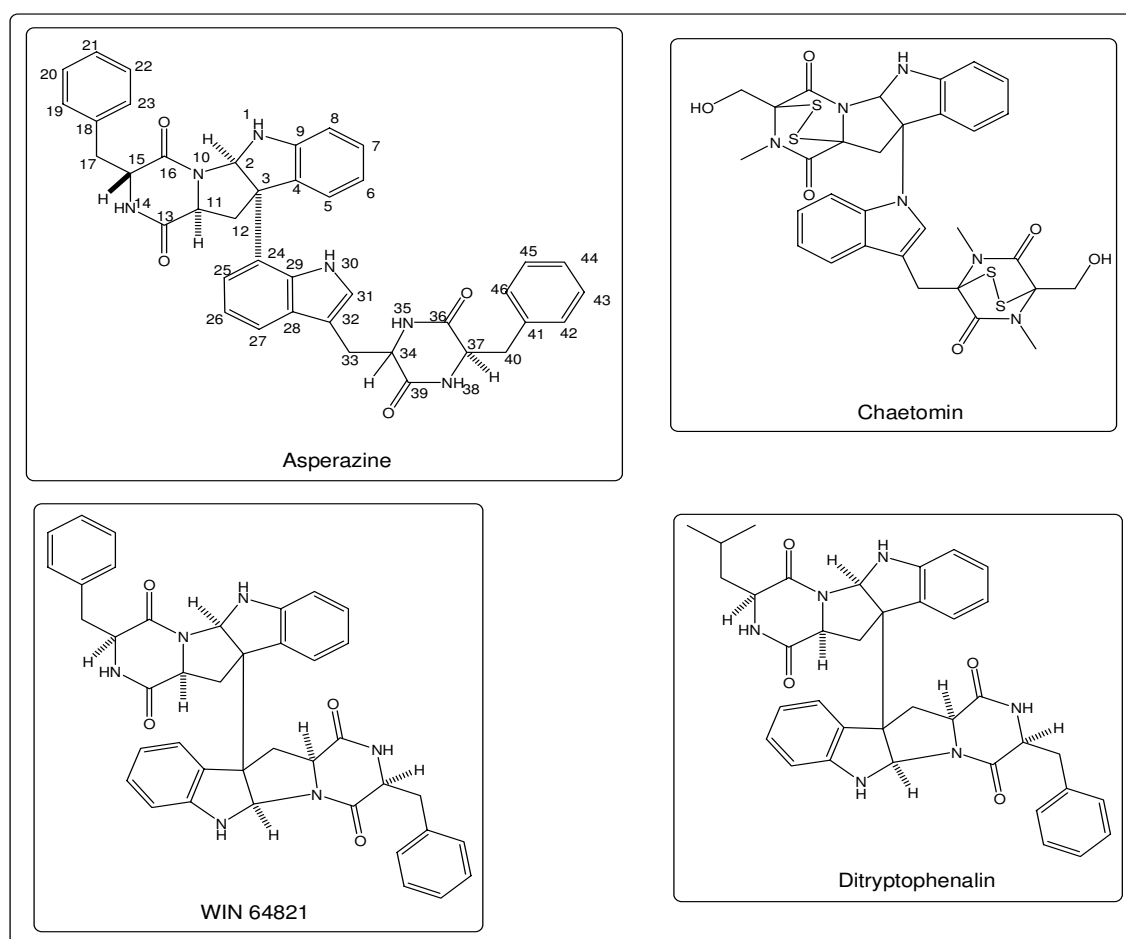


Figure 3.1.2.4.1. Structure of previously reported diketopiperazines

On the other hand, the presence of an indoline substructure in the northern part of the molecule was confirmed by an observed ABCD spin system involving the protons at δ 6.71 (H-5), δ 6.57 (H-6), δ 7.08 (H-7) and δ 6.71 (H-8) in the COSY spectrum. This assignment was also supported by the HMBC correlations H-5/C-9, H-7/C-9, H-6/C-4, and H-8/C-4 as well as the correlation 1-NH/C-4. The position of H-2 at δ 5.72 was identified

by its coupling ($^3J_{HH}$ 4.0 Hz) to 1-NH (δ 7.33) as shown in the COSY spectrum. Since H-2 was present as a methine, it was assumed that C-2 in the indoline moiety was covalently bonded to N-10 in the diketopiperazine moiety. Moreover, the coupling between H-11 (δ 3.41) to a methylene group, H₂-12 (δ 3.33 and 2.05), in the COSY spectrum proved another linkage between the two moieties.

In the southern part, however, the NMR data showed the presence of an indole moiety, instead of an indoline as observed in the northern part of molecule. This assignment was supported by further careful NMR data analysis which indicated the presence of an aromatic proton at δ 7.19 (H-31) correlated to three aromatic carbons at δ 130.4 (C-28), δ 135.4 (C-29) and δ 109.0 (C-32). Moreover, four aromatic protons at δ 6.52 (H-24), δ 6.92 (H-25), δ 6.98 (H-26) and δ 7.52 (H-27) were assigned as a part of an ABCD system of an indole moiety as shown by their coupling in the COSY spectrum and the HMBC correlations H-24/C-28, H-26/C-28, H-25/C-29, and H-27/C-29.

The connectivity of this indole moiety to another diketopiperazine unit in the southern part of the molecule was determined by HMBC correlations of a methylene (H₂-33, δ 3.22 and 2.99) to C-28 (δ 130.4), C-31 (δ 126.5) and C-32 (δ 109.0), as well as the couplings of a methine at δ 3.60 (H-34) with H₂-33 and an exchangeable peak at δ 8.01 (35-NH). Meanwhile, the HMBC correlations of H₂-33 and 35-NH to a carbonyl carbon at δ 168.2 (C-39) as well as the HMBC correlation of H-34 (δ 3.60) to another carbonyl carbon at δ 167.7 (C-36) were observed. Finally, the presence of another phenylalanine subunit in the southern part of the molecule was evident not only by the presence a complex spin system involving five phenyl protons at δ 7.11 (H-42, H-44 and H-46) and δ 7.19 (H-43 and H-45), but also another spin system which was involved H-37, 38-NH and H₂-40. Moreover, this assumption was also confirmed by the HMBC correlations of H₂-40 (δ 3.07 and 2.88) to the carbonyl atom C-36 and the aromatic carbons at δ 137.0 (C-41), δ 130.4 (C-42/46) as well as the HMBC correlations of H-37 to the other carbonyl carbon C-39. The remaining HMBC and COSY correlations observed for this compound are described in detail in figure 3.1.2.4.2 and table 3.1.2.4.1.

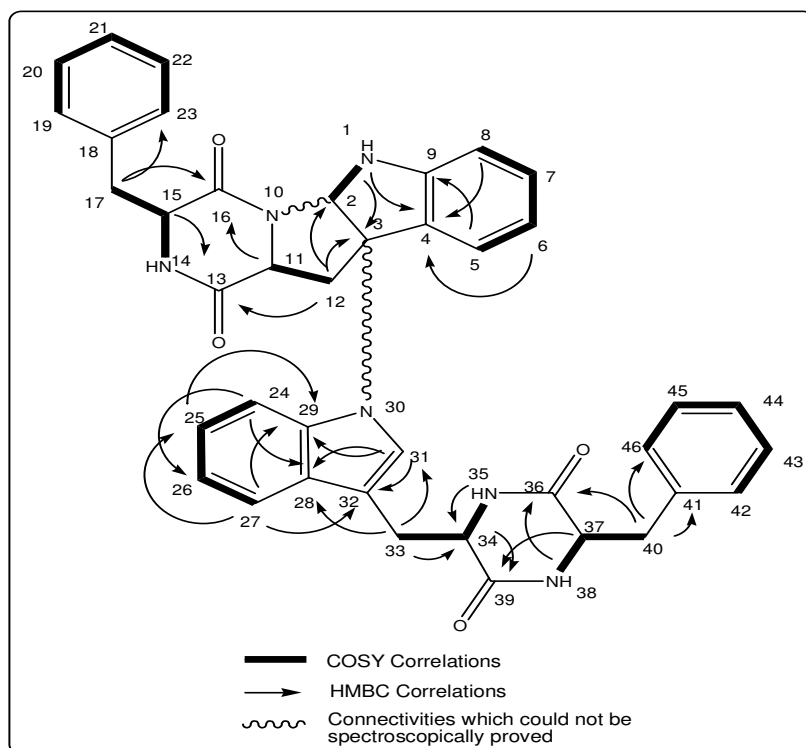


Figure 3.1.2.4.2. COSY (500 MHz) and selected HMBC correlations of ANE 4.9.4.D in DMSO- d_6

To sum up, the nature of ANE 4.9.4.D both in the northern and southern part of the molecule was basically identical to that in asperazine. Although it could not be proved by the performed spectroscopic experiments, it was concluded that the northern part was linked to the southern part at position N-30, instead of C-24 as featured in asperazin. This assumption was corroborated by the fact that H-31 appeared as a singlet in ANE 4.9.4.D, instead of doublet as in asperazine. Thus, the lower number of water exchangeable signal observed in the ^1H NMR spectrum of ANE 4.9.4.D supported this assignment. Furthermore, the indole portion in ANE 4.9.4.D had one extra proton (H-24) compared to that in asperazine. In addition, this type of connection (bridge) is also observed in chaetomin (McInnes et al., 1976), a known fungal metabolites which was also isolated in this study from the culture of *Chaetomium globosum* (figure 3.1.2.4.1 and section 3.1.3 below).

The relative stereochemistry of the stereocenters in ANE 4.9.4.D, notably C-2, C-11 and C-3, were determined using a ROESY experiment. The ROESY correlation of H-2 with H-11 as well as the correlations of H-2 and H-11 with aromatic protons in the southern part of the molecule suggested the close proximity of H-2, H-11, and N-30 at the endo-face.

Meanwhile, the lack of ROESY correlations and observable $^5J_{\text{H-H}}$ couplings between H-11 and H-15 in ANE 4.9.4.D suggested an anti-configuration for these two protons. It has been reported that an observable $^5J_{\text{H-H}}$ (~ 1 Hz) was consistent with the cis relationship between α -protons of diketopiperazine rings (Maes et al., 1986), such as in WIN 64821 (Barrow et al., 1993) and ditryptophenaline (Springer et al., 1977) (figure 3.1.2.4.1). The same assignment was also applied to H-34 and H-37. However, since the $^5J_{\text{HH}}$ might not be a reliable indication of stereochemistry (Varoglu et al., 1997) and some bonds always freely rotate, hydrolysis of ANE 4.9.4.D should be conducted to assign the absolute configuration of the phenylalanine residues. The complete assignment of the ROESY spectrum is shown in figure 3.1.2.4.3.

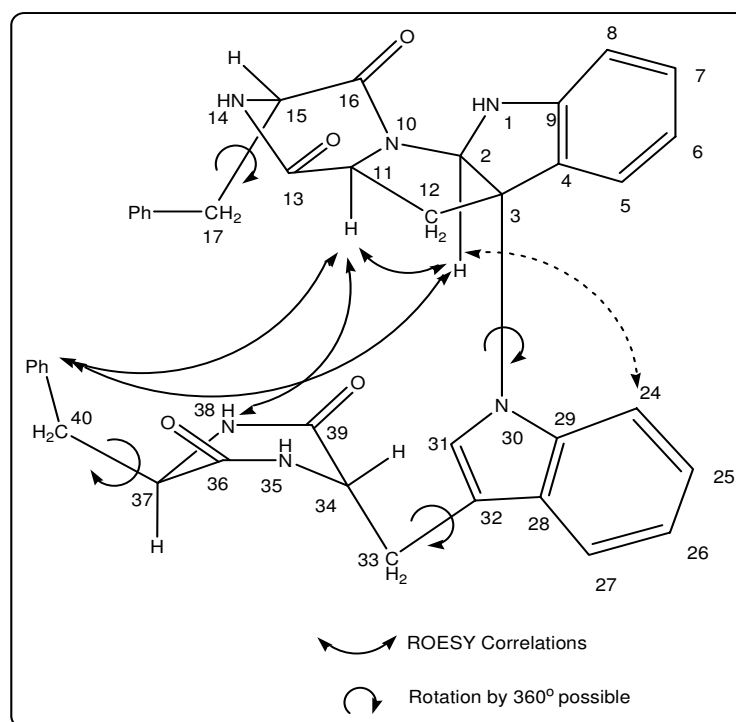


Figure 3.1.2.4.3 Some important spatial correlations in ANE 4.9.4.D based on ROESY experiment (600 MHz) in $\text{DMSO-}d_6$

A series of bioassays have been conducted to both ANE 4.9.4.D and the isolated congener asperazine. Although asperazine has been reported to be active in the cytotoxicity assay using human leukemia murine colon 38 and human colon H116 or CX1 cell lines (Varoglu et al., 1997), both ANE 4.9.4.D and the isolated asperazine did not show any activity in the cytotoxicity assay using L-5178Y cell line (mouse T-cell lymphoma) as well as antimicrobial, antifungal, and protein kinase assays conducted in this study.

Table 3.1.2.4.1 NMR data of ANE 4.9.4.D and isolated asperazine in DMSO-d₆ at 500 MHz (¹H) and 150 MHz (¹³C)

Position	ANE 4.9.4.D				Isolated asperazine				Reported asperazine (Varoglu, <i>et al.</i> , 1997) in CD ₃ CN, 500 MHz	
	¹ H δ (ppm) <i>J</i> _{H-H} (Hz)	¹³ C δ (ppm)	HMBC (H to C)	ROESY	¹ H δ (ppm) <i>J</i> _{H-H} (Hz)	¹³ C δ (ppm)	HMBC (H to C)	¹ H δ (ppm) <i>J</i> _{H-H} (Hz)	¹³ C δ (ppm)	
1	7.33 d (4.0)	-	3,4	8,24	6.65 d (3.2)		2	6.14 b		
2	5.72 d (4.0)	82.0	3	11,12B,24,42, 43,44,45,46	5.84 d (3.2)	82.4		5.71 d (1)	84.20	
3		71.4				56.8			59.28	
4		129.4				132.2			134.16	
5	6.71 d (8.0) ^o	123.4	3,7,9	12A,12B,33B	6.75 d (7.2) ^o	123.2	7,9	6.82 dd (7 ; 1)	121.48	
6	6.57 ddd (8.0 ; 7.6 ; 0.9)	119.4	4,8		6.60 ddd (7.6 ; 7.2 ; 0.9)	118.2	4,8	6.66 dd (7 ; 1)	120.93	
7	7.08 m	130.8	5,9		7.10 ddd (7.9 ; 7.6 ; 0.9)	128.2	5,9	7.12 m	130.45	
8	6.71 d (8.0) ^o	111.0	4,6	1	6.75 d (7.9) ^o	110.2	4,6	6.82 d (7.5)	112.41	
9		147.0				147.5			148.57	

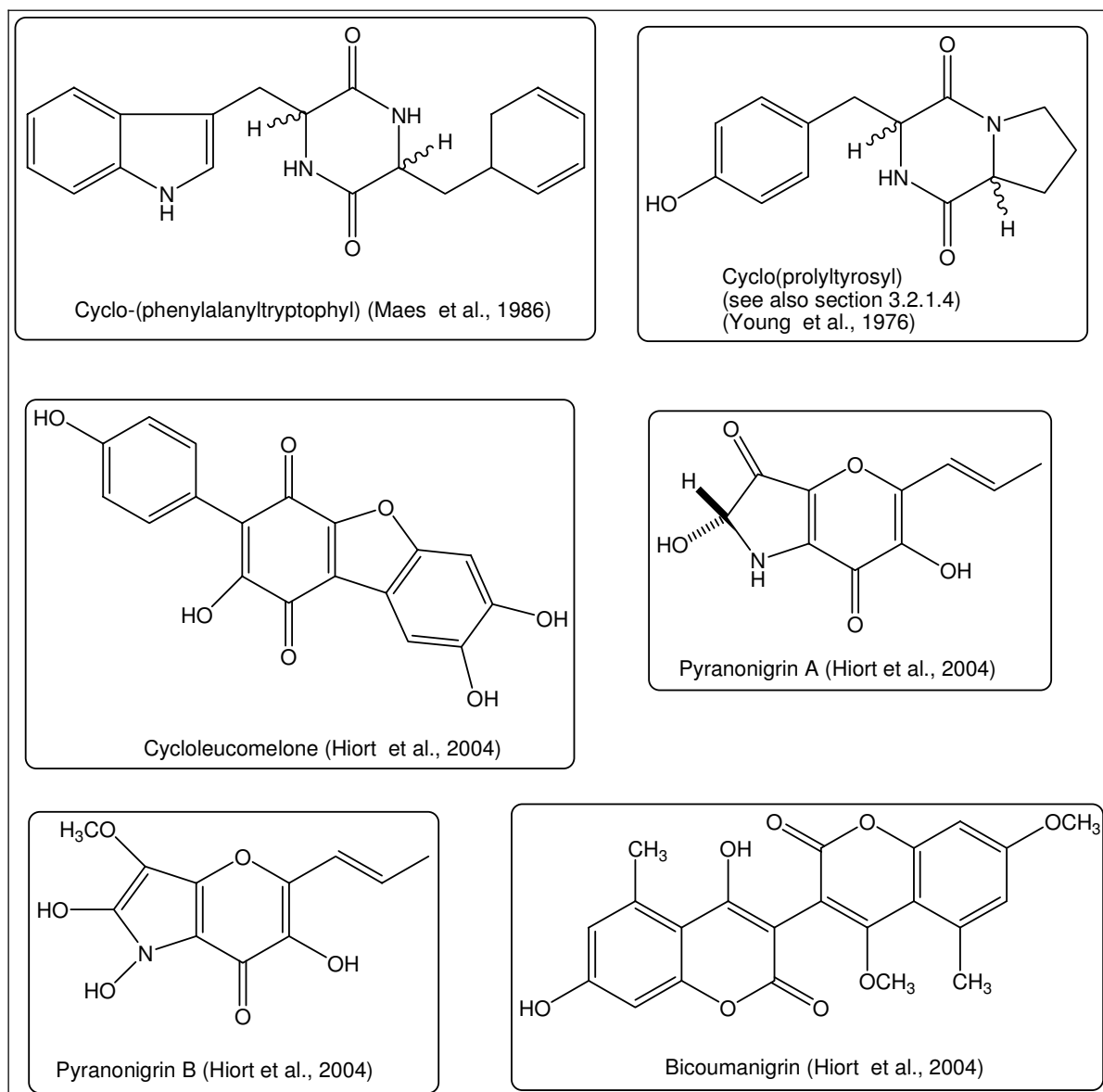
21	7.11 m*	127.5	19/23		7.11 m ^s	127.2	19,23	7.12 m	128.98
24	6.52 d (8.4)	112.8	26,28	1,2,11,12A		123.9			126.31
25	6.92 ddd (8.4 ; 7.3 ; 0.9)	122.4	27,29		6.92 d (6.7)	118.8	27,29	7.12 m	120.24
26	6.98 ddd (7.7 ; 7.3 ; 0.9)	120.0	24,28		6.97 dd (7.9 ; 6.7)	118.8	24,28	7.12 m	120.61
27	7.52 d (7.7)	120.0	25,29,32	33A, 34	7.52 d (7.9)	118.8	25,29,32	7.48 d (7.1)	119.02
28		130.4				129.4			130.45
29		135.4				132.8			135.45
30					9.63 d (1.9)		29,32	8.61 b	
31	7.19 s ^s	126.5	28,29,32	Too complex	6.96 d (2.5)	125.0	32	6.92 d (2.5)	125.20
32		109.0				109.0			111.1
33	A 3.22 dd (14.6 ; 4.9) B 2.99 dd (14.6 ; 4.4)	29.5	28,31,32, 34,39	12B 27,35	3.14 dd (17.3 ; 4.1) 2.89 dd (17.3 ; 4.2)	n.d	31,32,34	A 3.09 dd (14.5 ; 5.5) B 3.05 dd (14.5 ; 3.5)	30.20
34	3.60 b	55.5	33,36	14,27	3.38 b	54.5	32	3.51 ddd (6 ; 5.5 ; 3.5)	56.36
35	8.01 d (1.9)		34,39	33A,33B	8.00 d (1.3)		39	6.16 b	
36		167.7				167.0			169.64
37	4.10 ddd	59.0	38,40	17A,17B	4.02 ddd	58.2	39,40,41	4.12 ddd	60.46

	(6.3 ; 4.4; 4.1)					(6.9 ; 4.7 ; 4.1)				(6 ; 5 ; 4.5)	
38	8.36 d (4.1)	36	11,40B,42/46	8.17 d (4.1)			36,37			6.49 d (4.5)	
39		168.2						167.9			168.84
40	A 3.07 dd (13.8 ; 6.3) B 2.88 dd (13.6 ; 4.4)	38.0	36,37,41, 42/46 38,42/46	2.98 dd (13.5 ; 6.9) 2.70 dd (13.5 ; 4.7)	11,42/46		36,37,41, 42/46 36,37,41, 42/46	38.8		A 3.06 dd (14 ; 6) B 2.93 dd (14 ; 5)	40.72
41		137.0						136.0			137.72
42/46	7.11 m*	130.4	40,44,42/4 6	7.11 m [§]	2,11,12A,38,40A, 40B		40,44,42/46	129.4		7.12 m	131.63
43/45	7.19 m [§]	129.0	41,43/45	7.19 m [#]	2,11,12A		41,43/45	127.8		7.12 m	130.15
44	7.11 m*	127.5		7.11 m [§]	2,11,12A		42,46	126.8		7.27 m	128.72

^h hidden under residual solvent or water signal ; ^{0,*;§,#} mutually overlapped ; n.d not detected

3.1.2.5 Known Isolated Metabolites from *A. niger*

In this study, some known metabolites have been also successfully isolated and identified from *A. niger* (see figure below). They were then submitted to the cytotoxicity, antimicrobial, antifungal, and protein kinase assays, but only some of them showed activities. In the cytotoxicity assay, only malformin A1 was active against the L5178Y cell lines at ED₅₀ 0.21 µg/ml. On the other hand, RF 3192-C and atromentin were the only *A. niger* metabolites which inhibited several protein kinases (see section 3.3). In the antibacterial and antifungal assays, none of them were active against *Bacillus subtilis* or *Cladosporium herbarum*, respectively.



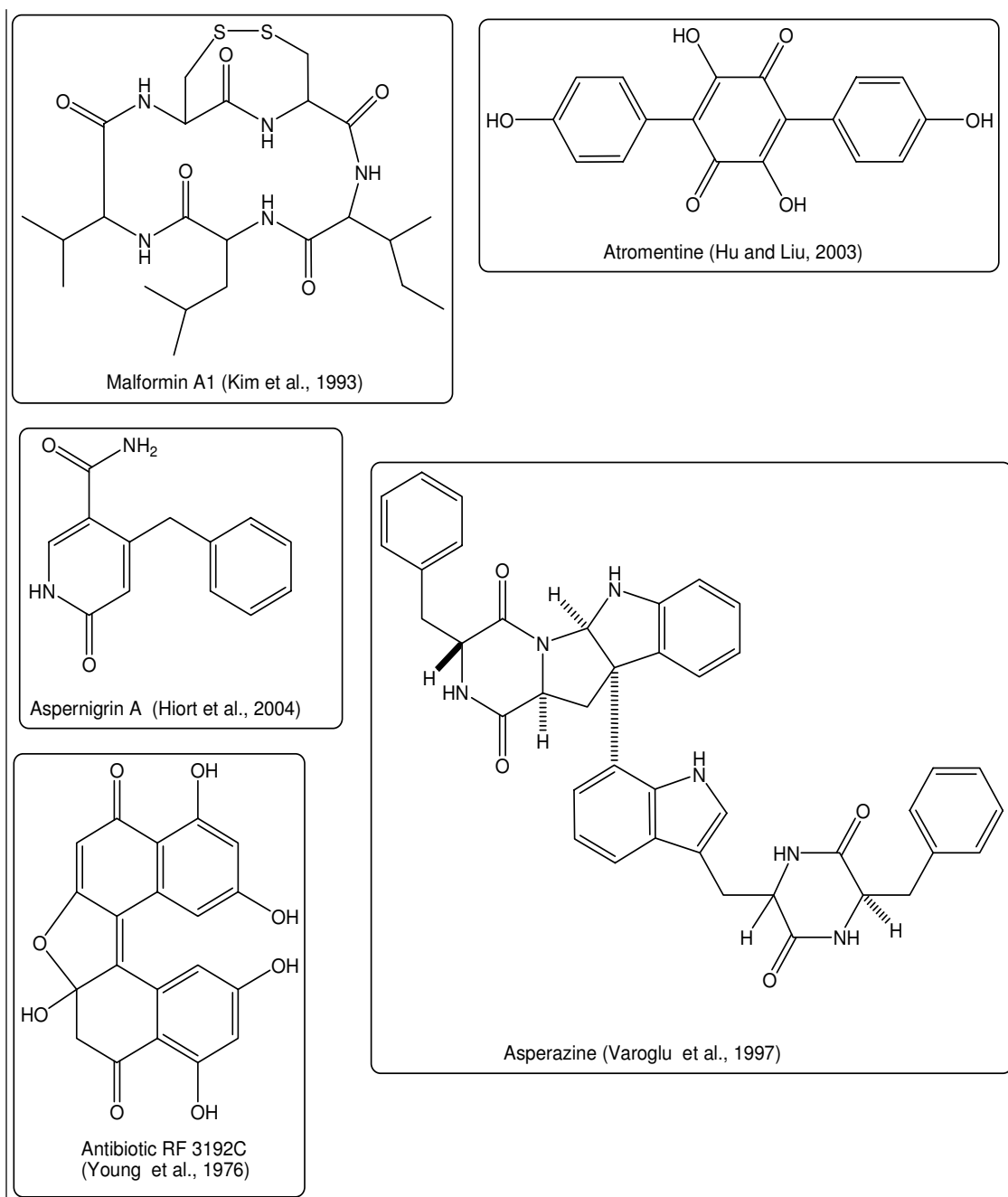
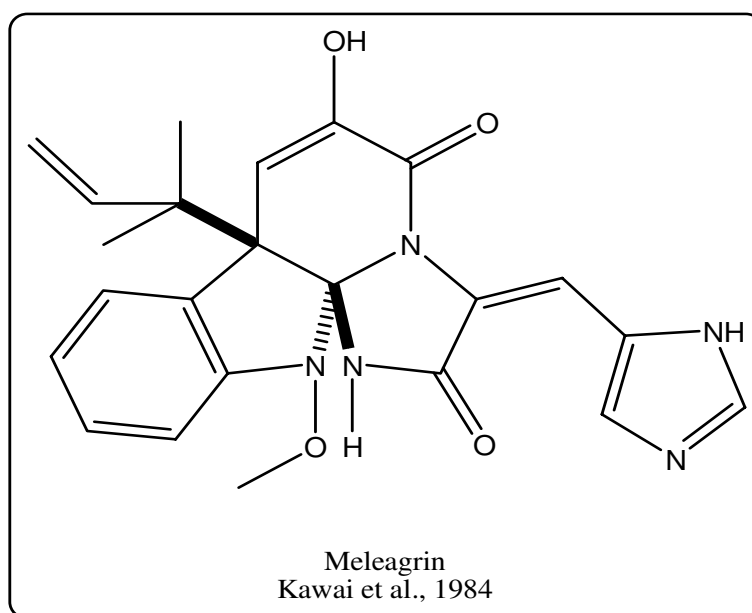


Figure 3.1.2.5.1 Known metabolites isolated from *A. niger*

3.1.3 Melegarin, a Known Secondary Metabolites from an Unidentified Fungus

Melegarin is a known fungal metabolite which has been reported from *P. melegrinum* (Nozawa et al., 1979). In this study, the compound was isolated from an unidentified fungus that found to be associated with an unidentified sponge collected in Pulau Seribu (Indonesia)

in 2002. This compound was the only secondary metabolite found in the ethyl acetate extract of the fungus which was grown only at a small scale, i.e. 300 mL culture media.

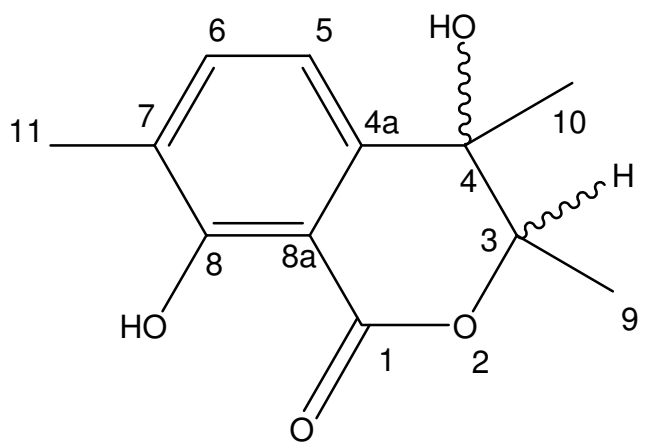
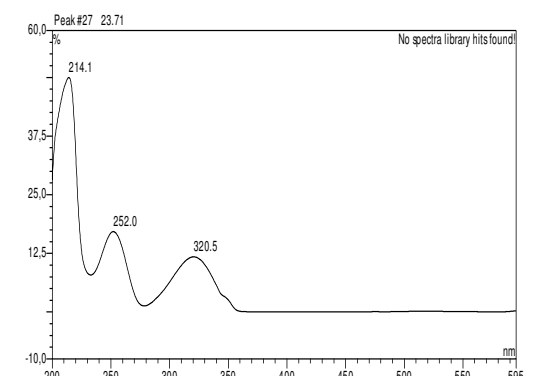
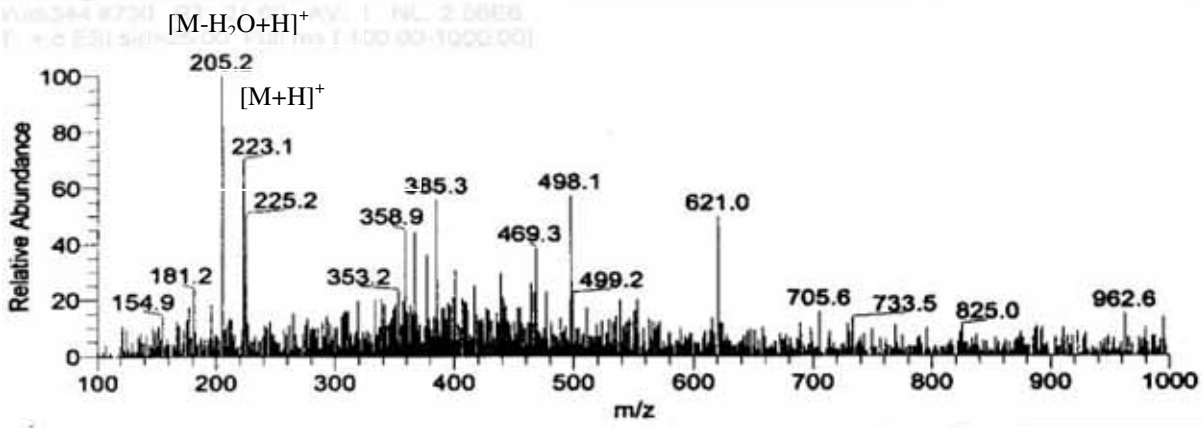


Since meleagrins A is a known compound isolated from *P. meleagrinum* (Kawai et al., 1984), the structure elucidation of this compound will not be discussed in this report. Moreover, it did not show any activity in the cytotoxicity assay using the L 5178Y cell line as well as antimicrobial and antifungal activity towards *B. subtilis* and *C. herbarum*, respectively. However, it showed the inhibitory properties against selected protein kinases (see section 3.3).

3.2 New Secondary Metabolites from Plant Endophytic Fungi

3.2.1 New Secondary Metabolites from *Pestalotiopsis longisetula*

3.2.1.1 PL 3.8 D

New Gamahorin Derivate (PL 3.8.D)	
Synonym(s)	: 4,8-dihydroxy-3,4,7-trimethylisochroman-1-one
Biological Source	: <i>P. longisetula</i>
Sample code	: PL 3.8.D
Amount	: 1.0 mg
Molecular Formula	: C ₁₂ H ₁₄ O ₄
Molecular Weight	: 222 g/mol
Solubility	: CH ₃ OH
Physical Description	: Brown solid
HPLC Retention Time (R _t)	: 23.73 min (Standard gradient)
Structure	UV Spectrum
	
(+)-ESI-MS	

PL 3.8.D was isolated from the ethylacetate extract *P. longisetula* as a brown solid showing a pseudomolecular ion at m/z 223.1 $[M + H]^+$ in the positive mode ESI-MS. The NMR data analysis and UV maxima at λ_{\max} 214.1, 252.0 and 320.5 nm suggested a relationship to gamahorin, a known fungal metabolite which was also isolated from this study. Compared to the one of gamahorin showing only two methyl doublets, the ^1H NMR spectrum of PL 3.8.D displayed one methyl doublet and two methyl singlets. Moreover, the ^1H NMR spectrum indicated the presence of only one methine quartet coupled to the methyl doublet.

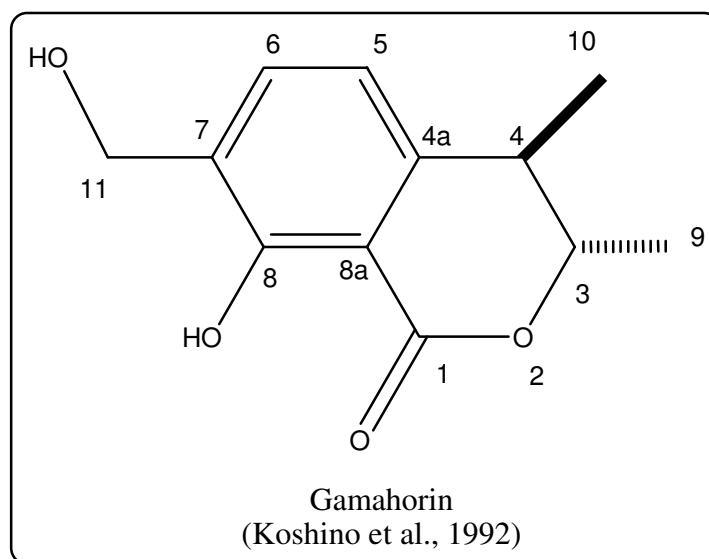


Figure 3.2.1.1.1 Gamahorin, a known fungal metabolite analogous to PL 3.8.D

Since the compound was isolated only in a small amount, the HMBC spectrum showed only the correlations of the methyl protons. The presence of a methyl group (H_3 -11) at δ 2.21 as a substituent in ring A was confirmed by HMBC correlations of H_3 -11 to aromatic carbons at δ 137 (C-6), δ 125 (C-7), and δ 160 (C-8). In the other part of the molecule, another methyl singlet at δ 1.34 (H_3 -10) was assigned based on its HMBC correlations to carbons at δ 149 (C-4a), δ 70 (C-4) and δ 82 (C-3). Meanwhile, the HMBC correlations of H_3 -9 (δ 1.42) to C-3 and C-4 as well as the coupling ($^3J_{\text{HH}}$ 6.6 Hz) between H_3 -9 and H-3, a methine proton at δ 4.54, confirmed the position of the methyl doublet in the molecule.

However, since the NMR experiment was run in CD_3OD the presence of hydroxyl groups at 8-OH and 4-OH could not be proved in this study. Moreover, the presence of a δ -lactone ring was assumed only by the planarity and the calculation of the molecular weight in the molecule. The remaining HMBC correlations of this compound and its analog gamahorin are described in detail in figures 3.2.2.2 and 3.2.2.1.

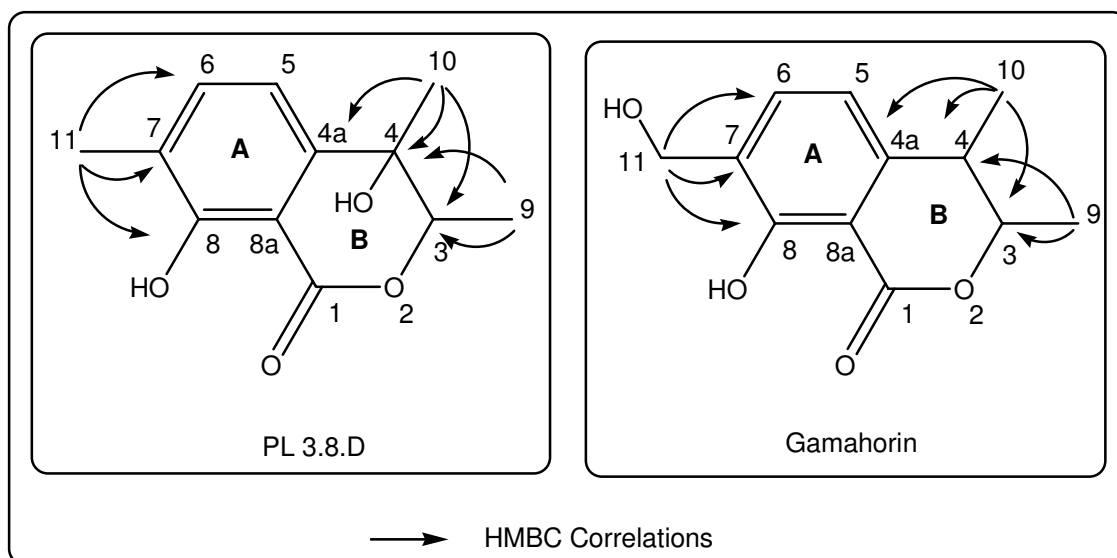


Figure 3.2.1.1. HMBC correlations of PL 3.8.D and gamahorin

Table 3.2.1.1 NMR data of PL 3.8.D in CD₃OD at 500 MHz (¹H) and 125 MHz (¹³C)

Position	PL 3.8.D in CD ₃ OD			Isolated gamahorin in CD ₃ OD			Known gamahorin (Koshino et al., 1992) in CDCl ₃	
	¹ H δ (ppm) J _{H-H} (Hz)	¹³ C ^{a,b} δ (ppm)	HMBC (H to C)	¹ H δ (ppm) J _{H-H} (Hz)	¹³ C ^{a,b} δ (ppm)	HMBC (H to C)	¹ H δ (ppm) J _{H-H} (Hz)	¹³ C ^a δ (ppm)
1	-	n.d		-	n.d			169.1
2	-	-		-	-			
3	4.54 q (6.6)	82		4.55 dq (6.6 ; 6.3)	82		4.53 dq (6.6 ; 6.5)	81.1
4	-	70		2.93 dq (6.6 ; 7.1)	30		2.88 dq (6.6 ; 7.1)	37.3
4a	-	149		-	145			143.3
5	7.05 d (7.5)	115		6.89 d (7.7)	117		6.78 d (7.6)	116.4
6	7.45 d (7.5)	137		7.62 d (7.7)	135		7.50 d (7.6)	135.3
7	-	125		-	128			127.7
8	-	160		-	160			160.1
8a	-	n.d		-	n.d			107.2
9	1.42 d (6.6)	14	3,4	1.45 d (6.3)	20	3,4	1.48 d (6.5)	19.7
10	1.34 s	22	3,4,4a	1.35 d (7.1)	17	3,4,4a	1.36 t (7.1)	17.4
11	2.21 s	16	6,7,8	(2H) 4.65 s	59	6,7,8	(2H) 4.73 d (6.0)	61.1
4-OH	-	-		-	-			
8-OH	-	-		-	-		11.5 s	
11-OH	-	-		-	-		2.35 t (6.0)	

^a Derived from HMBC spectrum ; n.d : not detected

^b Derived from HMQC spectrum

3.2.1.2 PL 5.12.A

PL 5.12.A	
Synonym(s)	: 6-(2-Hydroxy-3-(hydroxymethyl)-5-methylphenoxy)-2-hydroxy-3-(3-methylbut-2-enyl)benzoic acid
Biological Source	: <i>P. longisetula</i>
Sample code	: PL 5.12.A
Amount	: 2.5 mg
Molecular Formula	: C ₂₀ H ₂₂ O ₆
Molecular Weight	: 358 g/mol
Solubility	: CH ₃ OH
Physical Description	: Brown solid
HPLC Retention Time (R _t)	: 29.41 min (Standard gradient)
Structure	
UV Spectrum	
(+)-ESI-MS	

The ¹H NMR spectrum of PL 5.12.A showed the presence of four aromatic doublets resembling between δ 6.06 and 6.81, one olefinic singlet at δ 5.22, and three methyl groups at δ 1.62, δ 1.64 and δ 2.20. In addition, two doublets at δ 4.48 and 3.11 were assigned to

protons belonging to two methylene groups. A pseudomolecular ion at m/z 358.9 $[M + H]^+$ in the positive mode ESI-MS correlated to the molecular weight of 358 g/mol of this compound.

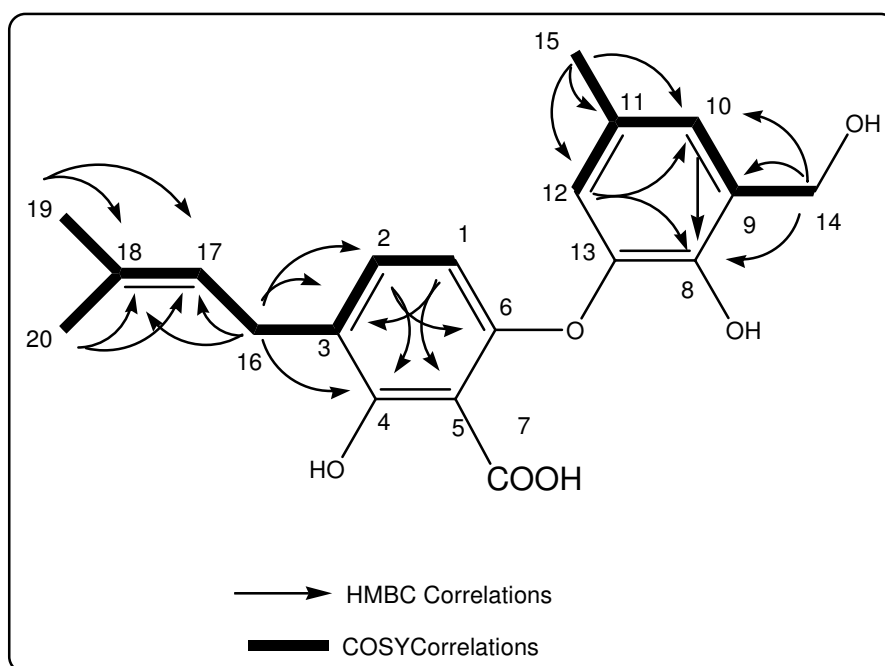


Figure 3.2.1.2.1 COSY (000 MHz) and HMBC correlations of PL 5.12.A in DMSO- d_6

The presence of a prenyl group was confirmed by long range couplings of the two geminal methyls at δ 1.62 (H_3 -19) and 1.64 (H_3 -20) with the olefinic proton at δ 5.22 (H -17) and the methylene protons at δ 3.11 (H_2 -16) as shown in the COSY spectrum (figure 3.2.1.2.1). Furthermore, the HMBC correlations of H_2 -16 to three aromatic carbons at δ 128.5 (C-2), 121.0 (C-3), and 158.5 (C-4) assigned the position of the prenyl group attached to C-3 in the A ring. Moreover, an ortho-coupling ($^3J_{HH}$ 8.2 Hz) between two aromatic protons at δ 6.06 (H -1) and δ 6.81 (H -2) confirmed the presence of the tetrasubstituted phenyl as A ring in this compound. However, since the compound was isolated only in a small amount, the presence of 4-OH and the carboxylic acid function (C-7) could not be directly detected in this study. The presence of these two functional groups as substituents in the A ring were assumed mainly by the chemical shift of C-4 (δ 158.5) and C-5 (δ 111.5) and consideration of the molecular weight.

In the other part of the molecule, a COSY correlation between two aromatic protons at δ 6.45 (H -10) and δ 6.66 (H -12) as well as one methyl at δ 2.20 (H_3 -15) and one methylene at δ 4.48 (H_2 -14) suggested the presence of 1,2,3,5-substituted aromatic ring system (B ring). The

HMBC correlations of H-10 and H-12 to an oxygenated aromatic carbon at δ 140.0 (C-8) confirmed this assignment. Furthermore, the HMBC correlations of H₃-15 to three aromatic carbons at δ 117.0 (C-10), 134.0 (C-11) and 115.0 (C-12) as well as the correlations of H₂-14 to C-8 (δ 140.0), C-9 (δ 135.0) and C-10 (δ 117.0) not only supported the previous assignment of the B ring, but also the positions of H₃-15 and H₂-14. However, the position of the two hydroxyls (8-OH and 14-OH) as well as the oxygen bridge that linked rings A and B could not be directly determined by the performed spectroscopical methods in this study.

Nevertheless, some reported fungal metabolites, such as isoemicellin (Bringmann et al., 2003) and variecoxanthone A (Chexal et al., 1975) (figure 3.21.2.2), supported the assignment for the placement of the hydroxymethyl function (CH₂OH) in the B ring and the oxygen bridge connecting rings A and B as well as the carboxylic acid function and 4-OH in the A ring. Assuming a biogenetic relationship, 8-OH in the B ring would result from a putative oxidative ring opening of isoemicellin or variecoxanthone.

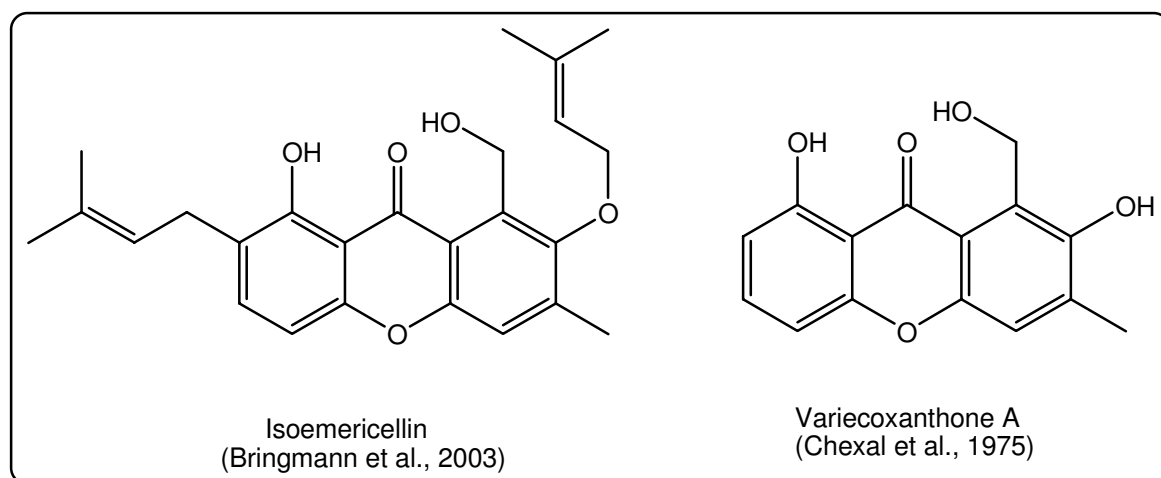


Figure 3.2.1.2.2. Some analogous compounds of PL 5.12.A

Table 3.2.1.2.1 NMR data of PL 5.12.A in DMSO-d₆ at 600 MHz (¹H) and 150 MHz (¹³C)

Position	¹ H δ (ppm) J_{H-H} (Hz)	¹³ C ^a δ (ppm)	HMBC (H to C)
1	6.06 d (8.2)	113.5	3,5,6
2	6.81 d (8.2)	128.5	4,6
3	-	121.0	
4	-	158.5	
5	-	111.5	

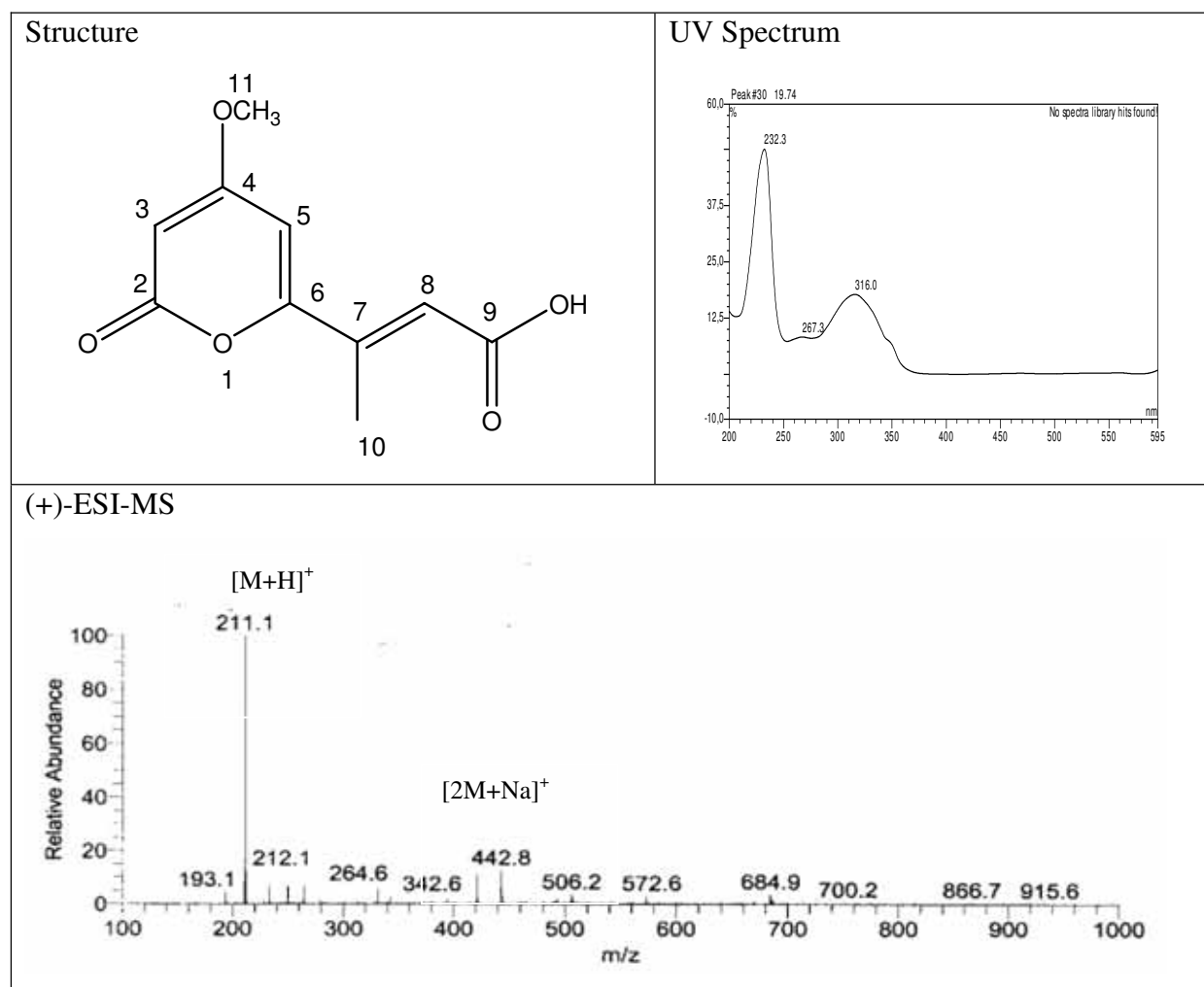
6	-	155.0	
7	-	n.d	
8	-	140.0	
9	-	135.0	
10	6.45 s	117.0	8,12
11	-	134.0	
12	6.66 s	115.0	8,10
13	-	n.d	
14	(2H) 4.48 d (5.5)	58.0	8,9,10
15	2.20 s	20.5	10,11,12
16	(2H) 3.11 d (7.3)	27.5	2,3,4,17,18
17	5.22 t (7.3)	123.0	
18	-	130.0	
19	1.62 s	117.0	17,18
20	1.64 s	25.0	17,18
4-OH	n.d	-	
7-OH	12.4 s	-	
8-OH	n.d	-	
14-OH	5.12 t (5.5)	-	

^a Based on HMBC and HMQC correlations

n.d : not detected

3.2.1.3 New Herbarin Derivate

PL 4.2.7.5	
Synonym(s)	: 3-(4-Methoxy-6-oxo-6 <i>H</i> -pyran-2-yl)but-2-enoic acid
Biological Source	: <i>P. longisetula</i>
Sample code	: PL 4.2.7.5
Amount	: 3.5 mg
Molecular Formula	: C ₁₀ H ₁₀ O ₅
Molecular Weight	: 210 g/mol
Solubility	: CH ₃ OH
Physical Description	: Yellowish brown solid
HPLC Retention Time (R _t)	: 19.76 min (Standard gradient)



PL 4.2.7.5. was isolated as a yellowish brown solid from the ethyl acetate fraction of *P. citreonigrum* after subsequent separation and purification using VLC, Sephadex LH-20 and silica column chromatography. Based on the retention times observed upon HPLC analysis under similar conditions, this compound was slightly more polar compared to PL 3.8.C and PL 5.12.A.

The UV spectrum pattern at (λ_{\max} 232.3 and 316.0 nm) indicated a close relationship to herbarin B, a known fungal metabolite which has a molecular weight of 210 g/mol and was isolated from *Cladosporium herbarum* (Jadulco et al., 2002). Moreover, a pseudomolecular ion at m/z 211.1 $[M + H]^+$ in the positive mode ESI-MS PL 4.2.7.5 supported the above assumption. As in the case of herbarin B (table 3.2.1.3.1), the ^1H NMR data of PL 4.2.7.5 indicated the presence of one methoxy group, one methyl group and three olefinic protons. However, the HMBC spectrum suggested that PL 4.2.7.5 differs to herbarin B with regard to the position of the methyl group (H₃-10) in the molecule.

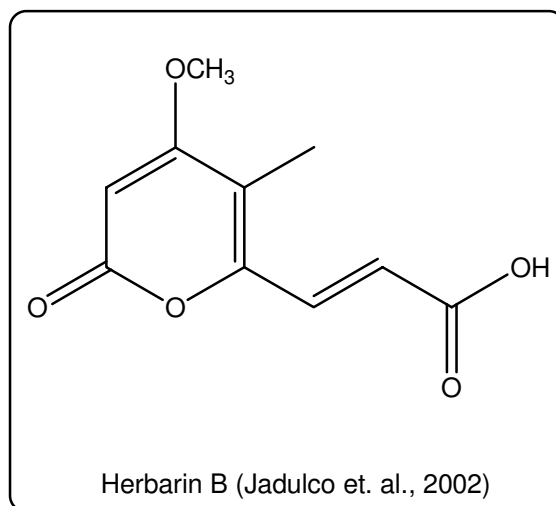


Figure 3.2.13.1. Herbarin B, an analogous compound of PL 4.2.7.5

The presence of two olefinic doublets at δ 5.56 (H-3) and δ 6.38 (H-5) as part of an α -pyron ring system was confirmed by the HMBC correlations of 4-OCH₃, H-3 and H-5 to an oxygenated olefinic carbon at δ 172.5 (C-4) as well as the coupling between H-3 and H-5 ($^4J_{HH}$ 2.0 Hz) as observed in the COSY system. Furthermore, this assignment was supported by the HMBC correlation of H-5 to C-6 (δ 161.5).

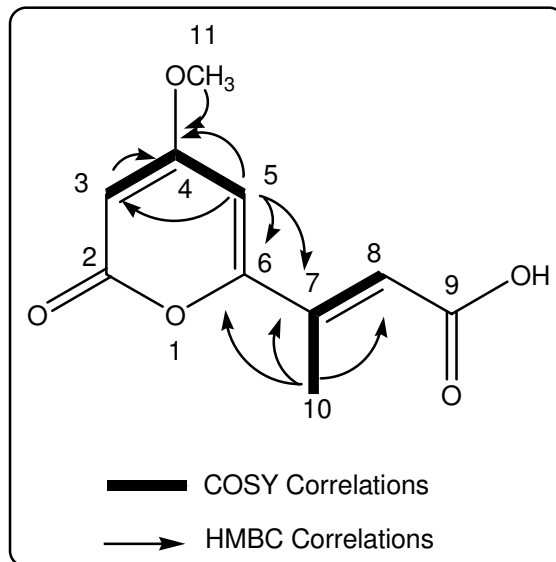


Figure 3.2.1.3.2 COSY (500 MHz) and HMBC correlations of PL 4.2.7.5 in MeOD

In side chain, the COSY correlation of H₃-10 (δ 2.21) with H-8 (δ 6.75) as well as the HMBC correlations of H₃-10 to C-6 (δ 161.5), C-7 (δ 134.0) and C-8 (δ 128.0) confirmed the position of H₃-10 (δ 2.21) attached to C-7. Consecutively, the HMBC correlations H-8/C-6, H₃-10/C-6, H-5/C-6 and H-5/C-7 assigned the position of the unsaturated side chain at C-6 in the α -

pyrone ring system. The HMBC and COSY correlations of this compound are described in detail in table 3.2.1.2.1 and figure 3.2.1.2.2.

Table 3.2.1.2.1 NMR data of PL 4.2.7.5 in MeOD at 500 MHz (^1H) and 125 MHz (^{13}C) and Herbarin B

Position	PL 4.2.7.5			Herbarin B (Jadulco et al., 2002) in MeOD	
	^1H δ (ppm) $J_{\text{H-H}}$ (Hz)	$^{13}\text{C}^{\text{a}}$ δ (ppm)	HMBC (H to C)	^1H δ (ppm) $J_{\text{H-H}}$ (Hz)	^{13}C δ (ppm)
2	-	n.d		-	172.1
3	5.65 d (2.0)	90.0	4,5	5.81 s	91.9
4	-	172.5			165.1
5	6.38 d (2.0)	102.5	3,4,6,7		110.5
6	-	161.5			152.6
7	-	134.0		7.5 d (15.4)	125.3
8	6.75 bs	128.0	6,7	6.64 d (15.4)	132.3
9	-	n.d			169.0
10	2.21 bs	14.0	6,7,8	2.13 s	9.3
OMe	3.87 s	57.5	4	3.97 s	57.5

^a Based on HMBC and HMQC correlations

n.d : not detected

3.2.1.4 Known Metabolites from *P. longisetula*

A series of known metabolites have been successfully isolated and identified from the ethyl acetate extract of *P. longisetula*. Since they are known metabolites, their structure elucidation is not discussed in detail in this report.

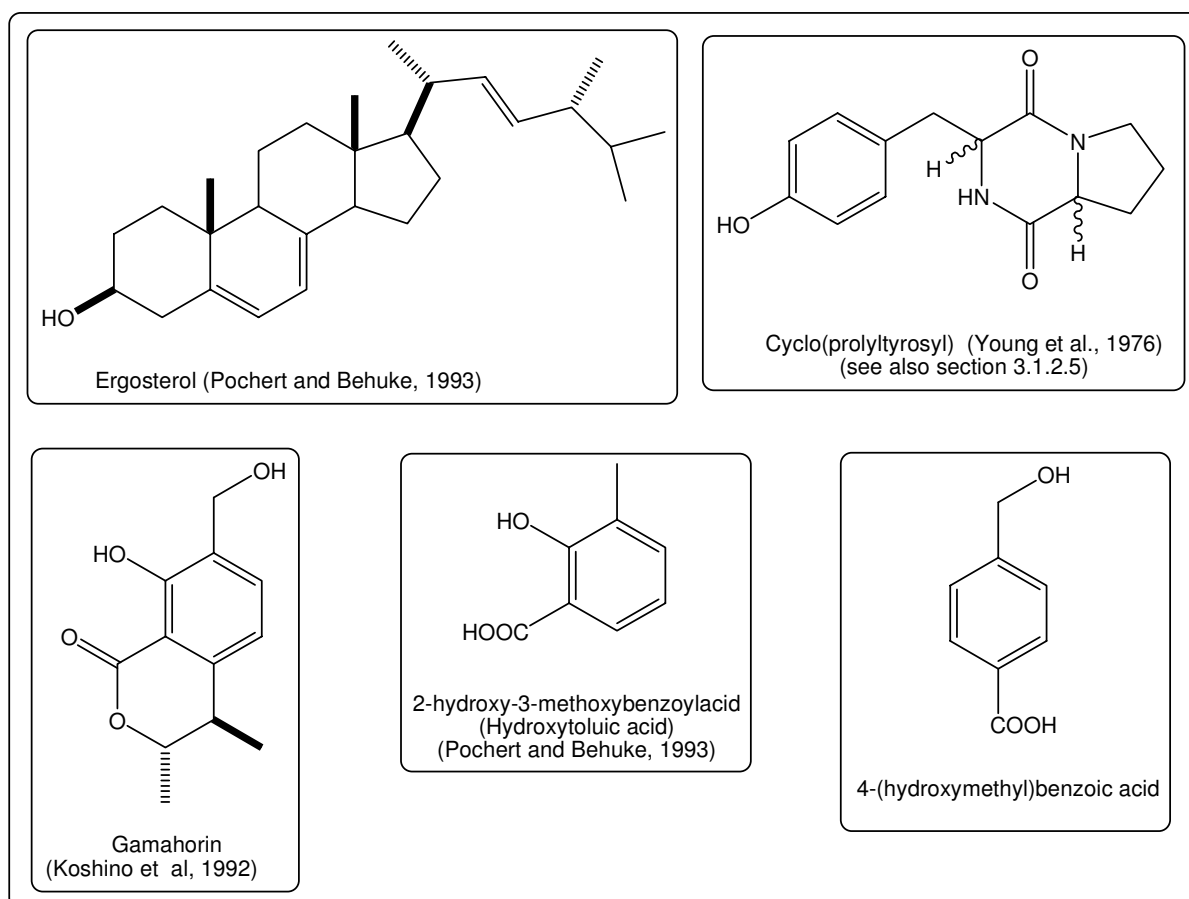


Figure 3.2.1.4.1 Known metabolites isolated from *P. longisetula*.

3.2.2 Chaetomin, a Known Secondary Metabolites from *Chaetomium globosum*

In this study, chaetomin was isolated from *C. globosum*, an endophytic fungus isolated from *Aglaia odorata* growing at the University green house. Chaetomin was the major compound of the ethyl acetate extract of *C. globosum* grown in a 300 mL liquid culture. Similar to other known compounds, the structure elucidation of chaetomin is not discussed in this report.

In the agar diffusion assays using *B. subtilis*, zones of inhibition of 10 and 11 mm were observed for a loading amount of 100 and 200 μg chaetomin, respectively. Furthermore, MIC₅₀ value of <1, <1, <50, >100, and >100 μg /mL chaetomin were observed on the assays using *Staphylococcus epidermidis*, *S. aureus*, *Enterococcus* sp., *Eschericia coli* and *Pseudomonas* sp., respectively.

On the other side, chaetomin showed a high cytotoxic activity toward the L5178Y cell line (ED₅₀ < 0.1 $\mu\text{g}/\text{ml}$). This data indicated that chaetomin is not only a potential antibacterial

agent, but also a highly cytotoxic substance. In addition, the inhibitory properties of chaetomin on selected protein kinases are described in section 3.3.

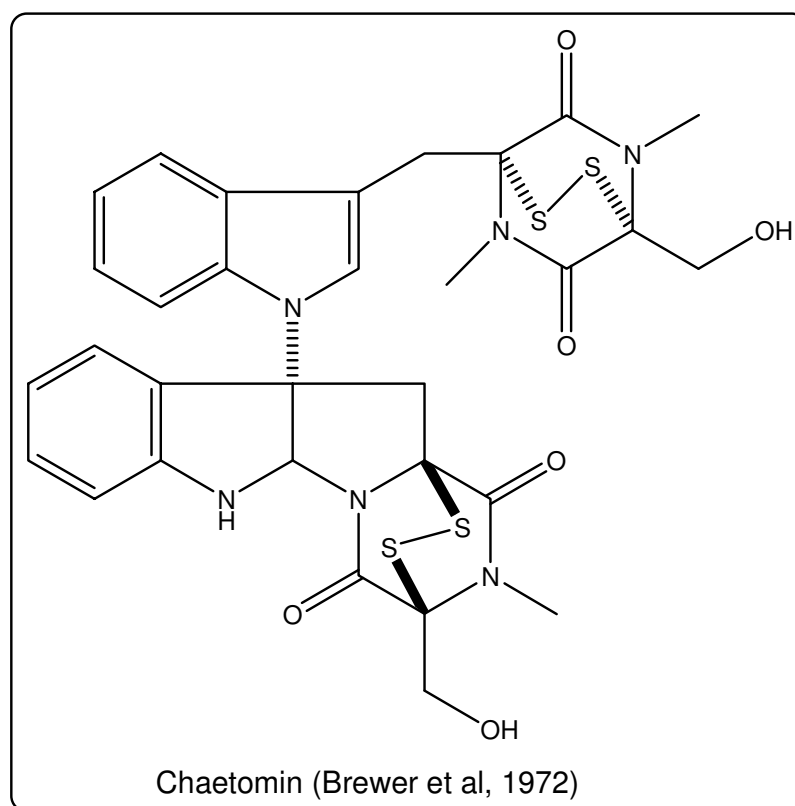


Figure 3.2.2.1 Chaetomin

3.3 The Biological Activity of Some Known Metabolites

Most of the known metabolites which have been isolated in this study were submitted to protein kinase assays. Four of them, as shown in table 3.3.1, showed pronounced activity toward selected protein kinases. Chaetomin, a metabolite from *C. globosum*, showed the strongest inhibitory activity to almost all selected protein kinases compared to other isolated compounds. In addition, the cytotoxicity assay indicated that the chaetomin is highly cytotoxic (see section 3.2.2).

Although its activity was not as strong as that shown by chaetomin, meleagrins still showed a considerable inhibition of some protein kinases, for example PLK-1, VEGF-R2 and SRC. The similar observations were also made for antibiobiotic RF 3192C and atromentine, two metabolites which were isolated from *A. niger*. They proved active towards a lower number of protein kinases compared to chaetomin.

Table 3.3.1 The Bioactivity of some known compounds towards selected protein kinases^{*)}

Family	Kinases	IC ₅₀ g/mL			
		Antibiotic RF 3192C	Atromentine	Meleagrinn	Chaetomin
Serine/threonine kinases	AKT1/PKB alpha	+	n.a	+	+
	ARK5	n.a	+	+	+
	Aurora A	+	+	+	+
	Aurora B	+	+	+	+
	CDK2/Cyclin A	n.a	+	n.a	+
	CDK4/Cyclin D1	+	n.a	+	++
	CK2-alpha 1	n.a	n.a	n.a	+
	COT	+	+	+	+
	PLK-1	+	+	+	+
	B-RAF-VE	+	+	+	+
	SAK	+	+	+	++
Receptor tyrosine kinase	EGFR	+	+	+	++
	EPHB4	+	+	+	+
	ERBB2	+	+	+	+
	FLT3	+	+	+	++
	IGF1-R	+	+	+	++
	INS-R	+	+	+	+
	MET	+	+	+	++
	PDGFR- beta	+	+	+	+
	TIE-2	+	+	+	++
	VEGF-R2	+	+	+	++
	VEGF-R3	+	+	+	++
Soluble tyrosine kinase	FAK	+	+	+	+
	SRC	+	+	+	++

^{*)} The assays was performed at ProQinase GmbH, Freiburg, Germany

n.a : not active ++ : very active + : active +- : moderately active - : weakly active

4 DISCUSSION

4.1 Secondary Metabolites from Sponge-Associated Fungi

4.1.1 Secondary Metabolites from *P. citreonigrum*

4.1.1.1 The Isolated Meroterpenes

4.1.1.1.1 Farnesylpyrophosphate and 3,5-Dimethylorselinic Acid as Precursors in the Fungal Meroterpenoid Biosynthetic Pathways

Natural products of mixed biosynthetic origins that are partially derived from terpenoids are often called meroterpenes. They could represent alkaloids, phenylpropanoids, or proteins containing terpenoid fragments. Simpson (1987), however, defined meroterpenoids as a more limited group, i.e., compounds of mixed polyketide-terpenoid origin. In this study, the isolated citreonigrins were identified as mixed polyketide-terpenoid metabolites which are biosynthetically related to other known fungal meroterpenoids, such as terretonin, paraherquonin, austin, dehydroaustin, andibenins, andilesins, and anditomin (figure 4.1.1.1.1). They differ from the known congeners with regard to the presence of a seven membered ring in a highly oxygenated compound.

As was already shown for other fungal meroterpenoids, the putative key step of the citreonigrin biosynthetic pathway is the alkylation of a bis-C-methylated tetraketide-derived phenolic precursor, i.e. 3,5-dimethylorsellinic acid, by farnesylpyrophosphate to give an intermediate cyclohexadienone (I). The epoxidation of intermediate I (in analogy to the respective steps in the biosynthesis of triterpenoids or steroids, respectively) followed by acid catalysed-epoxide ring opening initiates the cyclisation of intermediate II to generate a tetracyclic intermediate (III) (figure 4.1.1.1.2) (Ahmed et al., 1989).

In the following discussion, rings A and B will be referred to as the “Southern” part, while ring D and further rings formed in this region will be considered the “Northern” part of the structure. By convention, the numbering scheme of the farnesyl-derived parts followed by

the “classical” scheme also used for steroids, while the highly oxygenated and rearranged Northern part is numbered according to the respective atoms in the precursor 3,5-dimethylorsellinic acid which are indicated by numbers followed by a single prime symbol, i.e. C-1' to C-10'.

The oxidation of intermediate III results in the formation of a cyclo-hexanone intermediate (IV). Further biological Baeyer-Villiger type oxidation of intermediate IV would give an ϵ -lactone intermediate (V) which is then readily transformed into intermediate VI. Finally, the oxidation of intermediate VI leads to the formation of intermediate VII with an epoxide ring between C-4 and C-5 (Figure 4.1.1.1.3). This type of modification is also known in the biosynthetic pathway of andibenin B (McIntyre et al., 1984).

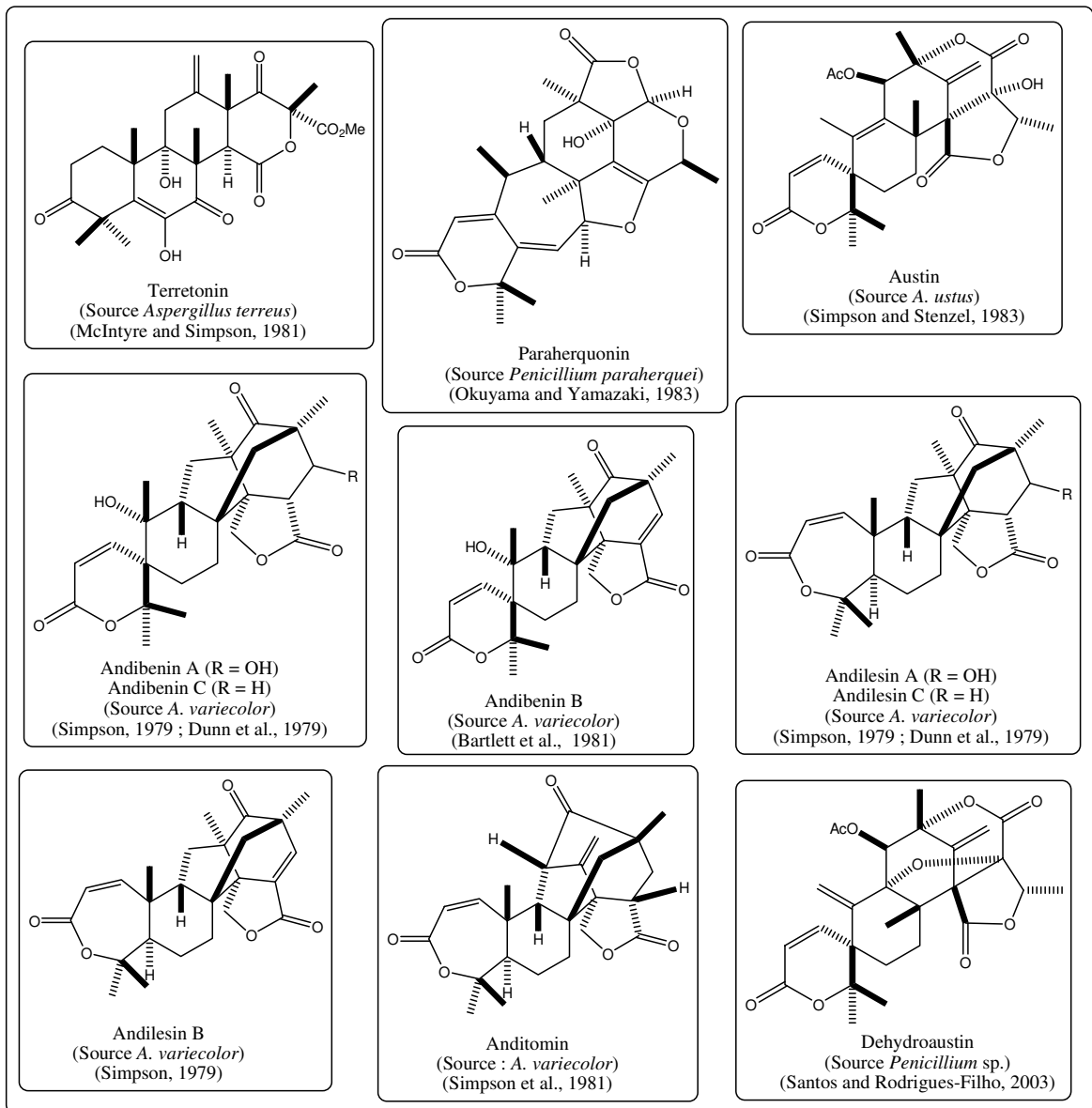


Figure 4.1.1.1.1 Some reported fungal meroterpenes

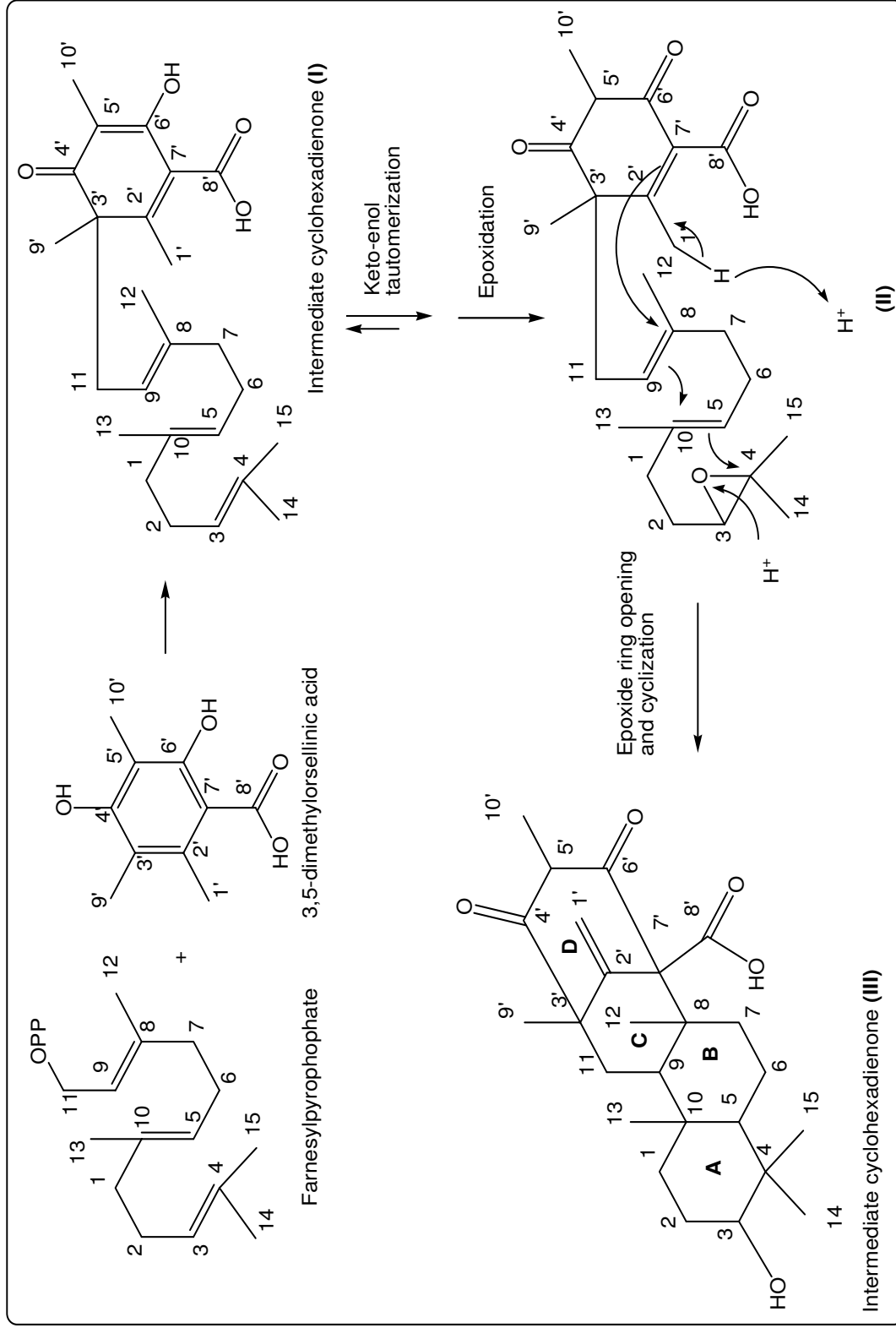


Figure 4.1.1.1.2. Initial steps of the fungal meroterpenoid biosynthetic pathway (Ahmed et al., 1989)

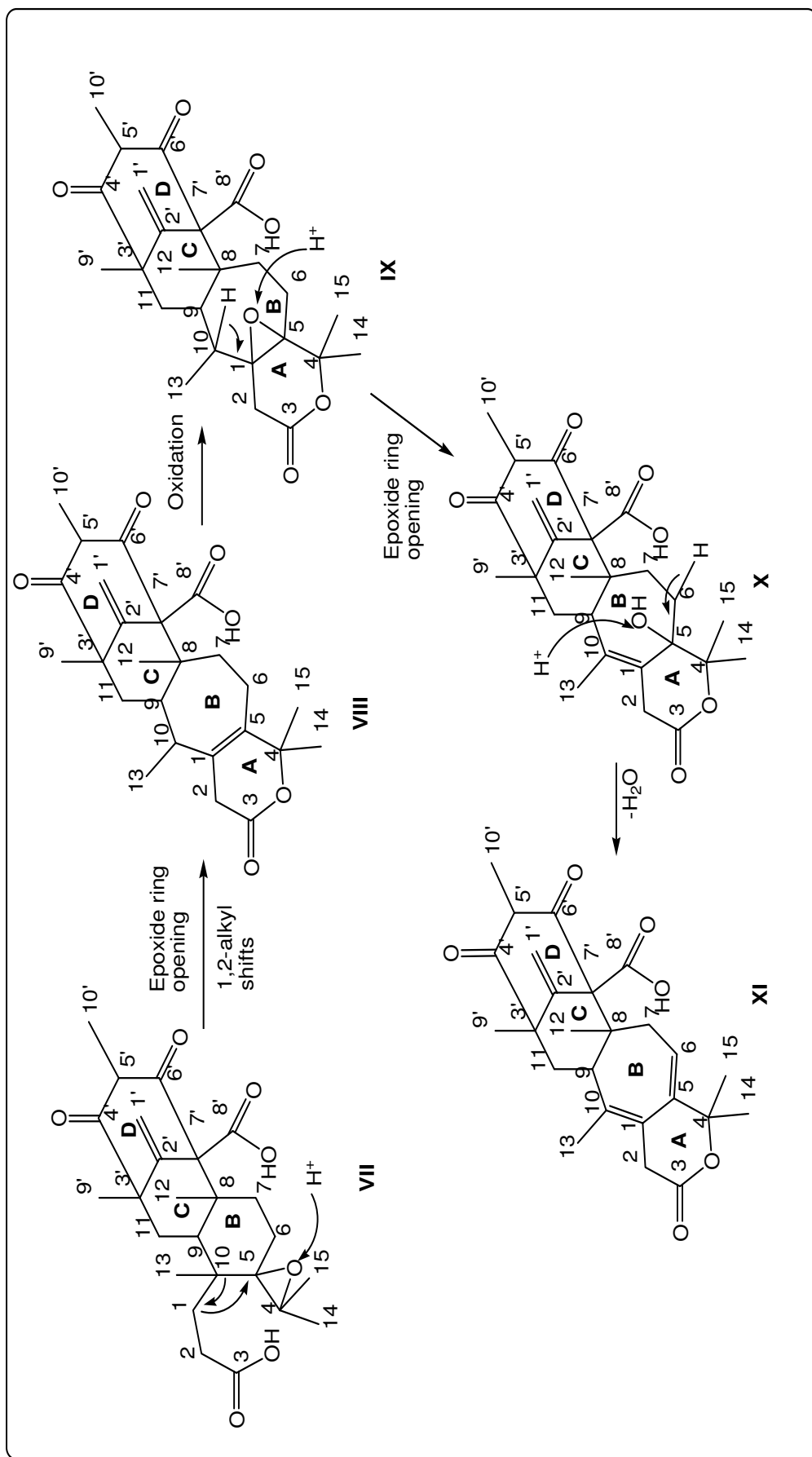


Figure 4.1.1.1.4. Proposed biosynthetic pathway of δ -lactone (A ring system) and seven membered ring (B ring) system formation in the Southern part of the citreonigrins

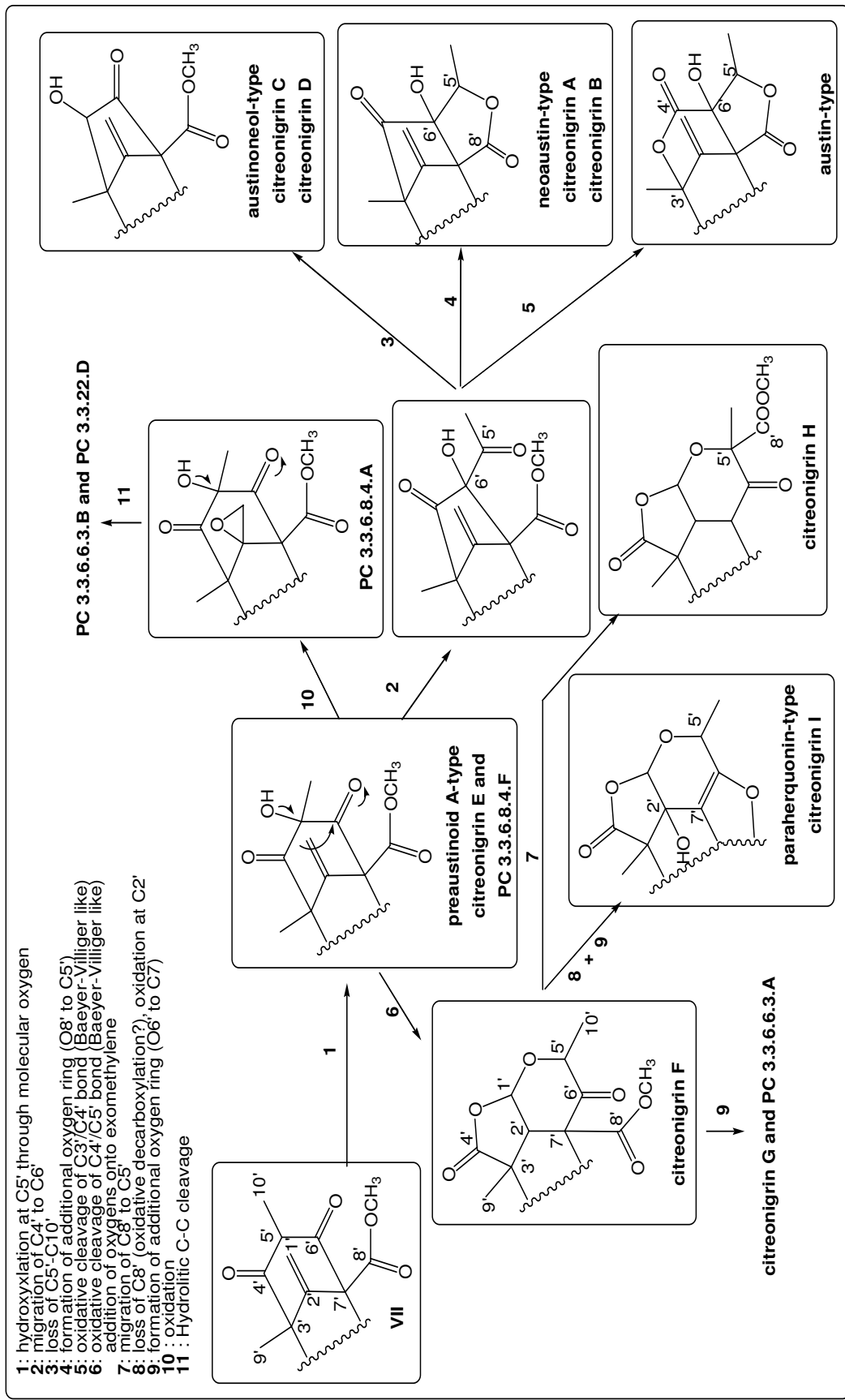


Figure 4.1.1.1.5 The proposed biosynthetic pathway for the Northern part of the citreonigrins

Acid-catalysed epoxide ring opening of intermediate VII followed by carbon-carbon cleavage would lead to the formation of the desired δ -lactone and 7-membered ring system of intermediate VIII. Further oxidation, acid catalysed epoxide ring opening and the elimination of a hydroxyl group under acidic conditions would yield cycloheptadiene intermediate XI which is ready to be converted to different type of meroterpenes including the isolated citreonigrins (fig. 4.1.1.1.4).

Meanwhile, figure 4.1.1.1.5 briefly describes the proposed hypothetical pathways for the formation of the various modifications in the Northern part of the citreonigrins. Similar to the Southern part, oxidation and acid catalysed-rearrangements dominate the pathways. Moreover, based on the chemical structural patterns in the Northern part, the isolated citreonigrins obtained during this study were then classified and grouped according to their known analogues.

The following sections describe the proposed hypothetical biosynthetic pathway of the isolated citreonigrins based on the known (reported) reaction mechanisms that are commonly involved and applied in the biosynthesis of terpenoid compounds.

4.1.1.1.2 Proposed Biosynthetic Pathways of New Preaustinoid A-Type Meroterpenes (Citreonigrin E, PC 3.3.6.8.4.A and PC 3.3.6.8.4.F)

Citreonigrin E is the simplest meroterpenoid which was isolated in this study. The Northern part of citreonigrin E is almost identical to that reported for preaustinoid A, A1 and A2 which were also isolated from *Penicillium* sp. (Santos and Rodrigues-Fo 2002 ; Santos and Rodrigues-Fo, 2003a) (figure 4.1.1.1.2.1). The different patterns in the Southern parts, however, indicate that preaustinoids would be putative precursors in the biosynthetic pathway of citreonigrin E as well as other isolated meroterpenes (figure 4.1.1.1.1.3, structure IV).

Hydroxylation at C-5' in intermediate XI followed by the methylation of free carboxylic acid at C-8' would convert intermediate XI into citreonigrin E (figure 4.1.1.1.2.2). Subsequent oxidation steps followed by acid catalysed epoxide ring opening initiates the formation of an oxygen bridge between C-7 and C-10 in the 7-membered ring system. In

addition, intramolecular rearrangements of intermediate XVI would give rise to the formation of an unsaturated δ -lactone ring system in PC 3.3.6.8.4.F. The epoxidation of the exo-methylene group in PC 3.3.6.8.4.F would cause the formation of the epoxide ring in PC 3.3.3.6.8.4.A.

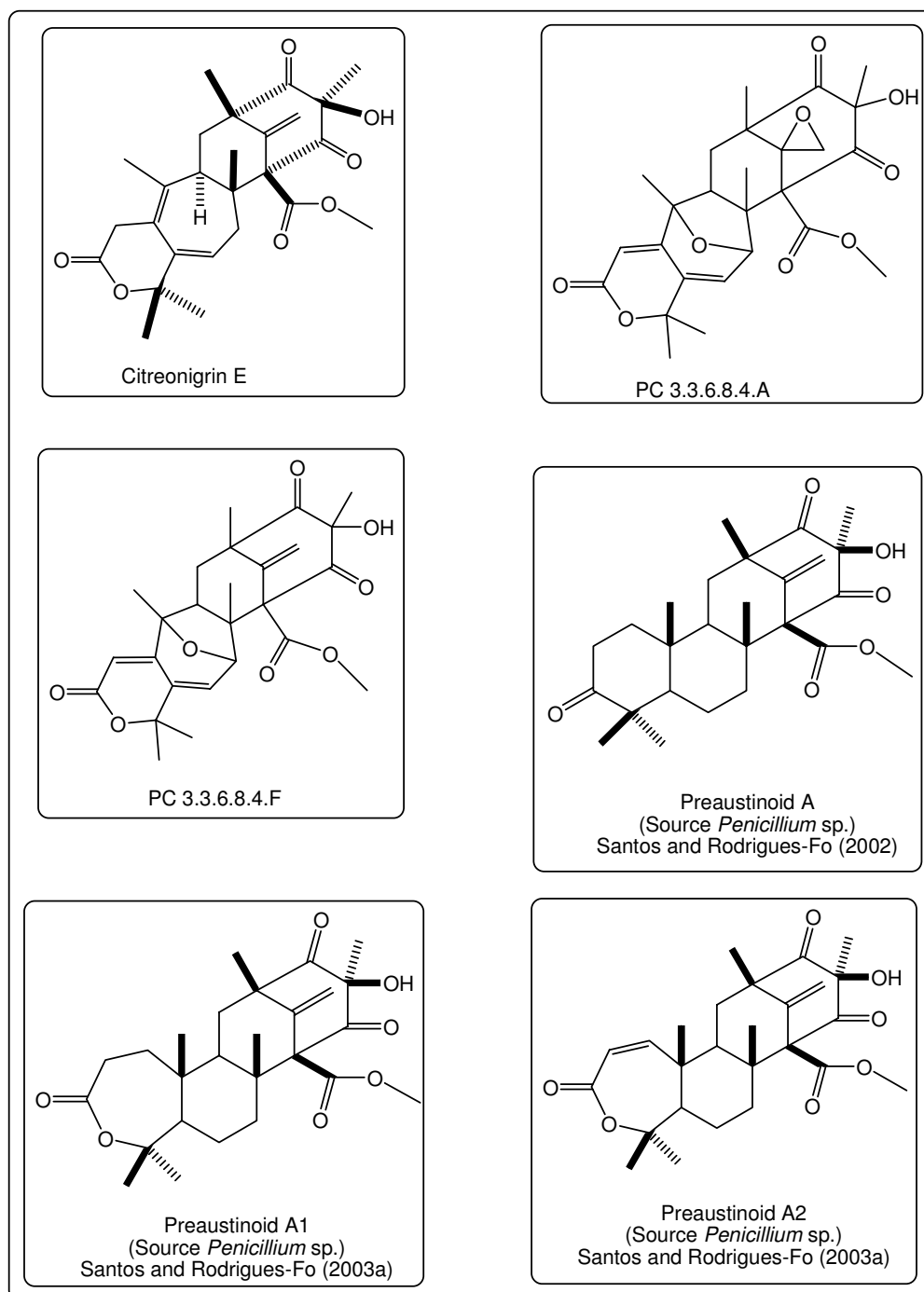


Figure 4.1.1.1.2.1 Structures of citreonigrin E, PC 3.3.6.8.4. A, PC 3.3.6.8.4.F and related known meroterpenes

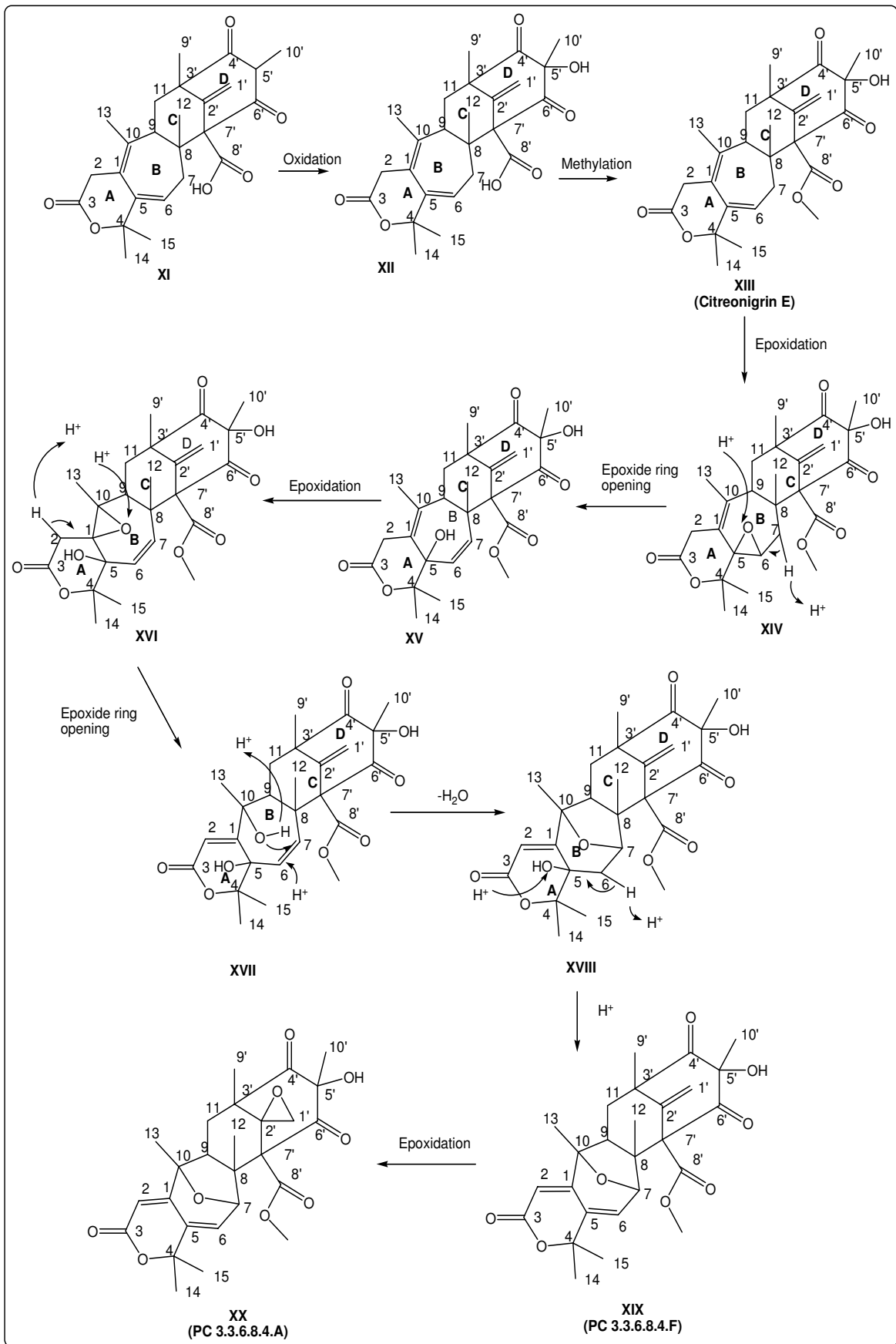


Figure 4.1.1.1.2.2. Proposed Biosynthetic Pathway of citreonigrin E, PC 3.3.6.8.4.F and PC 3.3.6.8.4.A

4.1.1.1.3 Proposed Biosynthetic Pathways of New Neoaustin-Type Meroterpenes (Citreonigrin A and B)

Structurally, the Northern part of citreonigrins A and B is almost identical to that of neoaustin (Santos and Rodrigues-Filho, 2003), a meroterpenoid which was also isolated from *Penicillium* sp. The spiro-lactone ring of neoaustin however, represents the main difference of this compound to citreonigrins A and B (figure 4.1.1.1.3.1).

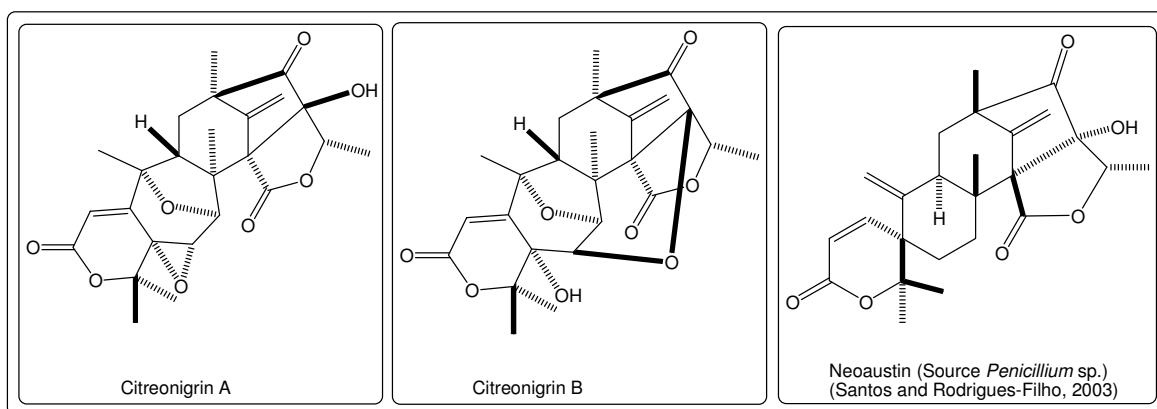


Figure 4.1.1.1.3.1. Structures of citreonigrin A, citreonigrin B and the related neoaustin

Biogenetically, both citreonigrin A and B are supposed to be formally derived from subsequent oxidation and rearrangement of PC 3.3.6.8.4.F. The acid-catalysed modifications of the cyclo hexadione ring of PC 3.3.6.8.4.F results in a cyclo pentanone intermediate (XXI). Reduction of keto C-5' in intermediate XXI followed by hydrolysis and lactonisation would give to the formation of intermediate XIII with a new γ -lactone saytem, ring E. A similar reaction sequence has been proposed in the biosynthesis of austin (Ahmed, et al., 1989). Further oxidation and acid catalysed- epoxide ring opening would subsequently convert intermediate XIII into citreonigrin A and citreonigrin B (figure 4.1.1.1.3.2). On the other hand, it also seems possible that the modifications in the Northern part described above represent the initial steps of the biosynthesis, followed by transformation in the Southern part which would be analogous to the respective events outlined in the previous chapter for citreonigrin E, PC 3.3.6.8.4.A and PC 3.3.6.8.4.F.

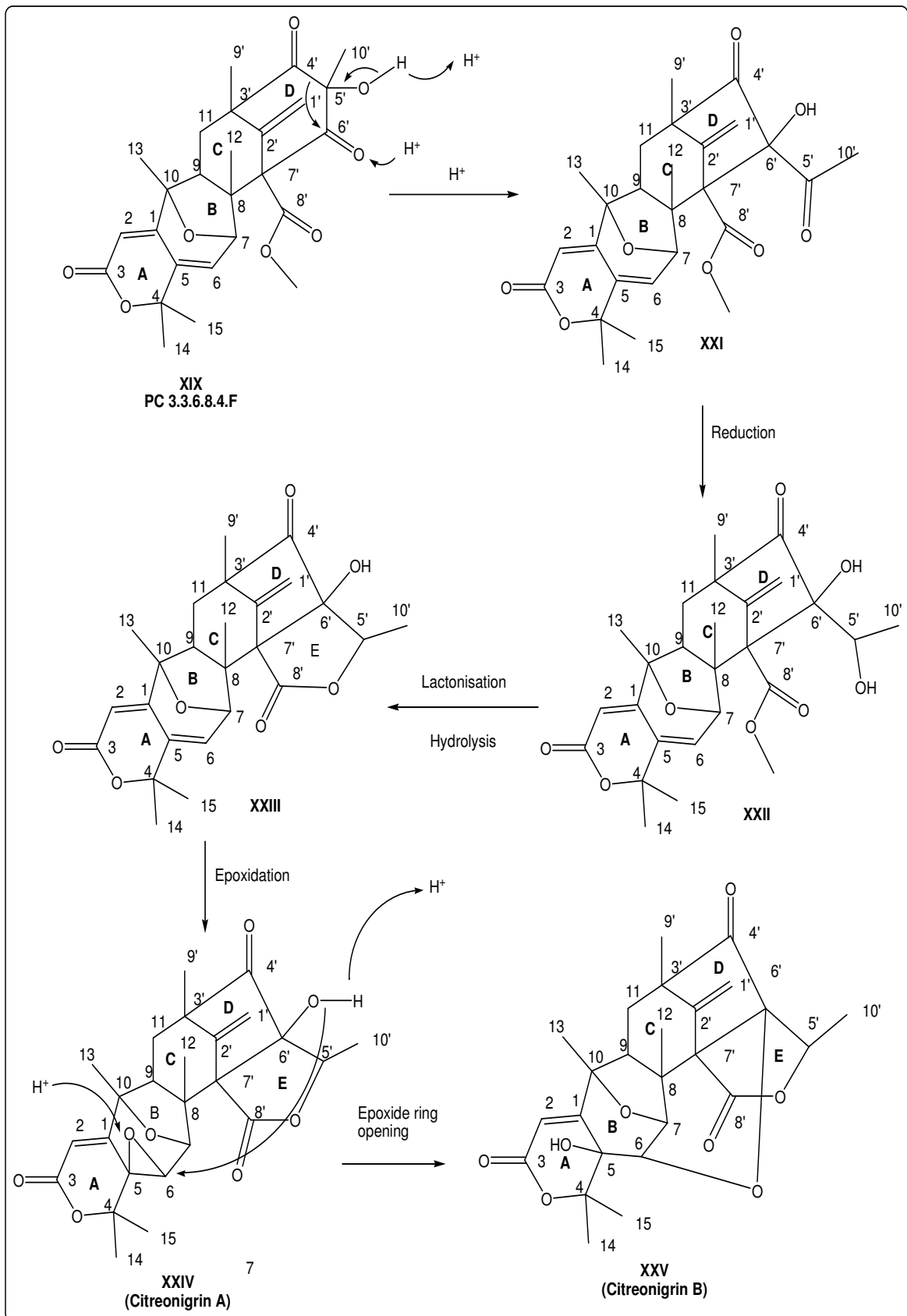


Figure 4.1.1.1.3.2. Proposed biosynthetic pathway of citreonigrin A and citreonigrin B

4.1.1.1.4 Proposed Biosynthetic Pathways of New Austinoneol A Type Meroterpenes (Citreonigrin C and D)

The Northern part of citreonigrins C and D is very closely related to that of austinoneol A (figure 4.1.1.1.4.1), a known meroterpene which was also isolated from *Penicillium* sp (Santos and Rodrigues-Filho, 2003). Biogenetically, both citreonigrin C and D are supposed to be formally synthesized from PC 3.3.6.8.4.F. The first step of the conversion of PC 3.3.6.8.4.F into citreonigrin C and D would be the oxidation of the double bond at C-5 and its conversion onto an epoxide ring. Further Baeyer Villiger type oxidation results in the formation of a 7-membered lactone D ring in intermediate XXVIa. Ring contraction and intramolecular rearrangement followed by the reduction of C-6' converts intermediate XXVIa into citreonigrin C. Finally, acid catalysed-deacetylation of citreonigrin C and isomerization by tautomerization would yield citreonigrin D. The details of the hypothetical conversion of PC 3.3.6.8.4.F into citreonigrin C and D are described in figure 4.1.1.1.4.2. Again, the sequence of events concerning the Northern and Southern part may be reversed.

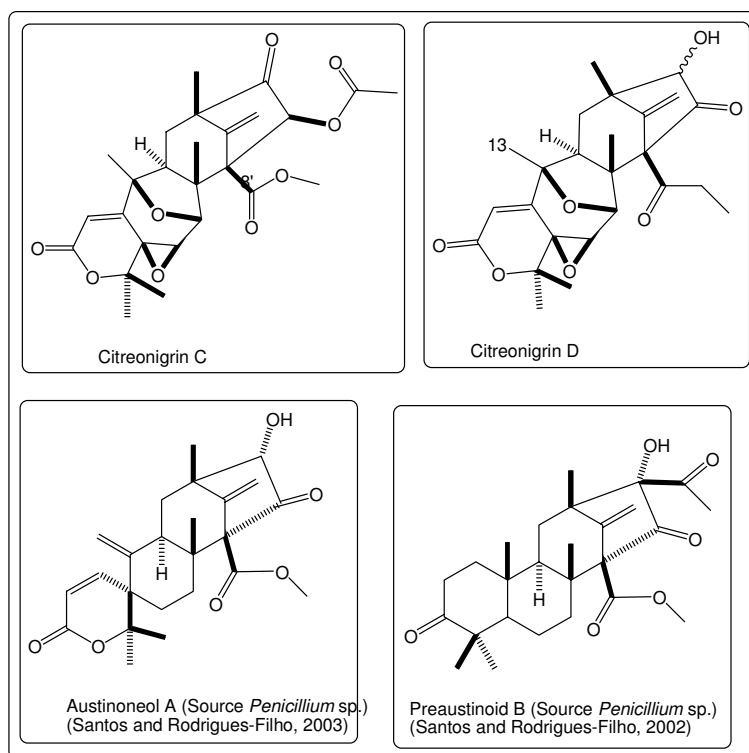


Figure 4.1.1.1.4.1 Structures of citreonigrin C, citreonigrin D and austinoneol A, a structurally related known meroterpenoid

An alternative biosynthetic pathway of citreonigrin D is summarized in figure 4.1.1.1.4.3. As compared to the previous pathway, the Baeyer-Villiger oxidation of PC 3.3.6.8.4.F in this scheme would take place between C-4 and C-5 resulting in intermediate XXVI b. The elimination of the hydroxyl group at C-6 followed by deacetylation produces citreonigrin D. It is difficult to decide which of the two pathways is more likely, since with citreonigrin C and preaustinoid B1 (Santos and Rodrigues, 2003) both possible keto and acetyl ester combinations at C-4'/C-6' have been observed in nature.

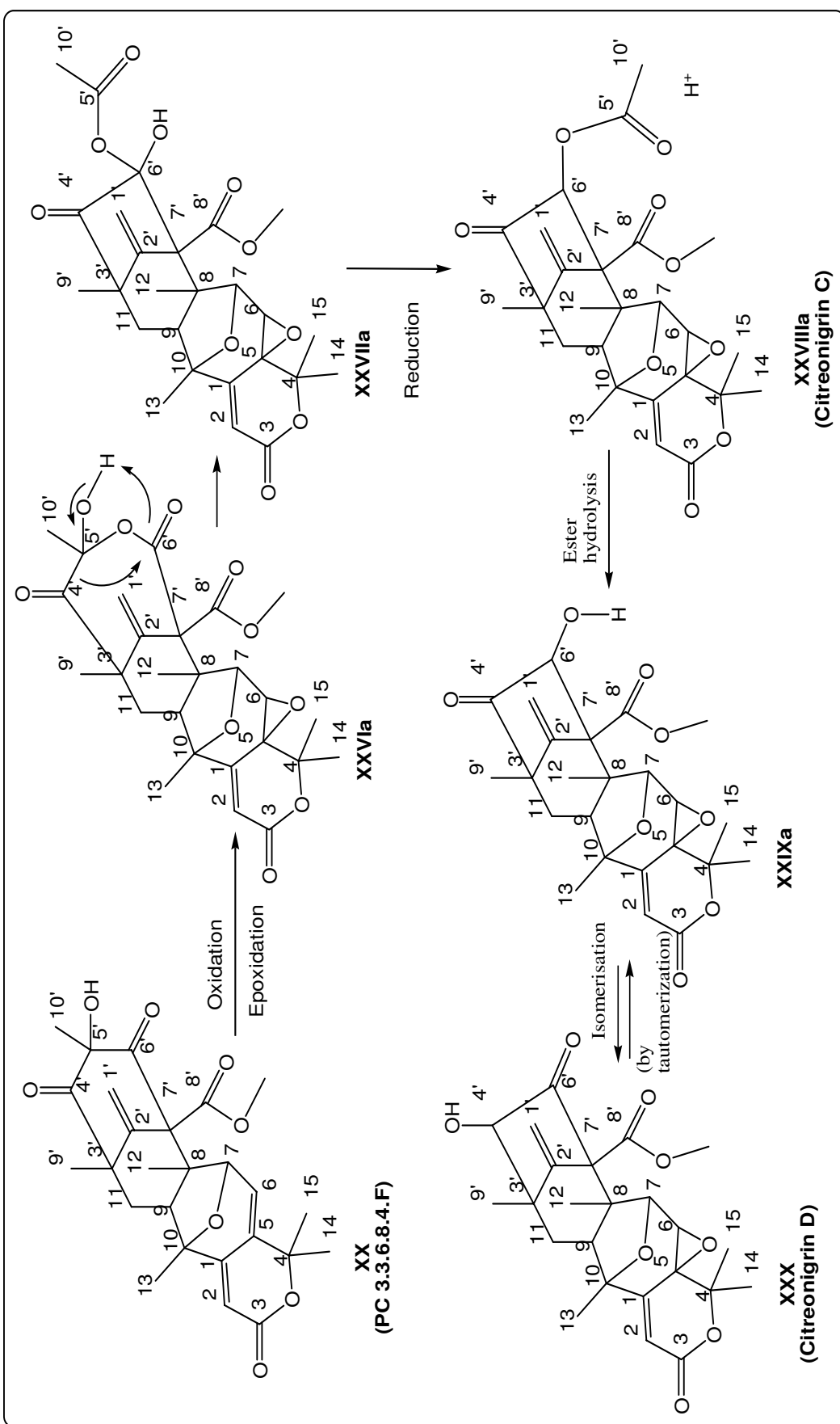


Figure 4.1.1.1.4.2. Proposed Biosynthetic Pathway of citreonigrin C and citreonigrin D

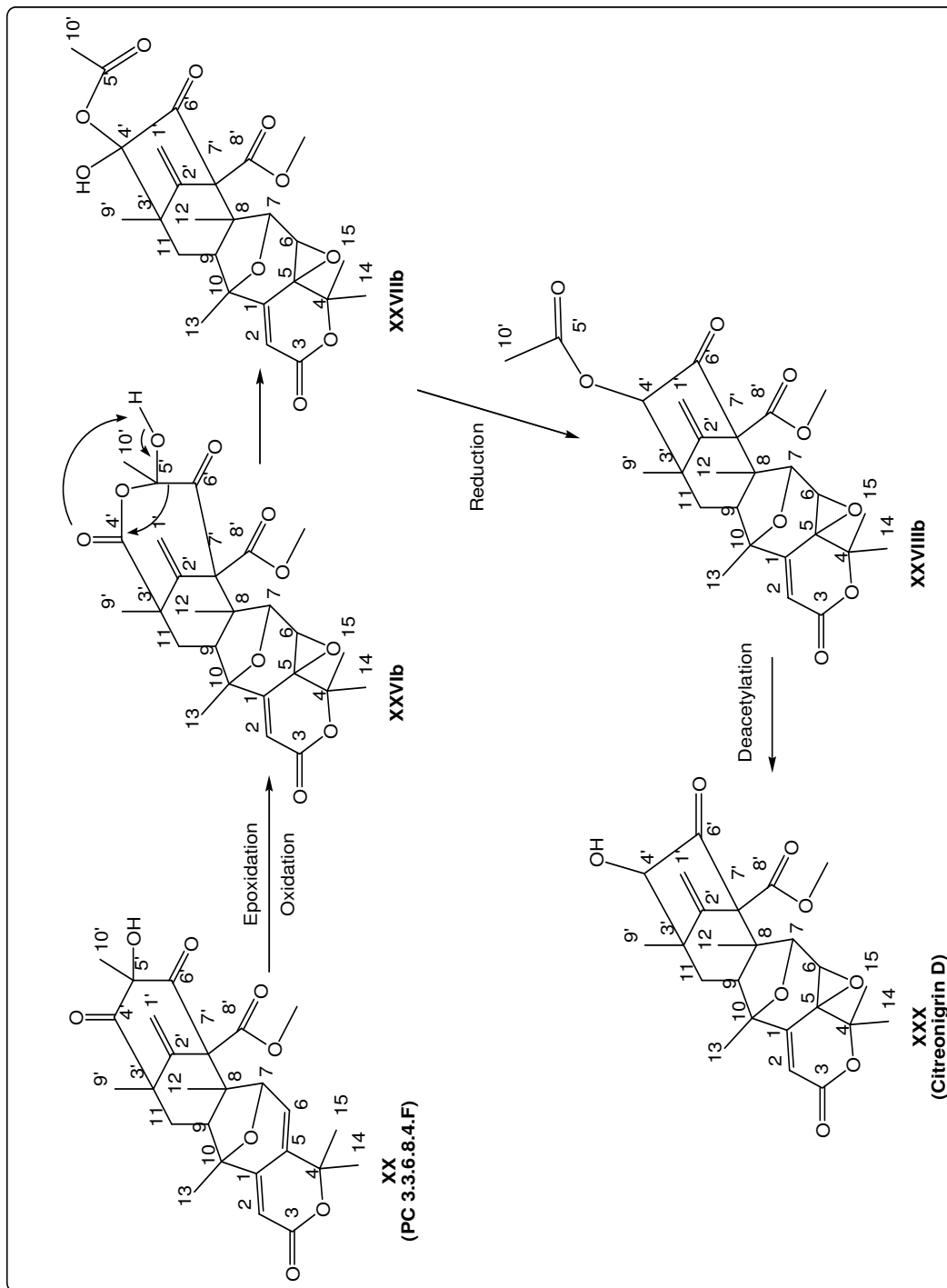


Figure 4.1.1.1.4.3. Proposed alternative biosynthetic pathway of citreogrignin D

4.1.1.1.5 Proposed Biosynthetic Pathways of Paraherquonin-Type Meroterpenes (Citronigrin F, G, H, I, and PC 3.3.6.6.3.A)

Citronigrin F is presumably produced from citronigrin E through a subsequent oxidation and rearrangement process. Although the proposed pathway for the conversion of citronigrin E to citronigrin F could not be as clearly defined in this study as in the previous three chapters, since putative intermediates have neither been isolated nor been described in the literature, it is assumed that two Baeyer-Villiger type oxidations between C-4' and C-5' (as shown in the formation of intermediate XXVIb) and subsequently between C-6' and C-5' could be involved in the pathway. In addition, a formal 1,3-acyl shift would result in the formation of citronigrin H (figure 4.1.1.1.5.1).

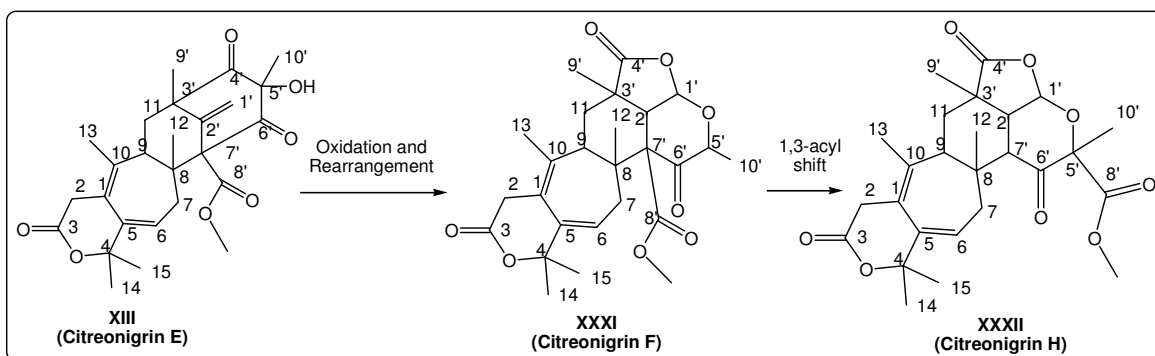


Figure 4.1.1.1.5.1. Proposed biosynthetic pathway of citronigrin F and H

On the other hand, modification of citronigrin F, especially in the Southern part, could lead to the formation of citronigrin G. The epoxidation of one double bond at the heptadiene ring in citronigrin F molecule followed by intramolecular rearrangement would result in the formation of a heptadienol intermediate XXXIV. Hydroxylation followed by double bond rearrangements, further hydroxylation and hemiacetal formation would result in the formation citronigrin G (figure 4.1.1.1.5.2).

As described in figure 4.1.1.1.5.3, the formation of citronigrin I is presumably derived from citronigrin G. Lost of water, ester hydrolysis and lost of carbondioxide would result in decarboxylation of intermediate XXXVIII. Further C-2 oxidation would yield citronigrin I, a compound which is an isomer to the known paraherquonin, a compound previously described from *Penicillium paraherquei*(Okuyama and Yamazaki, 1983) (figure. 4.1.1.1.1.1).

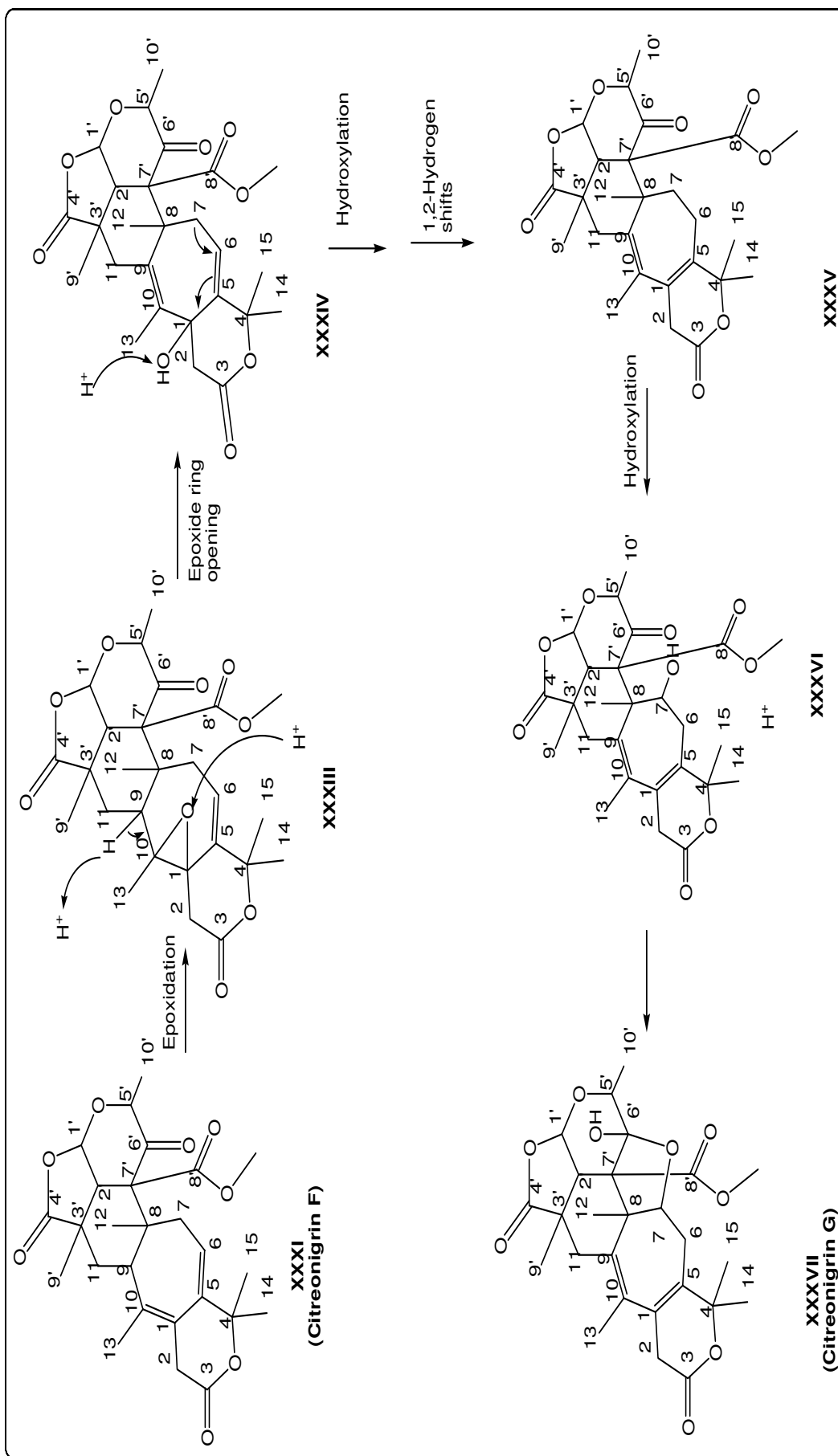


Figure 4.1.1.1.5.2. Proposed biosynthetic pathway of citreonigrin G

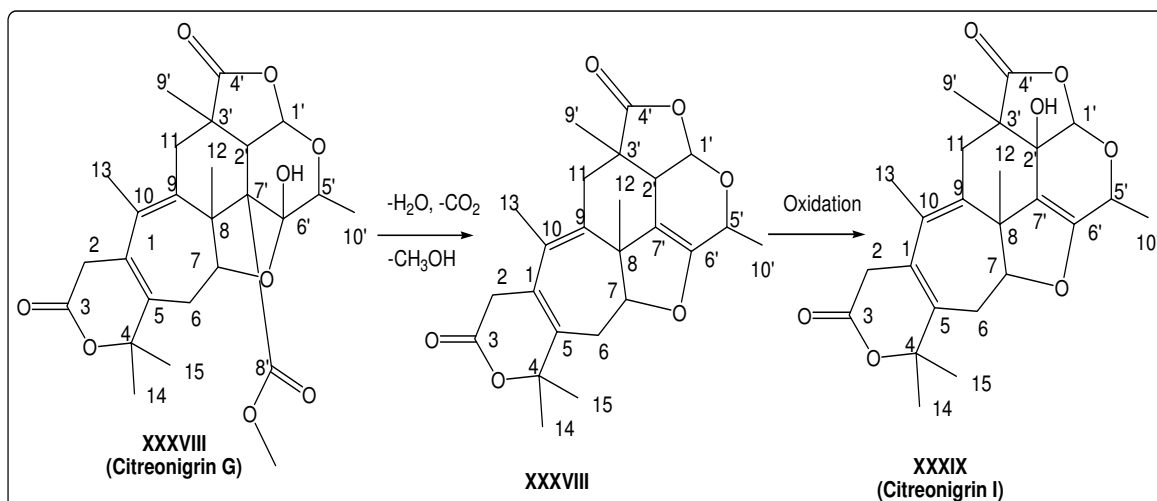


Figure 4.1.1.1.5.3 Proposed biosynthetic pathway of citreonigrin I

The structure similarity between PC 3.3.6.6.3.A and citreonigrin G indicated that PC 3.3.6.6.3.A could be derived from citreonigrin G. Figure 4.1.1.5.4 summarizes the hypothetical proposed scheme of the conversion of citreonigrin G into PC 3.3.6.6.3.A. Hydrolysis of the δ -lactone ring in citreonigrin G results in a free carboxylic acid function in intermediate XL. Further epoxidation followed by epoxide ring opening leads to the formation of intermediate XLII. Oxidative cleavage and loss of a C3 unit at C-5 and further double bond epoxidation in the seven-membered ring B yield PC 3.3.6.6.3.A.

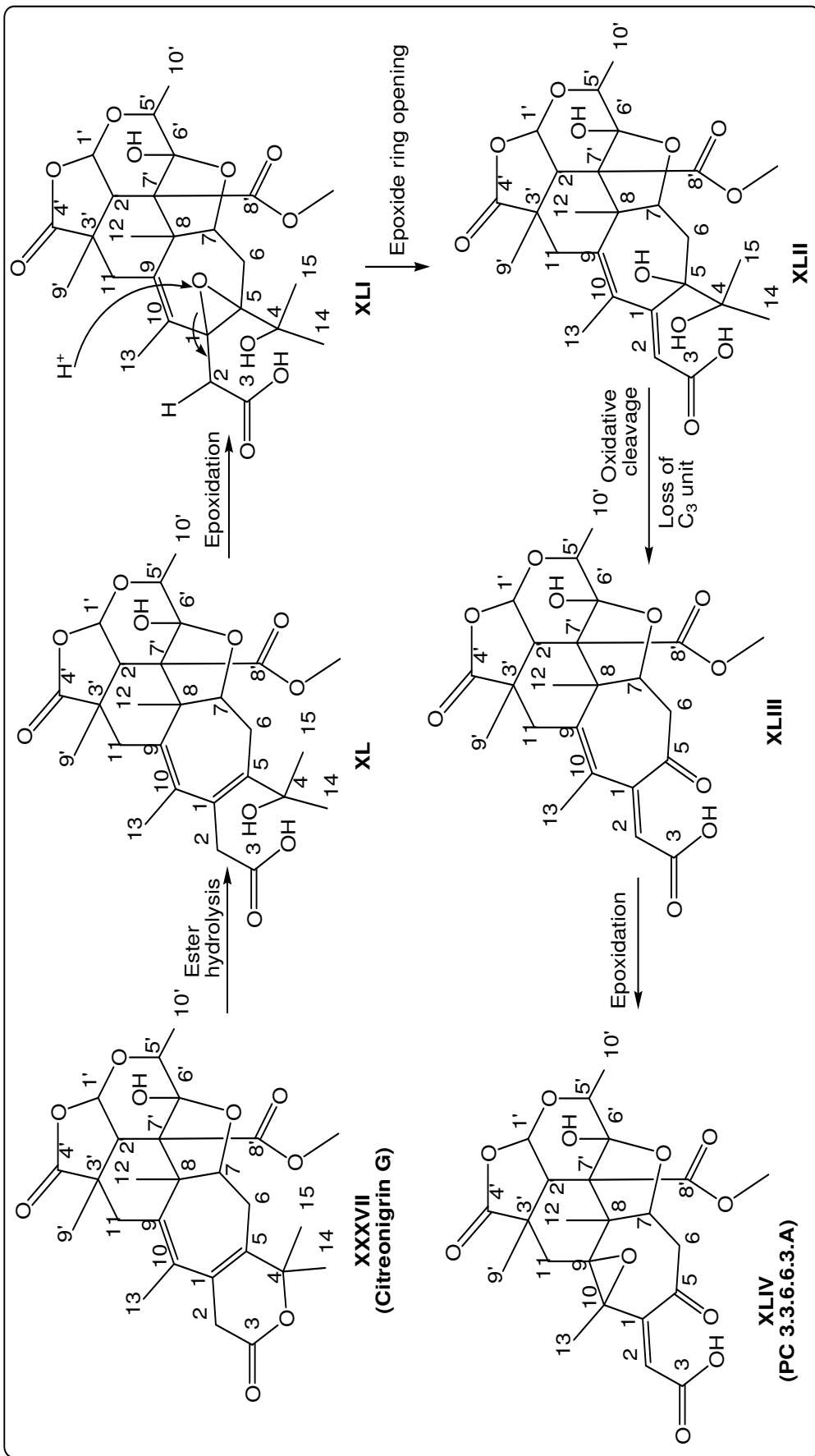


Figure 4.1.1.1.5.4 Proposed biosynthetic pathway of PC 3.3.6.6.3.A

4.1.1.1.6 Proposed Biosynthetic Pathways of PC 3.3.6.6.3.B and PC 3.3.22.D

Both PC 3.3.6.6.3.B and PC 3.3.22.D are supposed to be products of the intramolecular modifications of intermediate XII. The epoxidation of the exomethylene function C-1' would give the intermediate XLV which on a formal basis could easily be directly converted into PC 3.3.22.D (figure 4.1.1.1.6.1).

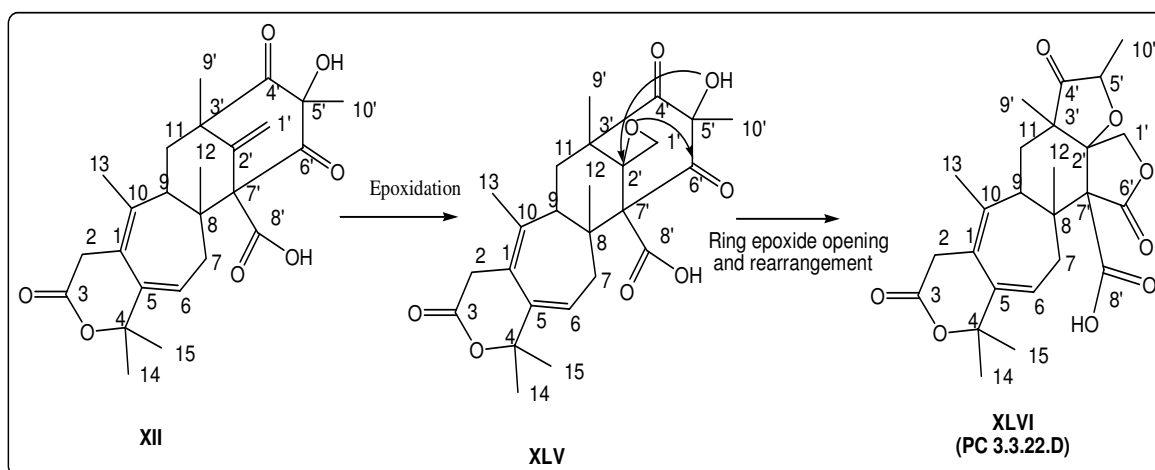


Figure 4.1.1.1.6.2. Proposed biosynthetic pathway of PC 3.3.22.D

Meanwhile, a Baeyer-Villiger type oxidation at C-6' and C-7' of intermediate XLV followed by the epoxide ring opening would lead to the formation of XLVIII. Further double bond rearrangement followed by keto-enol tautomerization results in intermediate L. This intermediate is then converted to intermediate LI by the formation of hemiacetal and acetal functions. Finally, the methylation of the free carboxylic acid would give PC 3.3.6.6.3.B (figure 4.1.1.1.6.2)

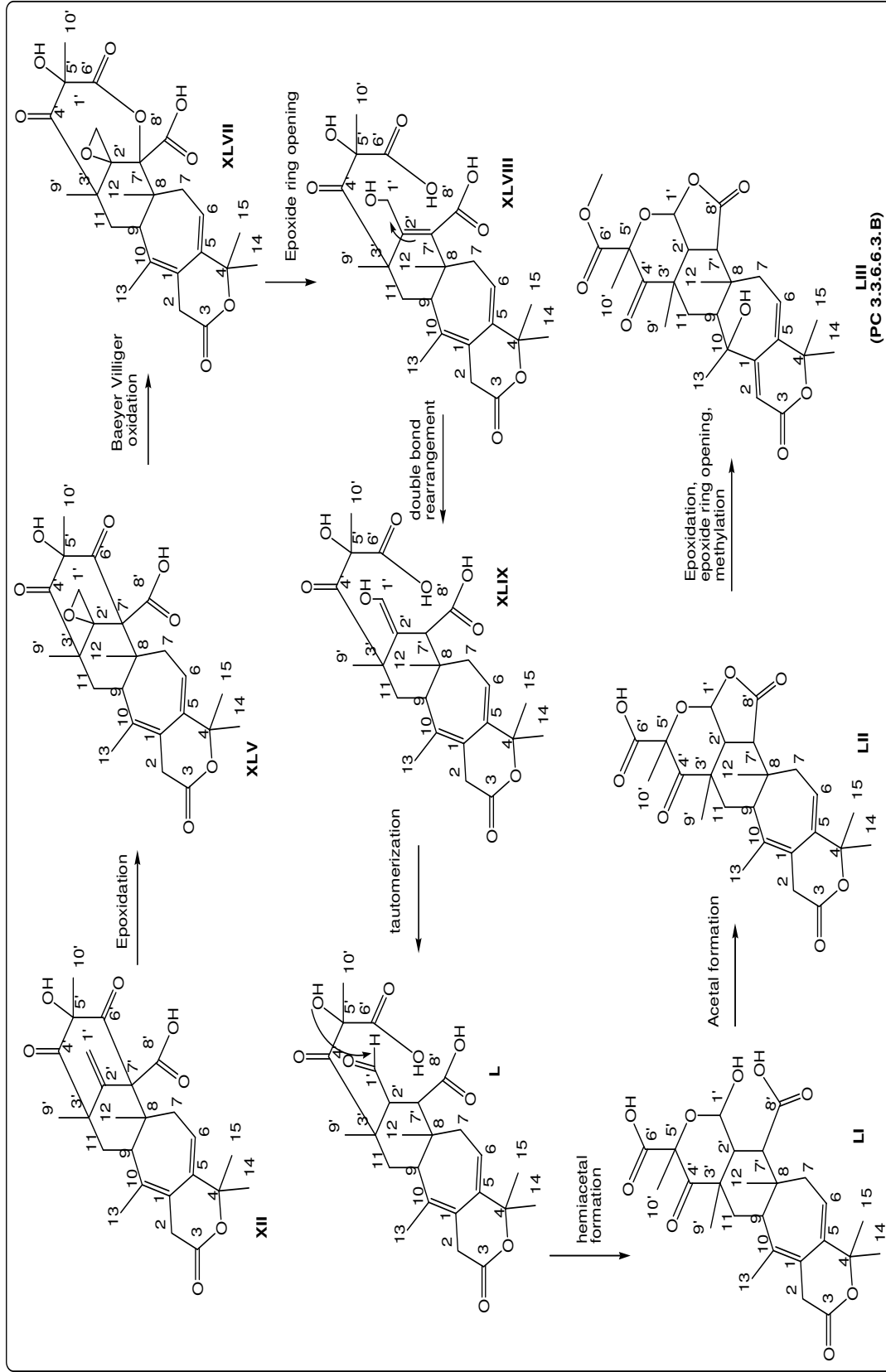


Figure 4.1.1.1.6.2. Proposed biosynthetic pathway of PC 3.3.6.3.3.B

4.1.1.1.7 Biological Activities of the Isolated Meroterpenes

Eventhough a series of meroterpenoids have already been reported, most of them lack a significant biological activity. Neoaustin and 7- β -acetoxy-dehydroaustin, which were isolated from *Penicillium* sp., are two of a few active fungal meroterpenoids. They were reported to exhibit moderate bacteriostatic effects toward *Escherichia coli* at dosages of 250 μ g/ml (Santos and Rodrigues-Filho, 2003).

Interestingly, andrastin A (Shiomi et al., 1999), isolated from *Penicillium* sp., has been reported not only to be active as protein farnesyltransferase inhibitor but also to enhance the cytotoxicity of vincristine in vincristine-resistant cells. The latter activity indicates that andrastin A might directly interact with P-glycoprotein and could inhibit the efflux of anti-tumor agents in drug resistant cells.

In this study, the isolated meroterpenes were submitted to bioassays to evaluate their pharmaceutical potential. Unfortunately, most of them did not show any activity when tested for antimicrobial, antifungal properties. Meanwhile, only citreonigrin E showed a weak activity (ED₅₀ 18.0 μ M) in the assays using the L-5178Y cell lines, while the other meroterpenoids did not show any cytotoxicity activity.

In protein kinase assays, however, only citreonigrin B exhibited inhibitory activities toward selected protein kinases. As the largest enzyme family encoded by the human genome, protein kinases have central roles in the regulation of most critical cellular processes. The over-expression and deregulation of protein kinases could lead to the aberration of cell proliferation, differentiation and activation that cause many diseases, including cancer, inflammation and diabetes. These facts underline the general importance of protein kinases as drug targets and the need for development of specific kinase inhibitors for the treatment of cancer, chronic inflammation, metabolic disorders and neurodegenerative diseases.

The assay using AKT1/PKB alpha gave an IC₅₀ value of only 4.1 mM for citreonigrin B. Human protein kinase B alpha/AKT1 is a protein serine/threonine kinase that regulates cell survival. The activation of this enzyme inhibits apoptosis and stimulates cell cycle

progression by phosphorylating numerous targets in various cell types, including cancer cells (Sun et al., 2001).

ARK5 is a serine/threonine kinase that plays a role in many cellular functions. The overexpression of this enzyme has been associated with tumor invasion and metastasis (colorectal neoplasm) (Kusakai et al., 2004). The assay using ARK5 gave only a very low activity of citreonigrin B in the lower molar range which was beyond the measured concentration.

Meanwhile, citreonigrin B showed a moderate inhibitory activity in the hyper micromolar range toward FAK. Focal-adhesion kinase (FAK) is a cytoplasmic protein tyrosine kinase acts as an important mediator of growth-factor signalling, cell proliferation, cell survival and cell migration. It has been reported that FAK is involved in tumour formation and progression, and its expression is increased in human tumours (McLean et al., 2005). These facts make FAK a potentially important new therapeutic target.

A moderate activity (IC_{50} 0.94 mM) was also shown when citreonigrin B was tested against IGF-1R. Insulin-like growth factor receptor (IGF-1R) is a receptor tyrosine kinase that plays a critical role in the establishment of a malignant cell phenotype. Interestingly, the targeting of IGF-1R can reverse the malignant phenotype in cancer cells and render them sensitive to apoptosis, without seriously affecting the biology of normal cells. For these reasons, IGF-1R seems to be a very promising target in cancer therapy, such as breast cancer (Zhang and Yee, 2000).

A stronger inhibitory activity (IC_{50} 68 μ M) was observed when citreonigrin B was tested against EPHB-4. EPHB-4 belongs to the EPH family of receptor tyrosine kinase which promote tumor angiogenesis by signalling through its membrane-bound ligand on endothelial cells and are thought to be involved in breast (Nooren et al., 2004), colon (Stephenson et al., 2001) and prostate (Xia et al., 2005) cancers.

A similar level activity of citreonigrin B was measured in the assay using SRC. SRC is a cytoplasmic tyrosine kinase which plays an important role in proliferation, adhesion and motility at the cellular level. In addition, it has been also reported that SRC is involved in

cell survival and intracellular trafficking in various specialized cell types. These facts suggest that Src inhibitors might have therapeutic value in the suppression of tumor growth, tumor angiogenesis and bone resorption (Susva, 2000), including tumor cells in breast (Biscardi et al., 2002) and colon (Dehm et al., 2001) cancers.

Compared to the structures of other isolated meroterpenoids, especially citreonigrin A, which were also submitted to the protein kinase assays but did not show any activity, citreonigrin B is the only isolated meroterpene which contains a hydroxyl group at C-5. Thus, the function arise whether the position of the hydroxyl group incorporated in a lactone ring system might trigger the activity of citreonigrin B. Unfortunately, there is not enough evidence to answer this question in this study although a similar phenomenon is also observed in the case of the isolated sesquiterpene lactones (see section 4.1.1.2.2).

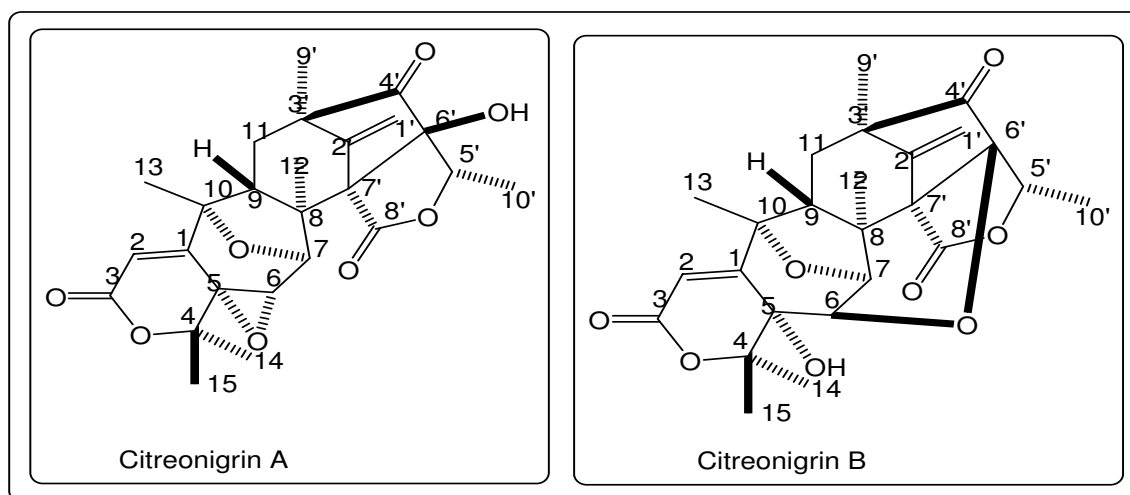


Figure 4.1.1.7.1. Structures of citreonigrin A and B

4.1.1.2 Sesquiterpene Lactones

4.1.1.2.1 Biogenesis of the Isolated Sesquiterpene Lactones

Structurally, the sesquiterpene lactones isolated in this study are related to the cinnamolide class of drimane lactones. Pebrolides (McCorcindale et al., 1981) and 2 α -hydroxydrimeninol (Pulici et al., 1996) are two of some reported fungal metabolites which belong to this class of compound (figure 4.1.1.2.1.1) isolated from *P. brevicompactum* and *Pestalotiopsis* sp., respectively.

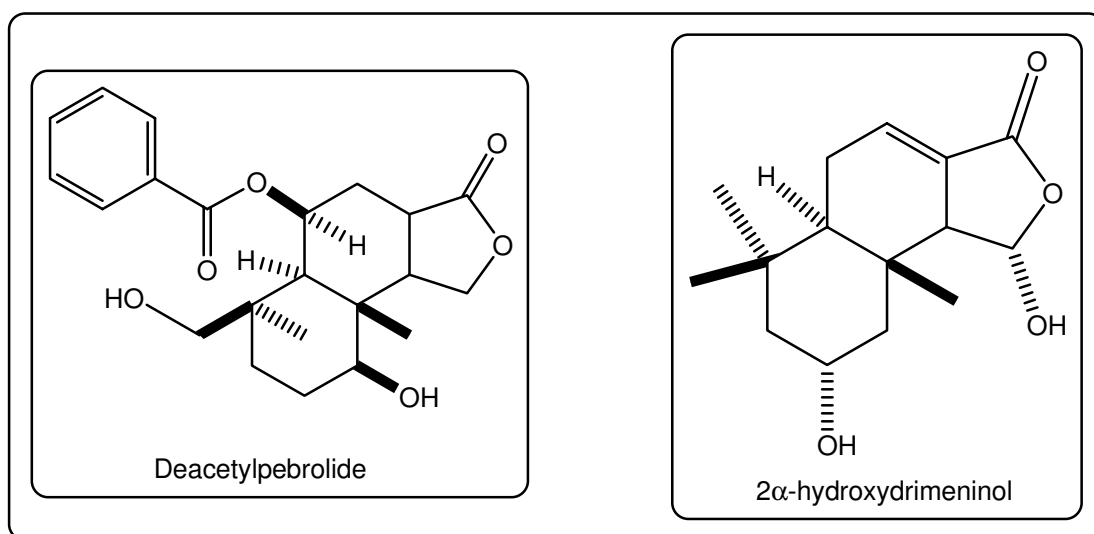


Figure 4.1.1.2.1.1. Two reported sesquiterpene lactones isolated from fungi

To date, there is no report which explains the biogenetic pathway of this class of compounds, especially in fungi. Based on the backbone pattern, however, these compounds seem to be biogenetically derived from farnesyl pyrophosphate a similar manner as described above for the meroterpenoid biosynthesis (figure 4.1.1.2.1.2).

KubaneK (KubaneK et al. 1997) investigated the biosynthetic pathway of terpenoids in dorid nudibranch *Cadlina luteomarginata*. In their investigation, they found that albicanyl acetate, a compound containing an exomethylene at C-8, would be directly derived from acetate units through the likely intermediate farnesylpyrophosphate (figure 4.1.1.2.1.3). Based on this report, a similar mechanism of cyclisation of farnesyl pyrophosphate and the formation of the δ -lactone ring system, following oxidation at C-12 to give citreodrimenes A – F can easily be derived (figure 4.1.1.2.1.4).

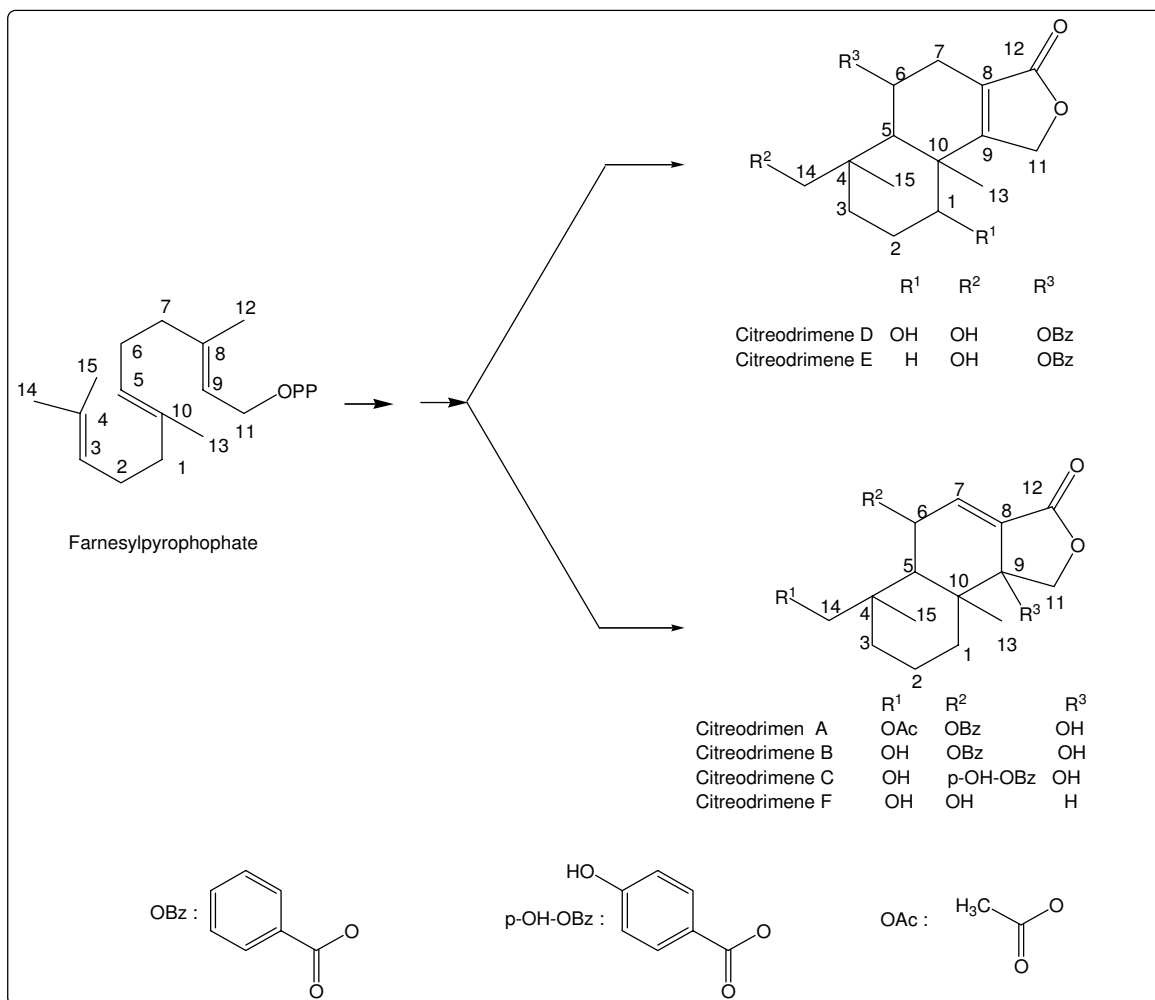


Figure 4.1.1.2.1.2. Putative biogenetic origin of the isolated sesquiterpene lactone backbones from farnesylpyrophosphate

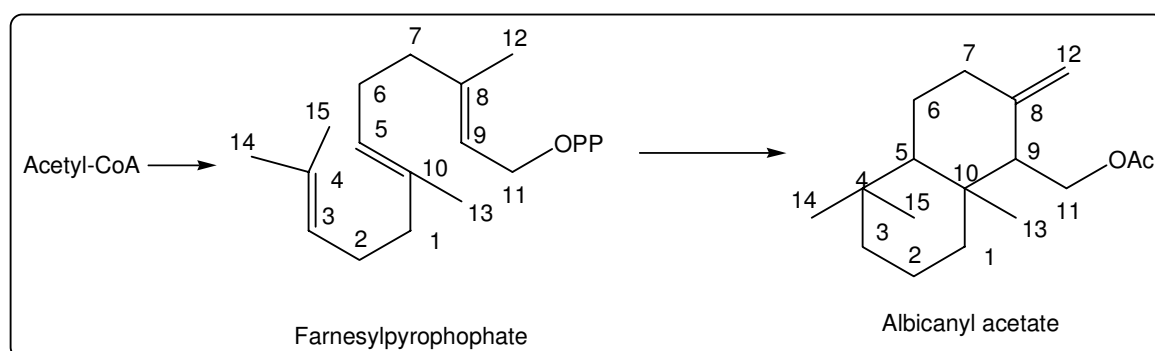


Figure 4.1.1.2.1.3. The conversion of farnesylpyrophosphate to albicanyl acetate (Kubane et al., 1997)

The formation of the sesquiterpenes is assumed to occur through a hypothetical intermediate LV, upon which, the formation of the δ -lactone ring would be initiated by the subsequent oxidation at C-12 followed by esterification between C-12 and C-11. Further double bond

rearrangements and oxidative steps would give rise to citreodrimenes A – F as described in figure 4.1.1.2.1.4.

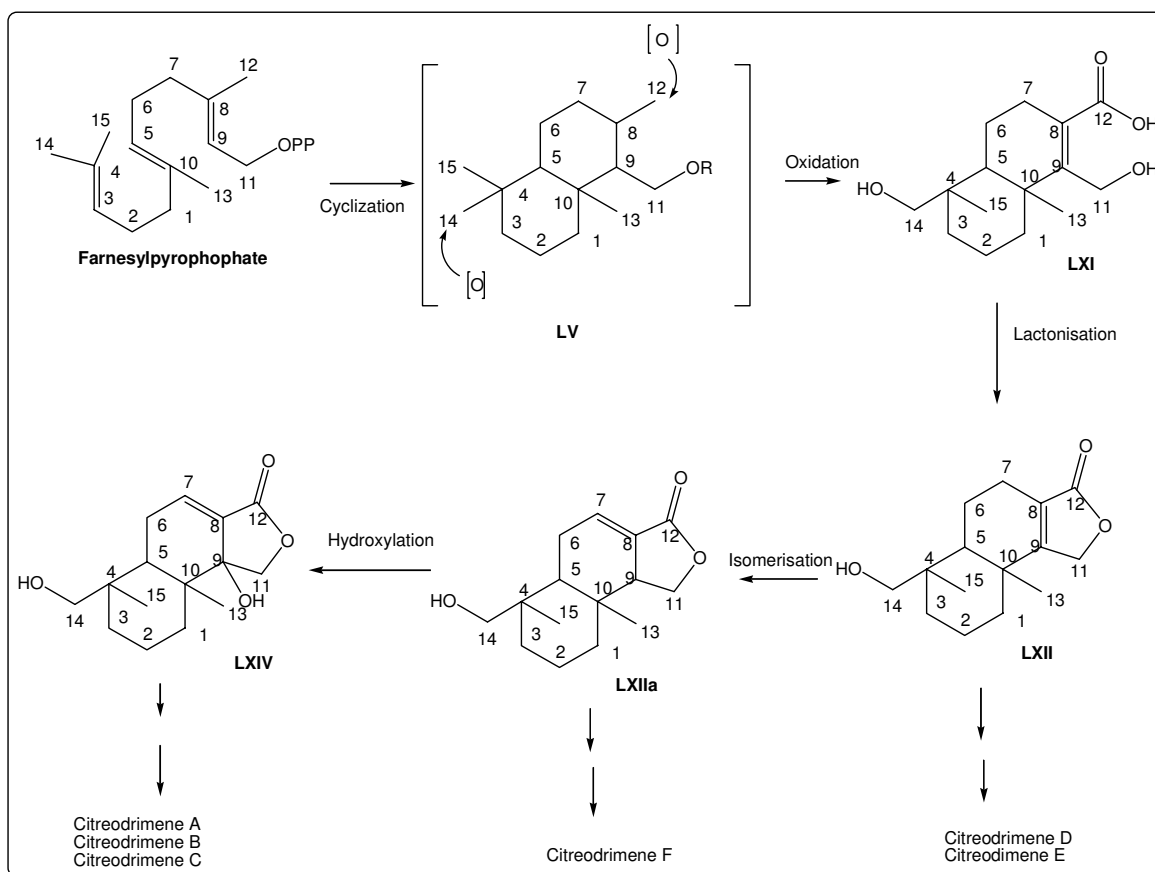


Figure 4.1.1.2.1.4. Proposed biogenetic pathway leading to the citreodrimene A –F.

4.1.1.2.2 Biological Activity and Structure Activity Relationships of the Citreodrimenes A - F

Sesquiterpene lactones are natural products occurring most widely in many plant families, primarily the Compositae (Asteraceae), and are known for their various biological activities, including cytotoxicity to tumor cells (Beekman et al., 1997). Over the past ten years, some sesquiterpenes with the various biological activities have been reported from fungal isolates, including marine fungi. Insulicolide A (Belofsky et al., 1998) is a marine fungal sesquiterpene lactone reported to be responsible for the HCT-116 colon carcinoma cell cytotoxicity in the crude extract of *A. varicolor* isolated from the surface of the Caribbean green alga *Penicillus capitatus*.

In this study, the isolated sesquiterpene lactones did not show any activity in the antifungal assays. Amongst the isolated sesquiterpene lactones, however, only citreodrimene A showed a weak antimicrobial activity on *B. subtilis* (9 mm diameter of inhibition zone for 100 µg of sample). Compared to the structure of citreodrimene B which was also submitted to the assays but did not show any antimicrobial activity, the activity of citreodrimene A is supposed to be affected by the presence of an acetate unit as esters at C-14.

In the cytotoxicity assays, citreodrimene A showed an ED₅₀ of 1.24 µM, against the L-5178-Y (mouse T cell lymphoma) cell line. In addition, a reduction of cell growth by 64 % in PC 12 (a red adrenal pheochromocytoma) and 20 % in HeLa (human cervix carcinoma) cell lines was caused by the substance at concentrations of 2.60 µM and 0.77 µM, respectively.

Citreodrimenes A and C showed ED₅₀ of 2.50 µM and 3.73 µM against the L-5178-Y and HeLa cell lines, respectively. In addition, the ED₅₀ of 4.15 µM and 18.10 µM were observed when citreonigrin A and C tested against HeLa cell line, respectively. On the other hand, citreodrimenes D, E and F did not show any activity when tested at the same concentration.

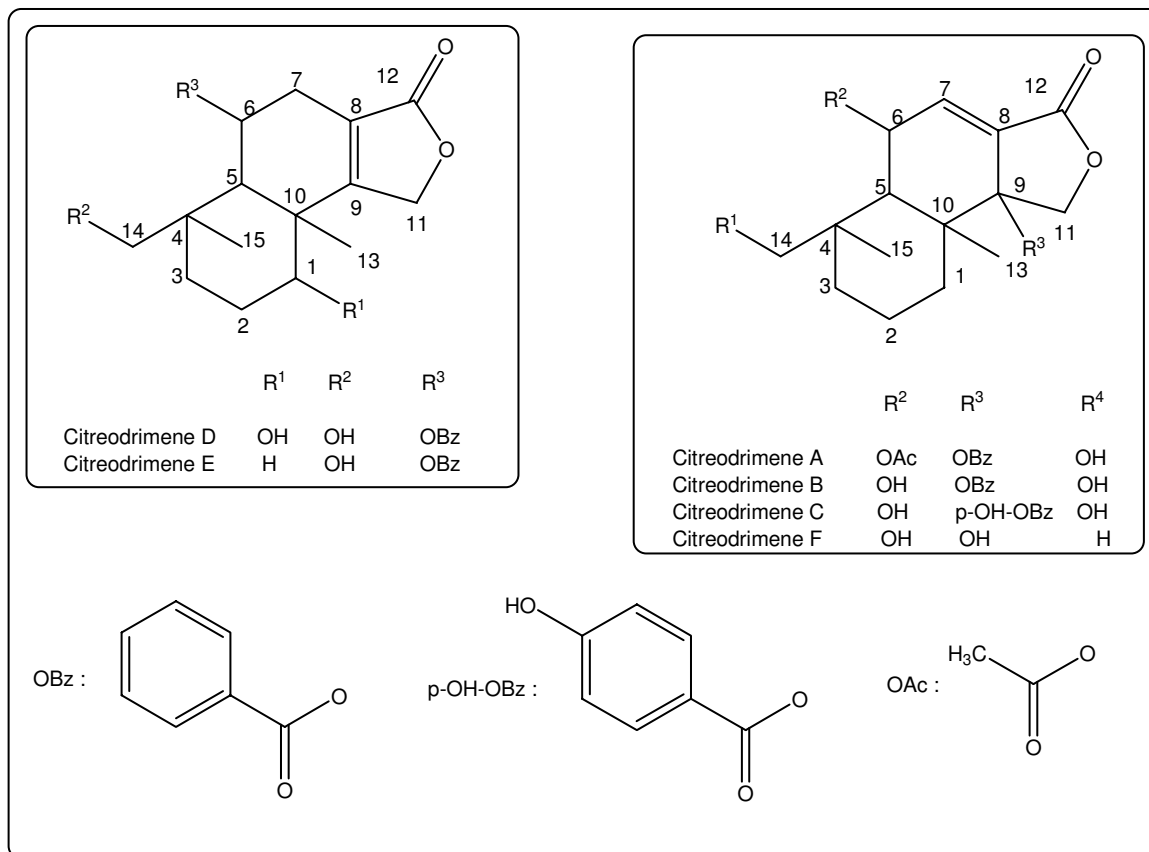


Figure 4.1.1.2.2.1. The structures of the isolated sesquiterpene lactones

Considering the structural similarities between citreodrimene A, B and C the differences to citreodrimene D, E and F, the presence of a hydroxyl group at C-9 alone or together with the α,β -unsaturated lactone functionality is assumed to be the trigger for the cytotoxicity of the active compounds. This assumption is also supported by the activity of insulicolide A (Belofsky et al., 1998) and pereniporin B (Kida et al., 1986) to colon carcinoma and leukemia cells, respectively.

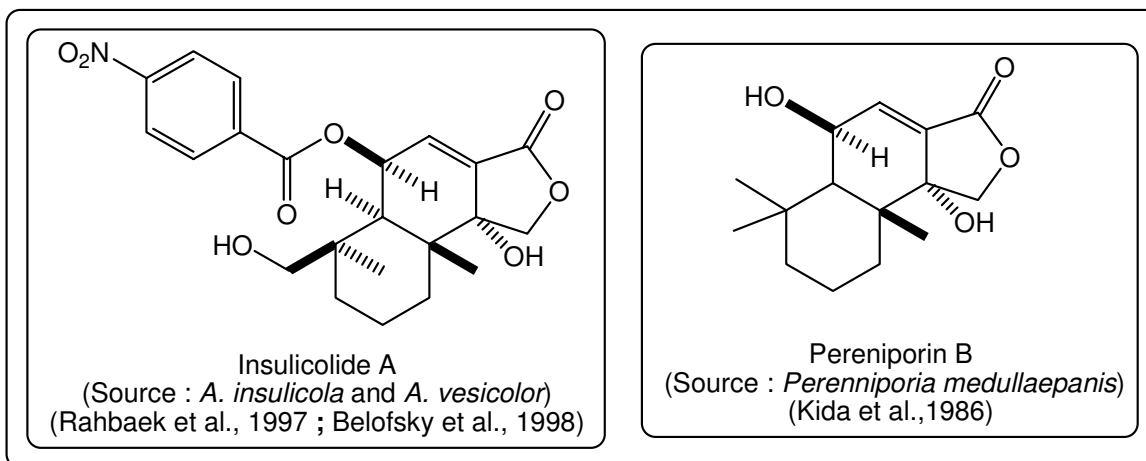


Figure 4.1.1.2.2.2 .The strutures of insulicolide A and pereniporin B

It has been reported that the cytotoxicity of sesquiterpene lactones could be attributed by the alkylation of biological nucleophiles by α,β -unsaturated carbonyl structures in a Michael-type addition (Beekman et al., 1997). This alkylation, presumably involving metabolically essential biomolecules, ultimately results in cell death (Belofsky et al., 1998). Nevertheless, this assumption would not explain the fact that citreodrimene F, a compound with a similar position of α,β -unsaturated carbonyl substructure like the active compounds, did not show any cytotoxicity activity. Furthermore, citredrimenes D and E, which also contain an α,β -unsaturated carbonyl substructure at a different position, did not show any cytotoxicity activity, but latter could be due to a steric hindrance of the assumed Michael-type addition.

It has also been found that sesquiterpene lactones inhibit a large number of enzymes involved in key biological processes, namely DNA and RNA synthesis, protein synthesis, purine synthesis, glycolysis, citric acid cycle, and mitochondrial electron transport chain (Beekman et al., 1997). For this reason, citreodrimenes A - F were subjected to protein-kinase assays. Unfortunately, only citreodrimene D proved active. A relative high activity of citreodrimen D was observed toward EPHB-4, while a lower activity was detected toward FAK.

A moderate activity of citreodrimene D was found in the assay using ERBB2. ERBB2 is a receptor tyrosine kinase which belongs to epidermal growth factor receptor (EGFR) family that plays an important role in the metastatic process of some gastric carcinomas (Lee et

al., 2005). Furthermore, a recent study indicated that ERBB2 mutations alone or together with K-RAS mutations may contribute to the development of some human cancers, such as gastric, colorectal, and breast cancers (Lee et al., 2006).

A moderate level of activities of citredrimene D were observed toward EGFR and VEGFR-3. The epidermal growth factor receptor (EGFR) is an important tyrosine kinase that plays an important role in the regulation of cellular signalling. It is frequently mutated in glioblastoma multiforme (GBM), one of the most aggressive types of brain cancer and one of the most resistant to treatment (National Cancer Institute, 2005). It has been also reported that EGF and VEGF families are overexpressed in human pancreatic cancers (Li et al., 2003). Meanwhile, vascular endothelial growth factor receptor-3 (VEGFR-3) is a protein tyrosine kinase that is overexpressed in human cancers and plays an important role in survival signalling. It has also been reported that VEGFR-3, in the presence of focal adhesion kinase (FAK), binds and suppresses apoptosis in breast cancer cells (Garces et al., 2006).

On the other hand, a very moderate activity of PC 3.3.14.G was observed against MET and SAK. MET is a receptor tyrosine kinase that has been shown to be overexpressed or mutated in a variety of solid tumors (Sattler et al., 2003), while SAK is a protein-serine/threonine kinase that is involved in cell proliferation (Fode et al., 1994).

4.1.1.3 14,15-Dihydroversmitatin and Vermistatin

14,15-Dihydrovermistatin is a new compound related to the known vermistatin which was also isolated in this study. The comparison of ^1H and ^{13}C NMR data together with the optical rotation value of the isolated 14,15-dihydrovermistatin and vermistatin indicated that the stereochemistry at C-3 of both compounds is identical to that reported for vermistatin in the original communication (Fuska et al., 1986).

It has been also reported that vermistatin is a phytotoxin and a cytotoxic agent (Fuska et al., 1986). Unfortunately, both 14,15-dihydrovermistatin and vermistatin isolated in this study did not show any activity in antimicrobial and antifungal assays. However, vermistatin showed a weak activity in the assay using L5178Y cell line. Preliminary assay

indicated that vermistatin (10 $\mu\text{g/ml}$ or 30 μM) suppressed the growth by 32.0 % cell growth compared to the untreated controls, while 14,15-dihydrovermistatin was inactive under the same conditios.

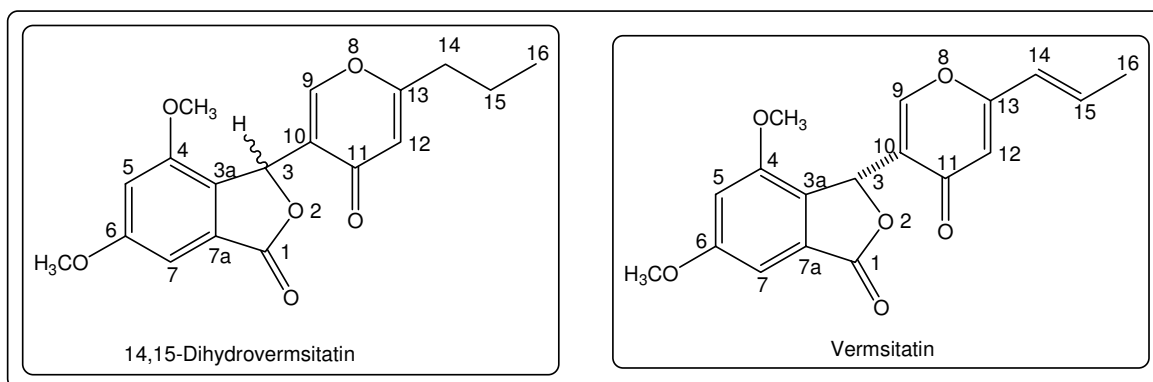


Figure 3.1.1.3.1 Structures of 14,15-dihydrovermistatin and vermistatin

A similar phenomenon was also observed in the protein kinase assays. The new compound, 14,15-dihydrovermistatin, did not show any activity, while vermistatin showed weak inhibitory activities toward the kinases Aurora A, Aurora B, CDK4/cycD1, ERBB2, IGF1R, BRAV-VE, VEGFR-2 and AKT1.

A weak activity of vermistatin was detected against Aurora B. Aurora B is protein serine/threonine kinase that is known as chromosomal passenger protein and is responsible for the proper progression of mitosis and cytokinesis ; it is overexpressed throughout the cell cycle in cancer cells (Abdullah et al., 2005).

A slightly higher activity of vermistatin was found against CDK4/CycD1. CDK4/CycD1 is a serine/threonine kinase that has an important role in the regulation of the cell cycles. Like other cyclin-dependent kinases (CDKs), it provides a means for the cells to move from one phase of the cell cycle to the next. Its role is positively regulated by cyclins, which are normally overexpressed in cancer cells, and negatively by CDK inhibitors, which are normally not expressed in cancer cells (Schwartz and Shah, 2005). In addition, a moderate activity of vermistatin was also observed in the assays using ERBB2 and IGF1R.

A similar activity of vermistatin, however, was observed when it was introduced to the assay using BRAF-VE, VEGFR-2, Aurora A and AKT1 kinases. BRAF is a serine/threonine kinase that belongs to the RAS/RAF/MEK/ERK/MAPK pathway, which is involved in the transduction of mitogenic signals from the cell membrane to the nucleus. BRAF is commonly activated by somatic point mutations in human cancers, predominantly in malignant melanoma (Davies et al., 2002) and papillary thyroid cancer (Ouyang et al., 2006). Meanwhile, vascular endothelial growth factor receptor-2 (VEGFR2) is a tyrosine kinase that has been reported to be implicated in the pathologic angiogenesis associated with tumor growth (Amino et al., 2006), such as breast cancer (Ryden et al., 2005).

The highest level of activity of vermistatin was observed in the assays using AKT-1 and Aurora-A. Aurora-A (also called aurora-2) belongs to a small family of mitotic serine/threonine kinases that regulates centrosome maturation, chromosome segregation, and cytokinesis. It has been reported to contribute to oncogenic transformation and is frequently overexpressed and amplified in many human tumor types (Warner et al., 2003), such as human pancreatic cancers (Li et al., 2003a).

4.1.2 Secondary Metabolites from *Aspergillus niger*

4.1.2.1 New γ -Pyrones (2-(hydroxy(phenyl)methyl)-4-pyrone and 6-benzyl-4-oxo-4H-pyran-3-carboxamide)

Both 2-(hydroxy(phenyl)methyl)-4-pyrone and 6-benzyl-4-oxo-4H-pyran-3-carboxamide were identified as a new γ -pyrone containing metabolites. These compounds are related to PAI 1/1 5, a new metabolite isolated from *Penicillium citreonigrum* (Brauers, 2003) which has not yet been published. Furthermore, some known *Aspergillus niger* metabolites which were also isolated in this study, such as pyranonigrins A and B (Hiort et al., 2004), contain γ -pyrone substructure. In the bioassays, however, these compounds did not show any activity, neither antimicrobial, antifungal, cytotoxic or protein kinase inhibiting activities.

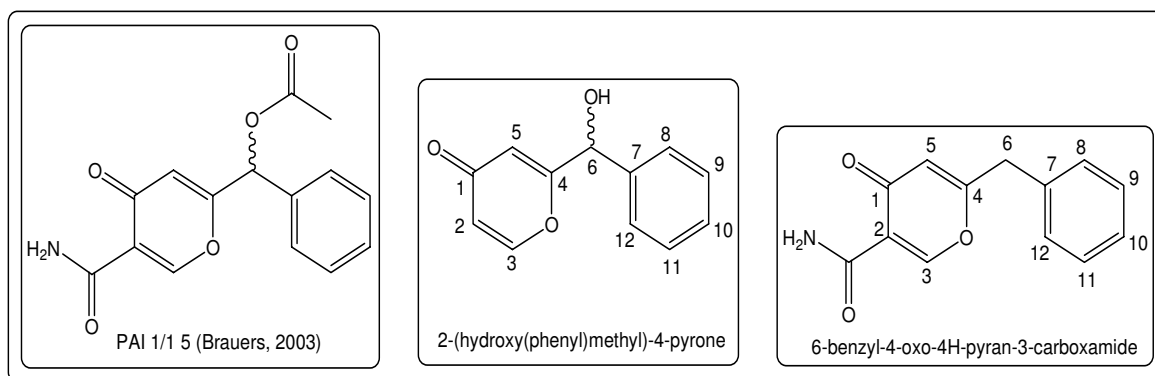


Figure 4.1.2.1.1 Structures of new γ -pyrones : 2-(hydroxy(phenyl)methyl)-4-pyrone, 6-benzyl-4-oxo-4H-pyran-3-carboxamide as well as PAI 1/5 (Brauers, 2003)

4.1.2.2 New Aflavinine Derivate

ANE 6.8.1.1 was the only indoloditerpene isolated in this study. Structurally, this compound is related to aflavinine and 10,23-dihydro-24,25-dehydro-21-oxo-aflavinine, two metabolites which have been reported from *Aspergillus tubingensis* (TePaske and Gloer, 1989). In comparison to the reported metabolites, the isolated ANE 6.8.1.1 differs mainly in the presence of 21-OH and the orientation of 19-OH.

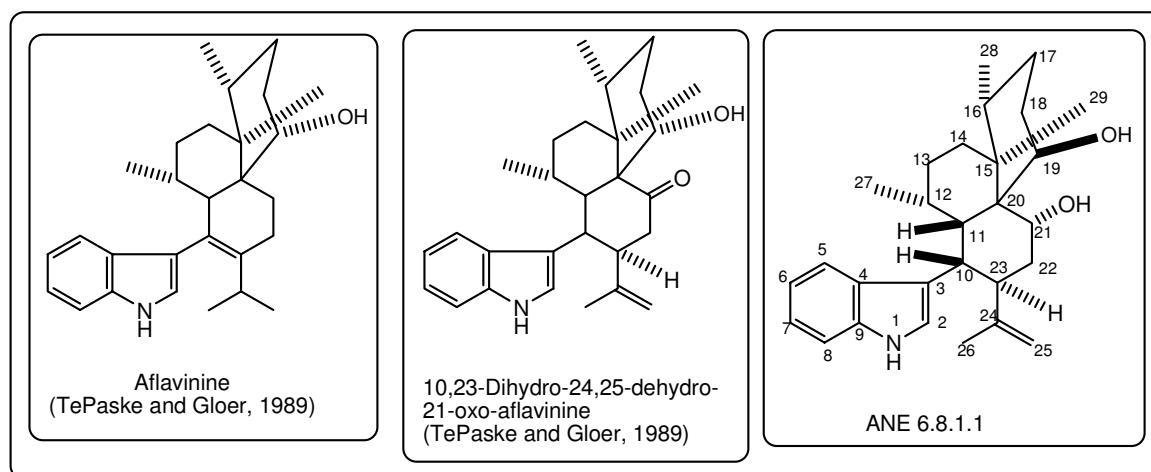


Figure 4.1.2.2.1 Structures of ANE 6.8.1.1, aflavinine and 10,23-dihydro-24,25-dehydro-21-oxo-aflavinine

The known aflavinine and its derivatives have been reported to exhibit anti-insecticidal activity, especially the ones isolated from *A. flavus* (Gloer et al., 1988). Since ANE 6.8.1.1 was isolated only in a small amount, the anti-insecticidal assay could not be conducted with this compound. However, the cytotoxicity assay using the L-5178Y cell line gave an

ED₅₀ value of 2.5 µg/mL. Meanwhile, the assays using the Hela cell line indicated only a low activity, i.e only 17 % growth inhibition at the concentration of 3 µg/ml, compared to the untreated controls.

In antimicrobial assays, ANE 6.8.1.1 showed a weak inhibitory activity in the assays toward *B. subtilis* (11 and 12 mm diameters for the inhibition zone upon loading amounts of 100 and 200 µg, respectively). Meanwhile, an MIC value of 100 µg/ml was measured for this compound in the assays using *S. epidermis* and *S. aureus*. Unfortunately, no activity was observed against assays using *Enterococcus sp.*, *Pseudomonas sp.* and *E. coli*.

4.1.2.3 New Asperazine Derivate

ANE 4.9.4.D was identified as a new metabolite belong to the diketopiperazine class of compound. Besides ANE 4.9.4.D, some others diketopiperazines, such as asperazine and cyclo(phenylalanyltryptophyl), were also isolated from the ethyl acetate extract of *Aspergillus niger*. Compared to asperazine, the lower solubility of ANE 4.9.4.D in methanol could be explained by the lower number of NH-groups which would decrease the capability to form the hydrogen bonds with solvent.

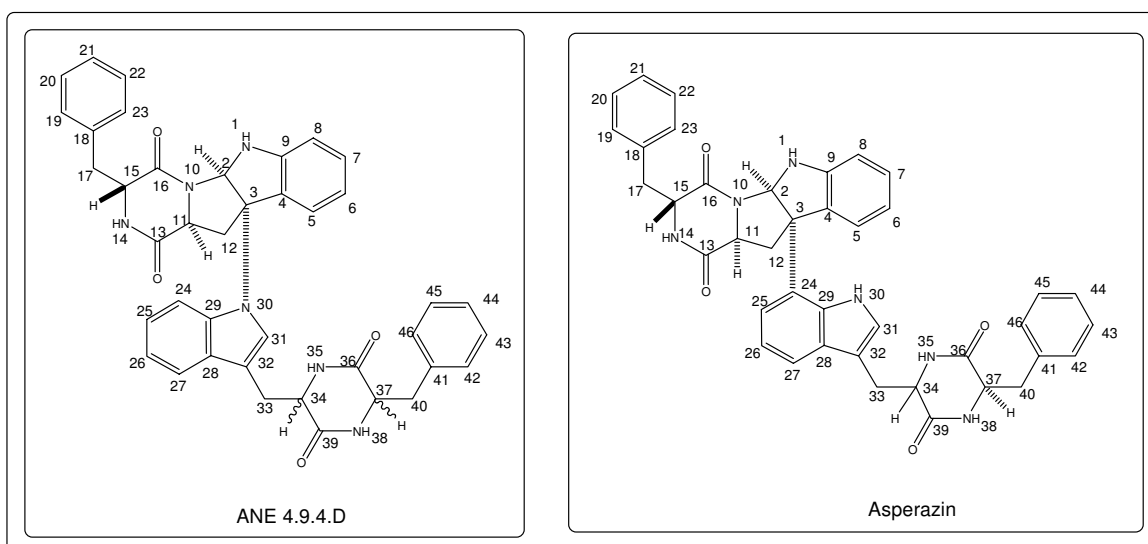


Figure 4.1.2.3.1 Structures of ANE 4.9.4.D and asperazine

In contrast to asperazine which has been reported to be active toward human leukemia murine colon 38 and human colon H116 or CX1 cell lines (Varoglu et al., 1997), both

ANE 4.9.4 D and the asperazine isolated in this study did not exhibit any cytotoxic activity against the L-5178Y (mouse T-cell lymphoma) cell line. Moreover, these two compounds also did not show any antibacterial, antifungal and protein kinase inhibitory activities.

4.2 Secondary Metabolites from Terrestrial Endophytic Fungi

4.2.1 Secondary Metabolites from *P. longisetula*

4.2.1.1 PL 3.8.D

Structurally, PL 3.8.D is related to the known antifungal compound gamahorin (Koshino et al., 1992), which was also isolated in this study. Unfortunately, both PL 3.8.D and the isolated gamahorin could not be submitted to any bioassay, including antifungal assays, because they were isolated only in small amounts.

Further small molecules which are related to PL 3.8.B were also isolated in this study, i.e. 2-hydroxy-3-methylbenzoic acid and 4-(hydroxymethyl)benzoic acid. In the previous time 2-hydroxy-3-methylbenzoic acid was also known as an analgesic and antiseptic agents but nowadays is no longer marketed due to toxic side effects (Dictionary Natural Products, 2004).

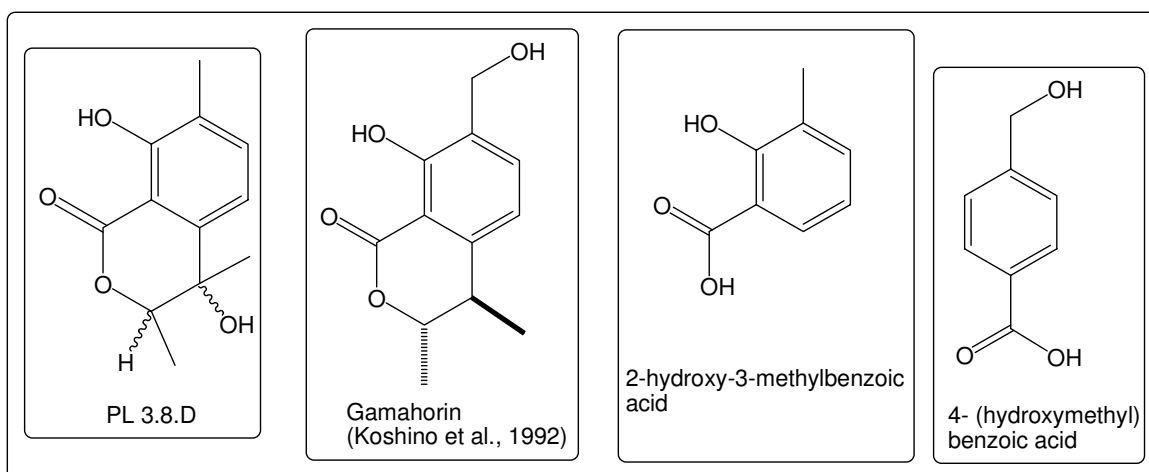


Figure 4.2.1.1.1 Structures of PL 3.8.D, gamahorin, 2-hydroxy-3-methylbenzoic acid and 4-(hydroxymethyl)benzoic acid

4.2.1.2 PL 5.12.A

Structurally, PL 5.12.A is closely related to the reported fungal metabolites variecoxanthone B (Chexal et al., 1975) and isoemicellin (Bringmann et al., 2003). PL 5.12.A differs from these compounds only in the absence of the xanthone core and the *O*-prenyl group. Instead, PL 5.12.A possesses a free carboxylic acid rather than the whole xanthone ring, while the *O*-prenyl group is replaced by an additional proton.

Since it was till required for further structural studies, PL 5.12.A has not yet been submitted to any bioassays. Nevertheless, the known isoemicellin was reported not to be active in cytotoxicity assays involved selected tumor cell lines (Bringmann et al., 2003).

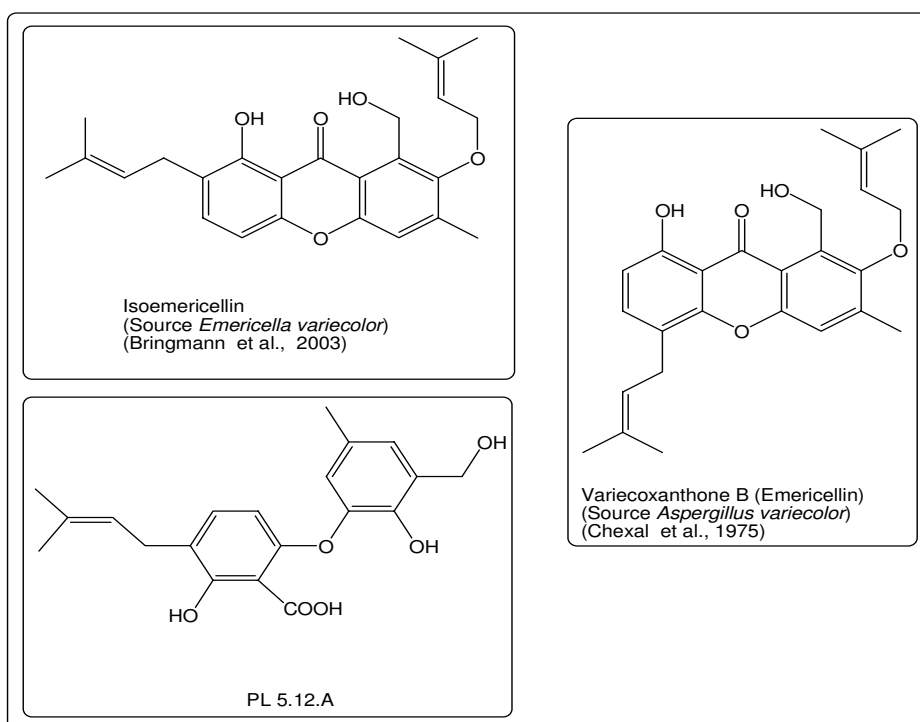


Figure 4.2.1.2.1 Structures of isoemicellin, emericellin and PL 5.12.A

4.2.1.3 PL 4.2.7.5

PL 4.2.7.5 is an isomer of herbarin B, a known metabolite isolated from *Cladopodium herbarum* which was associated with the sponge *Aplysina aerophoba*. Since the compound

was isolated only at low purity, it was not submitted to any bioassay. Furthermore, there is no report of any biological activity of its corresponding compound, herbarin B (Jadulco et al., 2002).

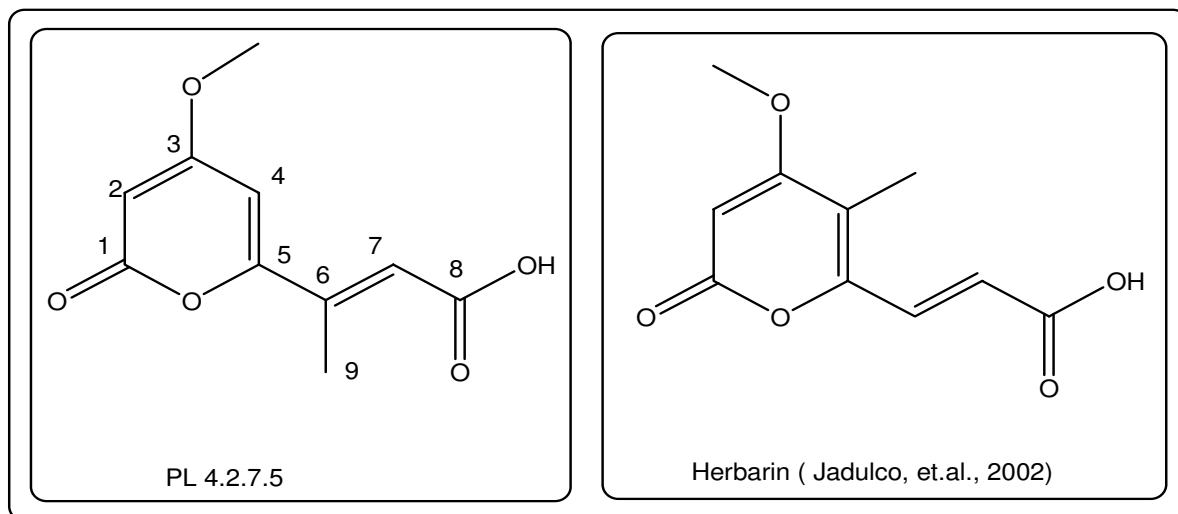


Figure 4.2.1.3.1 Structures of PL 4.2.7.5 and herbarin B

A remaining problem was the configuration of the olefinic group, viz the question whether the methyl group was on the same side of the double bond as the carboxylic group (cis-position) or not (trans-position). Some more NMR experiments are still needed in order to solve this problem.

4 CONCLUSION

Sponge-associated and plant endophytic fungi produce natural products with a large diversity of chemical structures which could not be synthesized for commercial purposes. In addition, most of them showed the biological activities in some pharmacological bioassay systems, thus they could be potential as lead structures for development new drugs.

The aim of this work was the isolation of secondary metabolites from sponge-associated and plant endophytic fungi followed by the structure elucidation and the examination of their pharmacological potential. Three sponge-associated fungi (*Aspergillus niger*, *Penicillium citreonigrum* and one unidentified fungi) as well as two plant endophytic fungi (*Pestalotiopsis longisetula* and *Chaetomium globosum*) were selected as the natural product sources and grown in a 300 mL liquid medium for three to four weeks. The ethyl acetate fractions were then subjected to some separation methods in order to isolate their secondary metabolite contents.

The isolation was performed using some different chromatography techniques and proceeded by the mass spectrometry (MS) and nuclear magnetic resonance (NMR) experiments to determine the molecular weight and structure elucidation of the isolated compounds, respectively. In addition, the X-ray crystallography was applied to some selected compounds in determining the absolute or relative configuration of the stereocenters in the molecule. Finally, some different bioassay techniques were performed to examine their anti-microbial, antifungal and cytotoxicity activities as well as inhibitory activities on some protein kinases.

Citreonigrin A – I, provided an extraordinary complex of meroterpene structure in which showed the new carbon skeleton in the natural products, were isolated from *P. citreonigrum* which was isolated in a sponge *Pseudoceratina purpurea* and collected in Bali Barat National Park, Indonesia (1996). Moreover, six new sesquiterpene lactones (citreodrimene A – F) and one new vermistatine derivative were also isolated from this fungus. On the bioassays, citreonigrin B and citreodrimene D showed the inhibitory activities on some protein kinases, while citreodrimene A, B and C showed the cytotoxicity

activities in the assay using L-5178Y (murine T-cell lymphoma) and HeLa (human cervix carcinoma) cell lines.

4.2.1.4 *Aspergillus niger* was an isolate from *Axinella damicornis* and collected in Elba at 1999. One new asperazine derivate, one new aflavinine derivate and two new γ -pyrone ((2-(hydroxy(phenyl)methyl)-4-pyrone and 6-benzyl-4-oxo- 4H-pyran-3-carboxamide) were succesfully isolated from this fungus. In the bioassays, the new aflavinine derivate showed not only the antimicrobial activities against *Bacillus subtilis*, *Staphylococcus epidermis* and *S. aureus*, but also the cytotoxic activities on the assays using L-5178Y, HeLa and PC-12 (rat adrenal pheochromocytoma) cell lines.

One plant endophytic fungus, *P. longisteula*, was isolated from *Aglaia odorata* grown in the green house of the Heinrich-Heine-Universität-Düsseldorf. One new gamahorin derivate, one new variecoxanthone derivate and one new herbarin derivate were successfully isolated from this fungus. Since they were isolated only in a small amount, these compounds were not submitted to the bioassays.

In general, more than fifty compounds have been successfully isolated from this study and at least thity of them, best of our knowledge, were new compounds. In this report, the discussion focuses only the new compounds. In addition to, the new activities of some known compounds, such as chaetomin (from *C. globosum*), meleagrín (from an unidentified fungus) and antibiotic RF-3192 C (from *A. niger*) are also briefly discussed in this report.

5 REFERENCES

- Abdullah, A., Foong, C., and Murata-Hori, M. (2005). Specific distribution of overexpressed aurora B kinase in interphase normal epithelial cells. **Cancer Cell International** 5, (31), Open access <http://www.cancerci.com/content/5/1/31>.
- Ahmed, S.A., Scott, F.E., Stenzel, D.J., Simpson, T.J, Moore, R.N., Trimble, L.A., Arai, K., and Vaderas, J.C. (1989). Studies on the biosynthesis of the mycotoxin austin, a meroterpenoid metabolite of *Aspergillus ustus*. **J. Chem. Soc, Perkin Trans1**, 807 – 816.
- Amino, N., Ideyama, Y., Yamano, Kuromitsu, S., Tajinda, K., Samizu, K, Hisamichi, H., Matsuhisa, A., Shirasuna, K., Kudoh, M. and Shibasaki, M. (2006). YM-359445, an orally bioavailable vascular endothelial growth factor receptor-2 tyrosine kinase inhibitor, has highly potent antitumor activity against established tumors. **Clinical Cancer Research** 12, 1630-1638.
- Bairati, C., Goi, G., Lombardo, A., and Tettamanti, G. (1994). The esters of p-hydroxybenzoate (parabens) inhibit the release of lysosomal enzymes by mitogen-stimulated peripheral human lymphocytes in culture. **Clin. Chim. Acta.** 224, 147 – 157.
- Barbel, J.A., Conford, J.L., Howard, T.D., and Sharples, D. (1986). The structure of citrinin in vivo. **J. Chem. Soc, Perkin Trans 1**, 2743 -2747.
- Barrow, C.J., Cai, P., Snyder, J.K., Sedlock, D.M., Sun, H.H., and Cooper, R. (1993). WIN 64821, a new competitive antagonist to substance P, isolated from *Aspergillus* species : Structure determination and solution conformation. **J. Org. Chem.** 58, 6016 – 6021.
- Bartlett, A.J., Holker, J.S.E., O'Brien, E., and Simpson, T.J. (1981). Biosynthesis of the meroterpenoid metabolite, andibenin B : Aromatic precursors. **J. Chem. Soc, Chem. Comm.**, 1198 – 1200.

- Beekman, A.C., Woerdenbag, H.J., Uden, W., Pras, N., Konings, A.W.T, Wikström, H.V., and Schmidt, T.J. (1997). Structure-cytotoxicity relationships of some helenanolide-type sesquiterpene lactones, **J. Nat. Prod.** *60*, 252 – 257.
- Belofsky, N., Jensen, P.R., Renner, M.K., and Fennical, W. (1998). New cytotoxic sesquiterpenoid nitrobenzoyl esters isolated from a marine isolate of the fungus *Aspergillus versicolor*. **Tetrahedron** *54*, 1715 – 1724.
- Bieber, B., Nüske, J., Ritzau, M., und Gräfe, U. (1998). Alnumycin a new naphthoquinone antibiotic produced by an endophytic *Streptomyces* sp. **J. Antibiot.** *51*, 381 – 382.
- Biscardi, J.S., Ishizawa, R.C., and Parsons, S.J. (2002). Tyrosine kinase signaling in breast cancer: epidermal growth factor receptor and c-Src interactions in breast cancer. **Breast Cancer Res.** *2* (3), 203-210.
- Bok, J.W., Lermer, L., Chilton, J., Klingeman, H.G., and Tower, G.H.N. (1999). Antitumor sterols from the mycelia of *Cordyceps sinensis*. **Phytochemistry** *51*, 891 – 898.
- Bradshaw, J., Butina, D., Dunn, A.J., Green, R.H., Hajek, M., Jones, M.M., Lindon, J.C., and Sidebottom, J. (2001). A rapid and facile method for the dereplication of purified natural products. **J. Nat. Prod.** *64*, 1541 – 1544.
- Brauers, G., Edrada, R.A., Ebel, R., Proksch, P., Wray, V., Berg, A., Gräfe, U., Schächtele, C., Totzke, F., Finkenzeller, G., Marme, D., Kraus J., Münchbach, M., Michel, M., Bringmann, G., and Schaumann, K. (2000). Anthraquinones and betaenone derivatives from the sponge-associated fungus *Microsphaeropsis* Species: Novel inhibitors of protein kinases. **J. Nat. Prod.** *63*, 739 – 745.
- Brauers, G.. (2003). Isolierung und Strukturaufklärung von neuen Naturstoffen aus schwamm-assoziierten Pilzen. **Dissertation**. Heinrich-Heine-Universität-Düsseldorf.

- Brewer, D., McInnes, A.G., Smith, D.G., Taylor, A., and Walter, J.A. (1978). The structure of chaetomin, a toxic metabolite of chaetomium cochliodes, by nitrogen-15 and carbon-13 nuclear resonance spectroscopy. **J. Chem. Soc, Perkin Trans 1**, 1248 -1251.
- Bringmann, G., Lang, G., Steffens, S., Gunther, E., and Schaumann, K. (2003). Evariquinone, isoemicellin, and stromemycin from a sponge derived strain of the fungus *Emericella varicolor*. **Phytochemistry** 63, 437 – 443.
- Butler, M.S. (2004). The role of natural products chemistry in drug discovery. **J. Nat. Prod.** 67, 2141 – 2153.
- Butler, M.S. (2005). Natural products to drugs : Natural products derived compounds in clinical trials. **Nat. Prod. Rep.** 22, 162 – 195.
- Calvo, A.M., Wilson, R.A., Bok, J.W., and Keller, N.P. (2002). Relationships between secondary metabolism and fungal development. **Microbiol. Mol. Biol. Rev.** 66 (3), 447 – 459.
- Chapman & Hall. (2004). **Dictionary of Natural Products**.
- Chexal, K.K., Holker, J.S.E., Simpson, T.J., and Young, K. (1975). The biosynthesis of fungal metabolites. Part V. Structure of variecoxanthenes A, B, and C, metabolites of *Aspergillus varicolor* ; Conversion of variecoxanthe A into (±)-De-C-prenylepishamixanthe. **J. Chem. Soc, Perkin Trans 1**, 543 – 548.
- Davies, H., Bignell, G.R., Cox, C., Stephens, P., Edkins, S., Clegg, S., Teague, J., Woffendin, H., Garnett, M.J., Bottomley, W., Davis, N., Dicks, E., Ewing, R., Floyd, Y., Gray, K., Hall, S., Hawes, R., Hughes, J., Kosmidou, V., Menzies, A., Mould, C., Parker, A., Stevens, C., Watt, S., Hooper, S., Wilson, R, Jayatilake, H., Gusterson, B.A, Cooper, C., Shipley, J., Hargrave, D., Pritchard-Jones, K., Maitland, N., Chenevix-Trench, G., Riggins, G.J, Bigner, D.D., Palmieri, G., Cossu, A., Flanagan, A., Nicholson, A., Ho, J.W.C., Leung, S.Y, Yuen, S.T., Weber, B.L., Seigler, H.F.,

- Darrow, T.L., Paterson, H., Marais, R., Marshall, C.J., Wooster, R., Stratton, M.R., and Futreal, P.A. (2002). Mutations of the *BRAF* gene in human cancer. **Nature** *417*, 949-954.
- DeBusk, L.M., Chen, Y., Nishishita, T., Chen, J., Thomas, J.W., and Lin, P.C. (2003). Tie2 receptor tyrosine kinase, a major mediator of tumor necrosis factor alpha-induced angiogenesis in rheumatoid arthritis. **Arthritis Rheum.** *48* (9), 2461 – 2471.
- Demain, A.L., and Elander, R.P. (1999). The β -lactam antibiotics : past, presence, and future. **Antonie van Leeuwenhoek** *75*, 5 – 19.
- Demain, A.L., and Fang, A. (2000). The natural functions of secondary metabolites. **Advances in Biochemical Engineering and Biotechnology** *69*, 1 – 39.
- Dehm, S., Senger M.A., and Bonham, K. (2001). *SRC* transcriptional activation in a subset of human colon cancer cell lines. **FEBS Letters** *487* (3), 367 – 371.
- Dunn, A.W., Johnstons, R.A.W., King, T.J., Lessinger, L., and Sklarz, B. (1979). Fungal metabolites. Part 7. Structure of C₂₅ compounds from *Aspergillus varicolor*. **J. Chem. Soc, Perkin Trans 1**, 2113 – 2117.
- Ebel, 1996, Secondary Metabolites From Marine-derived Fungi (in Press).
- van Elswijk, D.A., and Irth, H. (2003). Analytical tools for the detection and characterization of biologically active compounds from nature. **Phytochemistry Reviews I**, 427 – 439.
- Endo, A. (1979). Monacolin K, a new hypocholesterolemic agent produced by a *Monascus* species. **J. Antibiot** *32*, 852 – 854.
- Faulkner , D. J. (1998). Marine natural products. **Nat. Prod. Rep.** 113 - 120.

- Feher, M., Schmidt, J.M. (2003). Property distributions : Differences between drugs, natural products, and molecules from combinatorial chemistry. **J. Chem. Inf. Comput. Sci.** *43*, 218 – 227.
- Fenical, W. (1997). New pharmaceuticals from marine organisms. **Trens Biotechnol.** *15*, 339 – 341
- Fode, C., Motro, B., Yousefi, S., Heffernan, M., and Dennis, J. W. (1994). Sak, a murine protein-serine/threonine kinase that is related to the Drosophila polo kinase and involved in cell proliferation. **Proc. Natl. Acad. Sci.** *91 (14)*, 6388–6392.
- Franck, B., and Gehrken, H.P. (1980). Citreoviridine aus *Aspergillus terreus*. **Angew. Chem.** *92 (6)*, 484 – 486.
- Fuska, J., Fuskova, A., and Nemeč, P. (1979). Vermistatin, an antibiotic with cytotoxic effects, produced from *Penicillium vermiculatum*. **Biologia** *34*, 735 – 739.
- Fuska, J., Uhrin, D., Proska, B., Votický, Z., and Ruppeltdt, J. (1986). The structure of vermistatin a new metabolite from *Penicillium vermiculatum*. **J. Antibiot** *39*, 1605 – 1608.
- Garces, C.A., Kurenova, E.V., Golubovska, V.M., and Cance, W.G. (2006). Vascular endothelial growth factor receptor-3 and focal adhesion kinase bind and suppress apoptosis in breast cancer cells. **Cancer Research** *66*, 1446-1454.
- Ge, J., Ping, W., and Zhou, D. (2004). Characterization of a new species of taxol-producing fungus. **Nature and Sciences** *2 (1)* , 85 – 88.
- Gloer, J.B., TePaske, M.R., and Sima, S.J. (1988). Antiinsectan aflavinine derivatives from the sclerotia of *Aspergillus flavus*. **J. Org. Chem.** *53*, 5457 – 5460.
- Grove, J.F., MacMilan, J., Mulholland, T.P.C., and Rogers, M..A.T. (1952). Griseofulvin Part I. **J. Chem. Soc.** 3949 - 3958

- Guo, B. Dai, J., Ng S., Huang, Y., Leong, C., Ong, W., and Carte, B.K. (2000). Cytonic acids A and B: Novel tridepside inhibitors of hCMV protease from the endophytic fungus *Cytospora* species. **J. Nat. Prod.** 63, 602-604.
- Harvey, A. (1993). An introduction to drugs from natural products, in *Drugs from natural products, Pharmaceutical and agricultural*. Ellis Horwood.
- Harvey, A. (2000). Strategies for discovering drugs from previously unexplored natural products. **Drug Discovery Today** 5 (7), 294 – 300.
- Hickman. (1965). Fungal structure and organization, in : *The Fungi, an advance treatise*. Ainsworth and Sussman (eds.) Vol. I, 21 – 23, Academic Press, New York.
- Hiort, J., Maksimenka, K., Reichert, M., Perovic-Ottstadt, S., Lin, W.H., Wray, V., Steube, K., Schaumann, K., Weber, H., Proksch, P., Ebel, R., Müller, W.E.G., and Bringmann, G. (2004). New natural products from the sponge-derived fungus *Aspergillus niger*. **J. Nat. Prod.** 67, 1532 – 1543.
- Hofer, M.D., Fecko, A., Shen, R., Setlur, S.R., Pienta, K.G., Tomlins, S.A., Chinnaiya, A.M., and Rubin, M.A. (2004). Expression of the platelet-derived growth factor receptor in prostate cancer and treatment implications with tyrosine kinase inhibitors. **Neoplasia** 6 (5), 503 – 512.
- de Hoog, G.S., Guarro, J., Gene', Y., and Figuerres, M.J. (2000). **Atlas of Clinical Fungi**. 2nd edition, 14 – 18. CBS/Universitat Rovira i Virgile.
- Horn, W.S., Simmonds, M.S.J., Schwartz, R.E., and Blaney, W.M. (1995). Phomopsichalasin, a novel antimicrobial agent from an Endophytic Phomopsis Sp. **Tetrahedron** 51 (14), 3969 – 3978.
- Hu, L., and Liu, J-K. (2003). p-Terphenyls from Basidiomycete *Thelephora aurantiotincta*. **Z. Naturforsch.** 58c, 452 – 454.

- Hu, Y., Li, C., Kulkarni, B.A., Strobel, G., Lobkovsky, E., Torczynsky, R.M., and Porco, J.A.Jr. (2001). Exploring chemical diversity of epoxyquinoid natural products : Synthesis and biological activity of (-)-Jesterone and related molecules. **Org. Lett.** 3 (11), 1649-1652.
- Isaka, M., Jaturapat, A., Rukseree, K., Danwisetkanjana, K., Tanticharoen, M., and Thebtaranonth, Y. (2001). Phomoxanthonones A and B, novel xanthone dimers from the endophytic fungus *Phomopsis* species. **J. Nat. Prod.** 64, 1015-1018.
- Iseki, H., Ko, T.C., Xue, X.Y., Seapan, A., and Townsend, C.M.Jr. (1998). A novel strategy for inhibiting growth of human pancreatic cancer cells by blocking cyclin-dependent kinase activity. **J. Gastrointest. Surg.** 2 (1), 36-43.
- Izeradjene, K., Douglas, L., Delaney, A., and Houghton, J.A. (2004). Influence of casein kinase II in tumor necrosis factor-related apoptosis-inducing ligand-induced apoptosis in human rhabdomyosarcoma cells. **Clinical Cancer Research** 10, 6650-6660.
- Jadulco, R., Proksch, P., Wray, V., Sudarsono, Berg, A., and Gräfe, U. (2001). New macrolides and furan carboxylic acid derivative from the sponge-derived fungus *Cladosporium herbarum*. **J. Nat. Prod.** 64, 527 – 530.
- Jadulco, R., Brauers, B., Edrada, R.A., Ebel, R., Wray, V., Sudarsono and Proksch, P. (2002). New metabolites from sponge-derived fungi *Curvularia lunata* and *Cladosporium herbarum*. **J. Nat. Prod.** 65, 730 – 733.
- Jensen P.R., and Fenical . W. (2000). In *Drugs from the Sea*. Fusetani, N. (Eds.) , 6 – 29, Basel.
- Kalli, K.R., Falowo, O.I., Bale, L.K., Zschunke, M.A., Roche, P.C., and Conover, C.A. (2002). Functional insulin receptors on human epithelial ovarian carcinoma cells: implications for IGF-II mitogenic signalling. **Endocrinology** 143 (9), 3259 – 3267.

- Kashino, H., Yoshihara, T., Okuno, M., Sakamura, S., Tajimi, A., and Shimanuki, T. (1992). Gamahonolides A, B, and gamahorin, novel antifungal compounds from stromata of *Epichloe typhina* on *Phleum pratense*. **Biosci. Biotech. Biochem.** **56** (7), 1096 – 1099.
- Kawai, K., Nozawa, K., Nakajima, S., and Litaka, Y. (1984). Studies on fungal products. VII. The structure of meleagrine and 9-O-p-bromobenzoylmeleagrins. **Chem. Pharm. Bull.** **32**, 94 – 98.
- Keen, N., and Taylor, S. (2004). Aurora-kinase inhibitors as anticancer agents. **Nature Rev. Cancers** **4**, 927 – 936.
- Kida, T., Shibai, H., and Seto, T. (1986). Structure of new antibiotics, pereniporins A and B, from a Basidiomycete. **J. Antibiot.** **39**, 613 – 615.
- Kim, K.W., Sugawara, F., Yoshida, S., Murofushi, N., Takashi, N., and Curtis, R.W. (1993). Structure of malformin A, a phytotoxic metabolite produced by *Aspergillus niger*. **Biosci. Biotechnol. Biochem.** **57** (2), 240-243.
- Kobayashi, M., Uehara, A., Matsunami, K., Aoki, S., and Kitagawa, I. (1993). Trichoharzin, a new polyketide produced by the imperfect fungus *Trichoderma harzianum* separated from the marine sponge *Micale cecilia*. **Tetrahedron Lett.** **34**, 7925 – 7928.
- Kusakai, G., Suzuki, A., Ogura, T., Miyamoto, S., Ochiai, A., Kaminishi, M., and Esumi, H. (2004). ARK5 expression in colorectal cancer and its implications for tumor progression. **Am. J. Pathol.** **164**, 987-995.
- Kubanek, J., Graziani, E.I., and Andersen, R.J. (1997). Investigations of terpenoid biosynthesis by the dorid nudibranch *Cadlina luteomarginata*. **J. Org. Chem.** **62**, 7239 - 7246

- Larsen, T.O., Smedsgaard, J., Nielsen, K.F., Hensen, M.E., and Frisvard, J.C.(2005). Phenotypic taxonomy and metabolite profiling in microbial drug discovery. **Nat. Prod. Rep.** 22, 672 – 695.
- Lee, J.W., Soung, Y.H., Seo, S.H., Kim, S.Y., Park, C.H., Wang, Y.P., Park, K., Nam, S.W., Park, W.S., Kim, S.H., Lee, J.Y., Yoo, N.J., and Lee, S.H. **2006**. Somatic mutations of *ERBB2* kinase domain in gastric, colorectal, and breast carcinomas, **Clinical Cancer Research** 12, 57-61.
- Lee, J.W., Soung, Y.H., Kim, S.Y., Park, W.S., Nam, S.W., Kim, S.H., Lee, J.Y., Yoo, N.J., and Lee, S.H. (2005). ERBB2 kinase domain mutation in a gastric cancer metastasis. **APMIS** 113, 683–687.
- Lee, J.C., Strobel, G.A., Labkovsky, E., and Clardy, J. (1996) . Torreyanic acid : A selectively cytotoxic quinone dimer from endophytic fungus *pestalotiopsis microspora*. **J. Org. Chem** 61, 3232-3233
- Levine, S.G., and Hicks, R.E. (1971). Conformation of griseovulfin application. Application of NMR shift reagent. **Tetrahedron Lett.** 4, 311 - 314.
- Li, J. Y., Sidhu, R. S., Ford, E., Hess, W. M., and Strobel, G. A. (1998). The induction of taxol production in the endophytic fungus – *Periconia* Sp. from *Torreya grandifolia*. **J. Ind. Microbiol.** 20, 259–264.
- Li, J.Y., Harper, J.K., Grant, D.M., Tombe, B.O., Basyhal, B., Hess, W.M., and Strobel, G.A. (2001). Ambuic acid, a highly functionalized cyclohexane with antifungal activity from *Pestalotopsis* Sp. **Phytochemistry** 56, 463-468.
- Li, J, Kleeff, J., Guo, J., Fischer, L., Giese, N., Büchler, M.W, and Friess, H. (2003). Effects of STI571 (gleevec) on pancreatic cancer cell growth. **Mol. Cancer** 2 (32). Open access at <http://www.molecular-cancer.com/content/2/1/32>.

- Li, D., Zhu, J., Firozi, P., Abbruzzese, J.L., Evans, D.B., Cleary, K., Fries, H., and Sen, S. (2003a). Overexpression of oncogenic STK15/BTAK/Aurora A kinase in human pancreatic cancer. **Clinical Cancer Research** 9, 991-997.
- Long, L.M., and Troutman, H.D. (1949). Chloramphenicol (chloromycetin) VII. Synthesis through p-nitroacetophenol. **J. Am. Chem. Soc.** 71, 2473 – 2475.
- Macmillan, J.C, Hudson J.W., Bull, S., Dennis, J.W., and Swallow, C.J. (2001). Comparative expression of the mitotic regulators *SAK* and *PLK* in colorectal cancer. **Annals of Surgical Oncology** 8, 729-740 .
- Maes, C.M., Potgieter, M., and Steyn, P.S. (1986). NMR assignment, conformation, and absolute configuration of ditryptophenalin an model dioxopiperazines. **J. Chem. Soc., Perkin Trans. 1**, 861 – 866.
- Malmstrom, J., Christophersen, A., and Frisvad, J.C. (2000). Secondary Metabolites Characteristic of *Penicillium citrinum*, *Penicillium stecki* and related species, **Phytochemistry** 54, 301 – 309.
- Malmstrom, J., Christophersen, A., Barrero, F., Oltra, J.E., Justicia, J., and Rosales, A. (2002). Bioactive metabolites from a marine-derived strain of the fungus *Emericella varicolor*. **J. Nat. Prod.** 65, 364
- Matsunaga, K., Shizuri, Y., Yamamura, S., Kawai, K., and Furukawa, H. (1991). Isolation and structure of citreoindole, a new Metabolite of Hybrid Strain KO 0052 Derived from *Penicillium Citreo-viride* B. IFO 6200 and 4692. **Tetrahedron Letter**, 32 (47), 6883 – 6884.
- McInnes, A.G., Taylor, A., and Walter, J.A. (1976). The Structure of Chaetomin, **J. Am. Chem. Soc.** 98 (21), 6741
- McIntyre, C.R., and Simpson, T.J. (1981). Biosynthesis of terretonin, a polyketide terpenoid of *Aspergillus terreus*. **J. Chem. Soc., Chem. Comm**, 1043 – 1044.

- McIntyre, C.R., Simpson, T.J., Moore, R.N., Trimble, L.A., and Vederas, C. (1984). Biosynthesis of the meroterpenoid metabolite, andibenin B : Incorporation of sodium [1-¹³C, ¹⁸O₂]acetate and ¹⁸O₂, **J. Chem. Soc, Chem. Comm.** 1498 – 1499.
- McLean, G.W., Carragher, N.O., Avizienyte, E., Evans, J., Brunton, V.G., and Frame, C.M. (2005). The Role of focal adhesion kinase in cancer. A new therapeutic opportunity. **Nat. Rev. Cancer** 5 (7), 505 – 515.
- de Menezes, D.E.L., Peng, J., Garrett, E.N., Louie, S.G., Lee, S.H., Wiesmann, M., Tang, Y., Shephard, L., Goldbeck, C., Oei, Y., Ye, H., Aukerman, S.L., and Heise, C. (2005). CHIR-258: A potent inhibitor of FLT3 kinase in experimental tumor xenograft models of human acute myelogenous leukemia. **Clinical Cancer Research** 11, 5281-5291.
- National Cancer Institute. (22 November 2005). Mutations in glioblastoma in multiforme predict responded to target therapies. **NCI Cancer Bulletin** (online), 2 (45).
- Newman, D.J., Cragg, G.M., and Snader, K.M. (2000). The influence of natural products upon Drug discovery. **Nat. Prod. Rep.** 17, 215 – 234
- Newton, G.G.F., and Abraham, E.P. (1955). Cephalosporin C, a new antibiotic containing sulphur and D-a-aminoadipic acid. **Nature** 175, 548.
- Nishiyama, S., Shizuri, Y., Imai, D., and Yamamura, S. (1985). Structural and conformational studies on citreoviridinol and isocitreoviridinol : Syntheses of some 2,6-dioxabicyclo[3.2.1.]octanes. **Tetrahedron Lett.** 26 (27), 3243 – 3246.
- Nishiyama, S., Toshima, H., and Yamamura, S. (1986). Total syntheses of citreoviridinol and neocitreoviridinol. **Chem. Lett.** 1973 – 1976.

- Noren, N.K., Lu, M., Freeman, A.L., Koolpe, M., and Pasquale, E.B. (2004). Interplay between EphB4 on tumor cells and vascular ephrin B-2 regulates tumor growth. **Proc. Natl. Acad. Sci.** *101* (15), 5583 – 5588.
- Nozawa, K., and Nakajima, S. (1979). Isolation of radicicol from *Penicillium luteoaurantium*, and meleagrins, a new metabolite from *Penicillium meleagrinum*. **J. Nat. Prod.** *42*, 374 – 377.
- Nozawa, K., Sekita, S., Harada, M., Udagawa, S., and Kawai, K. (1989). Isolation and structures of two new indoloditerpenes related to aflavinine from a microsclerotium producing strain of *Aspergillus niger*. **Chem. Pharm. Bull.** *37* (3), 626 – 630.
- Numata, A., Amagata, T., Minoura, K., and Ito, T. (1997). Gymnastatins, novel cytotoxic metabolites produced by a fungal strain from a sponge. **Tetrahedron Lett.** *38* (32), 5675 -5678
- Okuyama, E., and Yamazaki, M., (1983). Paraherquonin, A new meroterpenoid from *Penicillium Paraherquei*. **Tetrahedron Lett.**, *24* (30), 3113 – 3114.
- Ouyang, B., Knauf, J.A., Smith, E.P., Zhang, L., Ramsey, T., Yusuff, N., Batt, D., and Fagin, J.A. (2006). Inhibitors of Raf kinase activity block growth of thyroid cancer cells with *RET/PTC* or *BRAF* mutations *In vitro* and *In vivo*. **Clinical Cancer Research** *12*, 1785-1793.
- Patwardhan, B., Vaidya, A.D.B., and Chorghade, M., (2004), Ayurveda and natural products drug discovery. **Current Science** *86* (6), 789 – 799.
- Pisano, M.A., Sommer, M.J., Brancaccio, L. (1989). Isolation of bioactive actinomycetes from marine sediments using rifampicin. **Appl. Microbiol. Biotechnol.** *31*, 609 – 612.
- Pochert, J.P., and Behuke, J. (1993). **Aldrich Library of 13C and 1H FT NMR Spectra**, *3*, 570B.

- Proksch, P., Edrada-Ebel, R.A., and Ebel, R. (2003). Drugs from the sea - Opportunities and Obstacles. **Marine Drugs** **1**, 5 – 17
- Pulici, M., Sugawara, F., Koshino, H., Uzawa, J., and Yoshida, S. (1996). A new isodrimeninol from *Pestalotiopsis* sp. **J. Nat. Prod.** **59**, 47 – 48
- Qiao, H., Hung, W., Tremblay, E., Wojcik, J., Gui, J., Ho, J., Klassen, J., Campling, B., and Elliot, B. (2002). Constitutive activation of met kinase in non-small-cell lung carcinomas correlates with anchorage-independent cell survival. **J. Cell Biochem.** **86** (4), 665-677.
- Kusakai, G., Suzuki, A., Ogura, T., Miyamoto, S., Ochiai, A, Kaminishi. M., and Esumi, H. (2004). ARK5 expression in colorectal cancer and its implications for tumor progression. **American Journal of Pathology** **164**, 987-995.
- Rabhaek, L., Christophersen, C., Frisvad, J., Benggaard, H.S., Larsen, S., and Rassing, B.R. (1997), Insulicolide A : A new nitrobenzoyloxy-substituted sesquiterpene from the marine fungus *Aspergillus insulicola*, **J. Nat. Prod.** **60**, 811 – 813.
- Reinhart, K., Gloer, J., Cook, J., Carter, Jr., Mizesak, S., and Scahilt, T. (1987). Structures of the didemnins, antiviral and cytotoxic depsipeptides from a caribbean tunicate, **J. Am. Chem. Soc.**, **103**, 1857 -1859.
- Rydén, L., Jirström, K., Bendahl, P.O., Fernö, M., Nordenskjöld, B., Stål, O., Thorstenson, S., Jönsson, P.E., and Landberg, G. (2005). Tumor-specific expression of vascular endothelial growth factor receptor 2 but not vascular endothelial growth factor or human epidermal growth factor receptor 2 is associated with impaired response to adjuvant tamoxifen in premenopausal breast cancer. **J. Clin. Oncol.** **23** (31), 4695 – 4704

- Safe, S., and Taylor, A. (1972). Sporidermis. Part XIII. Ovine III-thrift in Nova Scotia Part III. The characterisation of chetomin, a toxic metabolite of *Chaetomium cochliodes* and *Chaetomium globosum*. **J. Chem. Soc, Perkin Trans 1**, 472 – 479.
- Samson, R.A., Hoekstra, E.S., Frisvad, J.C., and Litenborg, O., (Eds.). (1995). **Introduction to Food-borne Fungi**. Centralbureau voor Schimmelcultures, Baarn.
- Santos, R.M.G., and Rodrigues-Fo, E. (2002). Meroterpenes from *Penicillium* sp Found in Association with *Melia azedarach*. **Phytochemistry 61**, 907 – 912.
- Santos, R.M.G., and Rodrigues-Filho, E. (2003). Structures of meroterpenes produced by *Penicillium* sp., an endophytic fungus found associated with *Melia azedarach*. **J. Braz. Chem. Soc. 14 (5)**, 722 – 727
- Santos, R.M.G., and Rodrigues-Fo, E., (2003A). Further meroterpenes produced by *Penicillium* sp., an endophytic fungus found associated with *Melia azedarach*, **Z. Naturforsch. 58c**, 663 - 669
- Sattler, M., Pride, Y.B., Ma, P., Gramlich, J.L., Chu, S.C., Quinnan, L.A., Shirazian, S., Liang, C., Podar, K., Christensen, J.G., and Salgia, R. (2003). A Novel small molecule Met inhibitor induces apoptosis in cells transformed by the oncogenic TPR-MET tyrosine kinase, **Cancer Research 63**, 5462 – 5469.
- Schmitz, K.J., Grabellus, F., Callies, R., Otterbach, F., Wohlschlaeger, J., Levkau, B., Kimmig, R., Schmid, K.W., and Baba, H.A. (2005). High expression of focal adhesion kinase (p125^{FAK}) in node-negative breast cancer is related to overexpression of HER-2/neu and activated Akt kinase but does not predict outcome. **Breast Cancer Res. 7**, R194 - R203.
- Shiomi, K., Tomoda, H., Otogura, K., and Omura, S (1999).Meroterpenoids with Various Biological Activities Produced by Fungi. **Pure Appl. Chem. 71 (6)**, 1059 – 1064.

- Simpson, T.J. (1979). Part I. The Structures of andibenins-A and -C, and andilesins-A, -B, and -C. Meroterpenoids from *Aspergillus varicolor*. **J. Chem. Soc, Perkins Trans** **1**, 2118 – 2121.
- Simpson, T.J and Wilkinshaw M.D. (1981). Anditomin, a new C₂₅ metabolite from *Aspergillus varicolor*. **J. Chem. Soc, Chem. Com.** 914 – 915.
- Simpson, T.J., and Stenzel, D.J. (1983.) Biosynthesis of Austin, a Polyketide-Terpenoid of *Aspergillus ustus*. **J. Chem. Soc., Chem., Comm.** 1042 – 1043.
- Simpson, T.J. (1987). Application of multinuclear NMR to structural and biosynthetic studies of polyketide microbial metabolites. **Chem. Soc. Rev.** *16*, 123 -160.
- Sings, H.L., and Rinehart, K.L. (1996). Compounds produced from potential tunicate-blue-green algal symbiosis, **J. Ind. Microbiol. Biotechnol** *7*, 385 – 396
- Sourvinos, G., Tsatsanis, C., and Spandidos, D.A. (1999). Overexpression of the *Tpl-2/Cot* oncogene in human breast cancer. **Oncogene** *18*, 4968-4973
- Springer, J.P., Buchi, G., Kobbe, B., Demain, A.L., and Clardy, J. (1977). The structure of ditryptophenalin, A new metabolite of *Aspergillus flavus*. **Tetrahedron Lett.** *28*, 2403 – 2406
- Staal, S.P. (1987). Molecular cloning of the akt oncogene and its human homologues AKT1 and AKT2: amplification of AKT1 in a primary human gastric adenocarcinoma, **Proc. Natl. Acad. Sci. U S A.** **84** (*14*), 5034–5037.
- Stephenson, S., Slomka, S., Douglas, E.L., Hewett, P.J., and Hardingham, J.E. (2001). Receptor protein tyrosine kinase EphB4 is up regulated in colon Cancer. **BMC Molecular Biology**, *2* (*15*), 1 – 9

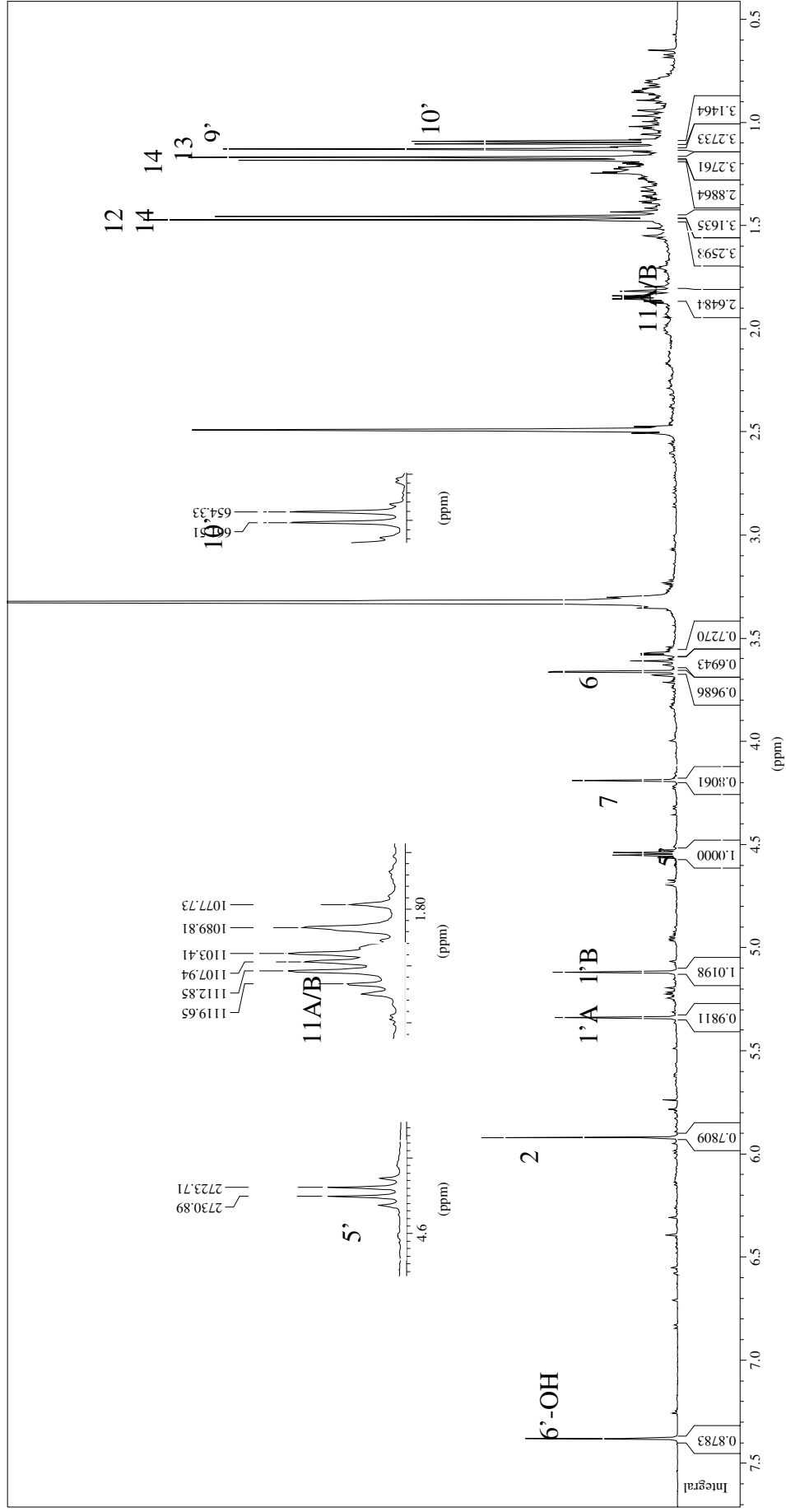
- Strobel, G.A.; Stierle, A.; Stierle, D., Hess, W.M. (1993). *Taxomyces andreanae* a proposed new taxon for a bulbiferous hypomycete associated with Pacific yew. **Mycotaxon** 47, 71–78.
- Strobel, G., Yang, X, Sears, J., Kramer, R., Sidhu, R. S., and Hess, W. M. (1996). Taxol from *Pestalotiopsis microspora*, an endophytic fungus of *Taxus wallichiana*. **Microbiology** 142, 435–440.
- Strobel, G. A., Ford, E., Li, J. Y., Sears, J., Sidhu, R. S., and Hess, W. M. (1999). *Seimatoantlerium tepuiense* gen. nov., a unique epiphytic fungus producing taxol from the Venezuelan-Guayana. **System. Appl. Microbiol** 22, 426–433.
- Strobel, G.A. (2002). Rainforest Endophytes and Bioactive Products. **Crit. Rev. Biotechnol**, 22 (4), 315 – 333.
- Strobel, G., Daisy, B., Castillo, U., und Harper, J. (2004). Natural Products from Endophytic Microorganisms **J. Nat. Prod.**, 67, 257 – 268.
- Susva, M., Missbach, M., Green, J. (2000). Src inhibitors: drugs for the treatment of osteoporosis, cancer or both? **Trends in Pharmacological Sciences** 21 (12), 489-495.
- Sun, M., Wang, G., Paciga, J.E., Feldman, R.I., Yuan, Z.Q., Ma, X.L., Shelley, S.A., Jove, R., Tsihchlis, P.N., Nicosia, S.V., and Cheng, J.Q. (2001). AKT1/PKB alpha kinase is frequently elevated in human cancers and its constitutive activation is required for oncogenic transformation in NIH3T3 cells. **Am. J. Pathol.**, 159 (2), 431 – 437.
- Tan, R.X., and Zou, W.X. (2001). Endophytes : a rich source of functional metabolites, **Nat. Prod. Rep.** 18 (4), 448 – 459.
- TePaske, M.R., and Gloer, J.B. (1989). Three new aflavinines from the sclerotia of *Aspergillus tubingensis*. **Tetrahedron** 45 (16), 4961 – 4968.

- Traber, R., Hofmann, H., Kuhn, M., and von Wartburg A. (1982). Isolierung und strukturermittlung der neuen cyclosporin E,F,G,H, und I. **Helv. Chim. Acta** 65, 1655 – 1677.
- Traber, R., Hofmann, H., Loosli, H.R., Ponelle, M., and von Wartburg A. (1987). Neue cyclosporine aus *Tolypocladium inflatum*. Die cyclosporine K – Z. **Helv. Chim. Acta** 70, 13 – 36.
- Varoglu, M., Corbett, T.H., Valeriote, F.A., and Crews, P. (1997). Asperazine, a selective cytotoxic alkaloid from a sponge-derived culture of *Aspergillus niger*. **J.Org. Chem.** 62, 7078 -7079.
- Vinokurova; N.G., Baskunov, B.P., Zelenkova, N.F., and Arinbasarov, M.U. (2004). The Alkaloids of *Penicillium aurantiogriseum* Dierckx (1901) var. *aurantiogriseum* VKM F-1298. **Microbiology** 73 (4), 414 – 419.
- Wall, E.M., Wani, M.C., Cook, C.E., Palmer, K.H., McPhail, A.T., and Sim, G.A. (1966). Plant antitumor agents I. The isolation and structure of camptothecin, a novel alkaloidal leukemia and tumor inhibitor from *Camptotheca acuminata*. **J. Am. Chem. Soc.** 88, 3888 – 3890.
- Wani, M.C., Taylor, H.L., Aall, M.E., Goggon, P., and McPhail, A.T. (1971). Plant antitumor agents VI. The isolation and structure of taxol, a novel antileukemic and antitumor. **J. Am. Chem. Soc.** 93, 2325 – 2327.
- Warner, S.L, Bearss, D.J., Han, H., and Von Hoff, D.D. (2003). Targeting Aurora-2 kinase in cancer. **Molecular Cancer Therapeutics** 2, 589-595.
- Weichert, W., Schmidt, M., Gekeler, V., Denkert, C., Stephan, C., Jung, K., Loening, S., Dietel, M., and Kristiansen, G. (2004). Polo-like kinase 1 is overexpressed in prostate cancer and linked to higher tumor grades. **Prostate** 60 (3), 240 – 245.

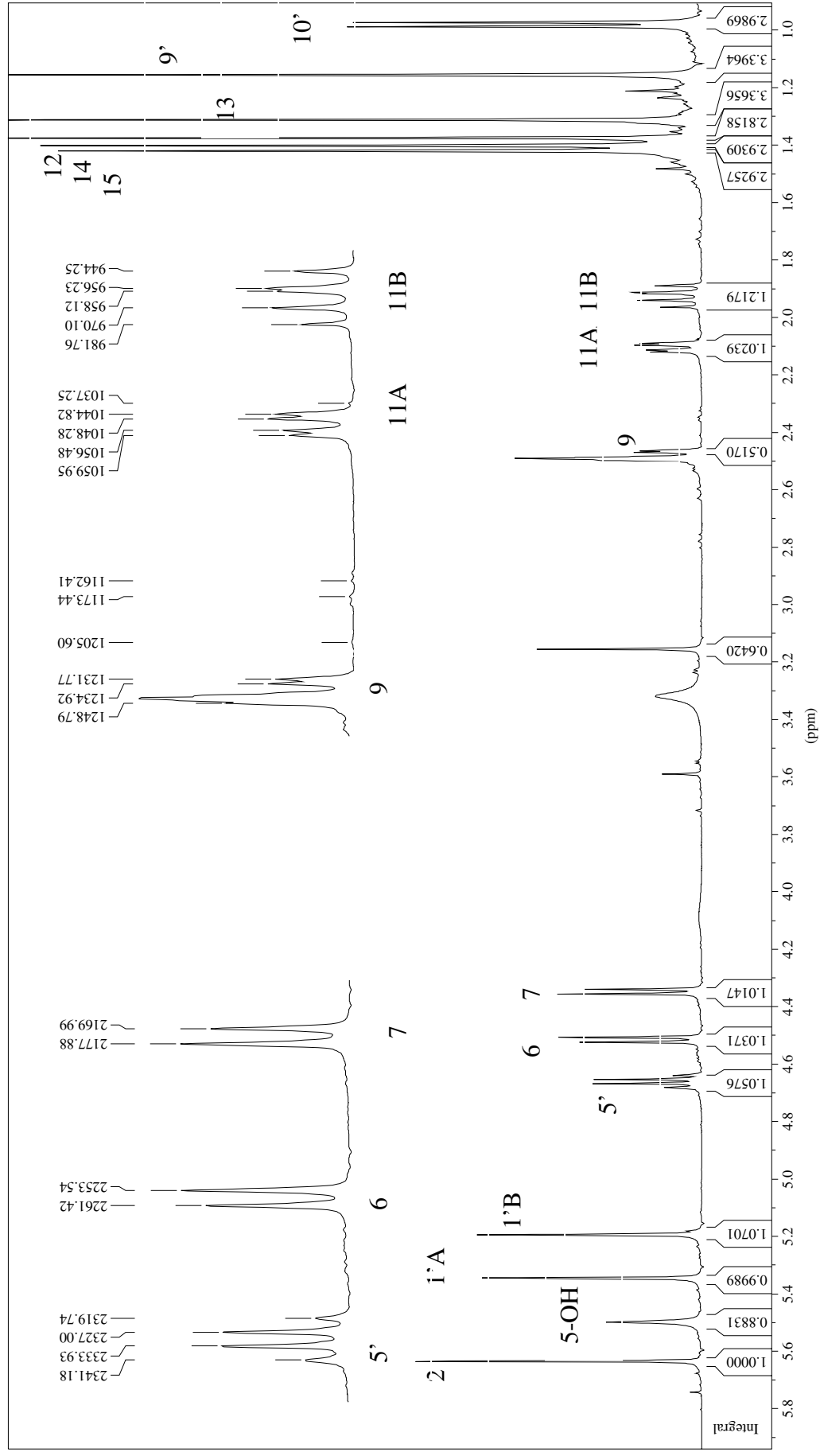
- Xia, G., Kumar, S.R., Masood, R., Zu, S., Reddy, R., Krasnaperov, V., Quinn, D.I., Henshal, S.M., Sutherland, R.L., Pinski, J.K., Daneshmand, S., Buscarini, M., Stein, J.P., Zong, C., Broek, D., Roy-Burman, P., and Gill, P.S. (2005). EphB4 expression and Biological Significance in Prostate. **Cancer Res.** 65 (11), 4623 – 4632.
- Young, P.E., Madison, V., and Blout, E.R. (1976). Cyclic peptide 15. Lanthamide-assisted ¹³C NMR and ¹H NMR analysis of preferred side chain rotamers in proline-containing cyclic dipeptides. **J .Am.Chem. Soc.** 98 (17), 5365 – 5370.
- Yu, Q., Sicinska, E., Geng, Y., Ahnstrom, M, Zagozdou, A., Kong, Y., Gardner, H., Kiyokawa, H., Harris, L.N., Stal, O., and Sicinski, P. (2006). Requirement for CDK4 kinase function in breast cancer. **Cancer cell** 9 (1), 23-32.
- Zhang, X., and Yee, D. (2000). Tyrosine kinase signalling in breast cancer: Insulin-like growth factors and their receptors in breast cancer. **Breast Cancer Res.** 2 (3), 170–175.

6 ATTACHMENTS

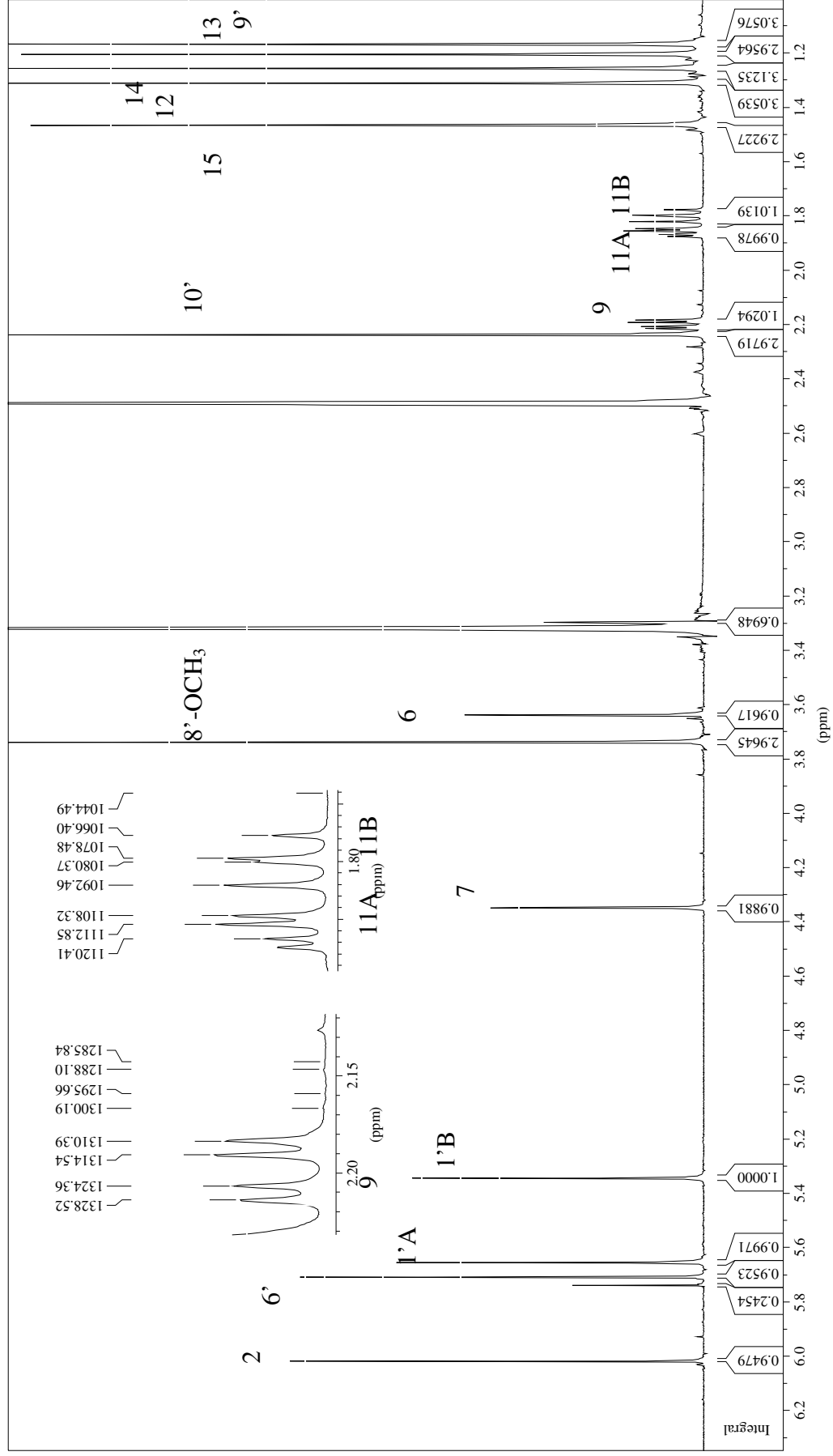
Attachment 1. The ^1H NMR spectrum of citreonigrin A



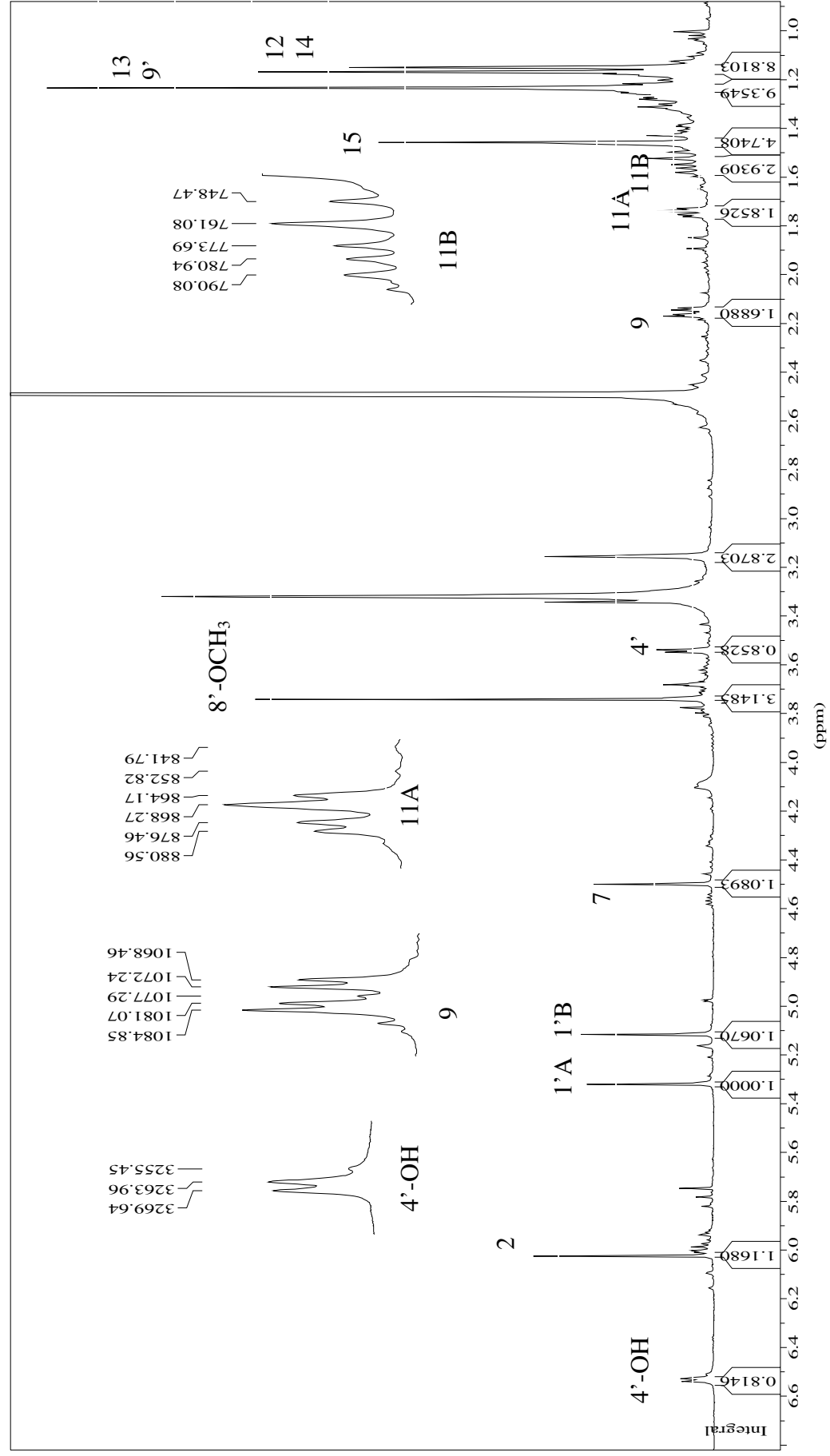
Attachment 2. The ^1H NMR spectrum of citreonigrin B



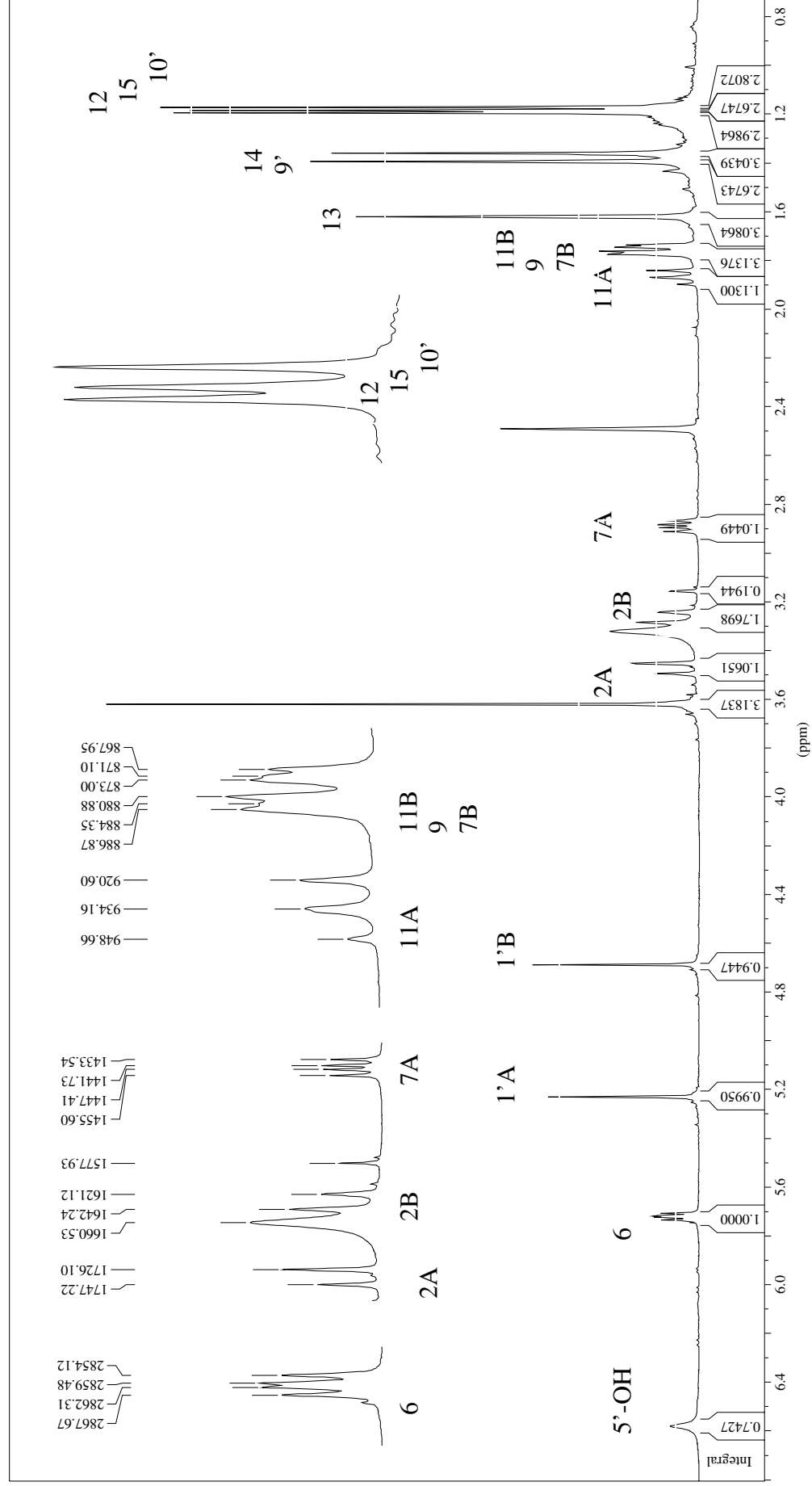
Attachment 3. The ^1H NMR spectrum of citreonigrin C.



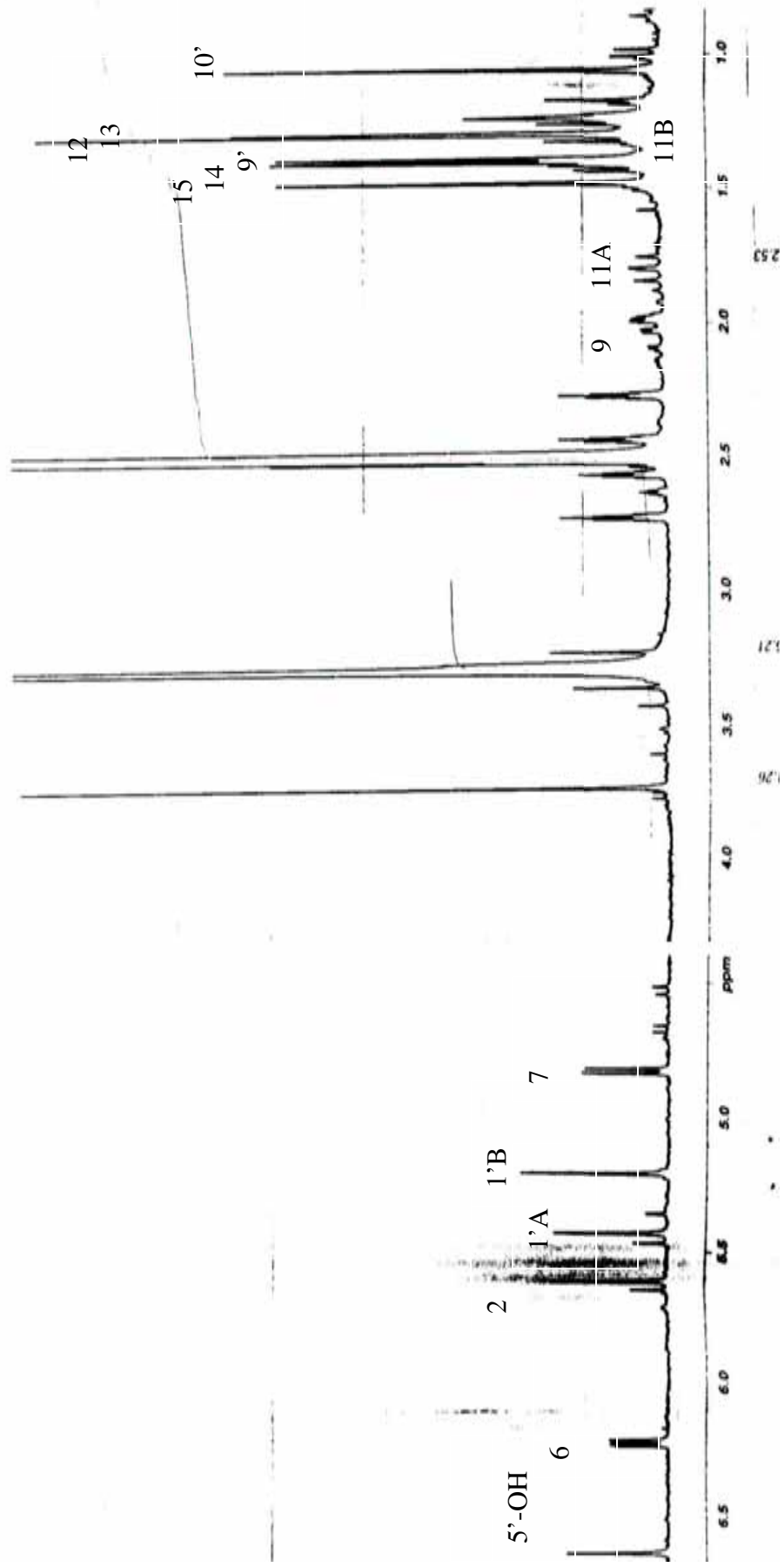
Attachment 4. The ^1H NMR spectrum of citreonigrin D



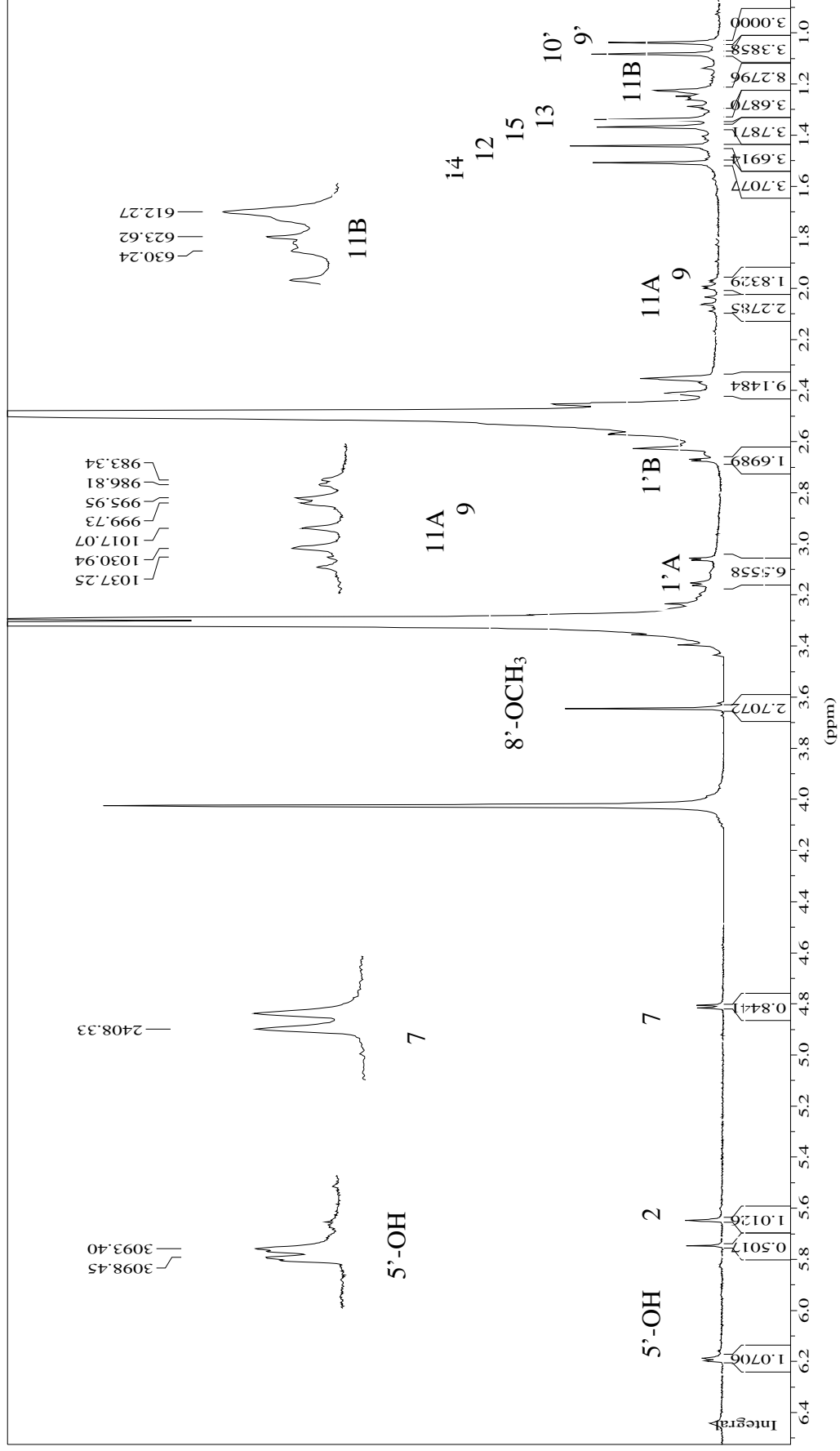
Attachment 5. The ^1H NMR spectrum of citreonigrin E



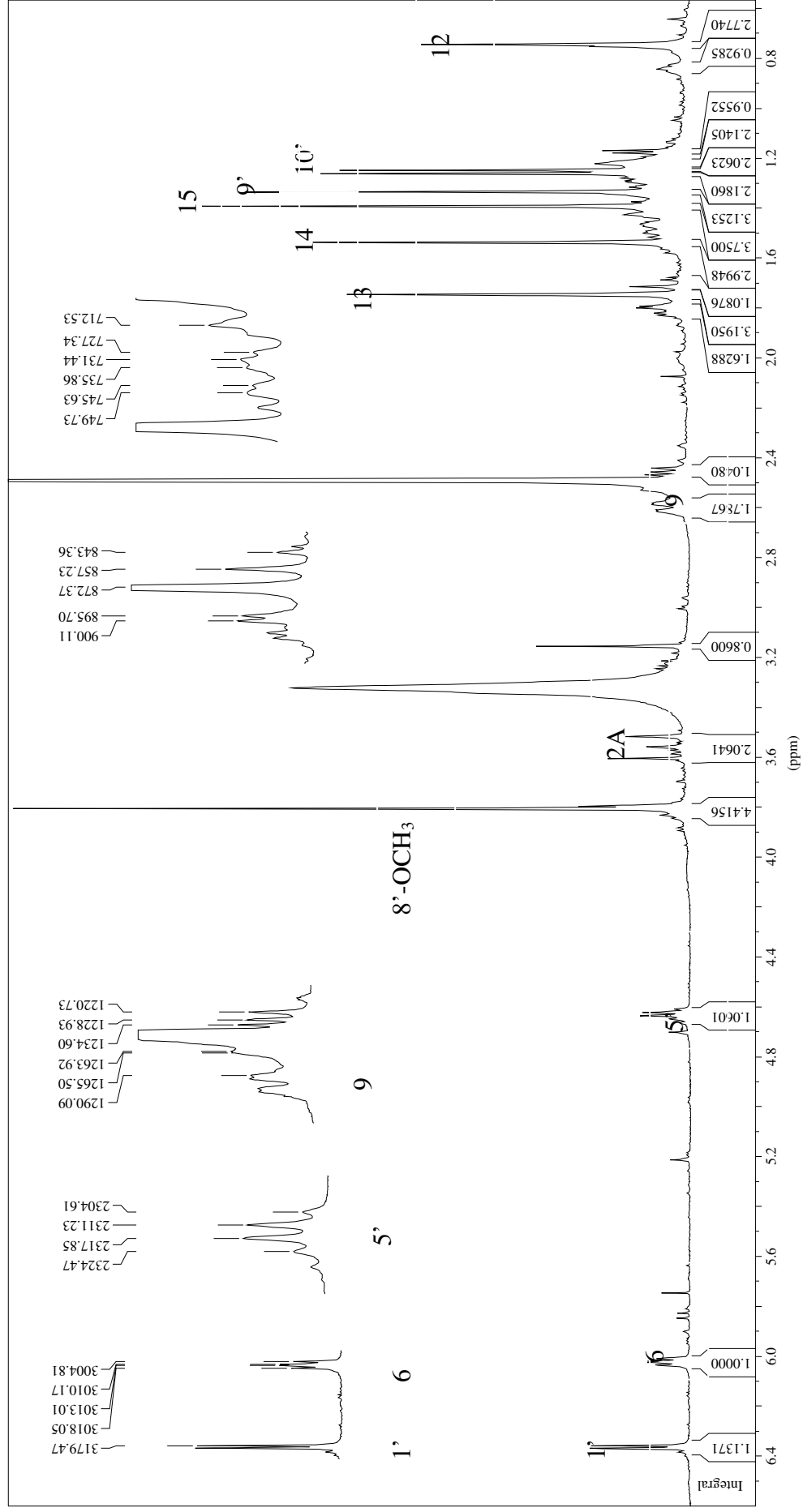
Attachment 6. The ^1H NMR spectrum of PC 3.3.6.8.4.F



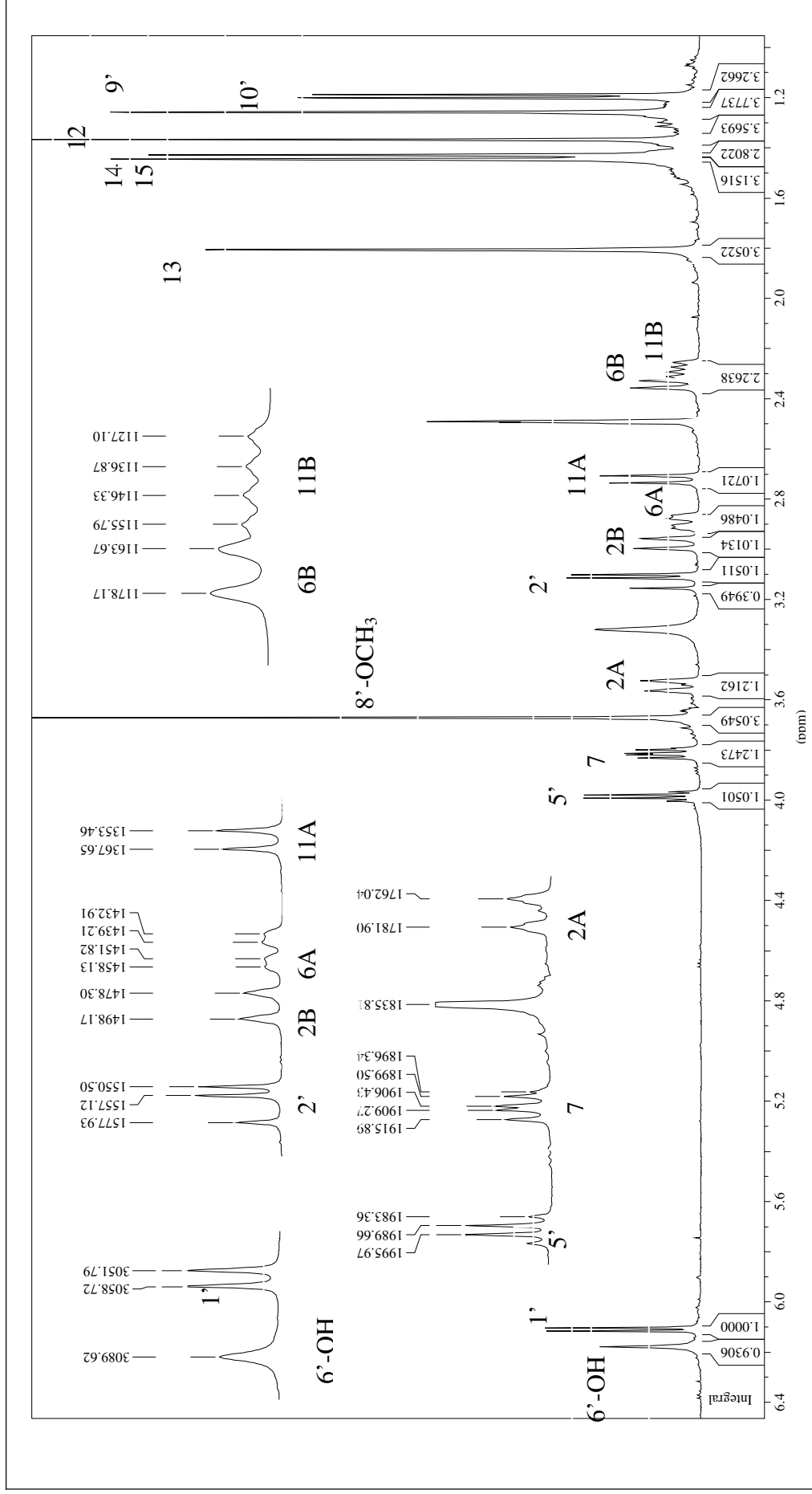
Attachment 7. The ^1H NMR spectrum of PC 3.3.6.8.4.A



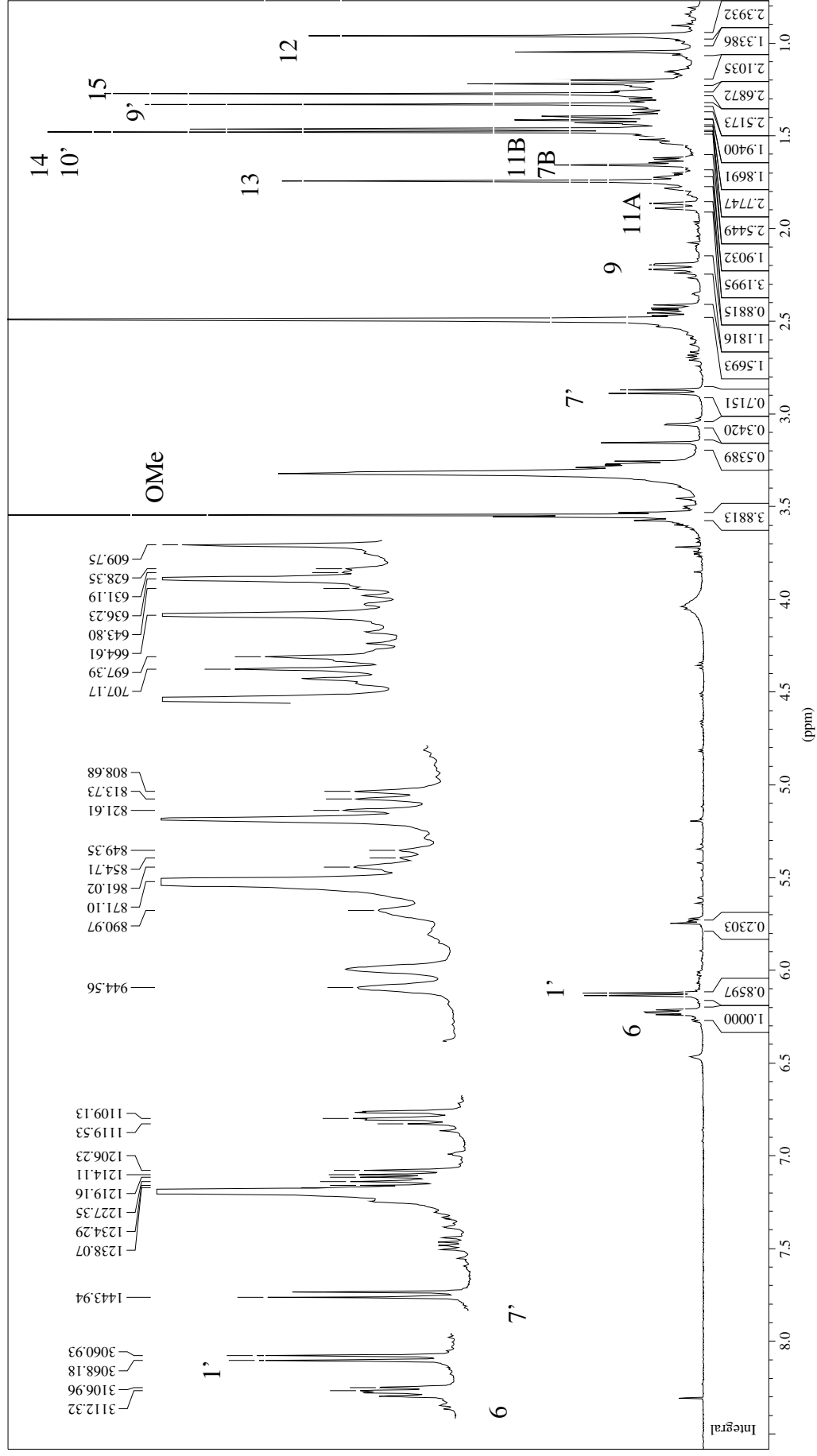
Attachment 8. The ^1H NMR spectrum of citreonigrin F



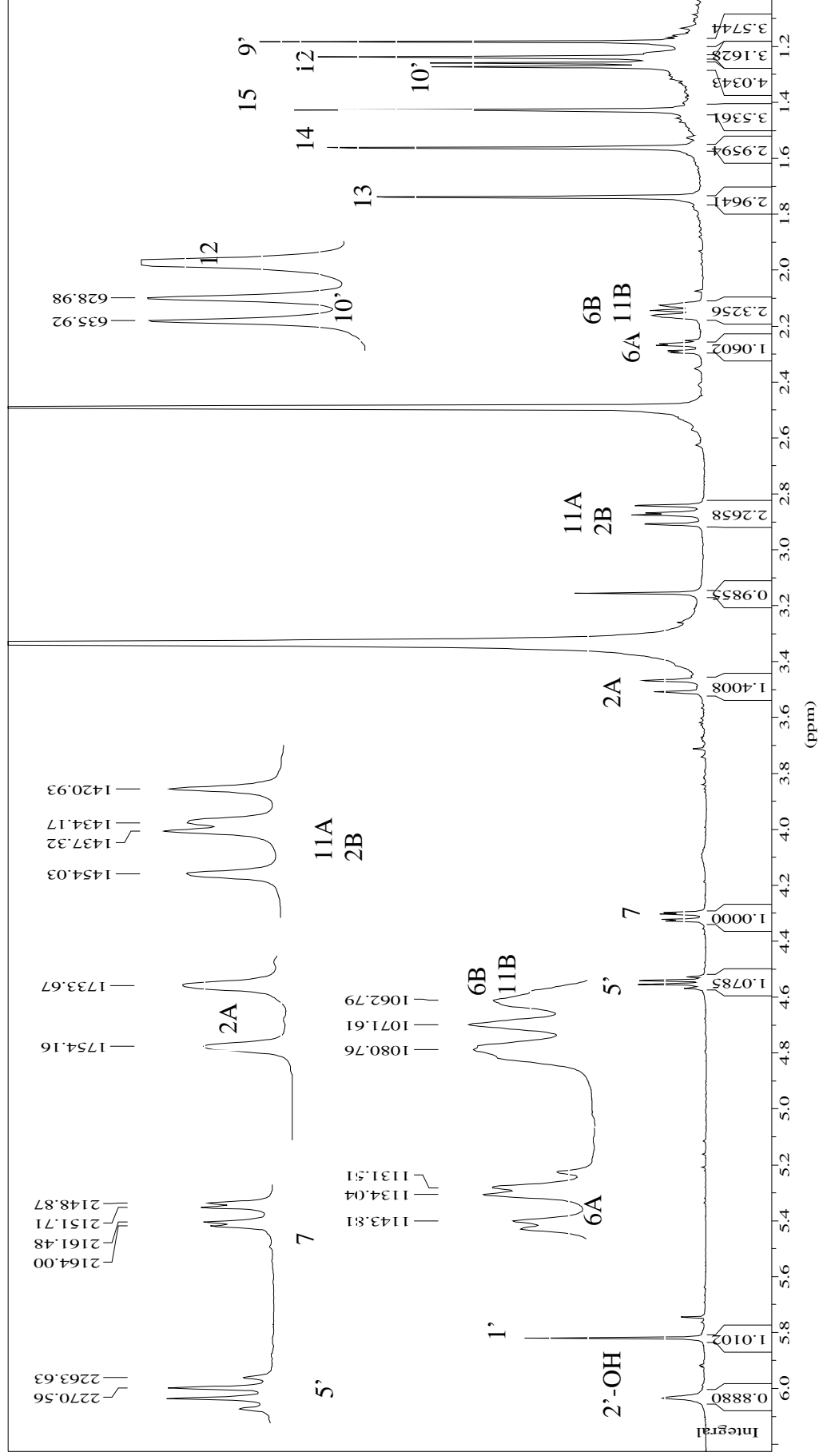
Attachment 9. The ^1H NMR spectrum of citreonigrin G



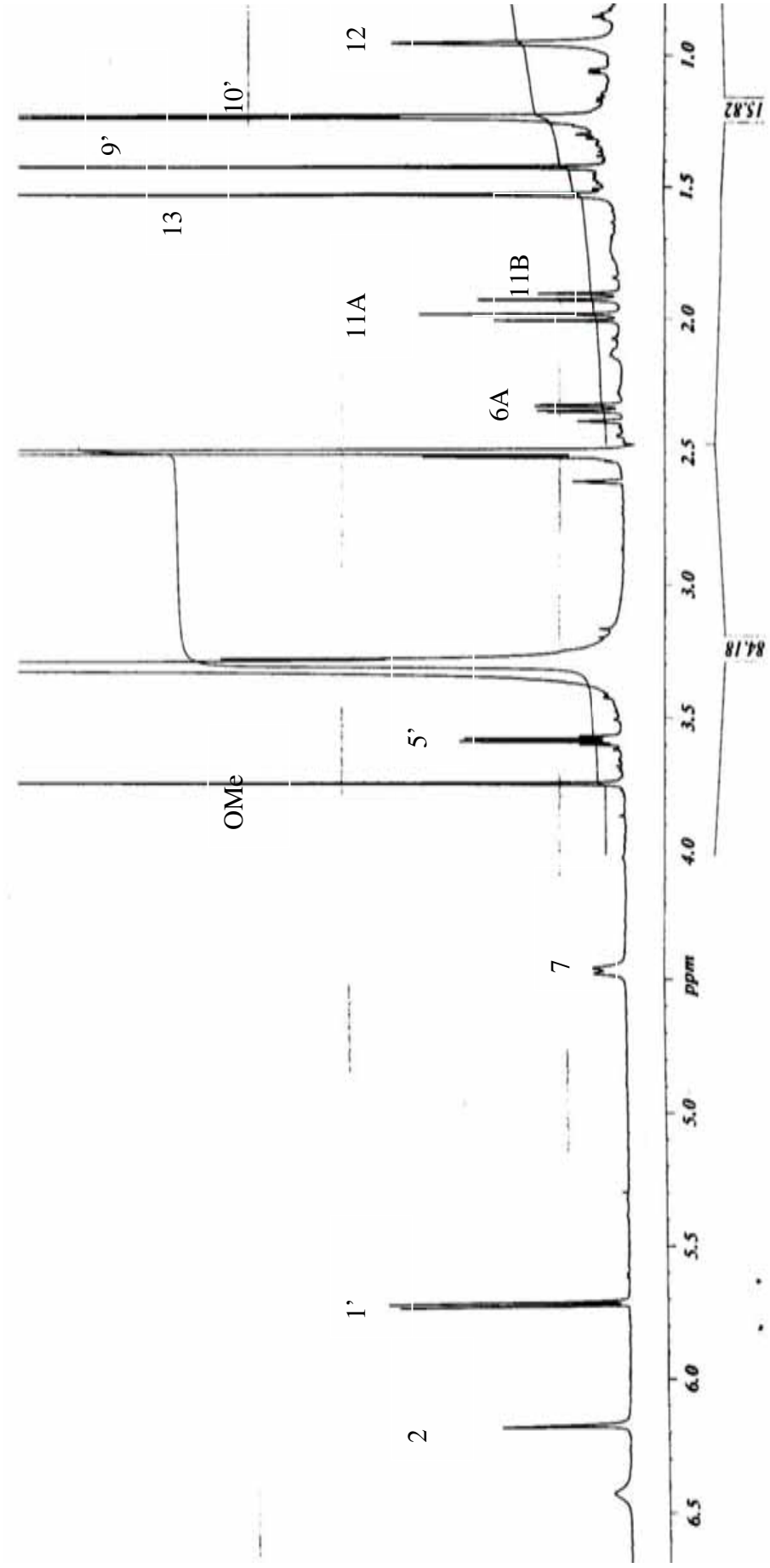
Attachment 10. The ¹H NMR spectrum of citreonigrin H



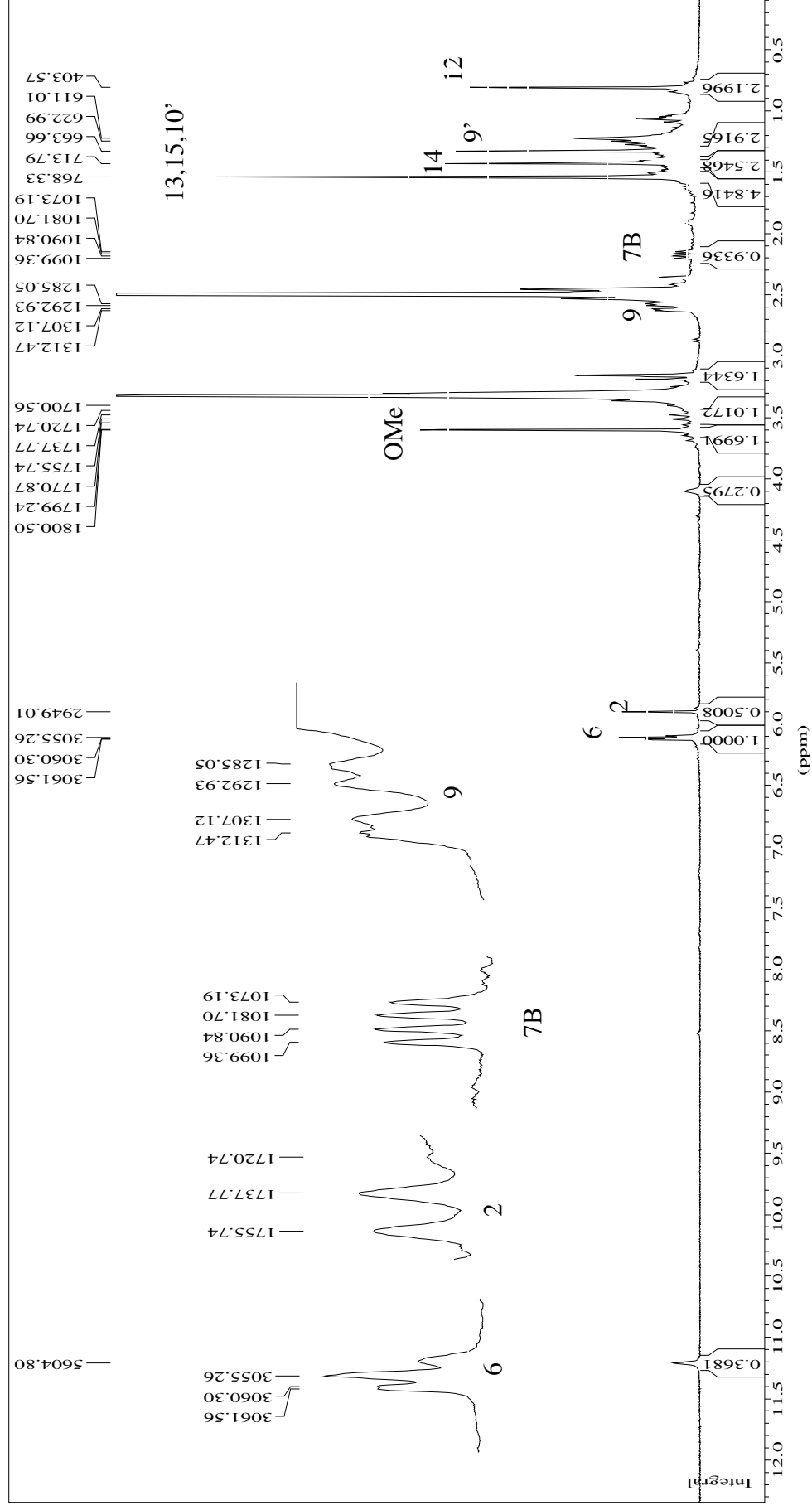
Attachment 11. ¹H NMR spectrum of citreonigrin I



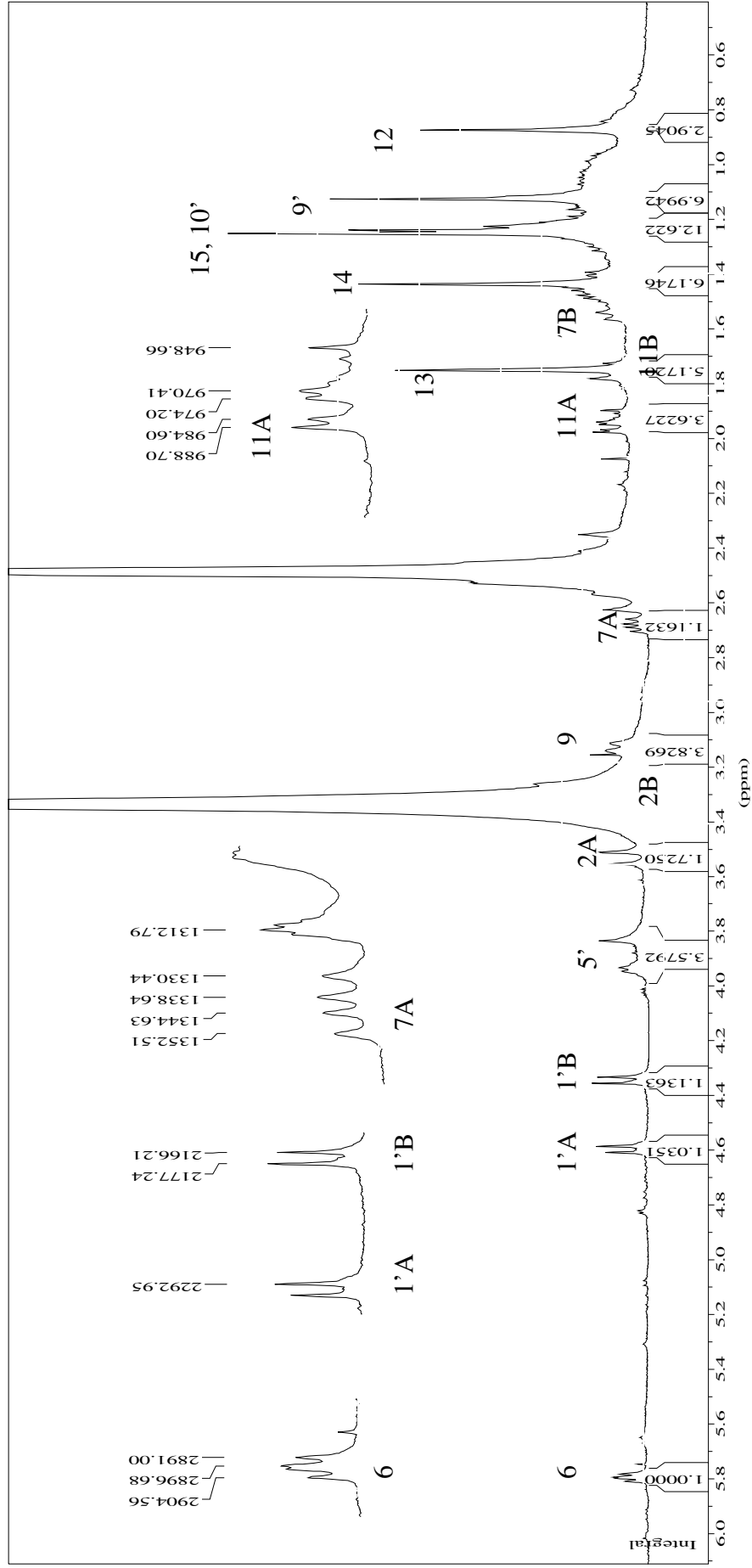
Attachment 12. The ^1H NMR spectrum of PC 3.3.6.6..3.A



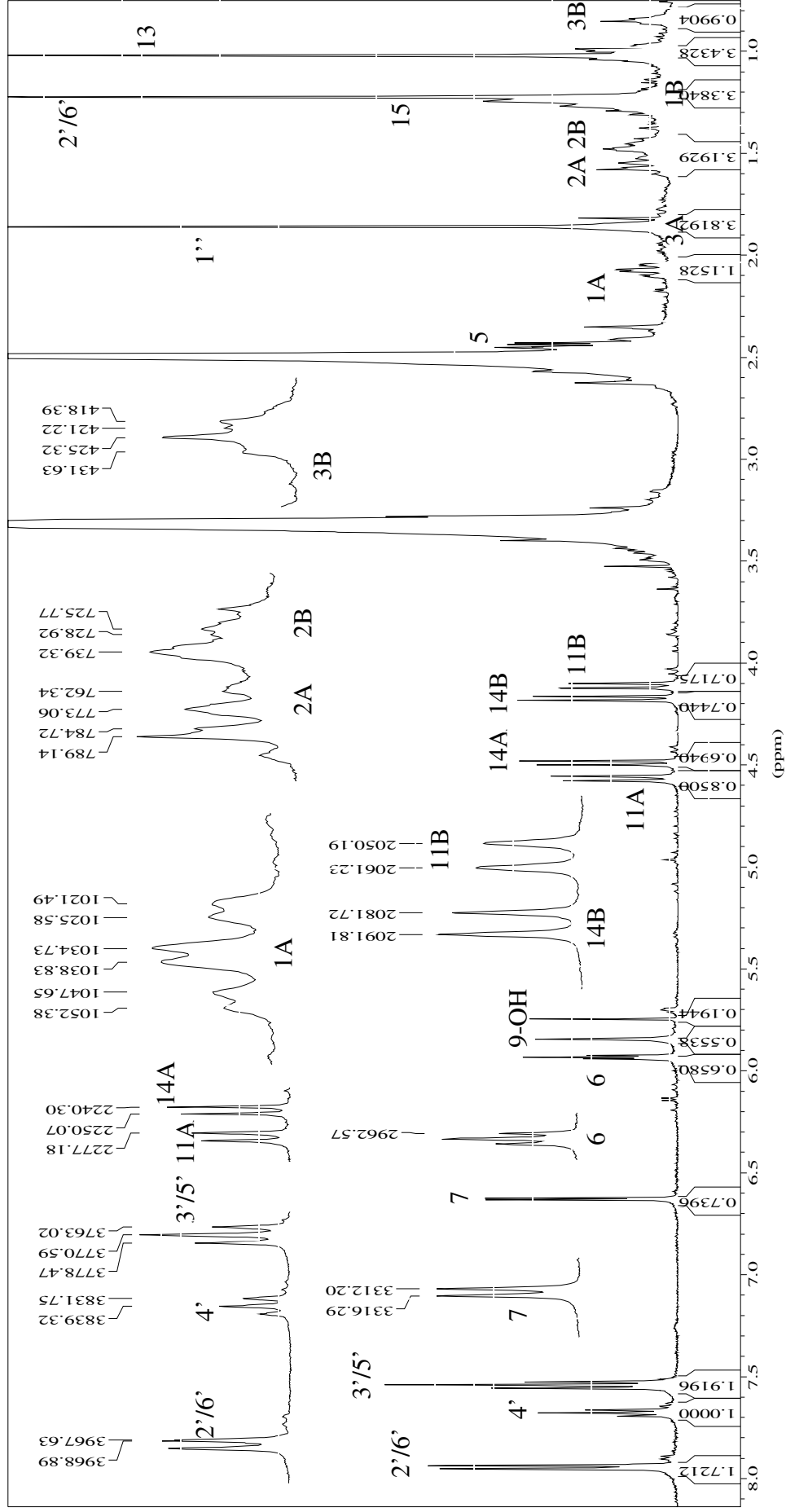
Attachment 13. The ^1H NMR spectrum of PC 3.3.6.6.3.B



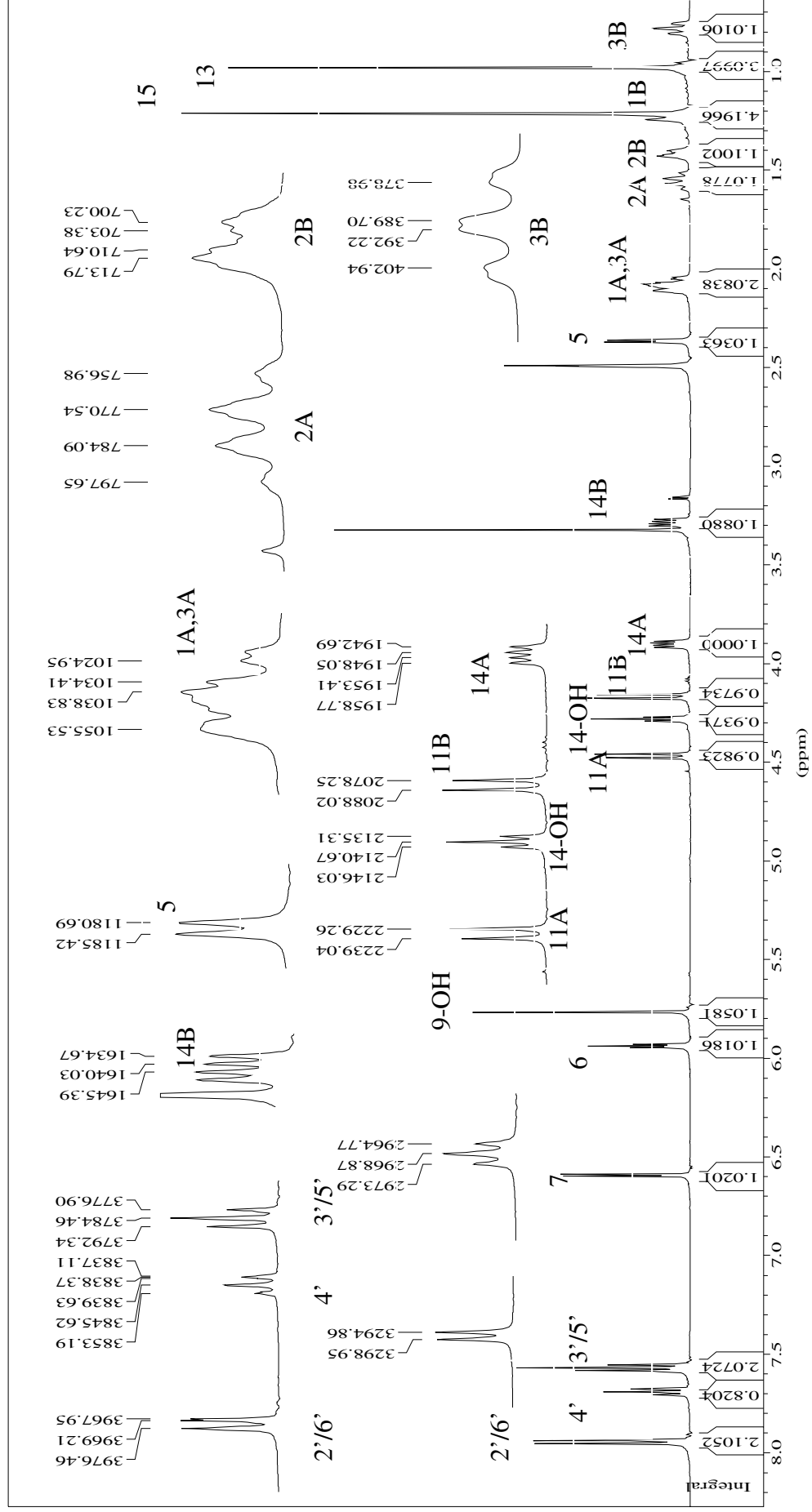
Attachment 14. The ^1H NMR spectrum of PC 3.3.22.D



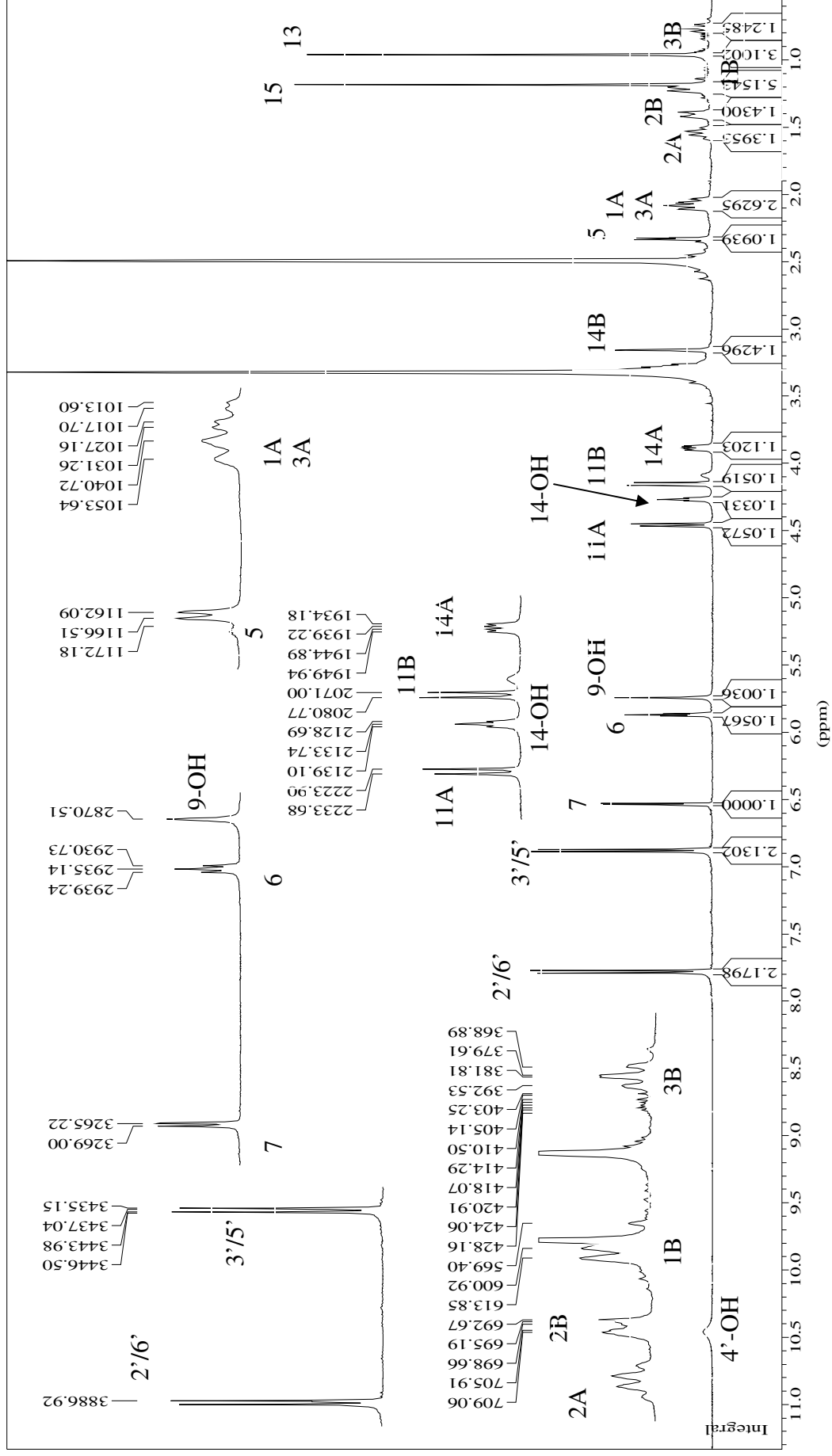
Attachment 15. The ^1H NMR spectrum of citreodrimene A



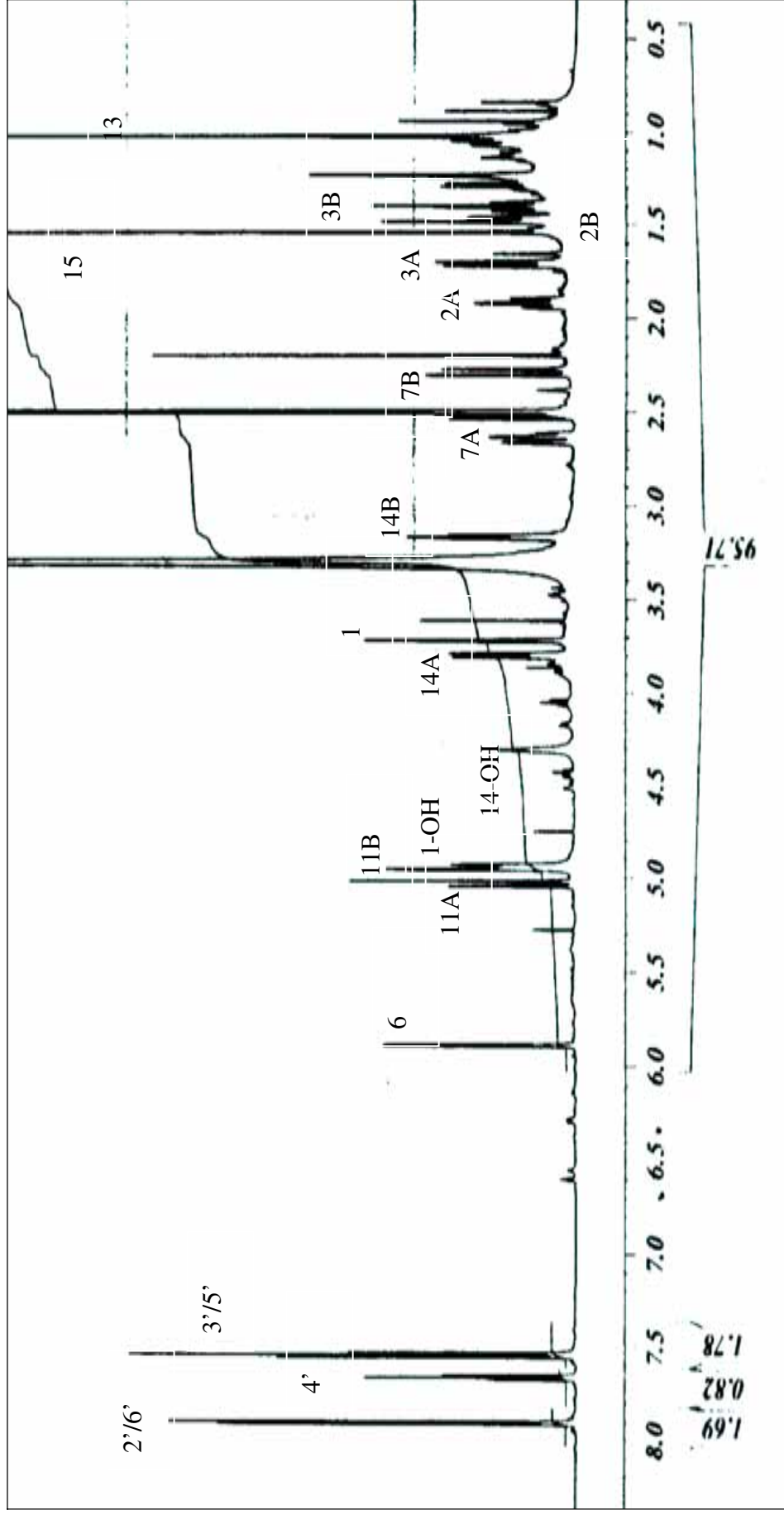
Attachment 16. The ^1H NMR spectrum of citredrime B



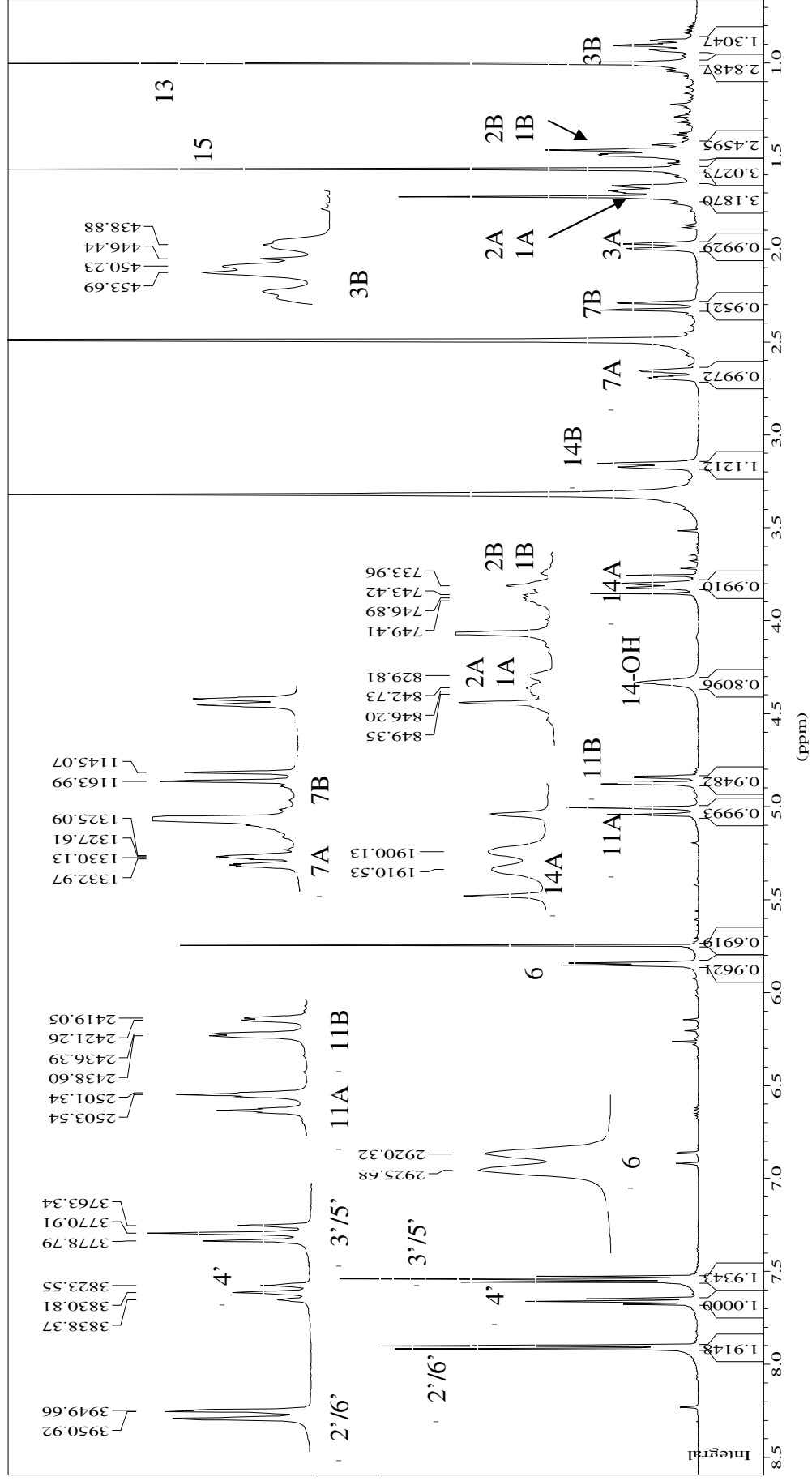
Attachment 17. The ^1H NMR spectrum of citreodrimene C



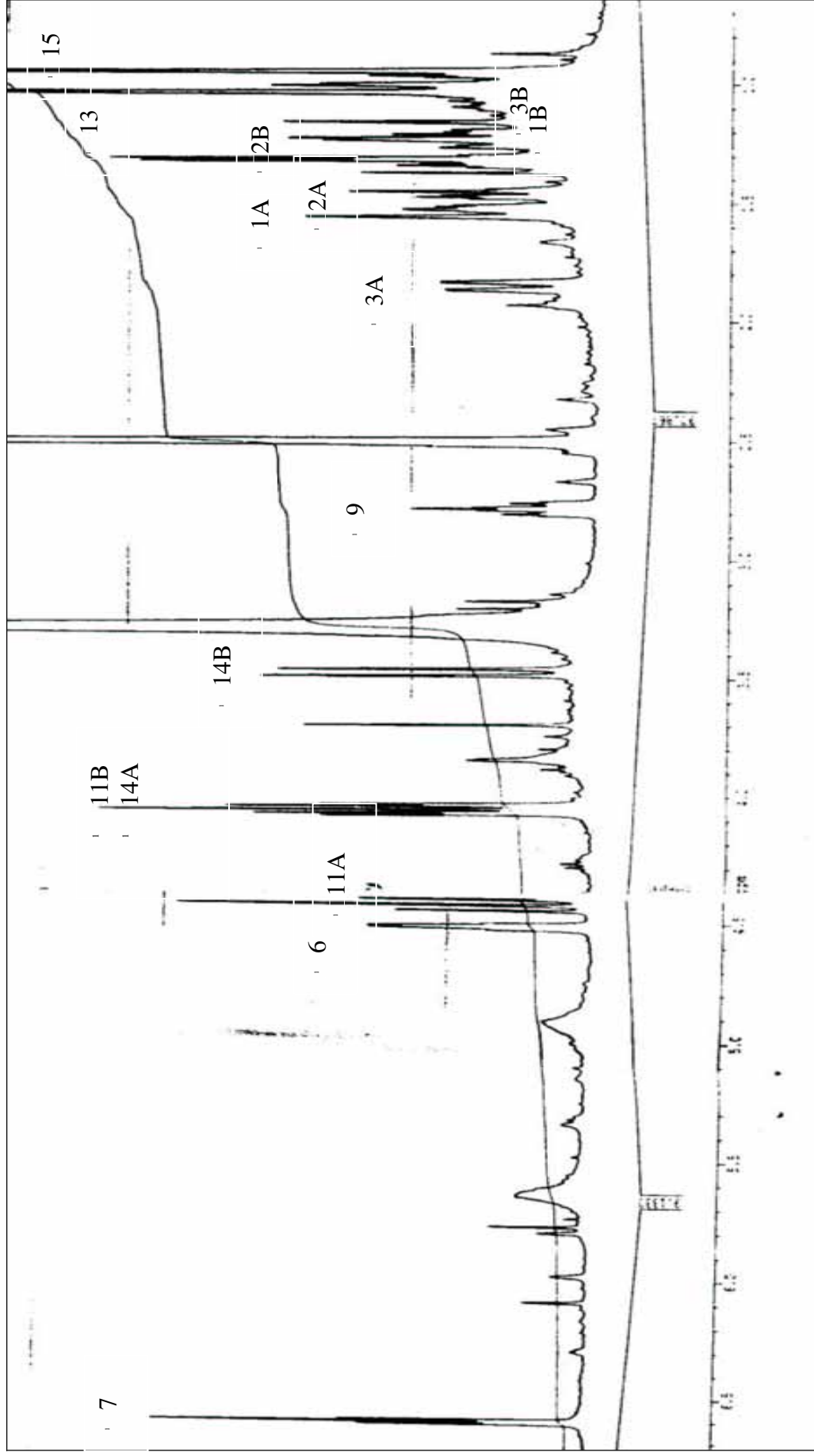
Attachment 18. The ^1H NMR spectrum of citreodrimene D



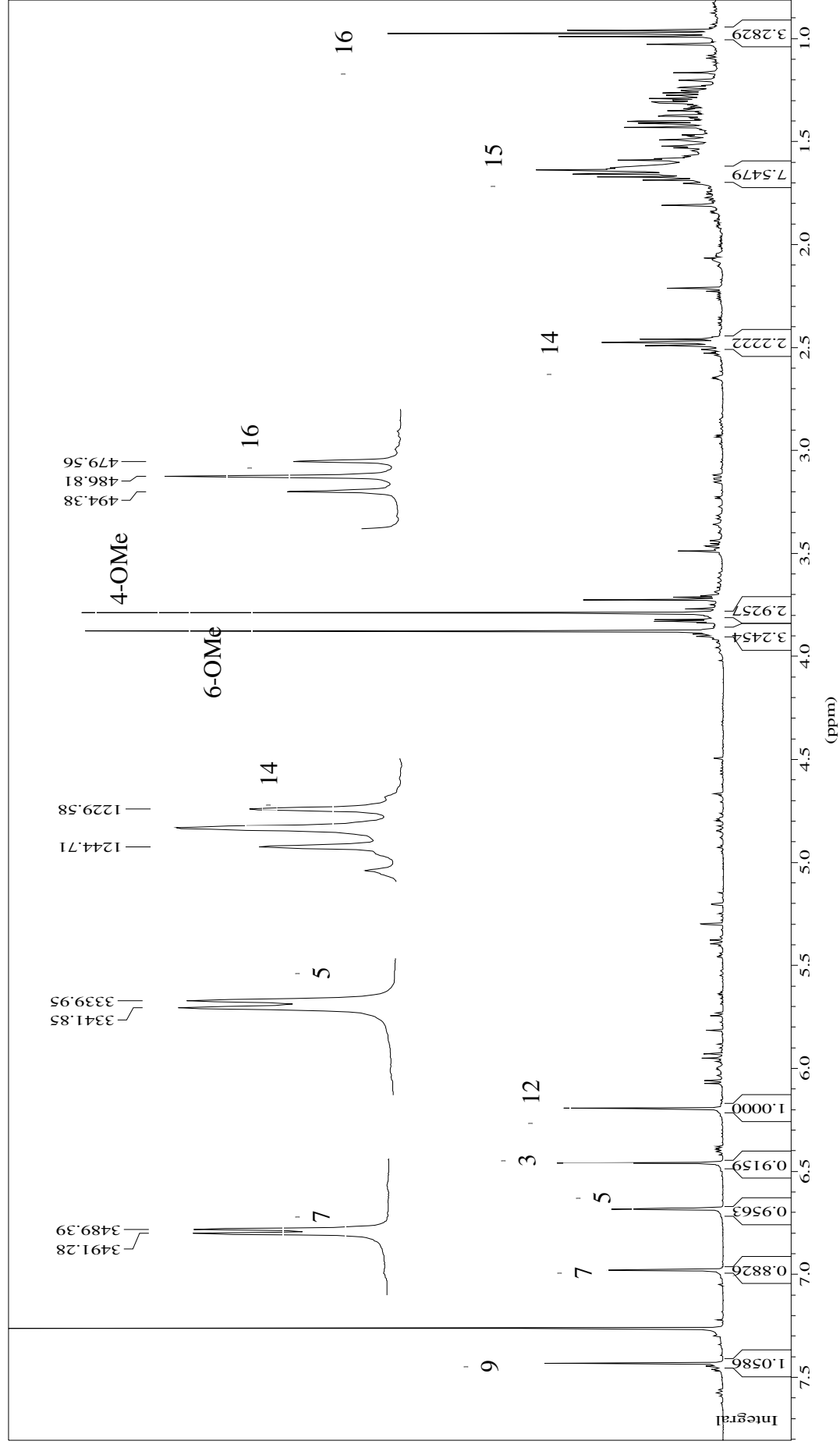
Attachment 19. The ¹H NMR spectrum of citreodrimene E



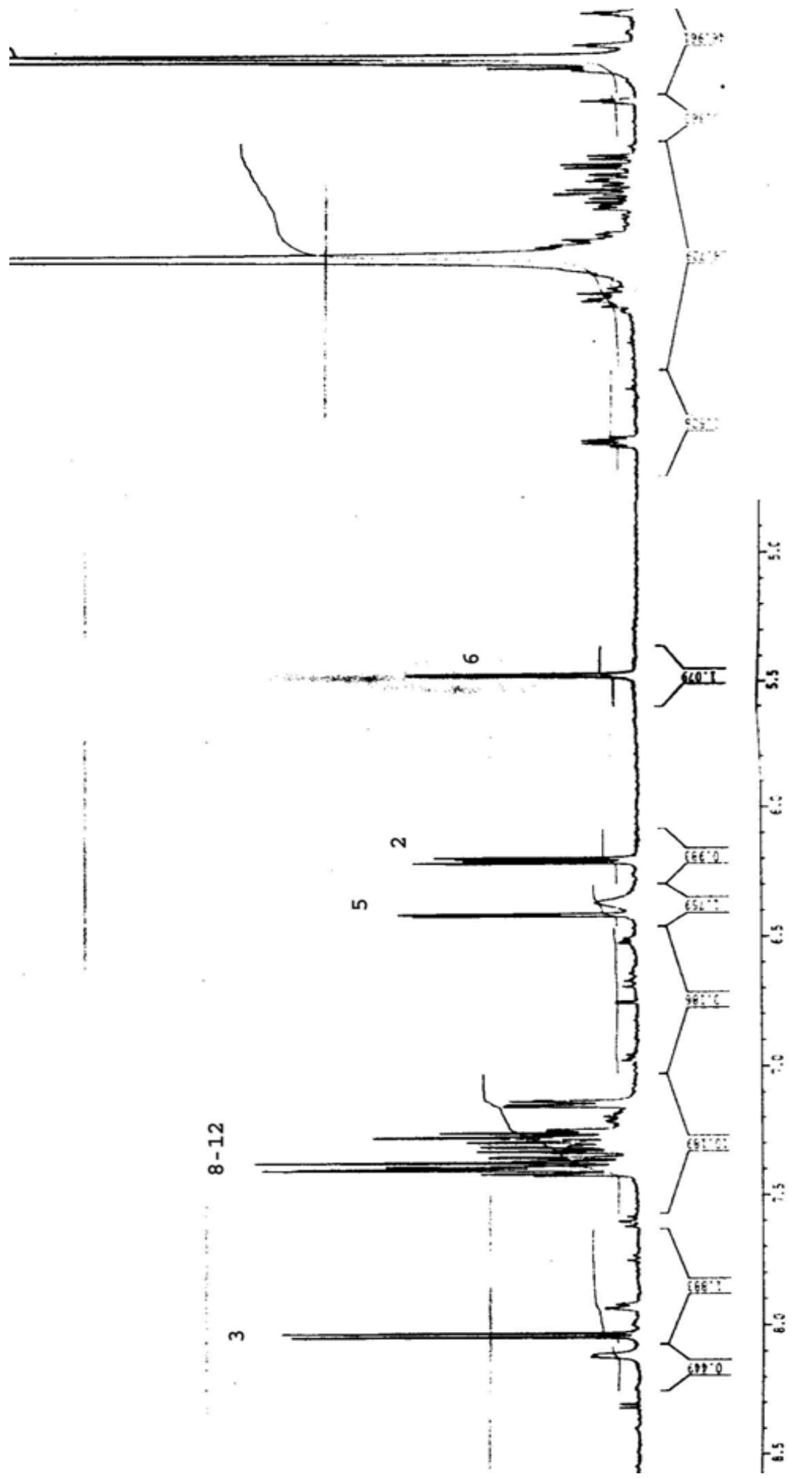
Attachment 20. The ^1H NMR spectrum of citreodrimene F in DMSO-d_6



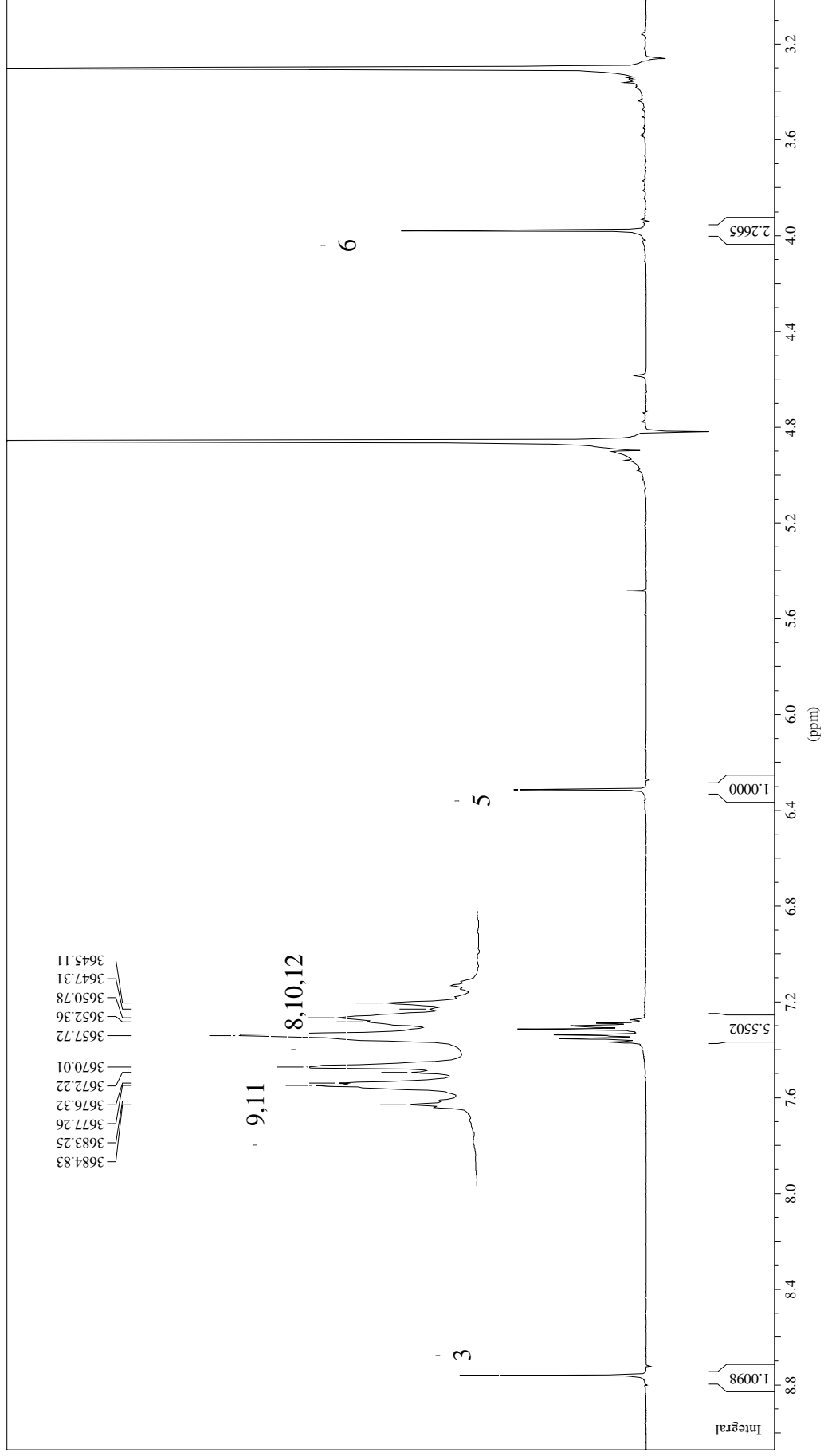
Attachment 21. The ¹H NMR spectrum of 14,15-dihydrovermistatin



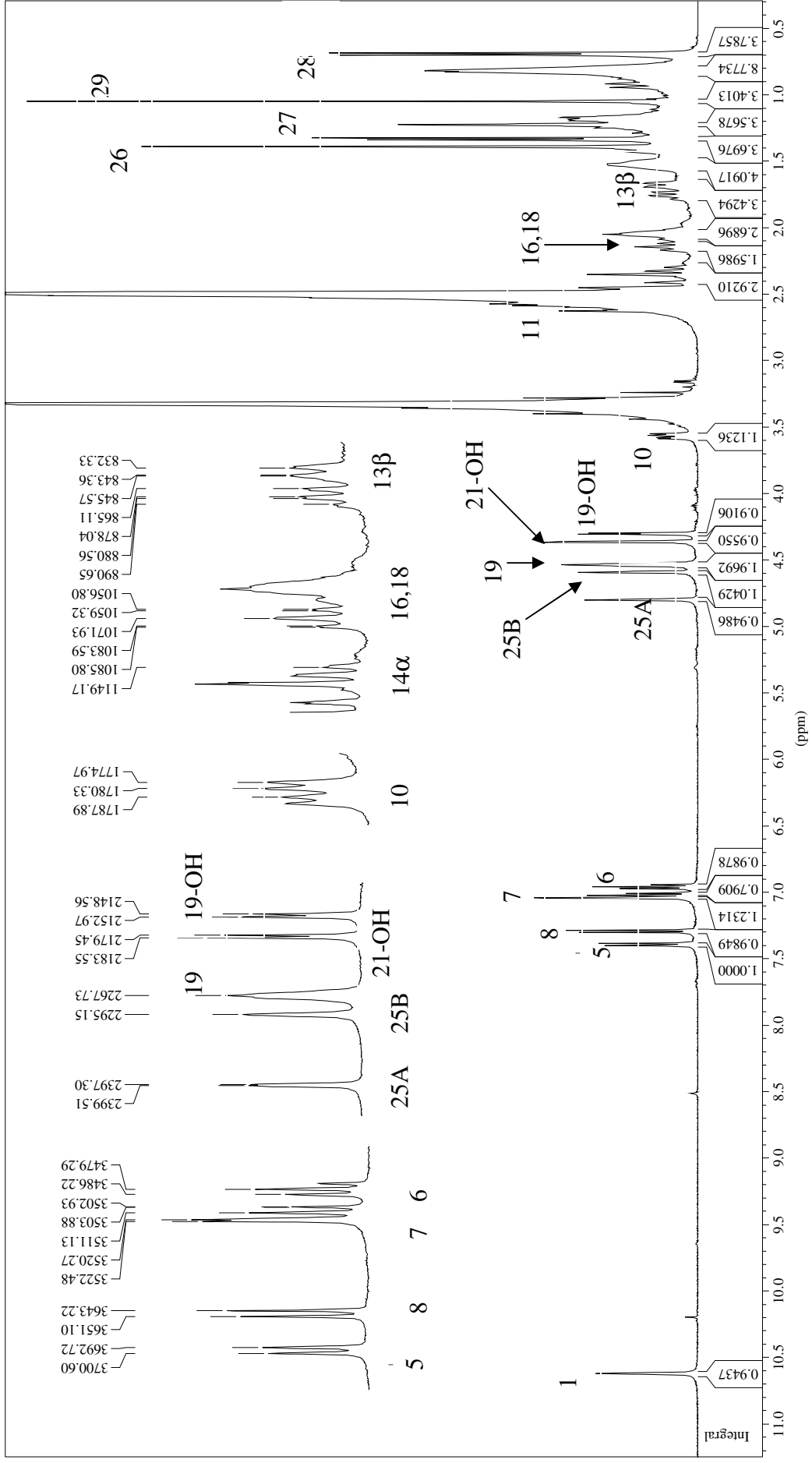
Attachment 22. The ^1H NMR spectrum of 2-(hydroxy(phenyl)methyl)-4-pyrone



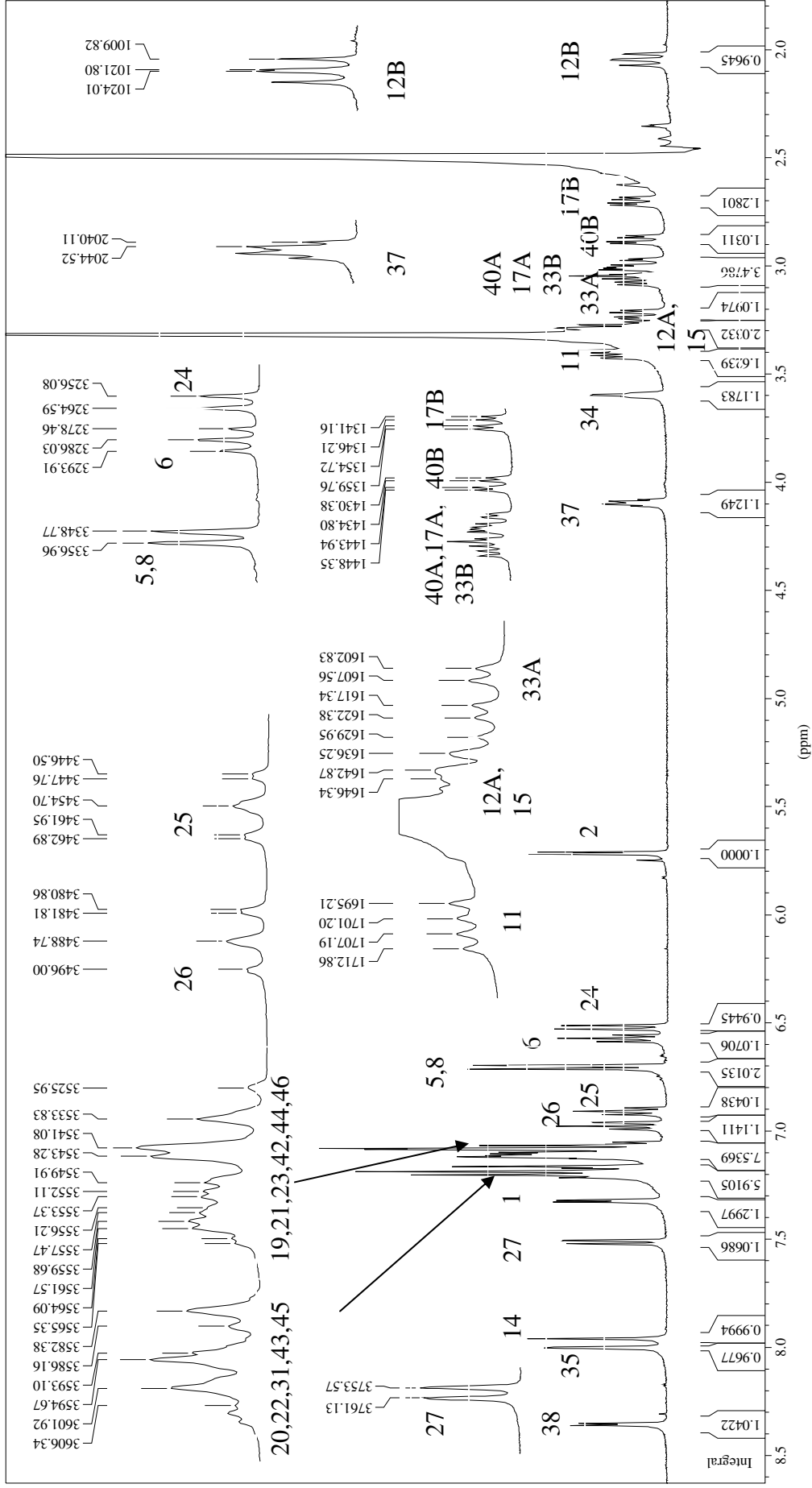
Attachment 23. The ¹H NMR spectrum of 6-benzyl-4-oxo-4H-pyran-3-carboxamide



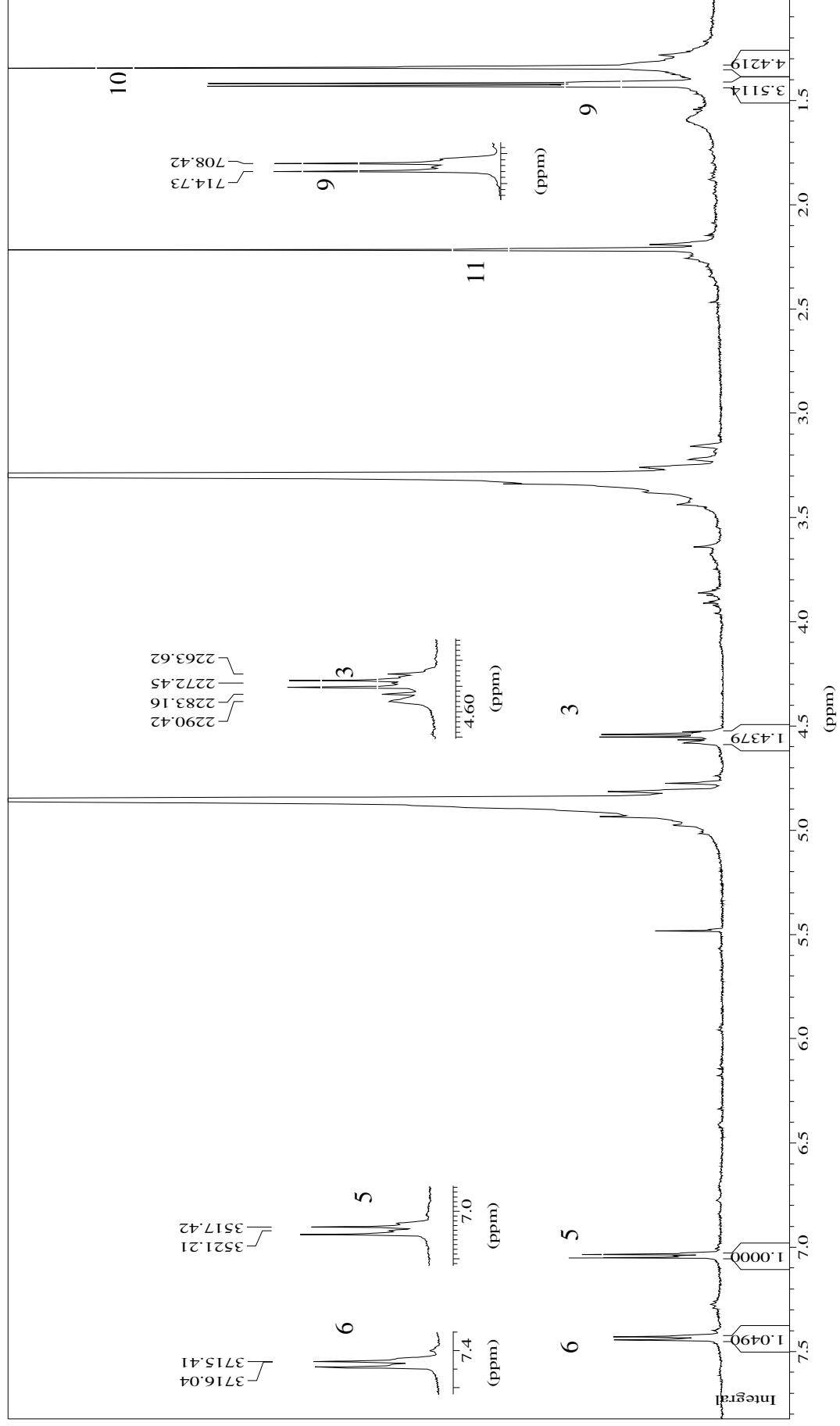
Attachment 24. The ¹H NMR spectrum of new aflavinin derivate (ANE 6.8.1.1)



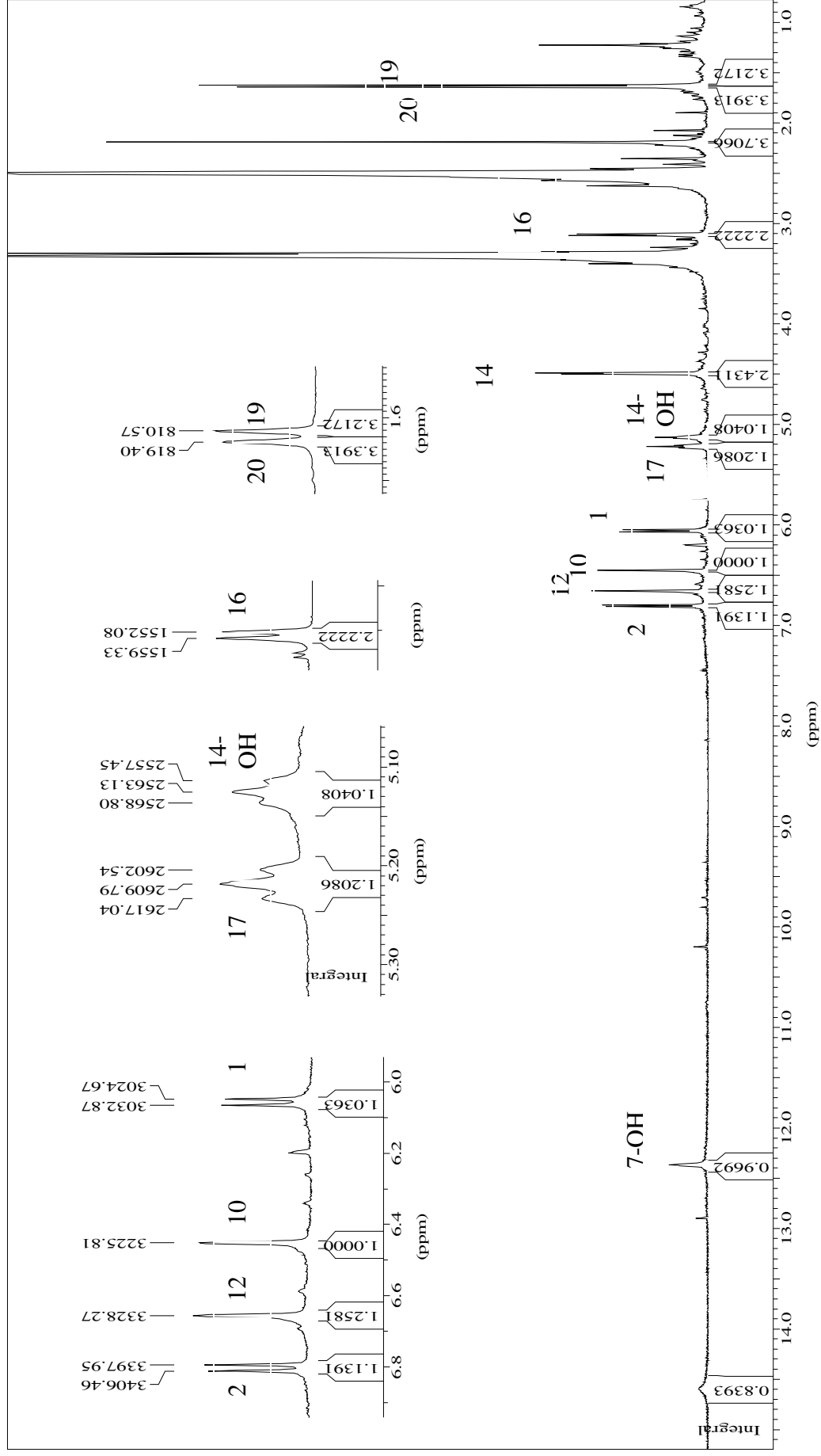
Attachment 25. The ^1H NMR spectrum of new asperazine



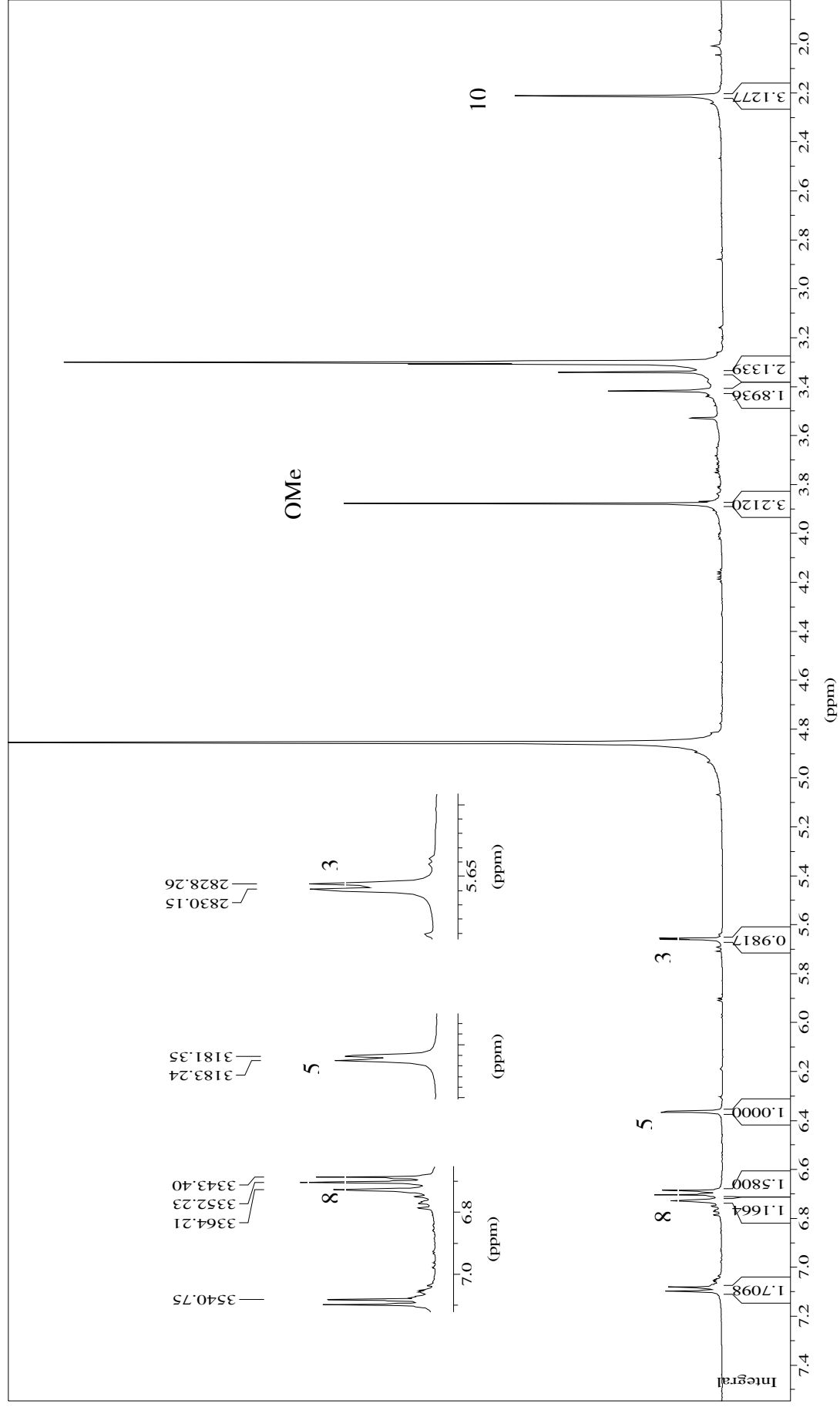
Attachment 26. The ^1H NMR spectrum of new gamahorin



Attachment 27. The ¹H NMR spectrum of PL 5.12.A



Attachment 28. The ^1H NMR spectrum of PL 4.2.7.5



LIST OF ABBREVIATIONS

b	: broad
BuOH	: butanol
COSY	: correlation spectroscopy
CDCl ₃	: deuterated chloroform
CHCl ₃	: chloroform
Cyc	: cyclin
CDK-2	: cyclin-dependant kinase-2
CK-2	: casein kinase-2
d	: doublet
DEPT	: distortionless enhancement by polarozation transfer
DMSO	: dimethylsulfoxide
DMSO-d ₆	: deuterated dimethylsulfoxide
ED	: effecive dose
EGF	: epidermal growth factor
EI	: electron impact ionisation
Eph	: ephrin
ESI	: electron spray ionisation
et al.	: et altera
EtOAc	: ethyl acetate
eV	: electron volt
FAK	: focal adhesion kinase
Fig	: figure
FLT-3	: Fms-like tyrosine kinase 3
g	: gram
HMBC	: heteronuclear multiple bond connectivity
HMQC	: heteronuclear multiple quantum connecticity
HPLC	: high pressure liquid chromatography
Hz	: hertz
IC	: inhibition concentration
IGFR	: insulin-like growth factor receptor
INS-R	: insulin receptor

L	: liter
LC	: lethal concentration
LC-MS	: liquid chromatography - mass spectrometry
m	: multiplet
M	: molar
MeOD	: deuterated methanol
MeOH	: methanol
Min	: minute
MS	: mass spectrometry
m/z	: mass per charge
n.a	: not active
n.d	: not detected
n.t	: not tested
nm	: nanometer
NMR	: nuclear magnetic resonance
n.t	: not tested
NOE	: nuclear overhauser effect
PDGFR	: platelet-derived growth factor receptor
ppm	: parts per million
PKC	: protein kinase C
PLK	: polo-like kinase
PTK	: protein tyrosine kinase
q	: quartet
ROESY	: rotating frame overhauser effect spectroscopy
RP	: reverse phase
RTK	: receptor tyrosine kinase
s	: singlet
t	: triplet
TLC	: thin layer chromatography
UV	: ultraviolet
VEGFR-3	: vascular endothelial growth factor receptor-3
VLC	: vacuum liquid chromatography

BIODATA

Name : Yudi Rusman
Date of birth : 01 December 1969
Place of birth : Bogor, Indonesia
Nationality : Indonesian
Address : 1. Himmelgeisterstrasse 81. 40225. Düsseldorf. GERMANY
2. Jl. Kebon Manggis I. No.H-6. Rt. 1/3.
Matraman. Jakarta Timur. 13150. INDONESIA

EDUCATION BACKGROUND

1975 – 1981 : Elementary School. SD Muhammadiyah 4. Palembang. Ind.onesia
1981 – 1987 : High School. SMPN-8 / SMAN-5 Palembang. Indonesia
1987 – 1993 : Graduate Study in Chemistry
Department of Chemistry. The University of Indonesia (Indonesia)
1997 – 2000 : Master Study in Biotechnology
Joint programme between Bandung Institute of Technology (Indonesia)
and School of Biotechnology and Biomolecular Science, The Univesity of
New South Wales (Australia)
2003 – 2006 : Doctor Study (Promotion) in Pharmacy
Institut für Pharmazeutische Biologie and Biotechnologie
Heinrich-Heine-Universität-Düsseldorf (Germany)

EMPLOYMENT RECORDS

1993 – 1994 : Research Department at PT Arindo Pacific Chemicals, Jakarta. Indnesia
1994 – Now : Research Centre of Pharmaceutical and Medicinal Technology.
The Agency for the Assessment and Application of Technology (BPPT).
Jakarta, Indonesia.

